Thymic Stromal Cells: Population Dynamics and Their Role in Thymopoiesis

Daniel Herbert Donald Gray

B.Sc.(Biomed)(Hons)

Department of Pathology and Immunology,

Monash University,

Melbourne, Victoria, Australia

Submitted to Monash University in accordance with the requirements

for the degree of Doctor of Philosophy

May 2003

Dedicated to the loving memory of Dorothy Worden Gray

ADDENDUM

DECLARATION

This thesis contains no material that has been accepted for the award of any other degree or diploma in any university or other institution. To the best of my knowledge, this thesis contains no material previously published or written by any other person, except where due reference is made in the text.

TABLE OF CONTENTS

TABLE OF FIGURES

CHAPTER ONE

CHAPTER THREE

CHAPTER FOUR

CHAPTER FIVE

CHAPTER SIX

CHAPTER SEVEN

ABSTRACT

The thymus is an essential component of the immune system. As the exclusive site of αβT-cell development, the thymus is absolutely required for the establishment of adaptive immunity. This unique function is imparted by the thymic stroma, which mediates the development of T-cells capable of responding to foreign antigen, while remaining tolerant of self. Despite the importance of stromal cells, our knowledge of their biology is relatively poor, partly due to technical limitations in studying this population. Consequently, major questions concerning the status of stromal cells as the thymus changes throughout life and how these cells guide the movement of thymocytes remain. This thesis establishes new ways of investigating stromal cells and applies these techniques to address such questions. The data presented demonstrates that the stroma is a more dynamic population than previously thought and leads to the proposal of new models for thymic epithelial cell differentiation, mature thymocyte export and the control of thymic homeostasis.

The complexity of the lympho-stromal interplay required for αβT-cell development is reflected by the heterogeneity of both lymphocytes and stromal cells. While panels of monoclonal antibodies have described many of the cellular components of these microenvironments, the means to quantify stromal cell subsets using flow cytometry has been poorly defined. The studies in Chapter Three refined and compared various stromal cell isolation procedures, and determined the effects of different digestion enzymes on important surface molecules. Three- and four-colour flow cytometric analysis was used to correlate established and novel stromal cell markers to define thymic fibroblasts, epithelium and a unique subset of endothelium that express MHC II molecules. This work provides the basis for the quantification and purification of the thymic stroma for further phenotypic, functional and genetic analysis.

This technique was employed in Chapter Four to describe fundamental parameters of thymic stromal cell biology. Quantitative and phenotypic analysis of the stroma in different thymic states throughout life revealed extensive changes in the number and composition of this population. These data show that the stroma expanded and contracted with overall thymocyte numbers. The dynamic nature of this association was confirmed upon examination of stromal cell proliferation capacities, suggesting continual turnover and remodeling of the stroma throughout life. Changes in the surface phenotypes of novel thymic epithelial subpopulations over time correlated with the provision of signals from thymocytes at particular stages of development. Age-related thymic involution was associated with a proportional loss of epithelium and skewing towards MHC II^{lo} and cortical subpopulations. This was corrected following sex steroid withdrawal, with the stroma regenerating to normal young numbers, albeit with delayed kinetics compared to thymocytes. Overall, these studies show that the thymic stroma continually develops and is capable of extensive expansion, remodeling and regeneration.

The requirement for the thymic stroma in many thymocyte developmental steps has been well established, but the mechanisms remain poorly characterised. Perhaps the least understood of these processes is the import and export of thymocytes into and from the organ. This has been partly due to a lack of appropriate cellular markers for the thymic microenvironments in which these events occur. The data presented in Chapter Five addresses this, characterising the distribution and biochemistry of a novel marker of thymic perivascular fibroblasts. The monoclonal antibody MTS-15 is shown to recognise a cell surface glycolipid expressed by pericytes of the thymus and spleen, adult connective tissues and discrete embryonic neural structures. Demonstration of MTS-15 antigen shedding was associated with a unique distribution of the determinant on leukocyte subsets. Biochemical and MALDI-TOF analysis indicates that the structure detected by MTS-15 is the terminal GalNAc carbohydrate of the globo-glycosphingolipid $GalNAc_2Gal_2GlcCer$. The restriction

of MTS-15 binding to thymic pericytes presents a unique opportunity to investigate the role of these stromal cells in thymic import and export.

Chapter Six focuses on the role of stromal cells in thymocyte emigration. By employing a novel fetal thymic organ culture system, the chemokine CCL19 (ELC, MIP3β or Exodus-3) was shown to elicit the export of mature thymocytes. RT-PCR analysis of purified thymic stromal cell subsets demonstrated that medullary epithelial cells and MTS-15$^+$ pericytes were the major sources of this chemokine in the thymus. The surface presentation of high levels of CCL19, but not CCL21 (a chemokine which binds to the same receptor, but does not mediate export), by MTS-15$^+$ pericytes and endothelial cells may account for the differential roles of these chemokines in thymic emigration. While the chemokine receptors CCR7 and CCXCKR seem to mediate epithelial CCL19 presentation, pericyte and endothelial presentation appear to occur via an as yet uncharacterised, trypsin-resistant interaction. This work defines a unique role for CCL19 and stromal cells of the thymic perivasculature in mature thymocyte emigration and proposes a mechanism by which this may occur.

LIST OF PUBLICATIONS

PUBLISHED JOURNAL ARTICLES

Prockop, S.E., Palencia, S., Ryan, C.M., Gordon, K., **Gray, D.**, Petrie, H.T. (2002) Stromal cells provide matrix for migration of early lymphoid progenitors through the thymic cortex. Journal of Immunology 169:4354-4361.

D.H.D. Gray, A.P. Chidgey, and R.L. Boyd (2002) Analysis of thymic stromal cell populations using flow cytometry. Journal of Immunological Methods 260,1-2:15-28.

T. Ueno, K. Hara, M. Malin, M. Swope Willis, **D.H.D. Gray**, U. Hopken, K. Matsushima, M. Lipp, T. Springer, R. Boyd, O. Yoshie and Y. Takahama. (2002) The role of CCR7 ligands in the emigration of T lymphocytes from the neonatal thymus. Immunity 16:205-218.

ABSTRACTS AND CONFERENCE PRESENTATIONS

D. H. D. Gray, A. P. Chidgey and R. L. Boyd (2003) "Population dynamics and lineage relationships of thymic stromal cells." Oral Presentation, ThymOz Conference.

D. H. D. Gray, A. P.Chidgey and R. L. Boyd (2002) "The thymic stroma is capable of rapid expansion during thymic regeneration." Oral Presentation, IgV Conference.

D. H. D. Gray, A. P.Chidgey and R. L. Boyd (2001) "Developmental changes in thymic stromal cells." Poster Presentation, ASI Conference.

D. H. D. Gray, A. P.Chidgey and R. L. Boyd (2001) "The role of stromal cells in thymic function." Oral Presentation, IgV Conference.

D. H. D. Gray, A. P. Chidgey and R. L. Boyd (2000) "Flow cytometric analysis of thymic stromal cells in embryonic, young and aged mice." Oral Presentation, ASI Conference.

D. H. D. Gray, B. J. Classon and R. L. Boyd (2000) "Characterisation of a novel glycolipid expressed by thymic stromal cells at the blood/thymus barrier." Oral Presentation, ASI Conference.

M. Milton, **D. H. D. Gray**, S. Zuklys, G. Hollander, R. L. Boyd and A. P. Chidgey (2000) "Genetic basis to the functional diversity of the thymic microenvironment" Poster Presentation, ASI Conference.

D. H. D. Gray, B. J. Classon and R. L. Boyd (2000) "Characterisation of a novel glycolipid expressed by thymic stromal cells at the blood/thymus barrier." Oral Presentation, Immunology Group of Victoria.

D. H. D. Gray, A. P. Chidgey and R. L. Boyd (2000) "Flow cytometric analysis of thymic stromal cells in embryonic, young and aged mice." Oral Presentation, Immunology Group of Victoria.

D. H. D Gray, B. J. Classon and R. L. Boyd (2000) "Characterisation of the thymic type I epithelial antigen recognised by the mAb MTS-15." Poster Presentation ThymOz 2000.

D. H. D. Gray, B. J. Classon and R. L. Boyd "Biochemistry and distribution of the thymic antigen recognised by the mAb MTS-15." (1998) Poster presentation, ASI Conference.

ACKNOWLEDGEMENTS

While it may have my name on the cover, this thesis embodies contributions from many people over the last 4 years. Without their support, this endeavour would not have been started, let alone completed. In this, the most important part of the book (ie. the only section most people will read), all of these people must receive a pat on the back.

The biggest thanks must to go to the ones that were there first. The work ethic required to complete this Ph.D. and certainly, the kind of person I am, is largely a reflection of the love and support provided by my family. Over time I've learnt that families like mine are not necessarily the norm, and that this particular group is made up of "exceptional specimens" (as Ma Gray would put it). More specifically, thanks must go to Douglas and Elisabeth for all of the encouragement and support over the last 25 years. Emma, thanks for providing a welcome refuge, replete with your awesome cooking and karate trophies. Thanks Tom for guiding me towards a misspent youth (computer games) and adulthood (scotch and computer games). I look forward to spending more time killing brain cells and aliens in your and Erin's new home. And thank you Charlotte, for all the late night chats, footy updates and countless lifts home. Together, these things maintain my perspective on all things.

For my perspective on this Ph.D., Richard Boyd has been the single most important influence. As a supervisor, Richard has provided many unique opportunities. A steady stream of conferences, collaborations and advice ensured that I've been given every chance to get a great start in science. In regards to this thesis, the opportunity to plot the line of enquiry, in conjunction with timely advice along the way, has shown me how to initiate and execute good science. I'm especially grateful for the willingness of the "world's busiest man" to drop whatever he's doing and help me out when necessary. As a character, Richard's humour and generosity has made my time in the lab very enjoyable. As has the introduction to the Scarpa Flow. Thank you, Richard.

One of the most important lessons I've learnt from Assoc. Prof. Boyd is the importance of collaboration in science. During the course of this Ph.D., I've been fortunate enough to form productive collaborations with some very brainy people. Thanks go to Dedreia Tull, Jody Zawadzki and Malcolm McConville for biochemical analysis of glycolipids, figures 5.8A

and B, as well as assistance with some of the methods text. Yousuke Takahama and Tomoo Ueno introduced me to the diverse world of chemokines and Japanese food (just don't say "aubergine"). They also contributed Figure 6.1 and much direction for the work presented in Chapter Six. I also gratefully acknowledge the provision of important reagents from Dale Godfrey, Philippe Naquet, Andy Farr, David Vremec, Ken Shortman, Adrian Liston and Chris Goodnow. This kind of input has allowed the research wheels to keep turning and take new directions.

Everything else arose from the unique environment that is the Boyd lab. Good science and good fun is mixed in very large parts by a group of fantastic members. It is rare to find such a close-knit group of friends and colleagues that make the long hours bearable, even fun. Thank you, Mark Malin for providing a constant source of amusement and assistance. Fortunately, your domestic "*farte blanche*" does not yet extend to the lab, because the atmosphere of the place will change if it does. Thanks also to Ann Chidgey for your advice and assistance over the years. Brendan "BJ" Classon also deserves my gratitude for his early supervision and advice regarding the MTS-15 work. Furthermore, thanks Stuart Berzins for the hilarious stories and practical advice on just about everything. I appreciated the timely corrections of this thesis, a few of which you may notice I agreed with. By the way, John Murphy would like to see you in his office. Jason Gill also deserves a big thank you for his intellectual input and advice, starting all those years ago as my third year demonstrator, right up to allowing me to use some of his pretty artwork in this thesis. Thanks also "Dirty" Dave Zammit for the beach volleyball chats and beer. Jayney, you've been an absolute delight to work with and tease. Thanks for your friendship and being such a sport. I must also acknowledge John Emmins, for his patient ear and awful jokes.

Morag Milton, your friendship and constant pestering to stop working so hard has helped me to maintain (relative) sanity. Thank you for that and the constant stream of CD's and videos, and sorry to hear about John Elliot. Adam, keep putting that reputation on the line and get that bloody X-box. Gabby, thanks for the help with references, Toolangi and restaurant suggestions. And other members that should be mentioned here include Libby, Cam-Tu, Eva, Samy, Elise, Kym, Lisa, Anne, Samantha, Lauren, Darren, Jade, Maree, Jarrod, Tracy and Alex. It's been fantastic working and socialising with you all, and I look forward to more of the same.

The setting for this unique lab has been an amazing department. The help provided by all academics has been invaluable, particularly Ban Hok Toh, Jenny Rolland, Ian van Driel, Paul Gleeson, Frank Carbone and Frank Alderuccio. Jim Goding deserves special mention for tearing strips off my first Ph.D. seminar, which didn't feel too great at the time, but put me on the right track with the MTS-15 project. Speaking of tearing strips, Dale "the biter" Godfrey has always been of assistance, whether it be by throwing beer all over me or nitpicking FACS profiles. This extends to the past and present members of the Godfrey enterprise. In no particular order, Kirsten, Daniel ("Plunger"), Jessica, Kon, Jared, Rachael and Nadine all deserve thanks for social and scientific input. Good luck with the next chapter at Melbourne University. Thanks especially Nadine, for your continued friendship and awesome curries (you really can cook well, you know). Elise, Gez, Plunger and Rachael have also been of great assistance making sure that bloody sorter behaves itself. Mel and Andrew deserve mention for their photography assistance and Dale Morris, Samantha, Karen and Jade made sure all my mice were well looked after. Thanks also to all the front desk boys, particularly filthy Benn.

Another integral cog of the department has been the Beer Room. Leon and Matt manfully maintained this facility, beyond the call of duty, for many years. Thanks Matty for all the beer and BBQs and Leon for all the drinks and advice (but you really shouldn't tease Dave so much). They were joined by many others already mentioned here, as well as Richard Coles (don't forget who carried you in your formative beach volleyball years) and Mark Coulson (stop playing with it and hand it in). I've lost more memories in that beer room and the College Lawn than I can remember. Other miscreants include Ben, Ed, and Cam (The Thornbury Boys), Petrea, "Potty" and Jerry. The magnificent bastards of Monster Piece Theatre and Struth provided outlets for physical aggression and teeth. Thanks also to my past and present housemates Terry, Darren, Rachael, Almut, Mark, Jessica, Ling, Preeti and Ina.

The final stages of the whole process have been especially enjoyable, due mostly to the love and support provided by Tracy Heng. Thank you for your companionship during the long hours and putting up with my crankiness and driving. I look forward to many more happy times with you and everyone mentioned above now that this thing is out of the way (assessors willing).

ABBREVIATIONS

BrdU	bromodeoxyuridine
CD	cluster of differentiation molecules
cTEC	cortical thymic epithelial cell
d	day
DN	double negative
DNase	deoxyribosenuclease
DP	double positive
ECGase	endoglycoceramidase
ECM	extracellular matrix
EDTA	ethylenediaminetetraacetic acid
EpCAM	epithelial cell adhesion molecule
E*n*	day of embryogenesis
FACS	fluorescence activated cell sorter
FcR	fragment crystallisable receptor
FCS	fetal calf serum
FITC	fluorescein isothiocyanate
hi	high
HSA	heat stable antigen
HSC	hemopoietic stem cell
HPTLC	high performance thin layer chromatography
HRPO	horse radish peroxidase
Ig	immunoglobulin
IL	interleukin

int	intermediate
kDa	kilodalton
lo	low
M	molar
mAb	monoclonal antibody
MALDI-TOF	matrix-assisted laser desorption/ionisation-time of flight
MHC II	major histocompatibility complex class II molecule
mo	month
mRNA	messenger ribonucleic acid
mTEC	medullary thymic epithelial cell
MTS	mouse thymic stroma
PBL	peripheral blood leukocytes
PBS	phosphate buffered saline
PVDF	polyvinylidene fluoride
RAG	recombinase activating gene
SDS-PAGE	sodium dodecyl sulfate polyacrylamide gel electrophoresis
SP	single positive
TcR	T-cell receptor
TEC	thymic epithelial cell
vs	versus
wk	week

Chapter One

Literature Review

INTRODUCTION

The thymus is the exclusive site of mainstream T-cell development. This function is fundamental to the establishment and maintenance of the adaptive immune system. Central to this unique function is the thymic stroma that mediates thymocyte differentiation. The various subpopulations of thymic stromal cells form discrete microenvironments within which the various thymocyte developmental steps occur. These interactions give rise to T-cells capable of responding to foreign pathogens while remaining tolerant of self tissue. Despite the importance of the thymic stroma, our current knowledge of their biology is lacking.

This review explores the role of thymic stromal cells in T-cell development and thymic organogenesis, highlighting recent advances in these areas. Evaluation of the literature concerning thymic disruption and regeneration reveals key roles for these cells in all aspects of thymic function. However, many fundamental questions concerning the thymic stroma remain unanswered.

1.1 THE THYMUS

The thymus is a bilobed, encapsulated organ situated in the upper thorax, anterior to the heart. Each lobe is comprised of numerous lobules bound by invaginations of the capsule, called trabeculae. The body of the thymus is divided into an outer region – the cortex, and an inner region – the medulla. These areas support different phases of T-cell development,

mediated by a diverse group of thymic stromal cells that are essential for the maturation of the itinerant thymocytes (Kendall, 1991).

Thymocyte precursors are derived from bone marrow hemopoietic stem cells (HSCs) and enter the thymus via the bloodstream. These cells then undergo a sequence of proliferation and differentiation as they migrate from the subcapsule, through the cortex and medulla, and are ultimately exported from the thymus as mature T-cells.

1.1.1 The thymic microenvironment

The thymic microenvironment comprises a meshwork of interconnected stromal cells through which thymocytes migrate and develop (Boyd et al., 1993). This microenvironment is established through the interplay of developing thymocytes with the thymic stroma (Ritter and Boyd, 1993). The latter consists of a diverse population of cells, including primarily epithelium, but also endothelium, fibroblasts, macrophages, dendritic cells and neuroendocrine cells (Boyd and Hugo, 1991). While collectively these cells are numerically minor (~1% of thymic cellularity), they provide an array of surface molecules, extracellular matrix elements and cytokines that are essential for the various stages of T-cell development (Anderson et al., 1996).

The thymic microenvironment can be divided into three main anatomical regions: the subcapsule, cortex and medulla (Fig. 1.1). Phenotypic differences between the stromal cells in these sites were identified by immunohistological analysis using panels of monoclonal antibodies (mAbs) raised against mouse stromal cells (Van Vliet et al., 1984; de Maagd et al., 1985; Lobach et al., 1985; Godfrey et al., 1988; Kampinga et al., 1989). These studies suggested that stromal cells in different regions may be specialised to mediate distinct T-cell developmental steps. More recently, functional studies of the various stromal

Figure 1.1 Schematic diagram of cellular constituents of the subcapsular, cortical and medullary thymic microenvironments.

Taken from (Boyd and Hugo, 1991).

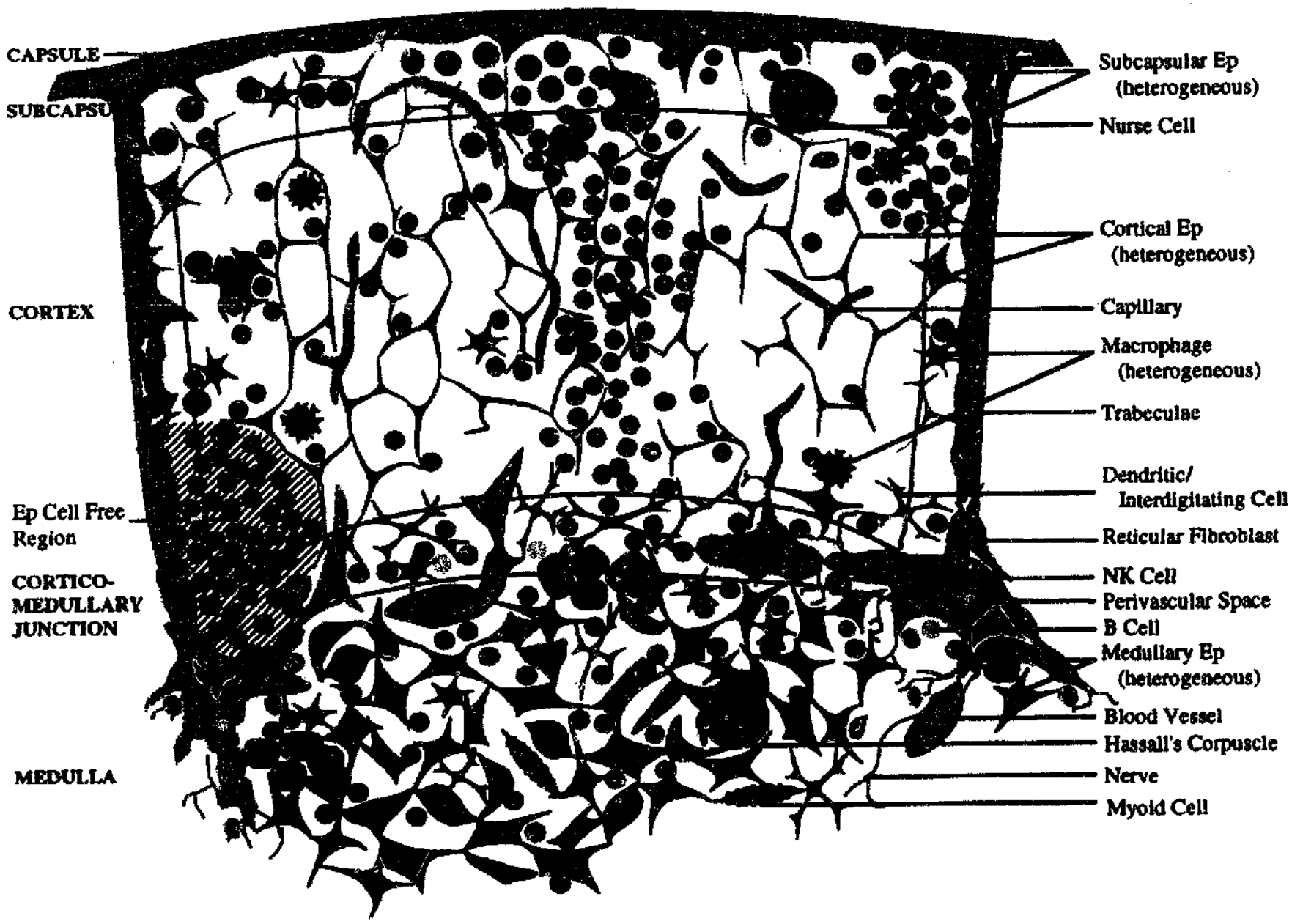
CAPSULE
SUBCAPSU
CORTEX
Ep Cell Free Region
CORTICO-MEDULLARY JUNCTION
MEDULLA
Subcapsular Ep (heterogeneous)
Nurse Cell
Cortical Ep (heterogeneous)
Capillary
Macrophage (heterogeneous)
Trabeculae
Dendritic/ Interdigitating Cell
Reticular Fibroblast
NK Cell
Perivascular Space
B Cell
Medullary Ep (heterogeneous)
Blood Vessel
Hassall's Corpuscle
Nerve
Myoid Cell

populations have defined many discrete roles that thymic cortical and medullary epithelium, fibroblasts and dendritic cells have in thymocyte development (Anderson and Jenkinson, 2001).

While the distinct microenvironments these stromal cell subsets constitute are essential for thymocyte differentiation, the development of these microenvironments likewise requires interactions with developing T-cells. The reciprocal interactions required to establish the various thymic microenvironments are referred to as "cross-talk" (Ritter and Boyd, 1993; van Ewijk et al., 1994). Studies of mutant mouse models in which thymocyte development is arrested at various stages revealed corresponding blocks in thymic stromal differentiation (van Ewijk et al., 2000a). Hollander et al. (1995) found that in the absence of very immature thymocytes, the cortical microenvironment did not form. Likewise, other studies have demonstrated the requirement for more mature thymocytes in the establishment of the thymic medulla (Shores et al., 1991; Mombaerts et al., 1992; Philpott et al., 1992; Palmer et al., 1993). It also appears that establishment of this microenvironment is influenced by spatial cues from the thymic vasculature (Anderson et al., 2000), an association that would facilitate emigration of mature medullary thymocytes. Despite the obvious importance of the vasculature and subcapsule as an interface between the circulation and thymus, these remain the least understood thymic microenvironments.

1.1.2 The thymic vasculature

During thymic organogenesis, branches of the internal thoracic artery penetrate the thymic capsule and, in association with connective tissue, divide and follow the lobular trabeculae. Blood vessels enter the thymic parenchyma at the cortico-medullary junction, surrounded by connective tissue and epithelium that form loose perivascular spaces containing many lymphocytes (Kato, 1997) (Ushiki and Takeda, 1997). From these vessels extend cortical capillaries tightly lined by thymic epithelial cells (Type I epithelium), once thought to form

the so-called "blood-thymus barrier" of the cortex (Marshall and White, 1961). It has since been found that soluble factors and cells can pass these cells to enter the thymus proper, showing that cortical thymocytes are not isolated from systemic antigens (Nieuwenhuis et al., 1988; Hoffmann-Fezer et al., 1989). The cortical capillaries loop back to drain into post-capillary venules within the perivascular spaces of the medulla (Kato, 1989). The perivascular spaces of the thymus are unique to this organ and the current evidence suggests they are the first and last thymic microenvironment encountered by thymocyte precursors and mature T-cells respectively.

Various precursor labeling experiments have shown that the sites of their entry into the thymus are the blood vessels at the cortico-medullary junction (Cantor and Weissman, 1976; Kyewski, 1987; Penit and Vasseur, 1988; Lind et al., 2001). Several studies have found that soluble peptides produced by thymic stroma are important in this process (Pyke and Bach, 1979; Champion et al., 1986; Wilkinson et al., 1999), and characterisation of chemokine candidates is ongoing (Norment and Bevan, 2000). The emigration of mature thymocytes from the thymus also seems to require chemoattractant signalling (Chaffin and Perlmutter, 1991; Rudolph et al., 1995), however the identity these factors remains undefined. While it is likely that stromal cells surrounding the vascular microenvironments of the thymus have a key role in these processes, studying these cells has been difficult to date. A lack of appropriate markers for these cells has precluded their purification for analysis of surface molecules and soluble factors involved in thymic immigration and emigration.

1.2 THYMIC T CELL DEVELOPMENT

Mainstream αβT-lymphocytes develop exclusively within the thymus from precursors derived from multipotential HSCs in the fetal liver or adult bone marrow (Carlyle and Zuniga-Pflucker, 1998a). Key features of thymocyte developmental stages include T-cell lineage commitment, T-cell receptor expression, thymocyte selection and emigration. These processes occur in a stepwise manner, dependent upon interactions with specialised stromal cells and growth factors in distinct microenvironments. The migration of developing thymocytes between thymic microenvironments is guided by overlapping gradients of various chemokines and adhesion molecules. The development of thymocytes can be tracked through the differential expression of CD3 and the CD4 and CD8 coreceptors. The most immature thymocytes are $CD3^-CD4^-CD8^-$ (triple negative, TN) which develop into $CD4^+CD8^+$ double positive (DP) cells, and ultimately $CD3^+CD4^+CD8^-$ or $CD3^+CD4^-CD8^+$ single positive (SP) T-cells (Nikolic-Zugic, 1991).

The following sections examine our current understanding of these processes, highlighting the key cellular and molecular requirements for thymic T cell development.

1.2.1 Hemopoietic stem cells and thymic colonisation

Hemopoietic stem cells (HSCs) give rise to all lymphoid, erythroid and myeloid blood cells. HSCs first develop in the yolk sac and fetal liver during embryogenesis, but reside in the bone marrow of adults as a self-renewing population (Bonifer et al., 1998). The differentiation of these cells is governed by interactions with their microenvironments. Thus, erythroid, myeloid and B lymphocytes all arise in the bone marrow, while T-lymphocytes almost exclusively develop in the thymus (Katsura and Kawamoto, 2001). Thymocyte progenitors first seed the embryonic thymic anlage prior to vascularisation at E10-12, through surrounding connective tissue (Anderson and Jenkinson, 2001). Adult blood-borne precursors enter via vessels at the cortico-medullary junction (see *1.1.2 Thymic*

vasculature) in what is thought to be a regulated manner (Foss et al., 2001). Whether these precursors differ from HSCs has proven difficult to determine, partly due to conflicting data concerning the lineage potential of the most immature thymocytes (for example (Wu et al., 1991a; Carlyle and Zuniga-Pflucker, 1998b; Kawamoto et al., 1998; Ohmura et al., 1999; Katsura and Kawamoto, 2001; Allman et al., 2003)). In particular, it is difficult to distinguish rapid differentiation upon entry into the thymic microenvironment from extrathymic differentiation prior to immigration. A recent study by Gounari et al., (2002) demonstrated pTα (a component of the pre-T-cell receptor) promoter activity prior to colonisation, supporting earlier work suggesting T-cell lineage commitment begins in common lymphoid progenitors before thymic immigration (Wu et al., 1991a; Rodewald et al., 1994). However, this does not seem to be a prerequisite for entry into the thymus, as a study by Allman et al., (2003) shows common lymphoid progenitors are not necessary for T cell development (supporting de Vries et al., (1992)).

The phenotype of the earliest thymocyte precursors is similar to that of bone marrow HSCs (lin^-, c-kit^+, Sca-1^+, $CD27^+$, IL-$7R\alpha^+$, $CD44^+$, $CD25^-$, $CD8^-$, $CD3^-$ (Allman et al., 2003)), however they also express low levels of CD4 (Wu et al., 1991b). These cells reside in the inner cortex and as they migrate through rest of the cortex towards the subcapsule, undergo further T-cell commitment and the early stages of thymocyte development (Lind et al., 2001).

1.2.2 Early T-cell development

The immature TN thymocytes of the thymus can be divided into 4 genetically and phenotypically distinct subsets based on the expression of the surface molecules CD25 (IL-2Rα chain) and CD44 (adhesion molecule) (Godfrey et al., 1993). Progression through each of these subsets correlates with important control points in T-cell differentiation (Godfrey and Zlotnik, 1993). The most immature of these subsets are $CD25^-CD44^+$ (DN1)

thymocytes, which include the $CD4^{lo}$ precursors mentioned previously, and bear T-cell receptor (TcR) genes in germline configuration (Godfrey et al., 1993; Oosterwegel, 1997). The proliferation and differentiation of these cells depends upon the provision of stromal derived cytokines, in particular, Stem Cell Factor (SCF, the ligand for c-kit) and IL-7 (Di Santo and Rodewald, 1998). Mice deficient in molecules essential to signalling by these growth factors show virtually no T-cell development beyond the DN1 stage, highlighting the importance of these cytokines in early thymocyte development (Rodewald et al., 1997).

Under the influence of these and other cytokines, these cells differentiate into DN2 thymocytes ($CD44^+CD25^+$), increasing in size, proliferating extensively (Penit et al., 1995) and upregulating pTα and CD25 expression. This subset also depends upon stromal cell support, with thymic epithelium and fibroblasts required for their differentiation into $CD44^-$ $CD25^+$ DN3 thymocytes (Godfrey and Zlotnik, 1993). The direct role for fibroblast extracellular matrix components in this development was demonstrated by Anderson et al., (1997), however subsequent differentiation can progress in the presence of thymic epithelial cells only. The transition from DN2 to DN3 thymocytes is accompanied by the initiation of TcRβ and γ chain gene rearrangement, leading to irreversible commitment to the T cell lineage (Godfrey and Zlotnik, 1993; Dudley et al., 1994; Godfrey et al., 1994). Recent studies have revealed a role for the surface receptor Notch-1 in governing these processes (MacDonald et al., 2001).

Notch signalling is an evolutionarily conserved pathway controlling multiple cell-fate decisions, initiated by interactions between Notch receptors and Notch ligands on neighbouring cells (Artavanis-Tsakonas et al., 1999). Mice deficient in Notch-1 receptor exhibit a block in T-cell development, with precursors instead giving rise to B-cells in the thymus (Radtke et al., 1999; Wilson et al., 2001). In contrast, overexpression of activated Notch-1 leads to DP T-cell development in the bone marrow (Pui et al., 1999). Together, these results strongly support the notion that Notch-1 signalling is critical for the earliest

stages of T-cell commitment. The Notch-1 ligand Delta-like-1 has recently been shown to mediate this process (Schmitt and Zuniga-Pflucker, 2002). The expression of this ligand by thymic epithelial cells suggests T-cell commitment is initiated within the thymic microenvironment (Harman et al., 2003). This interaction appears to be required for TcR β chain gene rearrangement, pTα upregulation and progression beyond the DN3 stage (Deftos et al., 2000; Reizis and Leder, 2002; Wolfer et al., 2002).

Following successful gene rearrangement, the TcRβ chain is expressed in association with the surrogate pTα protein to form the pre-TcR complex (Groettrup et al., 1993; Saint-Ruf et al., 1994). In a process termed β-selection, signalling through this complex via CD3 and lck transducers drives TcRα chain gene rearrangement, DN3 thymocyte proliferation and differentiation (Mallick et al., 1993; Dudley et al., 1994). This phase of pre-TcR mediated proliferation has been postulated to expand the potentially useful thymocyte repertoire prior to TcRα chain rearrangement and selection. The importance of the pre-TcR complex in early T-cell development is highlighted by studies of mice deficient in the pTα gene (Fehling et al., 1995). These mice exhibit a partial block in αβT-cell development at the DN3 stage, however some cells are rescued by accelerated TcRα chain gene rearrangement and expression (Buer et al., 1997). This rearrangement normally proceeds as the cells mature into the rapidly cycling $CD44^{-}CD25^{-}$ DN4 thymocytes, a transition that also requires input from the thymic epithelium (Godfrey and Zlotnik, 1993). DN4 thymocytes rapidly differentiate into the $CD4^{+}CD8^{+}$ DP subset of thymocytes, via an intermediate phenotype of $CD4^{+}CD8^{-}$ or $CD4^{-}CD8^{+}$, termed immature single positive (Hugo et al., 1990; Tatsumi et al., 1990). These cell subsets undergo several rounds of proliferation (Penit et al., 1988) until reaching the DP stage, where the newly expressed TcRα chain protein replaces pTα prior to further thymic selection.

While many of the factors governing early T-cell development have been elucidated, the precise nature of the stromal cell signals mediating each differentiation step remain

poorly understood. Promising avenues of research include the discovery of the Notch receptors and ligands influencing T-cell commitment, and the determination of the spatial relationship between the DN subsets and the thymic microenvironment. Future studies will hopefully characterise the molecular cues provided by stromal cells in these areas that drive thymocyte TcR expression prior to selection of useful clones.

1.2.3 Thymic Selection

The random nature of TcR gene rearrangement gives rise to a DP population of small, undividing thymocytes with an extremely diverse range of specificities for antigen. These cells undergo the processes of thymic selection to ensure only those thymocytes bearing TcRs of potential use to the organism mature into T-cells (Jameson and Bevan, 1998; Sebzda et al., 1999). The majority of DP thymocytes cannot recognise antigen presented by self-MHC molecules and in the absence of a survival signal from the thymic stroma, undergo programmed cell death within 3-4 days (Huesmann et al., 1991). Some DP thymocytes can escape this fate by continuing to rearrange their TcRα chain genes if the initial rearrangement is not productive, thereby increasing the yield of useful thymocytes (Petrie et al., 1993).

Those thymocytes bearing TcRs capable of recognising self-peptides presented by MHC molecules on thymic stromal cells are eligible for the processes of positive and negative selection. Positive selection refers to the provision of survival signals to thymocytes interacting with self-peptide:MHC complexes. Negative selection is the induction of apoptosis or inactivation of potentially autoreactive thymocytes, also via TcR interaction with self-peptide:MHC complexes. How these two very different outcomes are mediated by the interaction between TcR and self-peptide:MHC has been the topic of much research.

Two models have been proposed to distinguish the requirements for positive and negative selection. Both models (the qualitative and quantitative) focus on the role different forms of self-peptides in determining selection outcomes. While there is much experimental data supporting and contradicting each of these models, this review will focus only on the major features of this area (for a detailed review, see Sebzda et al., (1999)). The qualitative model proposes that different peptides promote positive or negative selection (Jameson et al., 1995). This model was primarily based on findings that antagonist peptide variants promoted positive selection, while agonist peptides resulted in deletion (Hogquist et al., 1994; Jameson et al., 1994) using distinct signalling pathways (for example, Sloan-Lancaster et al., (1994); Madrenas et al., (1995)). The avidity or quantitative model proposes that low avidity interactions induce positive selection, while high avidity interactions cause negative selection via the same signalling pathway (Ashton-Rickardt and Tonegawa, 1994; Williams et al., 1997). Support for this model came from experiments showing that the same peptide can induce positive and negative selection at low and high concentrations, respectively (for example Ashton-Rickardt et al., (1994); Sebzda et al., (1994)). In fixed concentration systems, it was found that positively selecting peptides (antagonists) had a lower TcR affinity than negatively selecting ones (agonists) (Alam et al., 1996). Collectively, the majority of the available data supports the avidity model of selection.

However, much of the current evidence for both of these models is based upon experiments using TcR transgenic mice that often exhibit higher and earlier expression of the TcR on thymocytes than normal animals. How the each transgenic system relates to the physiological signals delivered to developing thymocytes is not known. Furthermore, an assumption made by both models is that while costimulation by non-TcR molecules plays a role in distinguishing selection outcomes, the level of this stimulation remains constant between individual thymocytes, thereby emphasising the role of TcR self MHC:peptide interactions in positive and negative selection. This assumption may not be valid in light of

data suggesting different thymic stromal cell populations are responsible for positive and negative selection (most recently Capone et al., (2001)).

Several studies using transgenic mice expressing MHC molecules only in certain thymic microenvironments have suggested the cortical epithelium is unique in its ability to mediate positive selection (Benoist and Mathis, 1989; Bill and Palmer, 1989; Cosgrove et al., 1992; Laufer et al., 1996). Few of these studies rigorously analysed the expression of transgenes by thymic epithelial subsets during ontogeny and adulthood, which must be addressed to support these conclusions. There also remains the possibility that the lack of positive selection observed wnen MHC molecules are expressed only in the medulla may be due to a lack of accessibility by DP thymocytes, rather than an inability of medullary epithelium to mediate this process. These issues have been addressed tc some extent by the observation that isolated cortical epithelial cells can support positive selection in vitro, while stroma from other tissues cannot (Anderson et al., 1994) (Chidgey, unpublished). The conclusions from this and other work are that cortical epithelial cells express a unique co-receptor, or combination of co-receptors that mediate positive selection in conjunction with TcR recognition of MHC:peptide (Chidgey and Boyd, 2001; Hare et al., 2001).

Upon receiving the initial positive selection signal, DP thymocytes upregulate the TcR and transiently express the activation marker CD69. These cells require continual thymic epithelial cell contact to complete the differentiation process initiated by positive selection (Dyall and Nikolic-Zugic, 1995; Wilkinson et al., 1995) and migrate towards the medulla as they develop into mature $CD4^+CD8^-$ or $CD4^-CD8^+$ SP thymocytes.

Negative selection predominantly occurs in the medulla and its junction with the cortex (Surh and Sprent, 1994). Consistent with this, only the DP and the semimature HSA^{hi} $Qa\text{-}2^{lo}$ SP thymocyte subsets are susceptible to negative selection, the more mature HSA^{lo} $Qa\text{-}2^{hi}$ SP thymocytes are resistant (Kishimoto and Sprent, 1997). It is generally accepted that negative selection of thymocytes requires the ligation of costimulatory molecules, such

as CD28 (Kishimoto and Sprent, 2000). The lack of major negative selection defects observed in CD28 knockout mice (and other costimulatory molecule knockouts) has led to the suggestion that several different costimulation signals can be involved in negative selection (Kishimoto and Sprent, 1999). The potential of at least three different costimulatory molecules (CD5, CD28 and CD43) to cause deletion of immature SPs in conjunction with TcR ligation supports this hypothesis (Kishimoto and Sprent, 1999). These and other experiments demonstrate that distinct thymic microenvironments and costimulation mediate positive and negative selection.

Negative selection is mediated by thymic dendritic cells and, to some extent, medullary epithelial cells (Hoffmann et al., 1995; Sprent and Webb, 1995). Dendritic cells have been shown to be the most efficient mediators of negative selection, presumably due to high levels of MHC and costimulatory molecule expression (van Meerwijk et al., 1997; Anderson et al., 1998). Together, these cell types are estimated to induce the apoptosis of between 50% to 70% of the positively selected thymocyte repertoire (Ignatowicz et al., 1996; van Meerwijk et al., 1997; Zerrahn et al., 1997). In this way, negative selection induces central tolerance to self-antigens by purging autoreactive thymocytes from the repertoire prior to export. Central tolerance does not appear to be complete, as autoreactive T-cells have been detected in the periphery of mice and humans, however these are controlled by peripheral tolerance mechanisms (Sakaguchi et al., 2001).

The specialised roles different thymic stromal subsets in thymic positive and negative selection emphasise the necessity to consider selection outcomes in the context of the interacting cells and microenvironments (Fig. 1.2) (Klein and Kyewski, 2000). The various co-receptors and antigen processing pathways utilised by these cell types will impinge upon the signals delivered to developing thymocytes. This highlights the need for more detailed functional and phenotypic investigations of the various thymic stromal cell types to improve our understanding of how these cells mediate thymocyte selection.

Figure 1.2 Schematic diagram of thymocyte development in various thymic microenvironments.

Following precursor entry into the corticomedullary junction, DN thymocytes undergo early differentiation events mediated by interactions with cTECs and fibroblasts. As they traffic through the cortex towards the subcapsule, rearrangement of the TcRβ allows early selection and TcRα chain rearrangement. Following expression of the αβTcR, DP thymocytes must interact with cTECs to receive survival signals or undergo programmed cell death. Positively selected thymocytes upregulate αβTcR and CD69 as they migrate towards the medulla, during which time they are susceptible to negative selection induced by dendritic cells and mTECs. Following the final maturation events in the medulla, mature T-cells exit the thymus.

Adapted from Gill, (2002).

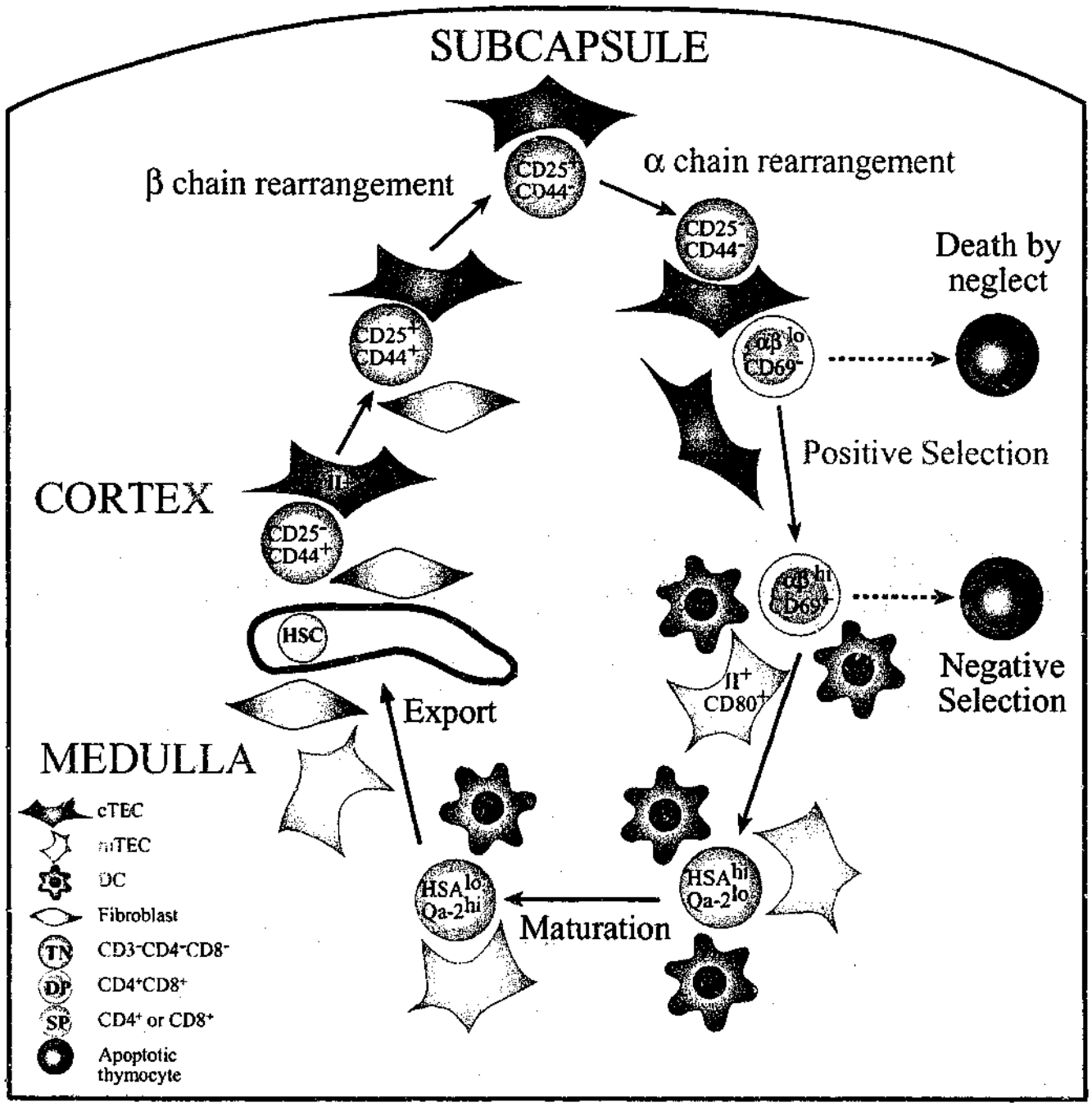
SUBCAPSULE
β chain rearrangement
α chain rearrangement
CD25+ CD44+
CD25- CD44-
CD25+ CD44+
αβlo CD69-
Death by neglect
Positive Selection
CORTEX
CD25- CD44+
HSC
αβhi CD69+
Negative Selection
Export
MEDULLA
II+ CD80+
HSAlo Qa-2hi
HSAhi Qa-2lo
Maturation
cTEC
mTEC
DC
Fibroblast
TN CD3-CD4-CD8-
DP CD4+CD8+
SP CD4+ or CD8+
Apoptotic thymocyte

1.2.4 The role of medullary epithelium in central tolerance

The high efficiency of central tolerance raises the question of how the thymus mediates the negative selection of thymocytes bearing TcRs specific for peripheral self-antigens. An emerging role for medullary thymic epithelial cells (mTECs) in the induction of central tolerance is yielding some answers to this question. Early reports indicating peripheral antigen expression in rare mTECs, were supported in several transgenic models where tissue-specific promoters were found to be active in these cells (Kyewski et al., 2002). A more comprehensive analysis of antigen expression by mTECs verified and extended these findings, establishing the "promiscuous" expression of tissue-specific antigens by mTECs (Derbinski et al., 2001). A role for this phenomenon in tolerance was described by experiments on mice deficient for *AIRE*, the gene defective in human autoimmune polyendocrinopathy syndrome type I. It was found that gene targeting of *AIRE* ablated peripheral gene expression by mTECs, resulting in the manifestation of a spectrum of organ-specific autoimmune diseases (Anderson et al., 2002).

A number of mechanisms have been proposed to mediate tolerance induction by these mTECs. The outcomes of thymocyte interaction with mTECs can vary from deletion (Klein et al., 1998; Klein et al., 2001) to functional inactivation of thymocytes (anergy) (Hoffmann et al., 1992; Schonrich et al., 1992). It has also been postulated that these rare peripheral antigen expressing cells may induce the development of immunoregulatory cells capable of controlling potentially autoreactive cells in the periphery (Kyewski et al., 2002). A recent study by Liston et al., (2003) demonstrated that negative selection of TcR transgenic thymocytes by ectopic antigen expressed by mTECs fails in the absence of AIRE expression. This strongly suggests expression of these tissue-specific elements by $AIRE^{+}$ mTECs induce central tolerance by deletion. Whether this is mediated directly by mTECs or by cross-presentation by thymic dendritic cells remains to be shown (Klein and Kyewski,

2000). Together, these studies highlight a unique role for medullary epithelium in central tolerance to peripheral antigens.

1.2.5 Thymocyte Maturation

Thymocytes surviving selection mature in the medulla for an average of 14 days before thymic export (Scollay and Godfrey, 1995). While much of this medullary maturation process is unknown, it is associated with phenotypic and functional changes in SP thymocytes. Recently selected thymocytes are $HSA^{hi}CD69^{+}CD24^{+}CD62L^{-}Qa\text{-}2^{lo}$ while recent thymic emigrants (RTEs) are $HSA^{lo}CD69^{-}CD24^{-}CD62L^{+}Qa\text{-}2^{hi}$ (Lucas et al., 1994; Gabor et al., 1997a). There is evidence that the early SP thymocytes are not functionally mature and only the more mature cells are capable of surviving in the periphery (Dyall and Nikolic-Zugic, 1995). These data suggest that functional maturity governs T cell export, rather than a passive process based on thymocyte age. In support of this, studies demonstrating the requirement of G-protein signalling for this process (Chaffin and Perlmutter, 1991), as well as a burst of mature thymocyte division just prior to export (Penit and Vasseur, 1997; Le Campion et al., 2002), indicate that thymic export is the consequence of an intrathymic signalling event. The nature of this signal required remains to be defined, however it is likely to involve input from medullary and perivascular stromal cells in this microenvironment.

1.2.6 Chemokines in intrathymic migration

During their development within the thymus, thymocytes migrate extensively within and between thymic microenvironments, remaining in constant contact with stromal cells (Fig. 1.2). The mechanisms controlling this trafficking remain poorly characterised, but evidence is emerging that chemokines and their receptors play important roles in this process (Norment and Bevan, 2000). Chemokines are small, soluble polypeptides that stimulate the migration of cells via G-protein coupled seven-transmembrane receptors (Murphy, 1994;

Rossi and Zlotnik, 2000). Individual chemokine receptors tend to be promiscuous in their specificity for particular chemokines. By analogy with other cell migration systems, the various phases of thymocyte migration are likely to be influenced by distinct (but probably overlapping) gradients of chemokines. In support of this hypothesis, recent studies have correlated differential chemokine receptor expression on thymocyte subsets and their chemokine ligands by thymic stromal elements (Norment and Bevan, 2000).

Based on their thymic expression profiles, several chemokine/receptor pairs have been investigated in the context of early, intermediate and late stages of thymocyte development. The expression of CXCR4 by DN thymocytes mediates their chemoattraction to the chemokine CXCL12 (SDF) (Kim et al., 1998) expressed by stromal cells in the outer cortex (Aiuti et al., 1999; Suzuki et al., 1999). While CXCR4 deficient thymocytes show no gross defects in development (Zou et al., 1998), several studies indicate a role for this interaction in early T-cell differentiation (Kawabata et al., 1999; Onai et al., 2000; Hernandez-Lopez et al., 2002). CXCR4 is downregulated in DP and SP thymocytes, suggesting as these cells mature they lose responsiveness to these signals (Norment and Bevan, 2000).

The trafficking of DP thymocytes into and through the cortex is likely to be influenced by CCL25/CCR9 interactions. CCR9 is upregulated on thymocytes after receiving signalling through the pre-T-cell receptor (Norment et al., 2000) while its ligand, CCL25 (TECK) is highly expressed by cortical epithelial cells (cTECs) (Wurbel et al., 2000). However, the ablation of this interaction does not significantly impinge on intrathymic thymocyte development, suggesting its loss can be compensated by other signals (Wurbel et al., 2001). Thymocytes that have recently undergone positive selection ($CD69^+$) upregulate CCR4 (Campbell et al., 1999) which mediates their chemotaxis towards CCL22 (MDC) producing medullary epithelium (Chantry et al., 1999). While no *in vivo* functional data has defined a role of this interaction in the thymus, there is some evidence that it may

facilitate negative selection by mTECs (Annunziato et al., 2000). As thymocytes mature beyond this stage, the upregulation of CCR4, CCR7, CCR8 and CCR9 implicate these receptors and their ligands in the migration of these cells to and through the medullary microenvironment (Campbell et al., 1999). Moreover, it has been found that both CCR4 and CCR9 mediate differential chemotaxis of $CD4^+SP$ and $C[illegible]SP$ thymocytes respectively (Norment and Bevan, 2000).

A role for chemokines in thymic emigration remains to be shown, however the sensitivity of this process to pertussis-toxin inhibition of G-protein signalling may point to a role for chemokine receptors (Chaffin and Perlmutter, 1991). The upregulation of CCR7 on SP thymocytes and the abundance of its ligands, CCL19 (ELC) and CCL21 (SLC) around medullary blood vessels make these molecules promising candidates for a role in thymic export (Annunziato et al., 2000). Certainly, SLC and CCR7 have an essential role in the homing of T cells to peripheral lymphoid organs, however no defect in T-cell export has yet been found in CCR7 or SLC deficient animals (Nakano et al., 1998; Forster et al., 1999; Gunn et al., 1999; Vassileva et al., 1999). While the differential expression of chemokines and their receptors by thymocytes and stromal cells points to roles in thymic migration and emigration (Fig 1.3), the *in vivo* functional data from various single chemokine knockout systems does not clearly support this. This is likely to be due to the redundancy of the chemokine signalling system, necessitating investigations of double and triple chemokine knockouts as well as the implementation of novel functional assays. Interactions between chemokines and the extracellular matrix emphasise the need to analyse thymic migration within the context of the microenvironments in which they occur (Savino et al., 2002a).

Figure 1.3 Schematic diagram of the differential expression of chemokines and their receptors, guiding developing thymocytes through thymic microenvironments.

CXCL12 and CXCR4 interactions are involved in DN thymocyte chemotaxis towards the subcapsule. Late DN and early DP thymocytes migrate towards CCL25 produced by cTECs. Following selection events, CCR4, CCR7 and CCR9 mediate migration into the medulla towards CCL19, CCL21, CCL22 and CCL25 produced in this microenvironment. The factors influencing thymocyte emigration remain to be defined, however CCR7 interactions with CCL19 and CCL21 have been proposed to play a role.

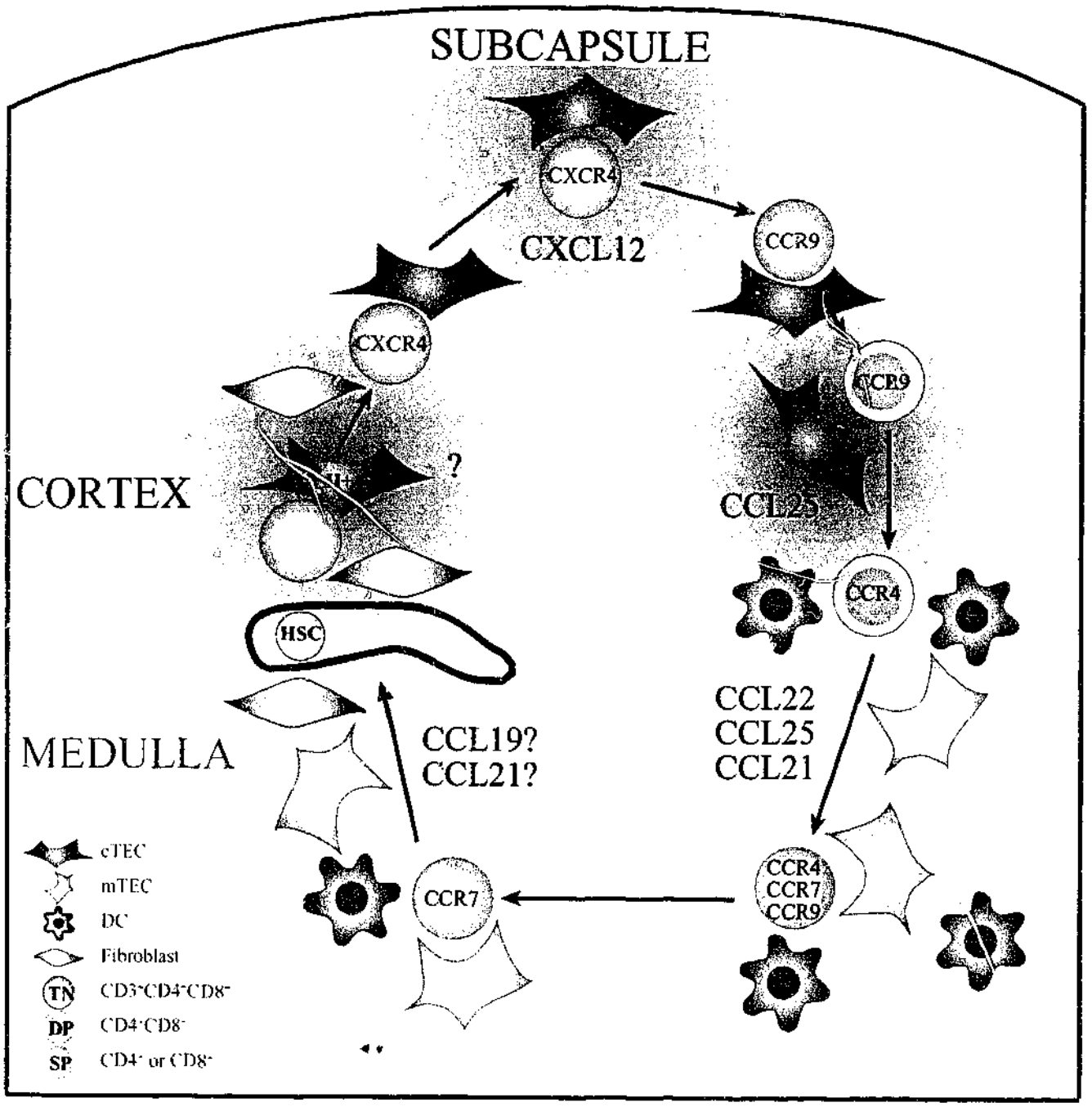
SUBCAPSULE
CXCR4
CXCL12
CCR9
CXCR4
CCR9
CORTEX
?
CCL25
CCR4
HSC
CCL22
CCL25
CCL21
MEDULLA
CCL19?
CCL21?
CCR4
CCR7
CCR9
CCR7
cTEC
mTEC
DC
Fibroblast
TN CD3-CD4-CD8-
DP CD4+CD8+
SP CD4+ or CD8+

Central to all of these studies is the role of the various stromal cell subsets in expressing and presenting the various chemokines responsible for directing thymocyte migration. Such studies will require the development of methods for purifying and analysing the surface phenotype of these cells.

1.3 THYMIC DEVELOPMENT

Despite the importance of thymic stromal cells in T-cell differentiation and immunological tolerance, surprisingly little is known about their cellular and molecular biology. Studies into their development throughout thymic ontogeny continue to be critical for understanding this enigmatic population. Thymic organogenesis is a complex series of developmental processes comprising input from all three embryonic germ layers under the control of discrete molecular cues. Of particular importance to the early stages of this process are the contributions made by mesenchymal elements. Upon HSC seeding of the primordial thymic microenvironment, differentiation and patterning of the organ occurs, highlighting the necessity for lymphostromal cross-talk. As regional changes form within the organ, the differentiation of cortical and medullary epithelium becomes evident. The cellular and molecular mechanisms responsible for the early and late stages of thymic epithelial cell development are only beginning to be elucidated.

1.3.1 Thymic organogenesis

The primordial murine thymus forms from an outpocketing of the third pharyngeal pouch endoderm, with contributions from neural crest mesenchyme of the third and fourth pharyngeal arches. While the possible involvement of ectoderm in this process is controversial, the pharyngeal endoderm and surface ectoderm are closely apposed during

thymus formation at E9.5-10.5. Early studies disagreed as to whether the ectoderm physically contributed to thymic epithelium (Smith, 1965; Cordier and Haumond, 1980). A seminal study by (Le Douarin and Jotereau, 1975) demonstrating that ectopically implanted pharyngeal pouch endoderm was sufficient to form the thymus suggests ectoderm does not contribute epithelium. Experiments identifying a common epithelial progenitor are consistent with this (Rodewald et al., 2001; Bennett et al., 2002; Gill et al., 2002), although ectoderm labelling experiments will be required definitively address the contribution of this germ layer to the thymus. The physical contribution of neural crest derived mesodermal cells to the thymic capsule and perivascular connective tissue has been established by cell lineage analyses (Le Lievre and Le Douarin, 1975; Jiang et al., 2000). Ablation of this contribution results in severe defects in thymus formation (Bockman and Kirby, 1984). The bilateral thymic rudiments formed by these interactions bud off the pharynx and move medially, ventrally and caudally to fuse at the midline above the heart by E12.5 (Fig 1.4).

Much of the recent literature concerning thymic organogenesis has defined aspects of the molecular control of these processes by transcription factors (Manley, 2000; Manley and Blackburn, 2003). Gene targeting of *Hoxa3,* a member of the *Hox* family of positional specification factors, resulted in athymia, demonstrating the requirement for this gene product in formation of the thymus (Manley and Capecchi, 1995). *Hoxa3* functions upstream of the homeobox-containing transcription factors *Pax1* and *Pax9*, both of which are required for early thymic organogenesis (Wallin et al., 1996; Peters et al., 1998; Hetzer-Egger et al., 2002). Candidate signalling molecules involved in regulation expression of these transcription factors that are expressed in the pharyngeal endoderm and have roles in the formation of other organs include fibroblast growth factors (FGFs), bone morphogenic proteins (BMPs) and sonic hedgehog (Manley, 2000). The genetic mutation causing the nude phenotype in mice and humans affects the transcription factor FoxN1 (whn), showing it

is essential for the developmental progression of the thymic rudiment (Nehls et al., 1994; Frank et al., 1999). FoxN1 deficient thymic epithelial cells were unable to attract lymphoid progenitors, nor expand or differentiate when they were introduced, suggesting a direct role in epithelial growth and differentiation (Blackburn et al., 1996; Nehls et al., 1996). A recent study has demonstrated that transcriptional control of *FoxN1* is mediated by Wnt signalling molecules produced initially by the thymic epithelium (E9.5-10.5), and later thymocytes (Balciunaite et al., 2002). Furthermore, this study suggested that Wnt signalling and *FoxN1* expression was necessary for the maintenance of TEC function beyond organogenesis.

Pax3 encodes a transcription factor expressed by neural crest cells that has been shown to influence thymic organogenesis. Pax3 deficient mice exhibit thymic hypoplasia due to defects in neural crest cell migration, highlighting the importance of the mesenchymal contribution to thymic development (Conway et al., 1997).

1.3.2 The role of thymic mesenchyme

It has been proposed that neural crest mesenchyme mediates thymic organogenesis in two ways (Anderson and Jenkinson, 2001). The first is by providing cues mediating the early development of the thymic rudiment (see *1.3.1 Thymic organogenesis).* This role does not appear to be exclusive to neural crest derived cells, as pharyngeal endoderm could induce non-pharyngeal mesenchyme to participate in thymic organogenesis (Le Douarin and Jotereau, 1975). This has since been supported by *in vitro* reconstitution studies showing that mesenchyme from other organs could support thymic epithelial cell development (Shinohara and Honjo, 1997). Therefore, it seems that during the earliest stages of thymic organogenesis, the pharyngeal endoderm provides inductive signals to recruit the neural crest mesenchyme (via BMP-signalling, (Ohnemus et al., 2002)), which in turn supports the initial growth and development of the epithelial rudiment. However, the molecular signals the mesenchyme provides the early epithelium

Figure 1.4 Schematic diagram of thymic organogenesis.

The thymic rudiment is formed from an outpocketing of the 3rd pharyngeal pouch. Under the influence of neural crest mesenchymal cells, the rudiment grows and buds off from the pharynx. By E12.5, the first haematopoietic precursors seed the thymic lobes through the mesenchymal capsule, leading to further differentiation of the early thymic epithelial cells. Taken from Manley, (2000).

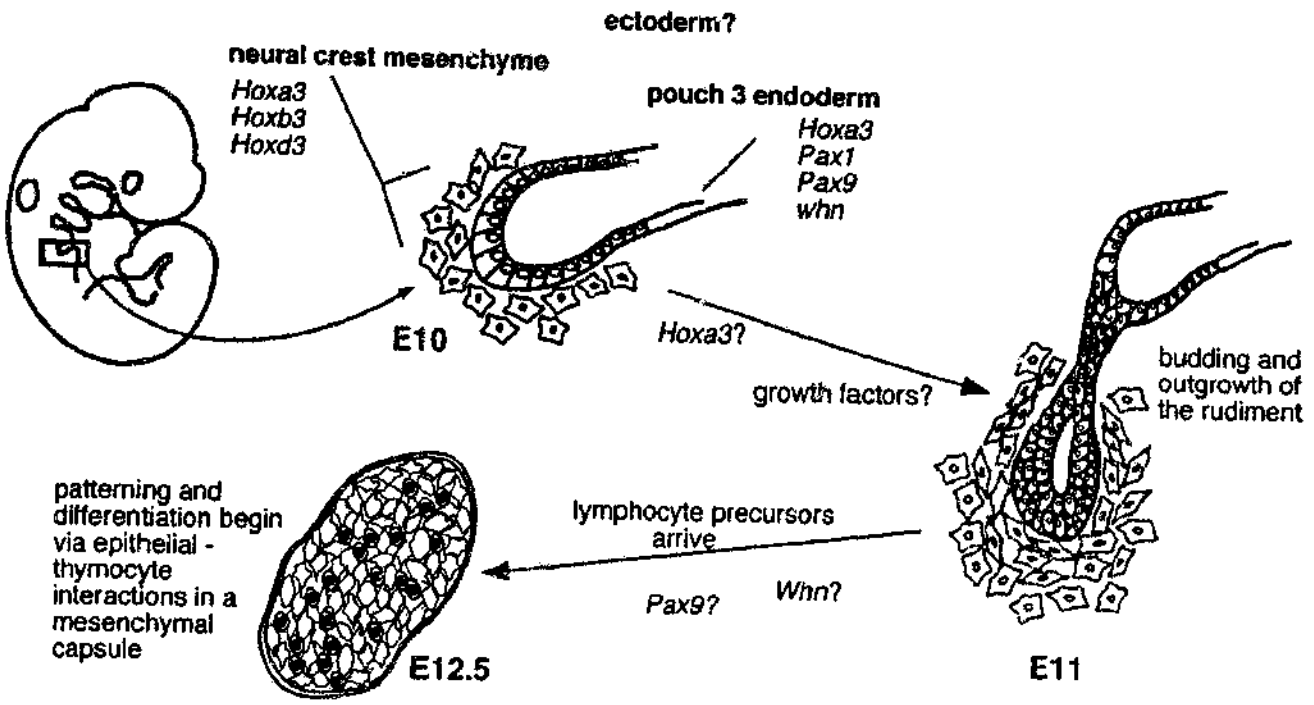
ectoderm?
neural crest mesenchyme
Hoxa3
Hoxb3
Hoxd3
pouch 3 endoderm
Hoxa3
Pax1
Pax9
whn
E10
Hoxa3?
growth factors?
budding and outgrowth of the rudiment
patterning and differentiation begin via epithelial - thymocyte interactions in a mesenchymal capsule
lymphocyte precursors arrive
Pax9?
Whn?
E12.5
E11

are yet to be fully characterised. By analogy with other organ developmental systems, the fibroblast growth factor (FGF) family of molecules has been suggested to play a role in early differentiation and proliferation of TECs. Indeed, a study by Revest et al., (2001) demonstrated that deficiency in the FGF receptor IIIb blocked thymic development beyond E12.5, and that the mesenchyme produces the main ligands that interact with this receptor (FGF7 and FGF10).

The second role for mesenchyme in thymic development is in the support of early thymocyte development. Experiments involving reaggregation of defined fetal thymic stromal elements with thymocyte precursors demonstrated the requirement for fibroblasts in the differentiation of DN2 into DN3 thymocytes (Anderson et al., 1993; Anderson et al., 1997). Suniara et al., (2000) extended these findings by showing that mesenchymal cells migrated into the thymus after lymphoid stem cell colonisation (E14), integrating with the network of epithelial cells and producing extracellular matrix constituents. In addition, this study demonstrated that these mesenchymal elements were essential for directly mediating the development of the earliest thymocyte precursors beyond the DN stage, and thereby indirectly facilitating further differentiation of the thymic epithelium.

1.3.3 Thymic epithelial cell development

While a general understanding of the major cellular influences upon TEC differentiation is emerging, the lineage relationships between the various subsets remains to be defined. Early studies into the development of the thymic epithelium suggested the cortical and medullary subsets arose from the ectoderm and endoderm, respectively (Cordier and Heremans, 1975; Cordier and Haumond, 1980). However, other research disputed this finding, suggesting the ectoderm did not physically contribute to the thymus (Smith, 1965; Le Douarin and Jotereau, 1975). More recently, evidence has emerged for a common embryological origin for TECs

(reviewed in Blackburn et al., (2002). The identification of small population of embryonic TECs recognised by cortical and medullary epithelial cell markers was taken to indicate a common stem cell gave rise to both subsets (Ropke et al., 1995). Analysis the expression of keratin subunits by TECs supported this hypothesis, detecting keratin-8 (K8; normally restricted to cTECs) and keratin-5 (K5; normally restricted to mTECs) double positive TECs at the cortico-medullary junction of the normal thymus (Klug et al., 1998). This study used mutant mice with various blocks in early thymocyte development to establish a precursor-product relationship between the $K8^+K5^+$ TEC population and $K8^+K5^-$ cortical epithelium, however it has not been established whether these double positive TECs can give rise to mTECs also. Elegant experiments using chimeric mice formed by injecting embryonic stem cells into blastocysts of different MHC haplotypes demonstrated that the medullary epithelial islets arise from single progenitors (Rodewald et al., 2001). Studies of the nude and embryonic thymus revealed another marker of early TECs in the cell surface reactive monoclonal antibody MTS-24 (Godfrey et al., 1990; Blackburn et al., 1996). Subsequently it was shown that purification, reaggregation and engraftment of embryonic $MTS\text{-}24^+$ TECs could reconstitute a complete thymic microenvironment, providing evidence for a single population capable of giving rise to all major TEC subsets (Bennett et al., 2002; Gill et al., 2002). However heterogeneity within the $MTS\text{-}24^+$ TEC population highlights the need for the development of clonal differentiation assays to identify a putative TE stem cell.

The early differentiation of TECs has been proposed to occur in two phases; a thymocyte independent and a thymocyte dependent phase (Klug et al., 2002). In an extension of their previous study, Klug et al., (2002) examined the keratin subunit expression of TECs throughout embryogenesis and in two mutant mouse models with severe early blocks in T-cell development. The finding that early embryonic epithelial microenvironment (E12.5-E15.5) exhibited pockets of medullary epithelial cells similar to

the postnatal mutant thymi, prompted the suggestion that thymocyte signals were not required for this process (Klug et al., 2002). It should be noted that the thymus of these and other knockout models do contain thymocytes, although these do not develop beyond the early DN stages. Therefore, it is possible that their input is required for the initial spatial separation of thymic elements producing various differentiation signals, leading to patterning of the organ. Additionally, the vascularisation and infiltration of mesenchymal cells that occurs during this phase may contribute inductive signals during this period.

The role of thymocyte development in TEC differentiation beyond this stage (the thymocyte dependent phase) has been well established ((Shores et al., 1991; Hollander et al., 1995b; van Ewijk et al., 2000a) reviewed in (van Ewijk et al., 2000b)). Without signals from thymocytes at the late DN and SP stages of development, cortical and medullary TECs do not fully develop. Furthermore, Hollander et al., (1995b) demonstrated the timing of these signals to be important. While the thymic microenvironments of CD3ε26 transgenic mice could be restored by normal bone marrow reconstitution of fetal mice, reconstitution of adults resulted in abnormal T-cell development and severe colitis (Hollander et al., 1995a). These findings have since been supported, defining a TEC developmental "window", whereby normal differentiation can be induced upon interaction with developing thymocytes only before the first week following birth (Wang et al., 1997; Klug et al., 1998). The provision of RAG^{null} bone marrow (thymocyte arrest at DN3) during this period is sufficient to induce the early differentiation of cTECs, such that full thymic restoration can be induced upon subsequent normal bone marrow reconstitution of adults (van Ewijk et al., 2000a). This next stage of restoration seems to involve proliferation of cTECs followed by their differentiation into mTECs, rather than expansion of pre-existing mTECs (Penit, 1996). Collectively, these studies describe early control points in the stepwise differentiation of TECs.

The cellular interactions mediating further TEC development are less clearly defined. Many models indicate that SP thymocytes induce mTEC differentiation and/or expansion; for instance, in TcRα chain deficient mice where nearly all thymocytes are blocked at the DP stage of development, the thymic medulla remains small and disorganised (Palmer et al., 1993) (*1.1.1 The thymic microenvironment*). Mature, peripheral T-cells and γδ thymocytes can also expand this microenvironment to some extent, with TcR:MHC interactions important in influencing its organisation (Ferrick et al., 1989; Surh et al., 1992a; Brabb et al., 1997). However, the broad phenotypic and ultrastructural heterogeneity within the mTEC population suggests there are more complex control points determining TEC fate (Farr and Rudensky, 1998; Farr et al., 2002). Differential expression of MHC molecules and CD80 distinguishes at least three mTEC subsets (Surh et al., 1992b; Nelson et al., 1993; Degermann et al., 1994). Whether these differences impact upon possible roles for these cells in negative selection remain to be defined.

Literature concerning the molecular control of late TEC development is sparse. A member of the NF-κB family of transcription factor subunits, RelB, is critical for the differentiation or expansion of mTEC subsets, however the upstream regulation of this gene in TECs is unknown (Burkly et al., 1995; Naspetti et al., 1997). A candidate for involvement in this signalling is keratinocyte growth factor (KGF, FGF-7), that has recently been found to drive expansion of the hypoplastic medullary epithelial compartment in *RAG*^{null} thymi (Erickson et al., 2002). Likewise, human cTEC differentiation can be influenced by viral induced interferon-β secretion (Vidalain et al., 2002), however a physiological role for either of these signalling pathways remains to be demonstrated.

In summary, our understanding of TEC development has recently grown extensively. Evidence for a single origin for the thymic epithelium has emerged, and early developmental control points and a framework lineage relationship proposed (Fig 1.5). However, the

Figure 1.5 A possible thymic epithelial cell lineage model.

The earliest endodermally-derived thymic epithelial cells mature into $K5^+K8^+$ TEC precursor cells, apparently under the influence of mesenchymal cells. Following recruitment of hematopoietic precursors, thymocytes development induces the differentiation of cortical ($K8^+$) and medullary TECs ($K5^+$).

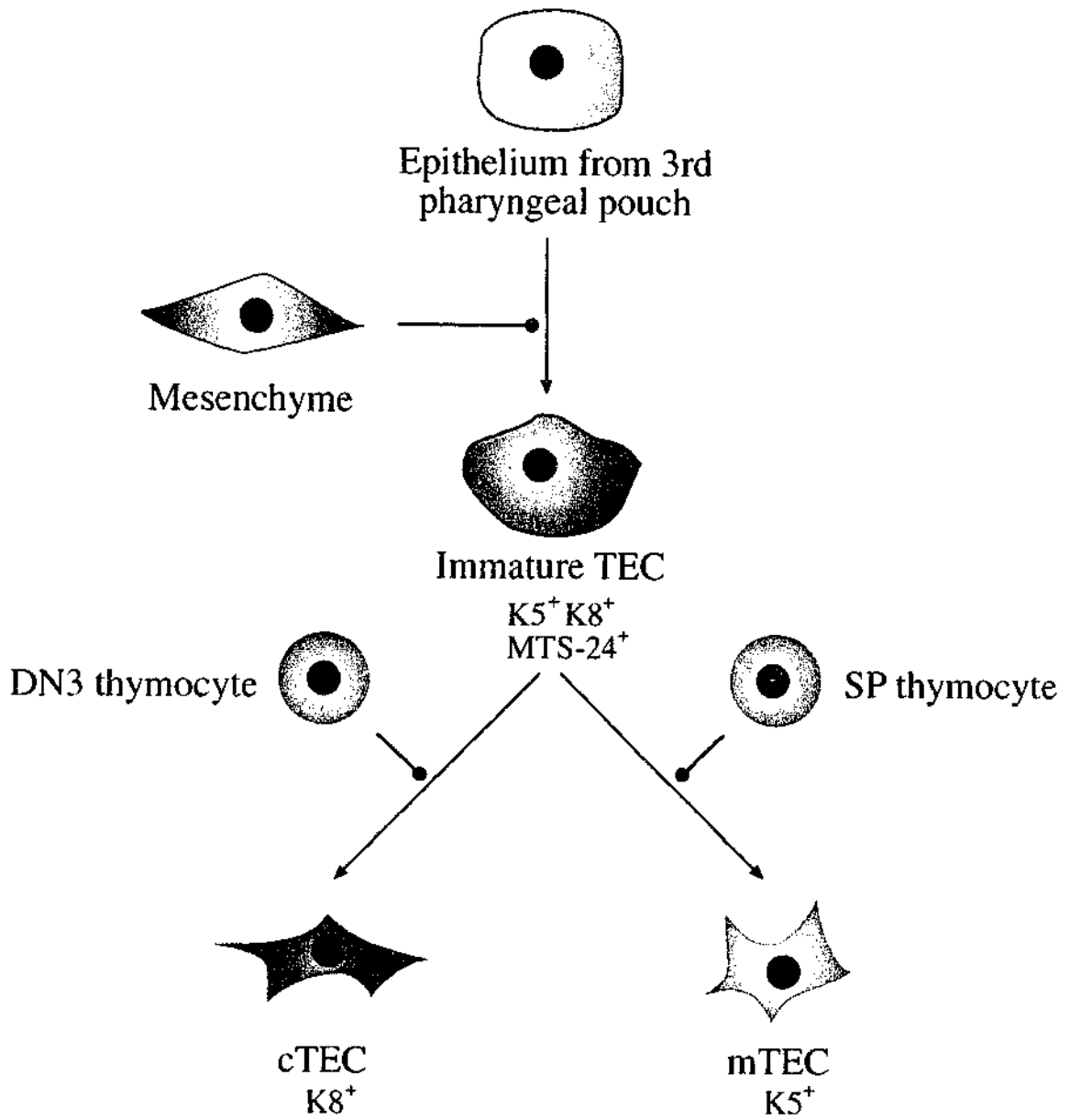
Epithelium from 3rd pharyngeal pouch
Mesenchyme
Immature TEC
K5+K8+
MTS-24+
DN3 thymocyte
SP thymocyte
cTEC
K8+
mTEC
K5+

absence of appropriate surface markers for the purification of these subsets currently hampers further understanding of TEC differentiation. Also, little is known about the molecular control of TEC biology. Developing a greater understanding of these processes will be essential for the design of strategies aimed at enhancing thymic-dependent immunity.

1.4 THYMIC DYSFUNCTION

The crucial role of the thymus in establishing and maintaining immunity while inducing self-tolerance is highlighted in instances of thymic dysfunction. Disruption of the thymus is a hallmark of many models of spontaneous organ-specific autoimmune disease. The decline in immune function and increased incidence of autoimmune disease upon thymic involution in the aged reinforces this link. A growing body of literature examines the possibility of regenerating the disrupted thymus to treat autoimmunity and T-cell depletion following bone marrow transplants. Given the importance of thymic stromal cells to thymocyte development, this compartment will be central to any strategy of thymus manipulation.

1.4.1 The thymus in autoimmunity

Early studies into the role of the thymus in immunity discovered that thymectomy of 3 day old mice resulted in various organ-specific autoimmune diseases (Nishizuka and Sakakura, 1969; Kojima et al., 1976; Kojima et al., 1980). Despite extensive research into these models, the reasons for these findings are not completely understood. Recently, several groups have found a link between autoimmune disease and the production of putative immunoregulatory $CD25^+CD4^+$ T-cells by the thymus after day 3 (Shevach, 2000). While thymectomised mice are deficient in these cells, transfer of $CD25^+CD4^+$ T-cells from intact mice can prevent autoimmune disease (Asano et al., 1996; Itoh et al., 1999). The

mechanism by which this effect is mediated, the antigen specificity of these cells and their targets remain unknown.

Other studies have found a link between thymic abnormalities and autoimmune disease. The potential for thymic defects to predispose autoimmunity has been demonstrated most recently by the finding that loss of peripheral antigen expression by mTECs compromises central tolerance (Anderson et al., 2002). Furthermore, the thymic microenvironment in many murine models of autoimmune disease is characterised by the presence of medullary epithelial cells in the cortex, large epithelial cell free regions, a reduction in the size of the medulla and dysregulated expression of stromal markers (Takeoka et al., 1995b; Takeoka et al., 1997; Taguchi et al., 1999). Extensive characterisation of intercrosses of one of these models, New Zealand black (NZB) mice, associated the thymic defect with disease and non-MHC genetic elements (Takeoka et al., 1995a). Similar findings were reported in non-obese diabetic (NOD) mice, where the severity of disease was linked to thymic defects that were not present in C57BL/6 H-2^{g7} congenic strains (Atlan-Gepner et al., 1999). NOD thymocytes also exhibit reduced susceptibility to negative selection, suggesting the thymic defect in this case may induce inappropriate T-cell development (Kishimoto and Sprent, 2001). However, this study did not find a similar impairment of negative selection of several other murine models of autoimmune disease, including NZB mice. While the disruption of the thymic microenvironment in various models of autoimmune disease is striking, as yet there is no evidence of a direct link between the two states.

1.4.2 Age-related thymic atrophy

A major anomaly of the immune system is the involution of the thymus with age. Despite its importance in maintaining a diverse peripheral T-cell pool, the thymus is dramatically reduced in size and function in the elderly. The time of onset of thymic atrophy in humans

remains controversial, but alterations in size and microenvironment are apparent 1 year after birth, with the most profound changes observed following puberty (Bertho et al., 1997; Mackall and Gress, 1997; Sutherland, 2001). In mice, it is a gradual process initiated following sexual maturity (Hirokawa et al., 1992). Involution is characterised by decreased thymic size, collapse of the cortex, infiltration of adipose tissue associated with large perivascular spaces, an indistinct cortico-medullary junction, decreased MHC II expression and reduction in thymic export (Farr and Sidman, 1984; Takeoka et al., 1996; Haynes et al., 2000b; Ortman et al., 2002). Despite a decrease in thymocyte numbers of up to 100-fold in the atrophied thymus, the major developmental subsets are retained at similar proportions as young, although a partial block between the DN1 to DN2 transition has been reported (Aspinall, 1997; Douek and Koup, 2000). It is not known whether microenvironmental collapse of the involuted thymus is accompanied by a reduction in stromal cell numbers or changes in their phenotype.

While the rate of mature T-cell export from the thymus remains the same (~1% per day), overall reduction in thymic size reduces the numbers of recent thymic emigrants to fewer than 5% of that of the young adult (Berzins et al., 2002). This has implications on the peripheral T-cell pool, as expansion of pre-existing memory cells compensates for reduced naïve input to maintain overall numbers (Haynes et al., 2000a). This leads to a narrowing of T-cell diversity that is associated with a declined T-cell function, resulting in reduced capacity to resist disease and an increased likelihood of autoimmune disease (Mackall and Gress, 1997; Aspinall and Andrew, 2000).

Current data suggest that while thymic atrophy is influenced by many factors, it is predominantly caused by sex steroids. There is some evidence that aged bone marrow contains reduced numbers of T cell progenitors and a reduced capacity to competitively repopulate young thymic lobes (Fridkis-Hareli et al., 1992; Globerson et al., 1992).

However, transfer of young bone marrow into aged recipients did not restore the involuted thymus (Mackall et al., 1998). Likewise, the inability of aged thymic lobes to reconstitute following grafting into young recipients further suggests the provision of normal bone marrow does not induce regeneration on its own (Utsuyama et al., 1995). On the other hand, when young recipients were gonadectomised, aged thymic grafts exhibited regeneration similar to young grafts (Utsuyama et al., 1995). This link between ablation of sex steroid action and reversal of thymic involution is well established in the literature (Olsen and Kovacs, 1996). Animals bearing defective androgen receptors did not exhibit age-related thymic atrophy (Olsen et al., 1991b). Those deprived of androgens demonstrated thymic regeneration which could be inhibited by administration of synthetic sex steroids (Kendall et al., 1990; Olsen et al., 1991a; Windmill et al., 1993; Olsen et al., 2001). Together these findings suggest an intrathymic role for androgens in mediating involution and regeneration.

1.4.3 Thymic regeneration

A logical means of ameliorating the problems associated with age-related thymic atrophy is by affecting thymic regeneration to restore its full functional capacity. This could be particularly useful in achieving accelerated immune reconstitution following the lymphopenia that accompanies radiation and chemotherapy. Slow immune recovery following these procedures has been associated with a reliance of peripheral expansion that skews the immune repertoire, and increased morbidity (Haynes et al., 2000a). Clinical studies of chemotherapy patients of varying ages demonstrated a significant inverse relationship between age and T cell recovery (Mackall et al., 1995; Small et al., 1999; Douek et al., 2000). Increased thymic output was found to correlate with increased naïve T-cell numbers and broader TcR repertoires (Mackall et al., 1995; Douek et al., 2000). In addition, the rate of $CD4^+$ recovery inversely correlates with the risk of developing opportunistic infections (Small et al., 1999). A corollary of these studies is that thymic regeneration

would be beneficial in the re-establishment of immunity.

One means of achieving thymic regeneration involves the ablation of sex steroids, removing their inhibitory effect upon the thymus (Berzins et al., 2002). Comprehensive studies by Sutherland, (2001) examined the immune reconstitution of aged or immunodepleted mice following castration, finding the attending thymic regeneration induced a return to young levels of T-cell development, thymic export, peripheral naïve T-cells and immune responsiveness to viral challenge. Analysis of prostate cancer patients undergoing sex steroid blockade by luteinising hormone-releasing hormone agonist (LHRH-A) treatment revealed a significant increase in naïve T-cells within four months of treatment, indicating chemical castration enhanced thymus function in humans (Sutherland, 2001). However, the means by which sex steroid ablation causes thymic regeneration is not known.

Thymic stromal cells appear to be the primary mediators of this effect. Olsen et al., (2001) used bone marrow transfer between normal and androgen receptor-deficient mice to demonstrate that androgens modulate thymic size by acting on stromal cells. This study extends earlier findings showing that progesterone and estrogen receptors on the thymic stroma are necessary for thymic involution mediated by these sex steroids (Staples et al., 1999; Tibbetts et al., 1999). The direct effects of sex steroid withdrawal on thymic stromal cells are not known, nor is the mechanism by which these cells drive thymocyte proliferation and differentiation to affect thymic regeneration. Furthermore, whether the restoration of thymocyte numbers and development is accompanied by a similar regeneration of the stromal compartment is an important question, yet to be addressed.

Other key factors that have been shown to have a regenerative effect on the thymus include IL-7 and keratinocyte growth factor (KGF) (Bolotin et al., 1996; Min et al., 2002). Importantly, KGF administration has been shown to specifically protect thymic epithelial cells from irradiation and chemotherapy regimes, as well as the damage caused during graft

versus host disease (Min, et al., 2002; Rossi et al., 2002). The emerging central role of these factors and the thymic stroma in thymic regeneration emphasises the need for further research in this area.

1.5 CONCLUSION

It is clear that thymic stromal cells mediate αβ T-cell development. The sequential differentiation of thymocytes occurs within thymic discrete microenvironments, initiated by specialised stromal cells. Thymic "crosstalk" between developing thymocytes and epithelial cells establishes these regions, however the molecular interactions involved in this process remain to be elucidated. The distinct stromal cell subsets controlling various thymocyte developmental steps have been determined, with the role of fibroblasts in early differentiation and the epithelium in selection events particularly notable. Major challenges presented in this area include the definition of the cTEC coreceptors required for positive selection, the mechanism by which ectopic gene expression by mTECs imposes tolerance to tissue-specific antigens and the molecular controls of thymocyte migration through and out of the thymus. An important technical requirement for research into these areas is the means to purify these cell subsets for molecular and phenotypic analysis, a procedure that has proven difficult to date. Studies into the developmental origins of thymic epithelium have provided some insight into how the various subsets of these cells arise and persist in the thymus. While current work focuses on the molecular control of this development, a greater understanding of the population dynamics and relationships is still required. What are the maturational stages of the thymic epithelial subsets? Is there an optimal thymocyte to stromal cell ratio? Can the thymic stroma remodel with age? The answers to these questions have implications for our general understanding of thymic function, as well as the development of strategies to regenerate thymopoiesis in immunosuppressed states.

CHAPTER 2

Materials and Methods

2.1 ANIMALS

CBA, C57Bl-6 and CBA x C57Bl/6 F1 mice were used throughout this study at the ages indicated for organs and cells. Embryological age was judged with the day of plug formation taken as E0.5. Mice were bred and maintained by the Monash University Central Animal Services.

2.2 TREATMENT OF ANIMALS

2.2.1 Surgical castration

Mice were anaesthetised by inhalation of 4% isofluorane in oxygen, maintained via a nose cone. Castration was then performed with a small scrotal incision made to reveal the testes, which were tied off with suture thread and removed with scissors. Incisions were sealed with 9mm autoclips (Becton Dickinson, U.S.A.) and cleansed with 70% ethanol. Sham castrated mice received the incision and the testes exposed but not removed.

2.2.2 Immunodepletion by cyclophosphamide treatment

Mice between 6-8 weeks of age were immunodepleted by two intraperitoneal injections of 200mg/kg body weight of cyclophosphamide (Pharmacia, Australia) in sterile PBS over two days.

2.2.3 Bromodeoxyuridine (BrdU) treatment

BrdU incorporation was initiated by one intraperitoneal injection of BrdU (1mg in sterile PBS) (Sigma, U.S.A.) and maintained by the administration of 0.8mg/mL of BrdU in sterile drinking water, which was made fresh and changed daily.

2.3 ANTIBODIES, IMMUNOCONJUGATES AND LECTINS

Specificity	Clone	Form	Source
Thymic fibroblasts	MTS-15	Hybridoma s/n	Boyd lab, Australia
		Biotinylated	Boyd lab, Australia
CD31 (PECAM)	MTS-12	Hybridoma s/n	Boyd lab, Australia
Primordial epithelium	MTS-24	Hybridoma s/n	Boyd lab, Australia
Thymic fibroblasts	ER-TR-7	Hybridoma s/n	Boyd lab, Australia
Keratin (wide screen)	Polyclonal	Purified	Dako, U.S.A.
CD8	53-6.7	APC	Pharmingen, U.S.A.
CD4	RM4-5	PE	Pharmingen, U.S.A.
B220	RA3-6B2	PE	Pharmingen, U.S.A.
TcRβ	H57-597	FITC	Pharmingen, U.S.A.
		APC	Pharmingen, U.S.A.
CD45.2	104	FITC	Pharmingen, U.S.A.
CD45	30-F11	PE	Pharmingen, U.S.A.
		APC	Pharmingen, U.S.A.
CD40	3/23	Purified	Pharmingen, U.S.A.
CD80	IG10	Purified	Godfrey lab, Australia
CD11c	HL3	Biotinylated	Pharmingen, U.S.A.
CD11b	M1/70	APC	Pharmingen, U.S.A.
Ly51	CDR-1	Hybridoma s/n	Boyd lab, Australia
	6C3	Biotinylated	Pharmingen, U.S.A.
		FITC	Pharmingen, U.S.A.
EpCAM	G8.8a	Hybridoma s/n	Farr lab, U.S.A.
		Biotinylated	Farr lab, U.S.A.

Fucose carbohydrates	UEA-1 lectin	Biotinylated	Vector, U.S.A.
TSA-1	GR-12	FITC	Boyd lab, Australia
ICAM-1	YN1/1.7.4	Hybridoma s/n	Boyd lab, Australia
FcR	2.4G2	Hybridoma s/n	Boyd lab, Australia
Thy1.2	121-112	Hybridoma s/n	Boyd lab, Australia
I-A/I-E	M5/114.15.2	PE	Pharmingen, U.S.A.
CCL19	Polyclonal	Biotinylated	R&D Systems, U.S.A
CCL21	Polyclonal	Biotinylated	R&D Systems, U.S.A.
Human Ki67	B56	FITC	BD Biosciences, U.S.A.
BrdU	Polyclonal	FITC	BD Biosciences, U.S.A.
Rat Ig	Polyclonal	FITC	Silenus, Australia
	Polyclonal	HRPO	Caltag, U.S.A.
	Polyclonal	APC	Caltag, U.S.A.
Rat IgG	Polyclonal	PE	Southern Biotechnologies, U.S.A.
	Polyclonal	Biotinylated	Vector, U.S.A.
	Polyclonal	Cy3	Amersham, U.K.
Rabbit IgG	Polyclonal	Alexa 568	Molecular Probes, U.S.A.
	Polyclonal	Cy5	Amersham, U.K.
Streptavidin		PerCP	Pharmingen, U.S.A.
		CyChrome	Pharmingen, U.S.A.
		APC	Pharmingen, U.S.A.

2.4 FLOW CYTOMETRY

2.4.1 Cell suspensions

Murine lymphoid cell suspensions were prepared by gently grinding organs between two frosted glass slides with cold FACS buffer (PBS, 1% FCS (v/v), 0.02% (w/v) NaN_3). Cells were washed in FACS buffer and recovered by centrifugation prior to immunofluorescent staining.

2.4.2 Thymic stromal cell isolation by collagenase digestion

The thymic stromal cell isolation procedure used was based on that developed by (Shortman et al., 1989). Two to three thymi were dissected from freshly killed mice and trimmed of fat and connective tissue. Small cuts into the capsules were made with a pair of fine scissors and the thymi were gently agitated in 50mLs of RPMI-1640 with a magnetic stirrer at 4°C for 30 minutes to remove the majority of thymocytes. The resulting thymic fragments were transferred into 10mLs of fresh RPMI-1640 and dispersed further with a wide bore glass pipette to free more thymocytes. Medium was changed 2-3 times after agitations, with fragments recovered by settling each time. The thymic fragments were then incubated in 5mLs of 0.125% (w/v) collagenase D with 0.1% (w/v) DNAse I (both from Boehringer Mannheim, Germany) in RPMI-1640 at 37°C for 15 minutes, with gentle agitation using a Pasteur pipette every 5 minutes. Enzyme mixtures with isolated cells were removed after fragments had settled, then replaced with fresh mixture for further incubation. Gentle mechanical agitation was performed with a yellow pipette tip or 3mL syringe and 26G needle to break up aggregates remaining in final digestions. After 3-4 digestions, cells were pooled and centrifuged at 450 g_{max} for 5 minutes, resuspended in 5mM EDTA in PBS + 1%FCS + 0.02% (w/v) NaN_3 (EDTA/FACS buffer) and allowed to incubate for 10 minutes at 4°C to disrupt rosettes. Cells were then passed through 100µm mesh to remove debris. Viable cells were stained with ethidium bromide/acridine orange and counted on a

haemocytometer on a fluorescent microscope, or using a Z2 Coulter Counter (Beckman Coulter U.S.A.) with viable cells gated according to cell size.

2.4.3 Comparison of thymic stromal cell isolation by collagenase/dispase or trypsin digestion

Thymi were removed and mechanically digested as above. The first enzymatic incubations were performed in collagenase, with final digestion of large aggregates performed in 5mLs of either collagenase, 0.125% (w/v) collagenase/Dispase (Boehringer Mannheim, Germany) with 0.1% (w/v) DNAse I in RPMI or 0.125% (w/v) trypsin (Boehringer Mannheim, Germany) in Ca/Mg-free HBSS for 30 minutes at 37°C with gentle agitation every 15 minutes. Five mLs of 0.1% (w/v) DNAse I in RPMI was then added to the trypsin digestion mixture and incubation resumed at 37°C for a further 15 minutes, with gentle agitation every 5 minutes. Cells recovered by centrifugation were resuspended in EDTA/FACS buffer and incubated at 4°C for 10 minutes, then passed through 100µm mesh before counting and staining.

2.4.4 Immunofluorescent staining for flow cytometry

Cells were washed in cold EDTA/FACS buffer and 3 x 10^6 cells dispensed into wells of a 96-well round-bottomed plate (an empty well was left between each sample). Primary antibody (30µL of hybridoma supernatant or purified antibody at a sub-optimal dilution) was incubated with resuspended cells for 20 minutes at 4°C, followed by two washes in 200µL of EDTA/FACS buffer. The secondary antibody was added, incubated and washed, before 10µL of 10% (v/v) normal rat serum in FACS buffer was added for 5 minutes at 4°C to block any remaining reactive sites of the secondary reagent. Biotinylated and direct conjugates were added, incubated and washed, followed by the appropriate streptavidin conjugate. After final incubation, cells were washed, then resuspended in 200µL of EDTA/FACS buffer for acquisition. Sample data from 1 x 10^4 $CD45^-$ (non-lymphoid) cells

or 1 x 10^5 lymphoid cells were acquired on a FACScalibur (BD Biosciences, U.S.A.) using up to four fluorescent channels (FL1 for FITC, FL2 for PE, FL3 for CyChrome and PerCP and FL4 for APC) and analysed using CellQuest software (BD Biosciences, U.S.A.). All compensations were performed on single colour labelling of stromal cells. An FcR block (clone 2.4G2 supernatant) was employed before antibody staining of dendritic cells, macrophages or MTS-15 staining of leukocytes.

2.4.5 Cell sorting

Cells were isolated and stained as above in large samples (1.0 x 10^7-5 x 10^7) and resuspended in EDTA/FACS buffer at 1.0 x 10^7 cells/mL. Sorting was performed on a FACStar^{PLUS} cell sorter (BD Biosciences, U.S.A.) at no more than 3.0 x 10^3 cells per second. Samples were collected in 30%FCS in RPMI-1640, recovered by centrifugation, counted and a sample analysed for purity. Populations were sorted to greater than 95% purity.

2.4.6 BrdU staining

Cells were prepared and surface labelled as described previously (sections *2.4.2* and *2.4.4*). Samples were then fixed in cold 0.5% w/v paraformaldehyde (BDH Laboratory Supplies, U.K.), 0.01% Tween-20 (BDH Laboratory Supplies, U.K.) in PBS overnight at 4°C in the dark. Cells were washed in PBS, recovered by centrifugation and incubated in DNAse I (50Kunitz) (Roche Diagnostics, Germany) for 30 minutes at 37°C. After washing, cells were stained with FITC conjugated anti-BrdU for 1 hour at room temperature.

2.4.7 Ki67 staining

Cells were prepared and surface labelled as described previously (sections *2.4.2* and *2.4.4*). Samples were then fixed in 0.5% w/v paraformaldehyde (BDH Laboratory Supplies, U.K.) in PBS for 30 minutes at room temperature in the dark. Cells were then washed in PBS, recovered by centrifugation and incubated in BD FACS Permeabilisation solution (BD

Biosciences, U.S.A.) for 30 minutes at room temperature in the dark. After washing, cells were stained with FITC conjugated anti-Ki67 for 30 minutes at room temperature, washed once more and prepared for flow cytometric acquisition.

2.4.8 Recombinant ELC treatment

Biotin conjugated anti-ELC at a sub-optimal labelling concentration was incubated at 4°C overnight with varying concentrations of recombinant ELC (R&D Systems, U.S.A.), starting at a 200 molar excess to antibody (0.42µg/mL) in FACS buffer. This mixture was used to stain cells prepared as described previously (section *2.4.2*). Preincubations of cells with recombinant ELC alone were performed for 30 minutes at 4°C prior to other antibody labelling protocols (section *2.4.4*).

2.5 IMMUNOHISTOLOGY AND CONFOCAL MICROSCOPY

Sections (12-14µm) were cut on a TissueTek II cryostat (Miles Scientific, U.S.A.) at –25°C and mounted on microscope slides before fixation in –20°C acetone for 30 seconds and air drying. Tissue sections were then washed in PBS for 5 minutes and incubated with 30µl of primary mAb for 15 minutes in a moist box at room temperature, followed by washing three times in PBS with gentle agitation for 5 minutes each. Secondary antibodies (30µl) were applied, incubated for 15 minutes, then washed from slides. For three-colour immunofluorescence, 10µL of 10%(v/v) normal rat serum was added to sections for 5 minutes at room temperature to block any remaining reactive sites of the secondary reagents, followed by addition of biotinylated and direct conjugates. After incubation and washing, streptavidin conjugates were incubated and washed before mounting with fluorescent mounting medium (DAKO, U.S.A.) using coverslips.

Images were acquired on a Bio-Rad (U.S.A.) MRC 1024 confocal microscope with a three-line Kr/Ar laser (excitation lines 488, 568 and 647nm) using the acquisition software

Bio-Rad (U.S.A.) LaserSharp v 3.2. Files were analysed using LaserSharp processing software.

2.6 CELL AND ORGAN CULTURE

2.6.1 Cell culture

Hybridomas, cell lines and MTE-1D:PBL or 3B6:PBL co-cultures were maintained in RPMI-1640 (Invitrogen, Australia) supplemented with 5% FCS (v/v) (CSL, Australia) and 2mM L-glutamine and incubated at 37°C in 8%CO_2-in-air. MTE-1D and 3B6 cells were harvested by trypsinisation in 0.125% w/v trypsin (Sigma, U.S.A.) in 5mM EDTA/PBS and washed in RPMI-1640 before counting and replating. MTE-1D cells were the generous gift of Philippe Naquet (Marseilles, France), while 3B6 cells were obtained from Dale Godfrey (Melbourne, Australia).

2.6.2 Fetal thymic organ culture (FTOC)

Thymus lobes were obtained from E15.5 fetal mice and cultured on sponge-supported filter membranes at an interface between 5% CO_2-in-air and 10% FCS, 50μM 2-mercaptoethanol, 2mM L-glutamine, 1 x non-essential amino acids, 10mM HEPES, 1mM sodium pyruvate, 100U/mL penicillin and 100μg/mL streptomycin in RPMI-1640 (Life Technologies, U.S.A.) for 5 days in a 37°C incubator. Lobes were then washed and submerged in 1.08 mg/mL Cellmatrix collagen gel (Type I-A, Nitta Gelatin, Japan) in a 30mm dish. This was filled with media and cultured at 37°C in 75% O_2 and 5% CO_2-in-air under an Axiovert S-100 microscope (Carl Zeiss, Germany) for monitoring by a time-lapse visualisation system equipped with a C4742-95 digital CCD camera (Hamamatsu Photonics, Japan) and Openlab software (Improvision Inc., U.S.A.).

2.6.3 Chemotaxis assay

Thymocyte cell suspensions (100µL with 5 x 10^5 cells) were placed in a Transwell chamber with a polycarbonate membrane (6.5mm diameter, pore size 5µm, Costar, U.S.A.) with 600µL of culture medium containing chemokines (all from R&D Systems). Cells were cultured for 90 minutes, recovered from the upper and lower chambers, counted and analysed for TcRβ expression by flow cytometry.

2.7 BIOCHEMICAL AND MOLECULAR TECHNIQUES

2.7.1 Tween-40 membrane preparations and Western blotting

Cell membranes were enriched by ultracentrifugation (100,000g_{max}) of Tween-40 disrupted tissue or cell preparations in 10mM Tris,140mM NaCl, 0.02%Na_3 (v/v) (Standring and Williams, 1978). Pellets were resuspended in a minimal volume of 10mM Tris, 140mM NaCl, 0.02% NaN_3 (v/v) and 1-2µL mixed with 2X reducing or non-reducing SDS sample buffer (5% SDS, 20% glycerol, 0.1% bromophenol blue (w/v) in 0.5M Tris-HCl with 0.1M DTT for reducing). Samples were boiled prior to loading on a 3% polyacrylamide stacking gel over a 16% polyacrylamide SDS resolving gel cast in a Dual Mini-gel Caster (Bio-Rad, U.S.A.). Electrophoresis was performed at 60mA per gel in 0.2M Tris-HCl pH 8.8 anode buffer and 0.1%SDS, 0.1M Tricine in 0.1M Tris-HCl pH 8.25 cathode buffer (Schagger and von Jagow, 1987). After tricine SDS-PAGE, western transfer onto PVDF membranes was performed using a Bio-Rad transfer system run at 30V (80mA) overnight in 20%(v/v) methanol in 0.25M Tris/0.2M glycine. Membranes were then blocked in 5% (w/v) casein for 2 hours, washed for five minutes three times in 0.05% (v/v) Tween-20 in PBS, then incubated with approximately 7.5mLs of MTS-15 hybridoma supernatant for 30 min at room temperature. Following washing, secondary antibodies in 5% (w/v) casein were incubated

on membranes for 30 min, then washed off prior to ECL-Plus detection (Amersham, U.K.) and exposure to autoradiography film.

2.7.2 MTS-15 antigen purification.

Mouse intestinal membrane preparation (4mL) was extracted with 15mL of chloroform, methanol (1:2 v/v), with intermittent sonication for 3h at room temperature and the extract recovered by centrifugation (1500rpm, 10min, room temperature). The pellet was further extracted with 5mL chloroform, methanol, water (1:2:0.8 v/v), with sonication for 1.5h at room temperature and centrifugation as above. The two supernatants were combined, water added to give a final chloroform, methanol, water ratio of 1:2:1.4 (v/v) and the two phases allowed to separate overnight at 4°C. The chloroform phase was dried under N_2 and resuspended in 500µL of chloroform, methanol (1:1 v/v). An aliquot (100µL) was applied over 17cm of a silica gel 60 aluminium-backed HPTLC plate (Merck, Germany) and developed for 10cm in chloroform, methanol, 1M ammonium acetate, 13M ammonium hydroxide, water (180:140:9:9:23 v/v). Silica bands of 2.5mm were scraped and the resolved glycolipids extracted with chloroform, methanol, water (1:2:0.8 v/v). Antigenic activity was identified by reanalysing each fraction by HPTLC and immunoblotting with MTS-15 (see below). A duplicate HPTLC plate was stained with orcinol/sulphuric acid reagent (3min, 80°C) for detection of carbohydrates.

2.7.3 HPTLC immunoblot analysis.

Chromatographed HPTLC plates were air dried and plastic coated with 0.1% (w/v) polyisobutylmethacrylate in n-hexane. Coated plates were dried and blocked in 5% (w/v) powdered skim milk in PBS, 0.02% (v/v) Tween-20 for 1h at room temperature. The HPTLC plates were probed with MTS-15 for 1h at room temperature followed by anti-rat Ig HRPO conjugated antibody (1:500, Dako, U.S.A.) in 5% (w/v) powdered skim milk in PBS,

0.02% (v/v) Tween 20 for 1h at room temperature. Detection of the secondary antibody was by ECL Western detection system (Amersham, U.K.).

2.7.4 GC-MS compositional analysis

HPTLC-purified MTS-15 antigen was subjected to methanolysis on 0.5M methanolic-HCL (50µl) for 16h at 80°C. The mixture was neutralised with pyridine (10µL), sugars re-N-acetylated by addition of acetic anhydride (10µL, 10min, room temperature) and dried under vacuum. The released monosaccharides were derivatised in 15µL pyridine, hexamethyldisilazane, trimethylchlorosilane (9:3:1 v/v) for 20min at room temperature and the solvent dried under N_2. The trimethylsilyl derivatives were resuspended in 50µL n-hexane and detected by gas chromatography mass spectrometry an a Hewlett Packard (U.S.A) GC system 6890 series/mass selective detector 5973 using a HP1 (Hewlett Packard, U.S.A.) capillary column.

2.7.5 MALDI-TOF-MS analysis.

HPTLC-purified MTS-15 antigen in 50% 1-propanol (0.3, ~1µg/µL) was analysed by matrix-assisted laser desorption ionisation/time of flight mass spectrometry on a Voyager-DE STR, Perspective Biosystem (PE Biosystems, Germany) in the positive ion/reflector mode. Saturated α-cyano-4-hydrocinnamic acid in 60% 1-propanol (0.3µl) was used as the matrix and GM1 was used as a standard.

2.7.6 Chemical and enzymatic treatments

Partial acid hydrolysis of the MTS-15 antigen was performed in 0.1M trifluoroacetic acid (100µL) for 2h at 100°C. The sample was dried under vacuum and residual trifluoroacetic acid removed by evaporating with toluene (2x20µL). Mild base hydrolysis was carried out in 0.1M methanolic-sodium hydroxide (50µL) for 2h at 37°C. The samples were neutralised with 1M acetic acid, then subjected to 1-butanol, water partitioning. The 1-butanol phase

containing the glycolipids was dried under vacuum. Endoglycoceramidase II ACT (EGCase II, 1μL, 1mU, Calbiochem, U.S.A.) digestions were performed in 20mM sodium acetate, pH 5.0 for 16h at 30°C. Lipidic digestion products were recovered by 1-butanol, water partitioning and the 1-butanol phase dried under vacuum. Coffee bean α-galactosidase (20μL, 1U, Boehringer Mannheim, Germany) treatments were performed in 0.1M phosphate-citrate, pH 6.0, 0.2% taurodeoxycholate for 48h at 37°C. Jack bean β-N-acetylhexaminidase (15μl, Oxford GlycoSystems, U.K.) treatments were carried out in 0.1M phosphate-citrate, pH 4.5, 0.1% taurodeoxycholate for 22h at 37°C. Chemical and enzymatic treatment products were resuspended in 50% 1-propanol (10μL), resolved by HPTLC and detected by orcinol and MTS-15 staining.

2.7.7 Reverse transcriptase PCR analysis of mRNA transcripts

Cells purified by cell sorting were washed and resuspended in a minimal volume of Trireagent (Molecular Research Center, U.S.A.). After vortexing, a one tenth volume of BCP phase separation reagent (Molecular Research Center, U.S.A.) was added, vortexed and incubated at room temperature for 15 minutes, followed by centrifugation to separate aqueous and organic phases. The aqueous phase was taken and added to yeast tRNA carrier (Invitrogen, U.S.A.) in isopropanol, mixed and incubated for 15 minutes at room temperature. Total cellular RNA was recovered by centrifugation and washed with 70% ethanol in water before air drying. RNA was reverse transcribed using Superscript II (Invitrogen, U.S.A.) and oligo-dT oligonucleotides (Invitrogen, U.S.A.) incubated at 42°C for 50 minutes, followed by inactivation at 70°C for 10 minutes. cDNA was PCR-amplified (30 cycles for HPRT; 35 cycles for chemokines and receptors) with Taq polymerase (Promega, U.S.A.) using the following primers.

Primer	**Sequence**
HPRT 5'	CACAGGACTAGAACACCTGC
HPRT 3'	GCTGGTGAAAAGGACCTCT
CCL19 5'	GCTAATGATGCGGAAGACTG
CCL19 3'	ACTCACATCGACTCTCTAGG
CCL21 5'	GCTGCCTTAAGTACAGCCAG
CCL21 3'	GTGTCTGTTCAGTTCTCTTGC
CCR7 5'	TTTTCCAGGTGTGCTTCTGC
CCR7 3'	TGTACGTCAGTATCACCAGC
CCXCKR5'	TTCAGATGCTGGAAATCGGC
CCXCKR3'	GCTTGGCAGAACTTAACAACG

PCR products were electrophoresed on a 1.5% agarose gel and visualised with ethidium bromide staining.

CHAPTER 3

Analysis of thymic stromal cell populations using flow cytometry.[1]

3.1 INTRODUCTION

The thymus provides a unique microenvironment that efficiently generates αβT-lymphocytes capable of responding to foreign peptide in the context of self-MHC. This microenvironment is established through the interplay of developing thymocytes with a non-lymphocytic component broadly termed the thymic stroma. The latter consists of a phenotypically diverse group of cells, including epithelium, endothelium, reticular fibroblasts, macrophages, dendritic cells and neuroendocrine cells (Boyd et al., 1993). These cells collectively provide cell surface molecules, cytokines and extracellular matrix elements that are essential for various stages of T-cell development (Anderson et al., 1996). While the various subsets of thymocytes in the thymus have been studied in depth, relatively little is known about the stromal cell types that influence their development.

Earlier ultrastructural studies initially demonstrated the diversity of thymic epithelial cells based on morphology and electron lucency, identifying six discrete subsets (types 1-6) (van de Wijngaert et al., 1984). Further investigations into thymic stromal cells (TSC) have involved immunohistological analysis using panels of monoclonal antibodies (mAbs) specific for stromal antigens (for example (Van Vliet et al., 1984); (de Maagd et al., 1985); (Lobach et al., 1985); (Godfrey et al., 1988)). Such work has defined stromal cells

---

[1] This chapter is based on the publication: **D.H.D. Gray**, A.P. Chidgey, and R.L. Boyd (2002) Analysis of thymic stromal cell populations using flow cytometry. Journal of Immunological Methods 260,1-2:15-28.

(particularly epithelial cells) into discrete subsets on the basis of morphology and the expression of intracellular and cell surface markers (Kampinga et al., 1989). However, the co-expression of these various markers and population kinetics of the stromal cell subsets have been difficult to evaluate by histological studies alone. A previous study attempting to resolve some of these issues using flow cytometric analysis of thymic stromal cells found extensive overlap between the distributions of determinants thought to be exclusive in their expression (Izon et al., 1994). Here, we describe the usage of multicolor flow cytometry to distinguish the various thymic stromal populations using mAbs to surface antigens.

The stromal cell yields from various enzymatic digestion methods are compared and the epitope sensitivities of important markers determined. As found previously, flow cytometry reveals a more extensive distribution of some stromal antigens than would have been predicted from immunohistology, highlighting the greater sensitivity of the former technique. However, exclusion of certain contaminating cell types has enabled clearer correlation of TSC reactive mAbs on stromal cell subsets. FACS purification of these stromal subsets will hopefully aid in the determination of the precise functional roles each of these cell types have in T-cell development. Furthermore, genetic and antigenic analysis of individual populations may lead to a better understanding of the molecules that mediate these functions.

3.2 RESULTS AND DISCUSSION

3.2.1 Analysis of Thymic Stromal Cells Isolated by Collagenase Digestion

To determine the enrichment and numbers of thymic stromal cells that could be obtained using collagenase digestion, cells isolated from a series of incubations were analysed for CD45 expression, which detects all cells derived from haematopoietic stem cells (HSCs) (reviewed by Thomas, (1989)). This enabled discrimination of $CD45^-$ epithelium, endothelium, fibroblasts and neuroendocrine cells from all other cells in the thymus.

Table 3.1 shows that incubation of thymic fragments in a series of three collagenase digestions released increasing levels of $CD45^-$ cells; very few were released by the initial agitation alone. The highest number and proportion of $CD45^-$ cells was obtained in the final digestion, resulting in an enrichment of these stromal cells of almost 30-fold (Fig. 3.1 A & B). This was verified by microscopic evaluation of the gradual enrichment of the larger of these cells throughout the course of the collagenase digestion (Fig. 3.1 C & D). This characteristic was also apparent with the high forward and side scatter properties of some $CD45^-$ cells, particularly in the final digest (Fig. 3.1 E & F). However, back-gating of $CD45^-$ events isolated in these digests revealed that there were also many small stromal cells, necessitating the inclusion of the larger thymocytes in a FSC:SSC stromal gate. Extremely high FSC or SSC events were excluded from the gate to minimise the risk of including doublets in the analysis.

	Total cells per thymus	Proportion of $CD45^-$ cells in digest	$CD45^-$ cells per thymus	Viability
Depletion	1.66×10^8	0.18%	8.30×10^4	96%
Collagenase 1	1.80×10^7	1.13%	5.76×10^4	98%
Collagenase 2	3.03×10^7	1.43%	1.21×10^5	97%
Collagenase 3	1.85×10^7	5.79%	3.26×10^5	97%
Total/thymus	2.33×10^8	0.25%	5.88×10^5	

Table 3.1 Yields and viability of total cells and $CD45^-$ cells released from a series of collagenase digestions of thymi.

The number of collagenase digestions required and cell numbers released at each step varied between experiments, however the trend of $CD45^-$ cell release remained the same. This data is representative of 5 experiments.

Figure 3.1 CD45$^-$ cells are enriched in the final collagenase digestion of 4wk old thymi. Cells from the thymocyte depletion step and the final collagenase digestion were analysed for CD45 expression (**A** and **B**). The larger stromal cells were apparent microscopically (**C** and **D**). This was reflected in more cells of high forward and side scatter properties being found in the collagenase digestion (**E**) than the depletion (**F**). Profiles are representative of 5 experiments.

Thymocyte Depletion

Collagenase Digestion

A.

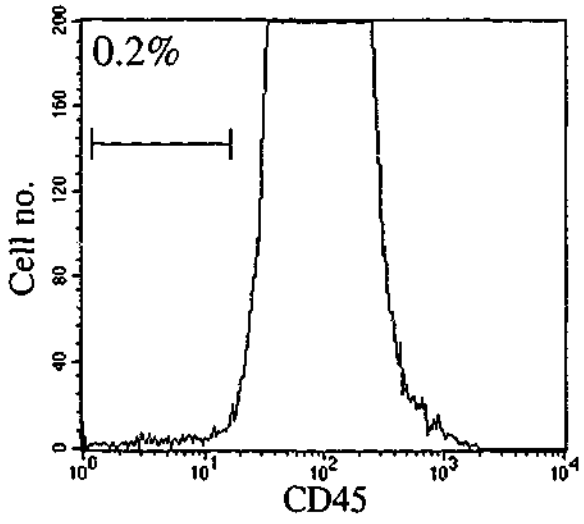

B.

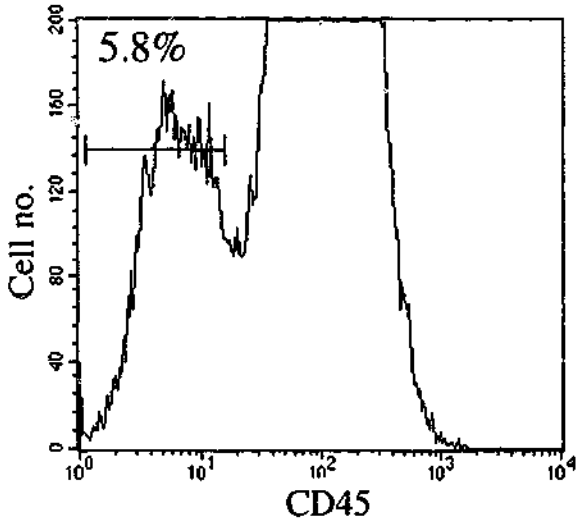

C.

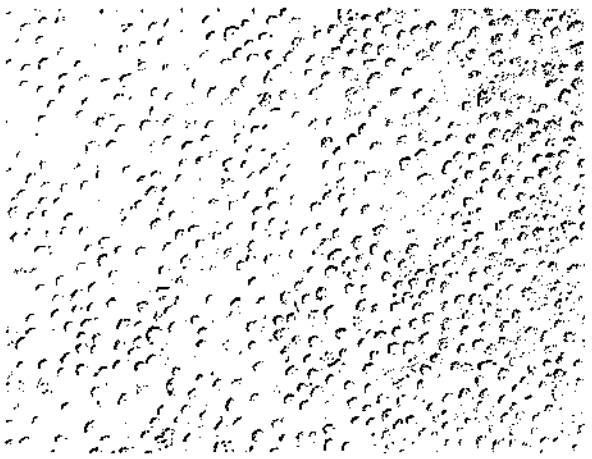

D.

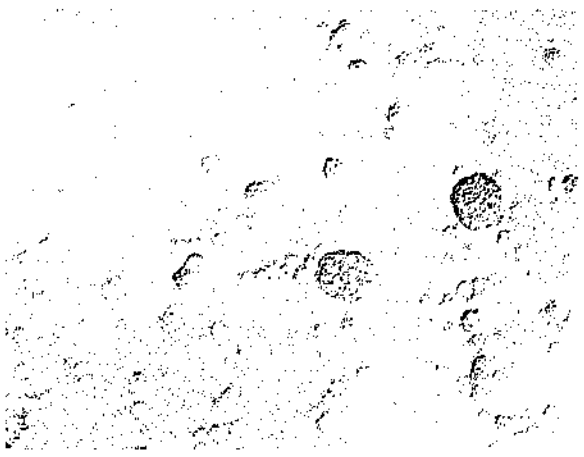

E.

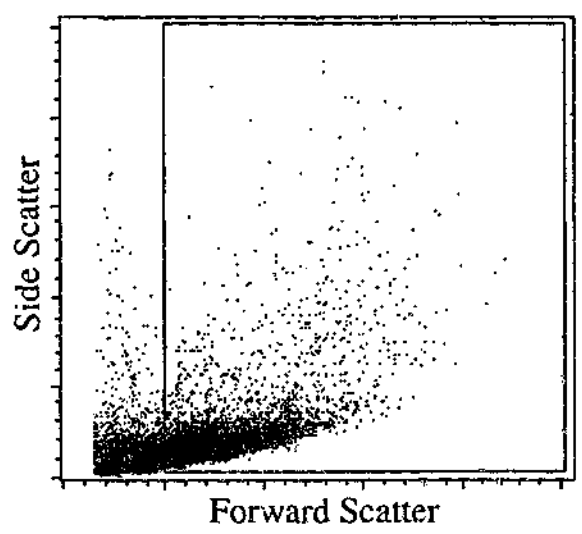

F.

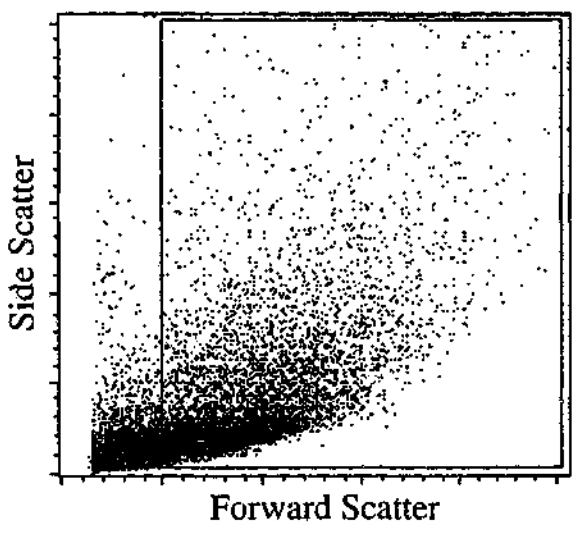

3.2.2 Comparison of Digestion Enzymes

Many previous studies into thymic stromal cells have used various isolation procedures that employ enzymes other than collagenase to dissociate the thymic tissue, in particular, collagenase/Dispase (Pircher et al., 1993) and trypsin (Jenkinson et al., 1992). In this study, these enzymes were used to gauge how effective each was in digesting the stromal cell aggregates that are normally left after the final collagenase digestion (Table 3.2).

Trypsin was the most effective, dissociating all thymic fragments and stromal aggregates into a single cell suspension thereby releasing all remaining stromal cells. The total $CD45^-$ cells isolated from this preparation represented the maximal recovery against which the other enzymes were compared. The recovery of almost 80% of CD45 negatives with collagenase digestion suggests that the undigested aggregates contained many thymic stromal cells (1.56×10^5 per thymus). Collagenase/Dispase dissociated some of these aggregates, recovering 94% of available $CD45^-$ stromal cells.

While Dispase and trypsin isolated more $CD45^-$ stromal cells, the possibility that these enzymes may cleave potentially important cell surface markers was assessed by incubating suspensions of stromal cells with these enzymes for 1 hour at 37°C, followed by immunofluorescent labeling. The summary of the epitope sensitivities of a variety of thymocyte and stromal antigens in Table 3.3 shows that collagenase digestion preserves all markers tested. Most of these molecules are also resistant to Dispase treatment however, CD4, CD8 and CD11c profiles did change with this enzyme. More than half of the epitopes tested were disrupted or cleaved entirely upon trypsin treatment, however some important markers (e.g. CD45, MHC II) were resistant.

	CD45$^-$ cells isolated in final digestion per thymus	Total CD45$^-$ cells isolated per thymus	Proportion of maximal recovery of CD45$^-$
Collagenase	3.26×10^5	5.88×10^5	79%
Collagenase/Dispase	4.40×10^5	7.02×10^5	94%
Trypsin	4.82×10^5	7.44×10^5	100%

Table 3.2 Comparison of CD45$^-$ cell yields using various digestion enzymes.

Thymi were digested in collagenase for two incubations, then the final digestion performed in collagenase, collagenase/Dispase or trypsin (data for previous collagenase digestions shown in Table 1). CD45$^-$ cell yields from the final and overall digestion are determined and the proportion of maximal recovery (trypsin digest) calculated. These data are representative of three experiments performed.

Marker	Collagenase	Collagenase/Dispase	Trypsin
CD45	+	+	+
CD4	+	+/-	-
CD8	+	-	-
CD11c	+	+/-	-
CD11b	+	+	+/-
MHC II	+	+	+
EpCAM	+	+	-
ICAM-1	+	+	+
PECAM	+	+	-
Thy1	+	+	+/-
TSA-1	+	+	+/-
CD40	+	+	+/-
B7.1	+	+	-
Ly51	+	+	+
CDR-1	+	+	+
MTS-15	+	+	+
UEA-1	+	+	+

Table 3.3 Epitope sensitivities to various digestion enzymes.

Isolated stromal cells were incubated in collagenase, collagenase/Dispase or trypsin and immunofluorescent staining with various mAbs analysed by flow cytometry. Epitopes that were resistant (+), partially resistant (+/-) or sensitive (-) to enzyme treatment were determined using histograms representative of 3 experiments.

3.2.3 Flow Cytometric Analysis of Thymic Stromal Cell Subsets

Pooled collagenase preparations enriched for thymic stromal cells were analysed further by flow cytometry for their autofluorescence. While these cells alone gave high signals in the FL1, 2 and 3 channels (Fig. 3.2A and Izon et al., (1994)), the majority of this background was due to autofluorescence from a population of $CD45^+$ cells (Fig. 3.2B). These highly autofluorescent, $CD45^+$ cells are probably thymic macrophages, as has been previously reported (Vremec et al., 2000), and are excluded from the analysis when gating on $CD45^-$ thymic stromal cells. Furthermore, it was found that $CD45^-$ cells exhibited little or no background staining due to non-specific binding of IgG (Fig. 3.2C) and did not express Fc-receptors (Fig. 3.2D). A population of thymic MHC^{hi} cells do express FcR and further analysis determined that these were myeloid derived cells and some lymphoid dendritic cells (data not shown), necessitating the use of an FcR block when staining for these cell types.

Further phenotypic analysis of thymic stromal cells was conducted using a panel of surface reactive mAbs. Of particular interest were thymic epithelial cells, which could be defined using the mAb G8.8a that recognizes EpCAM, expressed by thymic epithelium, dendritic cells and some thymocytes (Nelson et al., 1996). By first gating on $CD45^-$ stromal cells, the latter two cell types could be excluded, leaving only the epithelial cells staining positive with this marker.

Under these conditions, EpCAM positive cells comprised about 45-60% of $CD45^-$ cells in the pooled collagenase digestions and could be further divided into cortical and medullary epithelial cells using CDR-1 as a marker of cortical epithelium (Rouse et al., 1988) (Fig. 3.3A). In normal 4 week old mice, about half of the epithelium is $CDR\text{-}1^+$, the remainder presumably medullary epithelium (see later section).

Figure 3.2 Autofluorescence and FcR expression in collagenase digested preparations of 4wk old thymic stromal cells.

Autofluorescence of isolated cells alone extends up to 10^2 in the FL1, 2 & 3 channels (**A**). Analysis of CD45 expression vs. an empty FL3 channel reveals most of the high fluorescent signals are derived from a population of $CD45^+$ cells, while $CD45^-$ cells display a range of intensities (**B**). The histogram in **C** plots unlabelled $CD45^-$ cells (solid line) vs. an IgG2b isotype control detected by an anti-rat Ig FITC on $CD45^-$ cells (dotted line). Histogram **D** plots anti-FcR (clone F2.4G2) staining revealed by anti-rat Ig FITC gated on $CD45^-$ cells (solid line) and anti-FcR staining revealed by anti-rat Ig FITC gated on total MHC II^{hi} cells (dotted line). Profiles are representative of 3 experiments.

A.

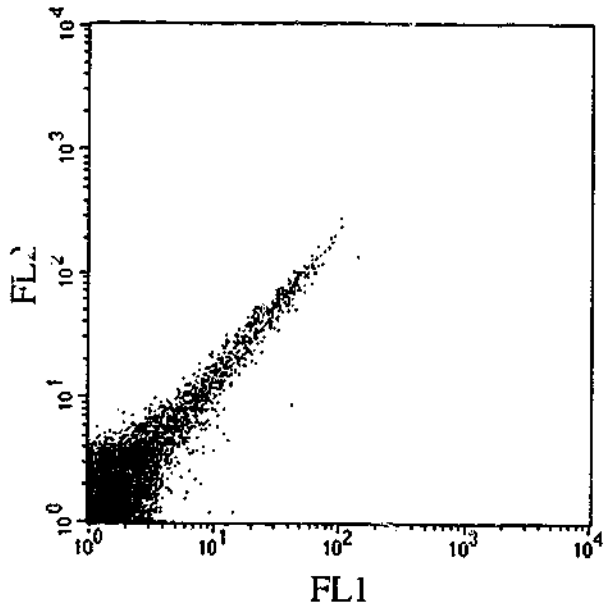

B.

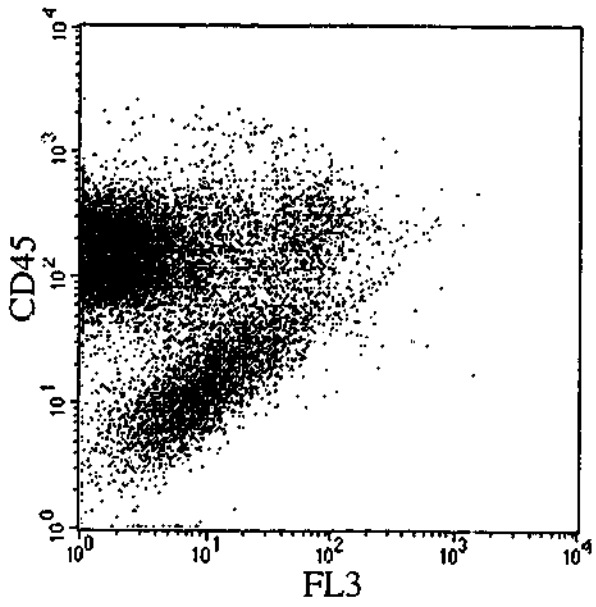

C.

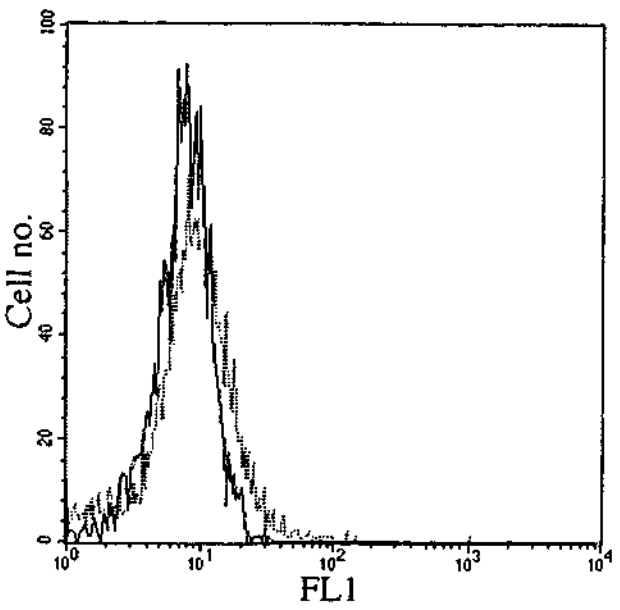

D.

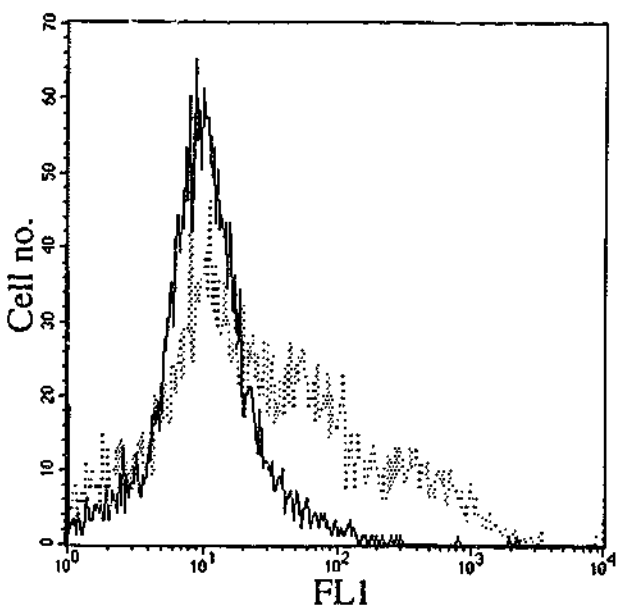

Figure 3.3 Phenotypic analysis of CD45$^-$ thymic stromal cell subsets defined by a panel of mAbs.

Collagenase digested CD45$^-$ stromal cells from 4wk old mice were gated and analysed for the expression of certain markers. Expression of EpCAM and CDR-1 allows distinction of cortical and medullary epithelium (**A**). All EpCAM$^+$ epithelial cells express MHC class II (**B**). CD31 positive endothelial cells comprise 11% of CD45$^-$ cells, half of which express low levels of MHC class II (**C**). Most cells expressing the fibroblast marker MTS-15 do not express MHC class II (**D**). MTS-15 is also expressed on the surface of some endothelial cells (**E**). As expected, MTS-15$^+$ fibroblasts do not express EpCAM (**F**). Representative profiles from three experiments shown.

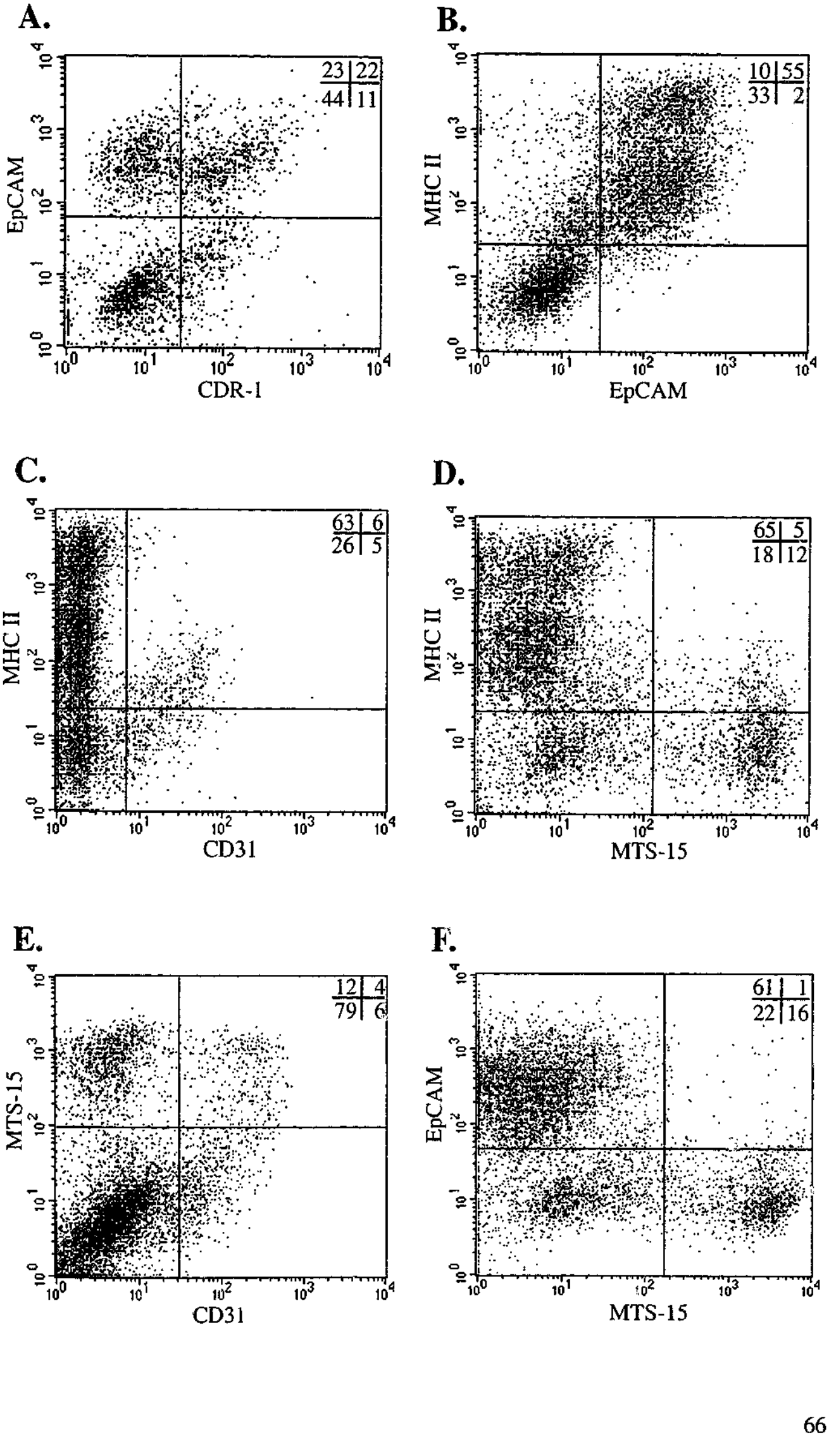
A.
EpCAM
CDR-1
23 22
44 11
B.
MHC II
EpCAM
10 55
33 2
C.
MHC II
CD31
63 6
26 5
D.
MHC II
MTS-15
65 5
18 12
E.
MTS-15
CD31
12 4
79 6
F.
EpCAM
MTS-15
61 1
22 16

Interestingly, all CD45$^-$/EpCAM$^+$ stromal cells expressed MHC class II, although at varying levels (Fig. 3.3B). This presumably reflects the antigen-presenting role these cells play in selecting developing thymocytes. Certainly, it has been demonstrated by (Jenkinson et al., 1992) that embryonic CD45$^-$/MHC class II$^+$ thymic stromal cells can mediate the development of double positive to functional single positive thymocytes. While this fraction includes both cortical and medullary epithelial cells, about half of the endothelial cells in the thymus (defined by expression of CD31) also expressed low levels of MHC class II (Fig. 3.3C). Whether these cells play a role in selection remains to be addressed. It is unlikely that they are primarily involved in positive selection because this appears to be a unique feature of cortical epithelium (Benoist and Mathis, 1989). They could, however, contribute to positive and negative selection by providing MHC/peptide ligands for thymocyte T-cell receptors, acting in cis with differentiating signals from cortical epithelium (Chidgey et al., 1998).

In addition to thymic epithelial and endothelial cells, fibroblasts constitute a major component of the stromal microenvironment in which thymocytes develop. These cells are important in forming the ECM components essential to CD4$^-$CD8$^-$ thymocyte development (Anderson et al., 1997), although other roles remain to be defined. The mAb MTS-15 recognizes a glycolipid antigen expressed on the surface of MHC class II$^-$ thymic fibroblasts that line the subcapsule and large blood vessels (Fig. 3.3D, 3.4A & B). However, this antigen also appears to be present on some MHC class II$^+$ cells (Fig. 3.3D). Four colour labelling examining MTS-15, MHC II and CD31 expression on CD45$^+$ stromal cells revealed that these MHC II/MTS-15$^+$ events are the MHC II/CD31$^+$ endothelial cells mentioned earlier (Fig 3.3E and data not shown). Whether the distinct phenotype of these endothelial cells relates to a specialised function within the thymus is an interesting, as yet unanswered, question.

Figure 3.4 MTS-15 recognises an antigen expressed by subcapsular and perivascular fibroblasts in the 4 week old thymus.

MTS-15 antigen can be detected around the subcapsule and large blood vessels of the medulla (green) with little colocalisation (yellow) with keratin positive epithelial cells (red) (**A**). More extensive colocalisation (yellow) is observed upon higher power examination of counterstaining of MTS-15 (green) with anti-CD31 (red) than with anti-keratin (blue) (**B**).

A.

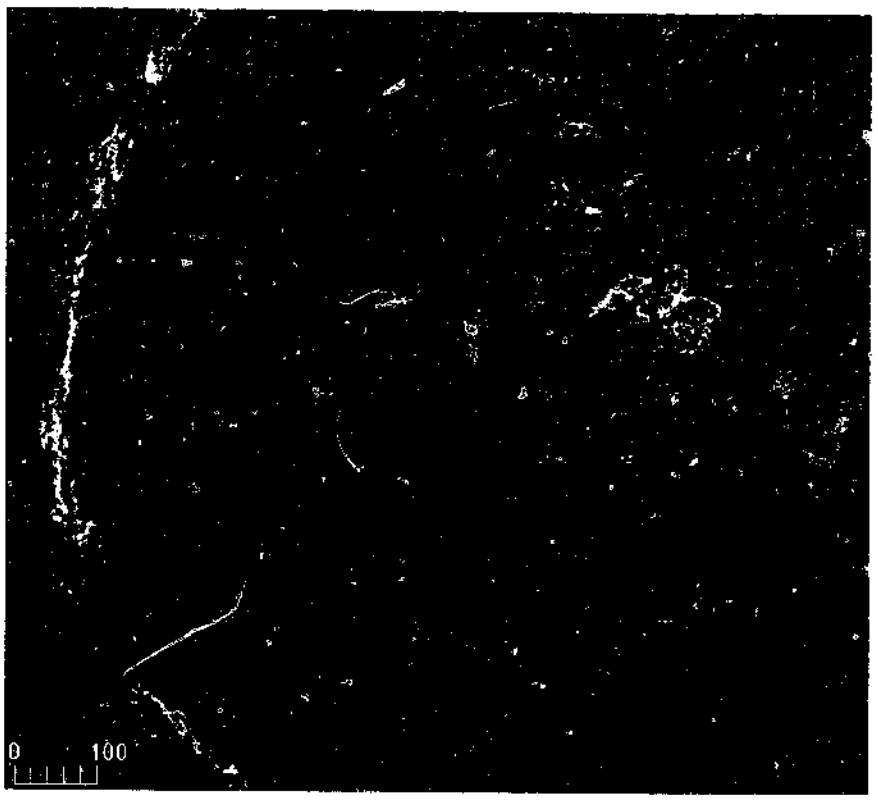

B.

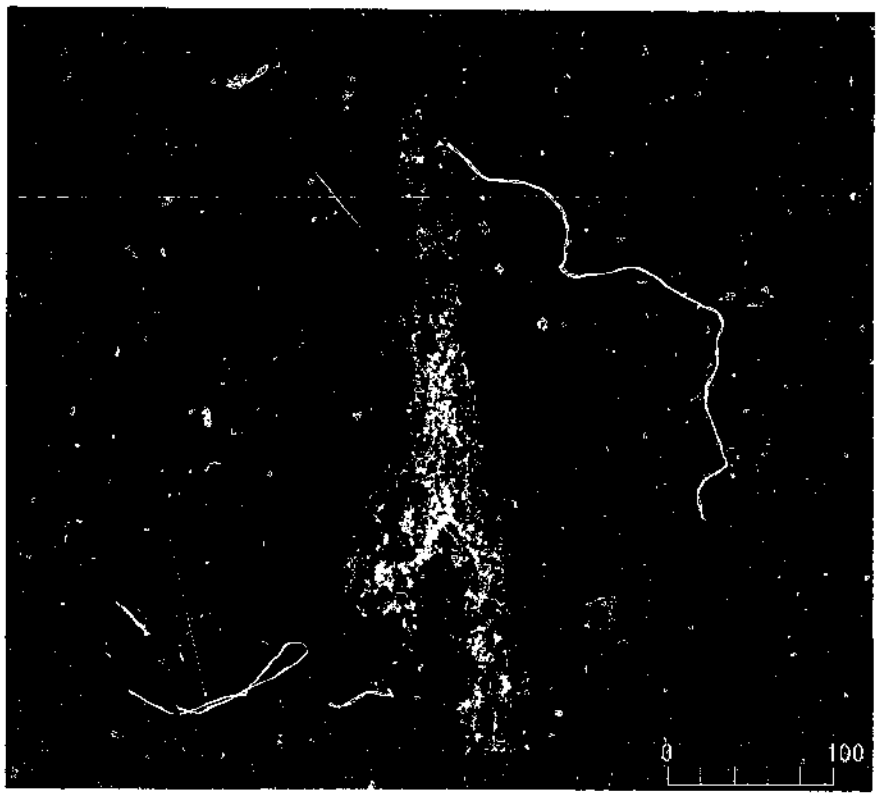

As would be expected, MTS-15 and anti-EpCAM define mutually exclusive populations of $CD45^-$ stromal cells (Fig. 3.3F). The remaining population of $CD45^-$/$EpCAM^-$/$MTS\text{-}15^-$ cells may include more fibroblasts and neuroendocrine cells.

The other major cellular components of the thymic stroma include the $CD45^+$ macrophages and dendritic cells. Thymic dendritic cells can be defined as $CD11c^{hi}$, MHC class II^{hi} cells (Fig. 3.5A) (Wu et al., 1995), while myeloid derived cells (predominantly macrophages) are $CD11b^{hi}$, $CD11c^{lo}$ (Kishimoto et al., 1989) (Fig. 3.5B). Thymic macrophages appear to be predominantly MHC class II^-, although there are some MHC class II high and low macrophages (Fig. 3.5C). These stromal cells are found to emerge at all stages of the collagenase digestion (including the thymocyte depletion step), although they are enriched in the final few digestions (data not shown).

3.2.4 Cortical and Medullary Epithelial Cell Markers

While it has been established that cortical and medullary epithelial cells play distinct roles in thymic selection (Klein and Kyewski, 2000), purification of these cell types will be essential for future functional and molecular studies. The mAbs CDR-1 and 6C3 have previously been used to define thymic cortical epithelial cells histologically (Rouse et al., 1988; Surh et al., 1992b). Furthermore, immunomagnetic and flow cytometric purification of cortical and medullary epithelial cells using CDR-1 has enabled comparisons of gene expression and antigen processing (Klein et al., 1998; Merkenschlager et al., 1999). Therefore, these markers were used to analyse the surface phenotype of cortical epithelial cells in more detail.

Figure 3.5 Thymic dendritic cells and myeloid derived cells in collagenase digested stromal cell preparations of 4wk old thymi.

Thymic dendritic cells can be defined by high expression of CD11c and MHC class II (**A**). Thymic myeloid derived cells are $CD11b^{hi}$ and $CD11c^{lo}$ (**B**). The few $CD11c^{hi}$, $CD11b^{+}$ events may represent myeloid derived dendritic cells. The $CD11b^{hi}$ cells can be divided into MHC class II positive and negative populations (**C**). Representative profiles from 3 experiments shown gated on total viable thymic stromal cells ($CD45^{-}$ & $CD45^{+}$).

A.

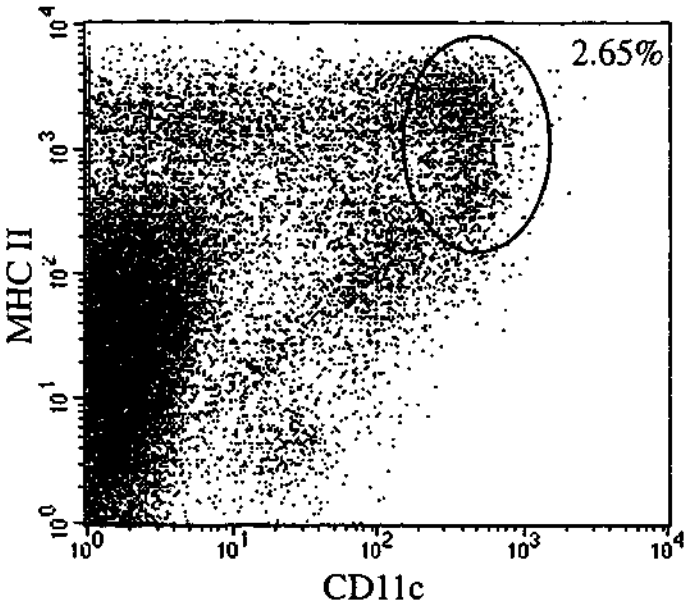
2.65%
MHC II
CD11c
10^0
10^1
10^2
10^3
10^4

B.

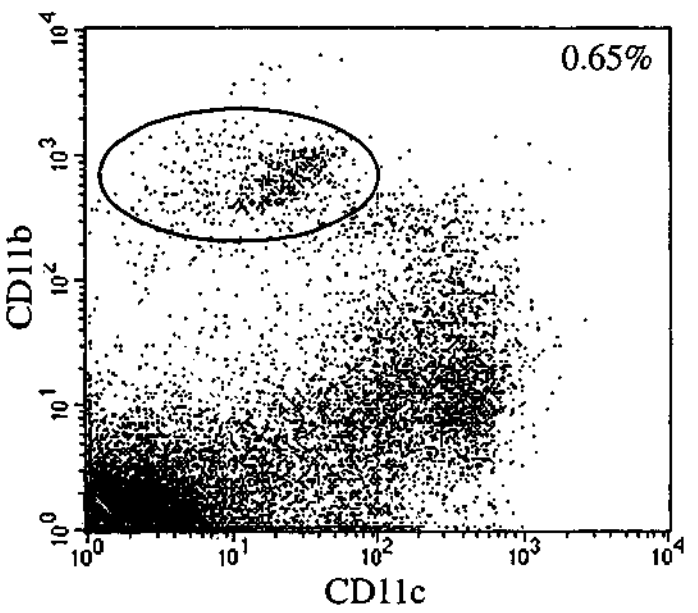
0.65%
CD11b
CD11c
10^0
10^1
10^2
10^3
10^4

C.

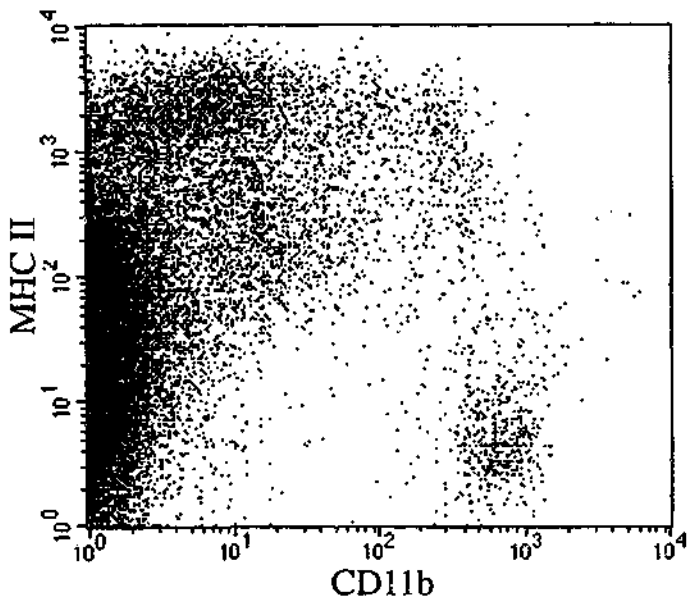
MHC II
CD11b
10^0
10^1
10^2
10^3
10^4

Both CDR-1 and 6C3 label a subset of EpCAM$^+$ cells (Fig. 3.3A and 3.6A), however each also recognizes a determinant expressed by some EpCAM$^-$ cells. The proportion of cortical and medullary epithelial cells tends to be roughly equal at 4 weeks of age, however it may vary during thymic development (ie. it appears to favour medullary epithelial cells in neonatal mice).

A direct comparison of the two cortical markers reveals that they label the same cells with similar intensities, suggesting they recognize distinct epitopes of the same molecule or complex (Fig. 3.6B). The antigen detected by 6C3 has been established as aminopeptidase A (Ly51) (Wu et al., 1990) that is also expressed on subsets of B-cell precursors and thymic dendritic cells (Wu et al., 1995). Studies using Ly51 deficient mice demonstrate that this enzyme is not essential for normal T and B cell development (Lin et al., 1998). By inference, CDR-1 may also recognize this molecule, however further studies will be needed to address this directly.

The non-epithelial reactivity of these two mAbs was further investigated by comparison to MTS-15 and CD31 (Fig. 3.6C and D), revealing that Ly51 is also expressed on some fibroblasts and endothelial cells. One of the few reagents specific for a determinant expressed on the surface of medullary epithelial cells that has been reported is the lectin Ulex Europaeus Aglutinin I (UEA-1) (Farr and Anderson, 1985). By immunohistology, it appears to label only a subset of medullary epithelial cells, so its reactivity by flow cytometry was of interest. The profile shown in Fig. 3.7A demonstrates the high expression of UEA-1 found on more than half of the EpCAM$^+$ cells and intermediate expression on the remaining epithelial cells. These UEA-1^{hi} cells are presumably the medullary epithelial cells

Figure 3.6 Cortical epithelial cell markers on neonatal thymus.

Representative profiles from 3 experiments are shown, gated on $CD45^-$ cells. Ly51 is expressed on an EpCAM negative subset of cells, as well as EpCAM positive cortical epithelial cells (**A**). CDR-1 and 6C3 (anti-Ly51) bind to the same cells at equivalent levels (**B**). Most of the EpCAM negative subset of 6C3 positive cells express the fibroblasts marker MTS-15 (**C**) and/or the endothelial marker CD31 (**D**).

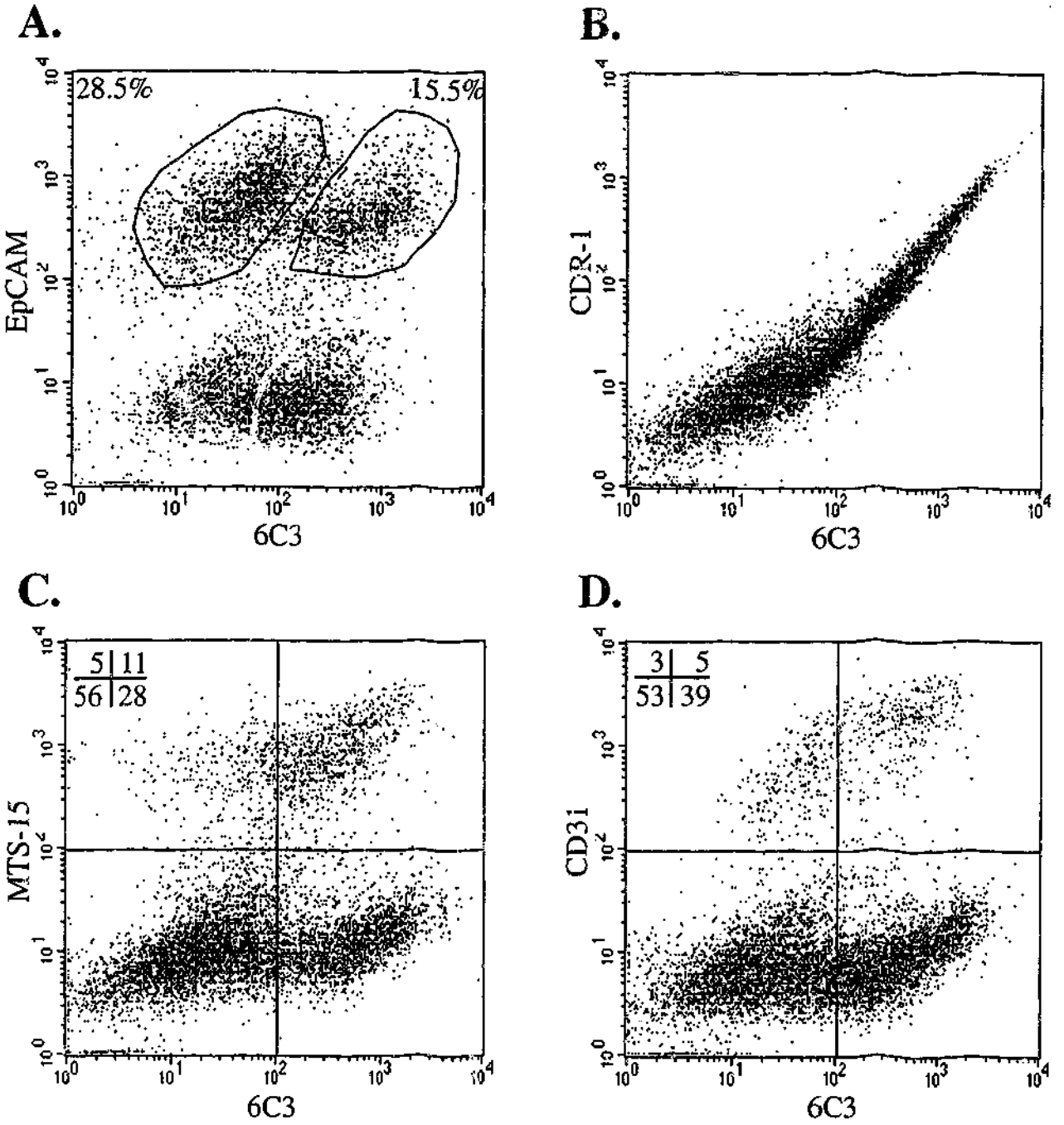
A.
28.5%
15.5%
EpCAM
6C3
B.
CDR-1
6C3
C.
5 | 11
56 | 28
MTS-15
6C3
D.
3 | 5
53 | 39
CD31
6C3

Figure 3.7 Medullary epithelial cell markers on the neonatal thymus.

All profiles are gated on $CD45^-$ cells. UEA-1 is highly expressed on a subset of $EpCAM^+$ cells (**A**). The remaining UEA-1 intermediate events co-express the cortical epithelial cell marker CDR-1 (**B**). Endothelial cells also express intermediate levels of UEA-1 (**C**). The remaining $CD31^-$, UEA-1^- events are presumably fibroblasts and neuroendocrine cells. Representative profiles from 3 experiments are shown.

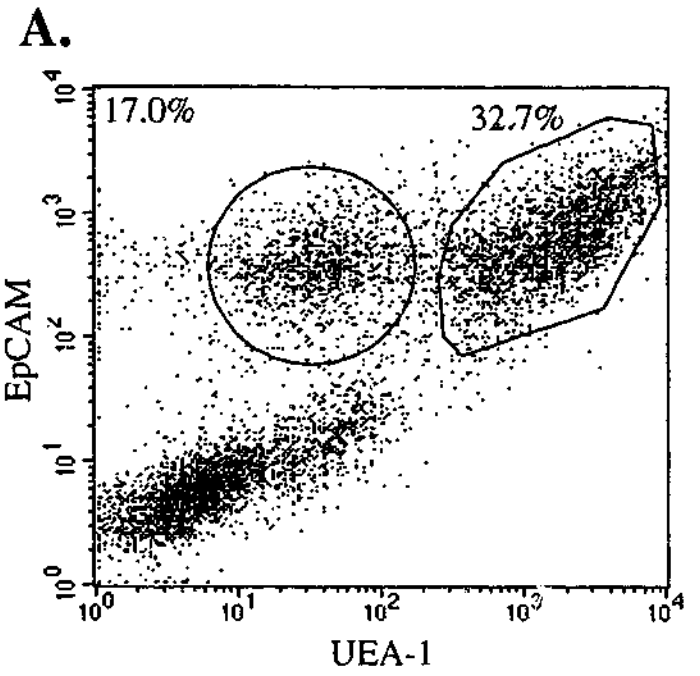
A.
17.0%
32.7%
EpCAM
UEA-1
B.
21%
CDR-1
UEA-1
C.
CD31
UEA-1

observed by immunohistology, since only the intermediates co-labeled with CDR-1 (Fig. 3.7B). Endothelial cells were also found to express intermediate levels of UEA-1 (Fig. 3.7C).

3.3 CONCLUSION

This study refines isolation protocols for thymic stromal cells and characterises the major subsets using a panel of surface reactive mAbs. Collagenase digestion of thymic fragments from 4 wk old and neonatal mice enriched CD45 negative and positive stromal cells appropriate for immunofluorescent labelling and flow cytometry. However, collagenase digestion did not dissociate all $CD45^-$ stromal cells, leaving up to 20% remaining as aggregates. Incubation with trypsin ensures maximal recovery but also cleaves many useful epitopes. The different properties of these enzymes will be an important consideration in the use of stromal cells for phenotypic, genetic and functional analyses.

The various thymic stromal cellular subsets were analysed using a panel of mAbs that had previously been defined using immunohistology. As in the previous study (Izon et al., 1994), a broader distribution of some of these antigens was found, perhaps due to the higher sensitivity of flow cytometry compared to immunohistology. However, the extent of overlap between subsets reported previously was reduced by the exclusion of $CD45^+$ stromal cells from the analysis. Thymic fibroblasts, endothelium, dendritic cells, myeloid cells, cortical and medullary epithelium can be defined into discrete populations using combinations of mAbs to provide quantitative data about the stromal microenvironment (summarised in Table 3.4). Future studies will focus on phenotypic and functional changes to these populations accompanying different thymic states.

Thymic Stromal Cell Subset	Surface Phenotype
Dendritic cells	$CD45^{+}$, $CD11c^{hi}$, MHC II^{hi}
Myeloid derived cells	$CD45^{+}$, $CD11b^{+}$, $CD11c^{-/lo}$, MHC $II^{-/+}$
Cortical epithelial cells	$CD45^{-}$, $EpCAM^{+}$, MHC II^{+}, CDR-1/$Ly51^{+}$, UEA-1^{lo}
Medullary epithelial cells	$CD45^{-}$, $EpCAM^{+}$, MHC II^{+}, CDR-1/$Ly51^{-}$, UEA-1^{hi}
Fibroblasts	$CD45^{-}$, MTS-15^{+}, $EpCAM^{-}$, MHC II^{-}
Endothelial cells	$CD45^{-}$, $CD31^{+}$, $EpCAM^{-}$, MHC $II^{-/lo}$, MTS-$15^{-/+}$

Table 3.4 Surface phenotypes of thymic stromal cell subsets.

CHAPTER 4

The population dynamics, phenotypic maturation and regenerative capacity of thymic stromal cells.

4.1 INTRODUCTION

T-cell development in the thymus is essential for the establishment and maintenance of the adaptive immune system. Thymic stromal cells mediate the various phases of thymocyte development to produce mature T-cells capable of responding to foreign antigen while remaining tolerant of self. It is well established that various subsets of stromal cells form microenvironments in the thymic subcapsule, cortex and medulla to facilitate distinct thymocyte maturational steps (Boyd et al., 1993). The formation and maintenance of thymic microenvironments requires reciprocal interactions between thymocytes and stromal cells, termed thymic "crosstalk" (van Ewijk et al., 1994). While much is known about the biology of thymocytes, our understanding of thymic stromal cells is lacking.

Early research demonstrated the heterogeneity of murine thymic stromal cells using monoclonal antibodies specific for various stromal determinants (for example Godfrey et al., 1988). These reagents have proven useful for defining the epithelium, endothelium, fibroblasts, dendritic cells and macrophages within thymic microenvironments. The thymic cortex is characterised by a meshwork of interconnecting, reticular cortical epithelial cells (cTECs) that can be identified by distinctive patterns of intracellular (eg. MTS-44, K8) and surface (eg. Ly51) antigen expression (Godfrey et al., 1988; Surh et al., 1992a; Klug et al., 1998). Markers such as K5, MTS-10 and UEA-1 distinguish mTECs from cTECs, and differential expression of MHC II and B7 indicates further heterogeneity within this

population (Farr and Anderson, 1985; Klug et al., 1998; Naquet et al., 1999). Early T-cell development involves the migration of immature double negative (DN, $CD4^-CD8^-$) thymocytes through the cTEC network towards the subcapsule (Lind et al., 2001). Fibroblasts that line this region facilitate DN thymocyte development through the provision of extracellular matrix components (Anderson et al., 1997). Maturing thymocytes then return through the cortex where cTECs mediate the process of positive selection, rescuing TcR^+ double positive thymocytes (DP, $CD4^+CD8^+$) capable of interacting with self-peptide:MHC from programmed cell death (Anderson and Jenkinson, 2001). Continued migration towards the medulla brings thymocytes in contact with dendritic cells and medullary epithelial cells (mTECs) that induce the apoptosis or anergy of potentially autoreactive thymocytes in a process termed negative selection (Sprent and Webb, 1995; Sebzda et al., 1999). Thymocytes surviving negative selection mature into $CD4^+$ or $CD8^+$ single positive (SP) T-cells within this microenvironment prior to export to the periphery. The precise role of mTECs in T-cell development is still unclear, however roles in tolerance induction to peripheral antigens and thymic emigration are emerging (Anderson et al., 2002; Ueno et al., 2002).

The generation and maintenance of these microenvironments requires the presence developing thymocytes. While medullary markers are detectable on rare TECs at E13, it is not until the appearance of the first SP thymocytes that medullary islets similar to those in adults become apparent (E15-17) (van Ewijk, 1991). Studies of mutant mice with various arrests in thymocyte development characterised corresponding blocks in thymic microenvironments. Thus, immature DN thymocytes were required to induce the development of cTECs, while mature SP thymocytes were necessary for normal medullary microenvironments (Hollander et al., 1995b; van Ewijk et al., 2000a). These microenvironmental arrests could be overcome by reconstitution with normal bone marrow,

although in the case of the cortex, this had to be performed before 1 week of age (Wang et al., 1997).

Analysis of the expression of keratin subunits at the various TEC developmental control points identified early $K5^+K8^+$ cells that could give rise to $K5^-K8^+$ cTECs, suggesting a precursor:product relationship (Klug et al., 1998). Direct evidence for a similar precursor of mTECs was provided by elegant experiments using chimeric mice (Rodewald et al., 2001). These studies have been supported by the finding that $K5^+K8^+$ TECs were present in a subpopulation of embryonic MTS-24^+ TECs that were capable of forming all thymic microenvironments in ectopic grafts (Bennett et al., 2002; Gill et al., 2002). Further assessment of the potential of various adult TEC subsets requires their purification for direct lineage analysis. The definition of TEC surface markers at various stages of differentiation is necessary for such experiments.

Once established, the various thymic microenvironments appear to remain relatively constant as the thymus expands during murine adolescence. Following puberty, circulating sex steroids cause the gradual involution of the thymus, resulting in a reduction of thymic size, disruption of architecture and reduced function (Staples et al., 1999; Tibbetts et al., 1999; Olsen et al., 2001). A decrease in numbers of recent thymic emigrants has been found to lead to the homeostatic expansion of peripheral memory T-cells, resulting in a narrowing T-cell diversity (Haynes et al., 2000a; Berzins et al., 2002). This has been associated with a reduced capacity to resist disease and increased likelihood of autoimmunity in the aged (Mackall and Gress, 1997; Aspinall and Andrew, 2000). One approach to ameliorate these problems involves sex steroid ablation to induce thymic regeneration. The regenerated aged thymus of castrated aged mice exhibited normal young architecture, levels of thymic export and peripheral immunity (Sutherland, 2001). While thymic stromal cells are central to sex steroid induced thymic involution and regeneration (Olsen et al., 2001), there is currently little data describing the status of this compartment in these thymic states.

In this study, flow cytometry was employed to enumerate thymic stromal cells in the embryonic, neonatal, adult, involuted and regenerating thymus. These data demonstrate that the stroma expands and contracts with changing thymocyte numbers, maintaining a relatively stable thymocyte to stromal cell ratio following puberty. Changes in the overall composition of the stroma were observed in the aged thymus. Castration of 12 month old mice induced stromal cell expansion and a restoration of subset ratios in the regenerating thymus. Analyses of Ki67 expression indicated that both medullary and cortical MHC II^{hi} TECs continued to divide throughout life. Phenotypic changes in TECs observed during embryogenesis and postnatal life showed a skewing from MHC II^{hi} cTECs to MHC II^{hi} mTECs. After one week post-parturition, the emergence of MHC II^{lo}/$CD40^{-}$/$CD80^{-}$ cortical and medullary TECs was apparent, coinciding with the reported "developmental window" of TEC differentiation (Wang et al., 1997). These findings were correlated with phenotypes observed in $RAG^{-/-}$ and $TcR\alpha^{-/-}$ mice, suggesting that DN and DP thymocytes induced changes in surface phenotype within the TEC population. This study provides fundamental data on thymic stromal cell biology, demonstrating a far more dynamic cell population than previously recognised.

4.2 RESULTS

4.2.1 $CD45^{-}$ thymic stromal cell numbers change with age.

To test the hypothesis that $CD45^{-}$ thymic stromal cell populations remodelled throughout varying thymic states, this population was quantified during ontogeny, steady-state adult expansion and thymic involution with age. Flow cytometric analysis of stromal cells (Chapter 3) at these phases of development was employed to enumerate total thymic cellularity and numbers of $CD45^{-}$ stromal cells (predominantly epithelium, fibroblasts and endothelium) per thymus.

Total thymic cellularity ($CD45^+$ and $CD45^-$ cells) roughly doubled each day during late embryogenesis and continued to expand following birth until peaking at 4 weeks of age (Fig 4.1 A). Following the onset of puberty (after 4 weeks), thymic cellularity decreased upon thymic involution, falling to neonatal levels at 12 months and beyond (Fig. 4.1 A & data not shown). $CD45^-$ cell numbers followed the trends in thymocyte numbers, expanding rapidly throughout thymic ontogeny and the neonatal period, until reaching a peak of 4.6×10^5 at 4 weeks of age (Fig. 4.1 B). Consistent with the declining cellularity of the involuting thymus, $CD45^-$ cell numbers steadily fell after 4 weeks to 2.0×10^5 at 12 months of age.

In terms of their relative proportions, $CD45^-$ thymic stromal cells composed 16% of the E14 thymus, representing a thymocyte to stromal cell ratio of 5.5 (Fig. 4.1 B and C). Upon extensive proliferation of thymocytes, the stromal proportion was diluted to about 1% by E18 and to 0.5% of thymic cellularity following birth. Postnatal changes in stromal cell composition were more obviously reflected in alterations of thymocyte to stromal cell ratios (Fig. 4.1 C). The steady neonatal increase in this ratio from about 200 to 480 in the 4 week-old thymus may reflect reduced stromal cell contact with thymocytes. This ratio fell following puberty and was maintained between 280 and 360 thereon, indicating a degree of flexibility in this index.

Taken together, these data support the hypothesis that stromal cells are capable of undergoing extensive numerical changes throughout varying thymic states in association with thymocytes, highlighting the integrated nature of thymopoiesis.

Figure 4.1 Thymic stromal cells change in number and proportion throughout development.

A. Developmental changes in total thymic cellularity with age, showing thymic expansion and involution. **B.** $CD45^-$ thymic stromal cell number per thymus (blue) and the proportion of thymic cellularity they constitute (red) changes over time. Means and standard errors from 2-5 experiments derived from collagenase/Dispase digests of at least 3 pooled thymi for each time point are shown for all graphs.

A.

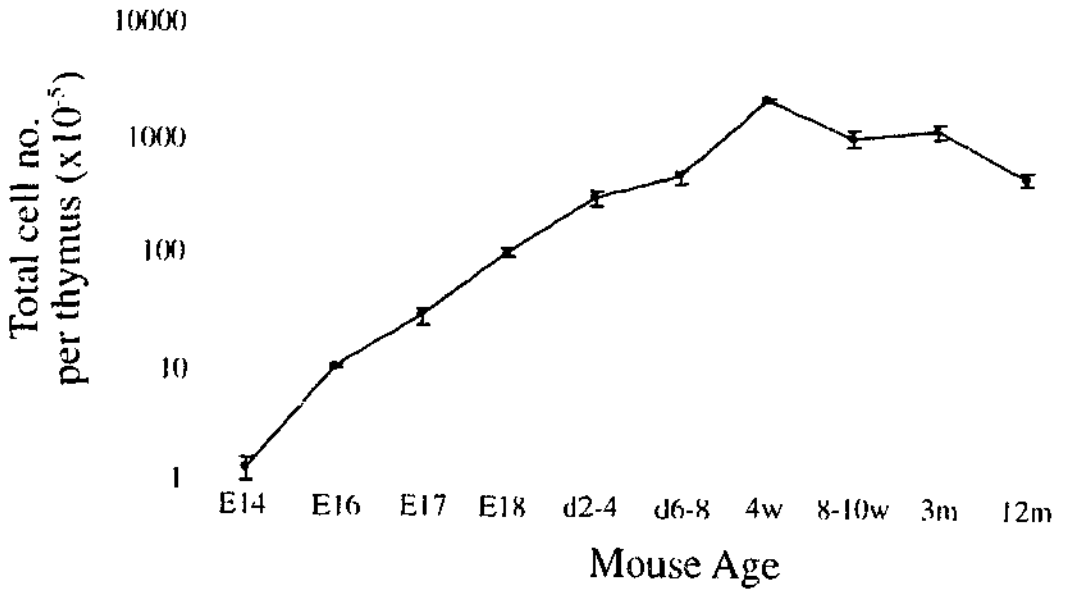
Total cell no. per thymus (x10⁻⁵)
10000
1000
100
10
1
E14
E16
E17
E18
d2-4
d6-8
4w
8-10w
3m
12m
Mouse Age

B.

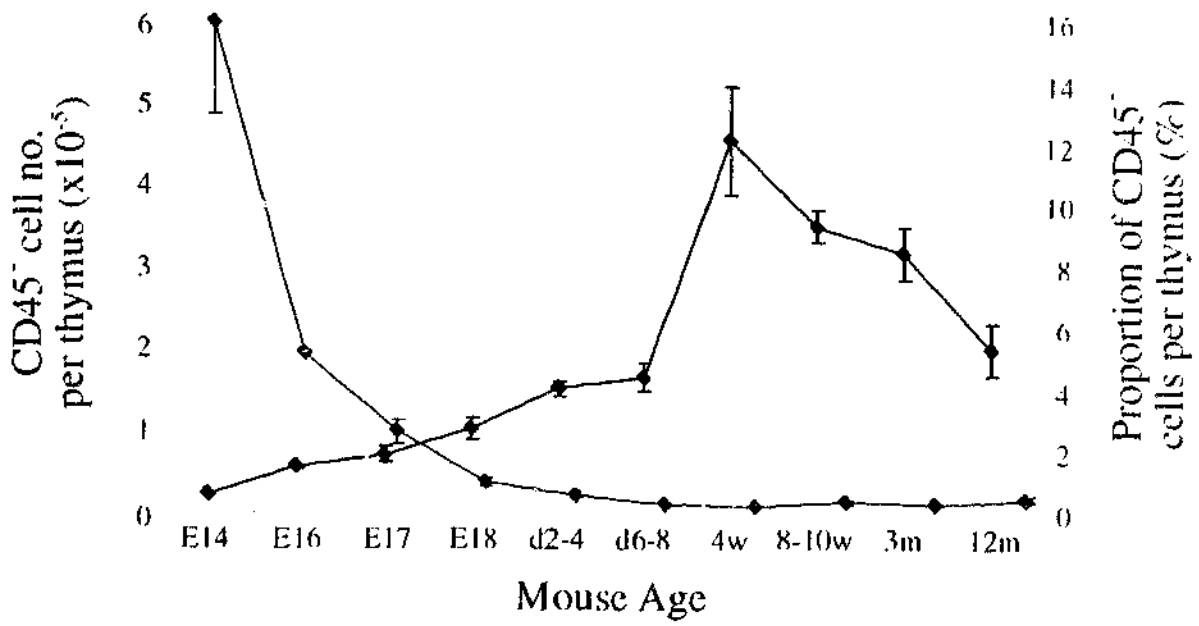
CD45⁻ cell no. per thymus (x10⁻⁵)
6
5
4
3
2
1
0
Proportion of CD45⁻ cells per thymus (%)
16
14
12
10
8
6
4
2
0
E14
E16
E17
E18
d2-4
d6-8
4w
8-10w
3m
12m
Mouse Age

C.


Thymocyte:CD45⁻ stromal cell ratio
600
500
400
300
200
100
0
E14
E16
E17
E18
d2-4
d6-8
4w
8-10w
3m
12m
Mouse Age

4.2.2 Alterations in CD45⁻ thymic stromal composition.

Given the changes in total stromal cell numbers throughout development, the composition of the CD45⁻ population was assessed at different time points. Monoclonal antibodies specific for thymic fibroblasts (MTS-15), endothelium (CD31) and the epithelial cells (MHC II) (Chapter 3) were used to characterise the phenotype of CD45⁻ stromal cells at various time points. Table 4.1 shows that the cell numbers for all subsets peaked at 4 weeks of age when the thymus was largest. In all but the 12 month time point, thymic epithelial cells (TECs) represented the major stromal cell type within this population, with proportions of thymic endothelium and fibroblasts remained relatively stable throughout.

Figure 4.2 (A) shows the relative proportions of different stromal cell subsets, excluding unlabelled events. Although subset proportions are relatively stable throughout late ontogeny and young adulthood, marked differences were apparent in the aged thymus. The proportion of TECs fell to almost half that of 4 week old mice, with a corresponding increase in fibroblasts. The ratio of TEC:fibroblasts was significantly lower in aged mice compared to 4 week old adults (Fig. 4.2 B).

4.2.3 TEC phenotype changes with age.

These changes in the major stromal cell populations with age prompted examination of TECs phenotype at these time points. All thymic epithelium ($EpCAM^+$) was found to express MHC II throughout life, although at varying levels (Fig 4.3A). Expression of the cortical epithelial cell marker Ly51 was used to differentiate MHC II^+ cTECs and mTECs (Surh et al., 1992b) (Chapter 3) (Fig 4.3B). Ly51 was also detected on MHC II^- fibroblasts (Chapter 3) (Fig4.3B). The costimulatory molecules CD40 and CD80 (B7.1), and the putative TEC precursor marker MTS-24 were found to be differentially expressed on TECs over time (Fig 4.3C, 4.3D and 4.3E).

Figure 4.2 The composition of the CD45$^-$ thymic stromal cell population differs between young and aged mice.

A. Percentage of CD45$^-$ thymic stromal cells that epithelium (EpCAM$^+$), endothelium (CD31$^+$) and fibroblasts (MTS-15$^+$) constitute at various ages. The numbers of CD45$^-$ stromal cells obtained per thymus for each time point are shown. Bar graphs of the ratios of TECs:fibroblasts (**B**), mTECs:cTECs (**C**), and MHC II^{hi}:MHC II^{lo} TECs (**D**) in 4wk old and aged (>12months old) thymi. Means and standard errors are plotted and groups were compared using a Mann-Whitney rank-sum U test. (* $p<0.05$, ** $p<0.01$, *** $p<0.001$).

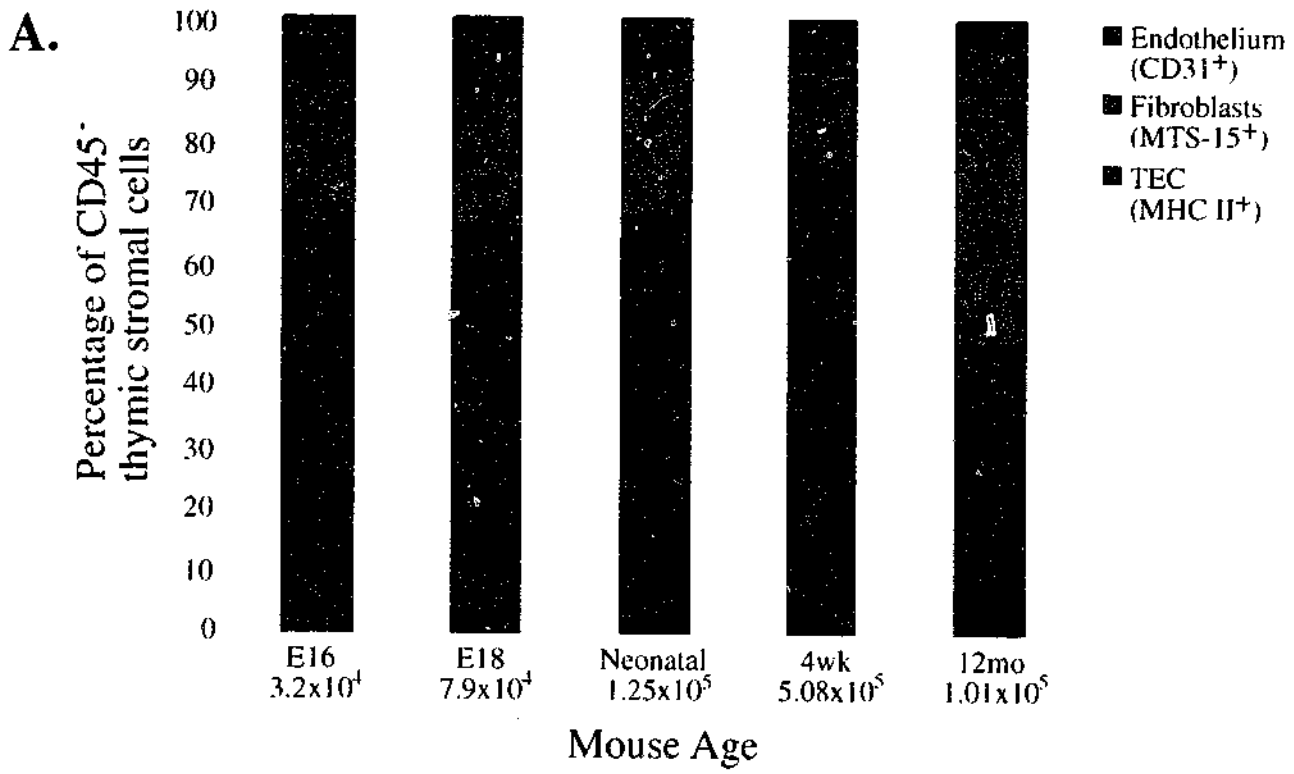
A.
Percentage of CD45⁻ thymic stromal cells
100
90
80
70
60
50
40
30
20
10
0
E16
3.2x10⁴
E18
7.9x10⁴
Neonatal
1.25x10⁵
4wk
5.08x10⁵
12mo
1.01x10⁵
Mouse Age
Endothelium (CD31⁺)
Fibroblasts (MTS-15⁺)
TEC (MHC II⁺)

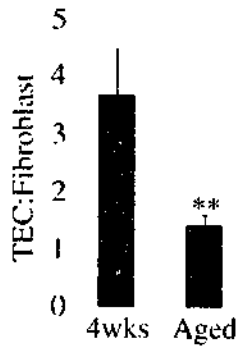
B.
TEC:Fibroblast
5
4
3
2
1
0
**
4wks
Aged

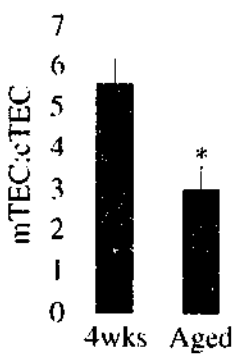
C.
mTEC:cTEC
7
6
5
4
3
2
1
0
*
4wks
Aged

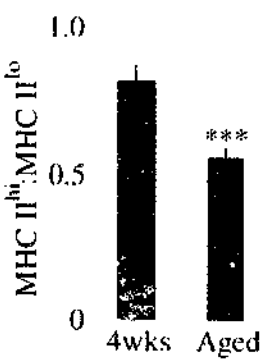
D.
MHC II^hi:MHC II^lo
1.0
0.5
0
***
4wks
Aged

Table 4.1 Numbers and proportions of CD45$^-$ thymic stromal subsets at various time points.

CD45$^-$ thymic stromal cell number and proportions are shown, followed by the percentage of this population constituted by epithelium (EpCAM$^+$), endothelium (CD31$^+$), fibroblasts (MTS-15$^+$) and events that do not label with any of these markers (other). Epithelial subsets (cTECs/mTECs and MHC II^{hi}/MHC II^{lo} TECs) are also shown, with bold numbers indicating proportions of total epithelium. Representative data from 2-5 experiments for each time point are shown.

	E16	E18	D5-6	4w	12m
Cells/thy ($x10^{-7}$)	0.10	1.22	8.82	22.9	2.96
$CD45^-$ no./thy ($x10^{-5}$)	0.45	1.29	1.42	5.31	1.60
$CD45^-$ %	4.46	1.05	0.30	0.23	0.54
TEC %	50.7	51.5	60.0	73.1	29.6
TEC no./thy ($x10^{-4}$)	2.26	6.64	8.52	38.8	4.7
Fibroblast %	14.8	16.5	20.0	14.9	25.9
Fibroblast no./thy ($x10^{-4}$)	0.66	2.13	2.84	7.92	4.14
Endothelium %	7.2	9.7	8.0	7.5	7.4
Endothelium no./thy ($x10^{-4}$)	0.32	1.25	1.14	3.99	1.18
Other %	27.3	22.3	12.0	4.5	37.1
Other no./thy ($x10^{-4}$)	1.22	2.88	1.70	2.39	5.92
cTEC %	**99.6**	**75.0**	**16.2**	**14.3**	**43.8**
cTEC no./thy ($x10^{-4}$)	2.25	4.98	1.38	5.55	2.07
mTEC %	**0.4**	**25.0**	**83.8**	**85.7**	**56.2**
mTEC no./thy ($x10^{-4}$)	0.01	1.66	7.14	33.25	2.66
mTEC:cTEC ratio	**0.00**	**0.33**	**5.17**	**5.99**	**1.28**
$MHC\ II^{hi}$ TEC %	**78.2**	**80.8**	**70.2**	**55.5**	**25**
$MHC\ II^{hi}$ TEC no./thy ($x10^{-4}$)	1.77	5.37	5.98	21.56	1.18
$MHC\ II^{lo}$ TEC %	**21.8**	**19.2**	**29.8**	**44.5**	**75**
$MHC\ II^{lo}$ TEC no./thy ($x10^{-4}$)	0.49	1.28	2.54	17.28	3.55
$MHC\ II^{hi}$:$MHC\ II^{lo}$ ratio	**3.59**	**4.21**	**2.36**	**1.25**	**0.33**
$MTS\text{-}24^+$ TEC %	-	**10**	**32.8**	**38.1**	**37.6**

Figure 4.3 Thymic epithelial cells change phenotype with age.

All dot plots are gated on $CD45^-$ thymic stromal cells isolated from at least 3 pooled thymii at the ages indicated and are representative of 2-5 experiments performed. **A.** Staining with antibodies to MHC II and EpCAM demonstrated that almost all TECs express MHC II A MHC II^{lo} population became apparent after 4 weeks of age. **B.** MHC II^{hi} TECs were found to express the costimulatory molecule CD40, and the majority co-expressed CD80 at 3 days of age (**C**). **D.** The cortical epithelial cell marker Ly51 discriminated two subsets of epithelial cells. The majority of $Ly51^+$ cTECs were MHC II^{lo} in adult mice. **E.** The putative precursor marker MTS-24 stained a subset of MHC II^{hi} TECs at early time points and MHC II^{lo} TECs in adult mice. **F.** Analysis of MHC II and EpCAM expression on neonatal TECs at 3, 8 and 16 days of age indicated the MHC II^{lo} population gradually emerges during the first week.

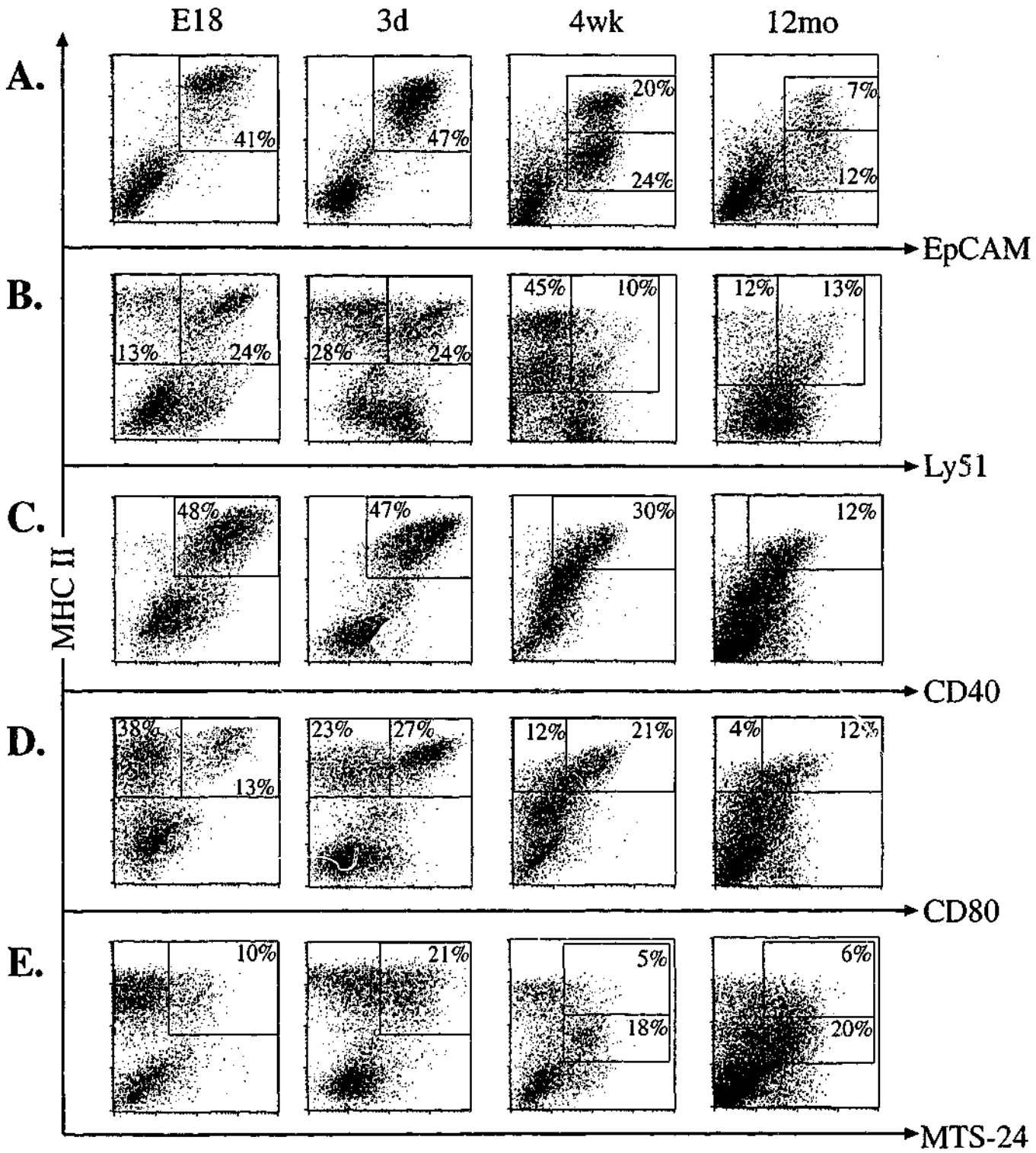
E18
3d
4wk
12mo
A.
41%
47%
20%
24%
7%
12%
EpCAM
B.
13%
24%
28%
24%
45%
10%
12%
13%
Ly51
C.
48%
47%
30%
12%
MHC II
CD40
D.
38%
13%
23%
27%
12%
21%
4%
12%
CD80
E.
10%
21%
5%
18%
6%
20%
MTS-24

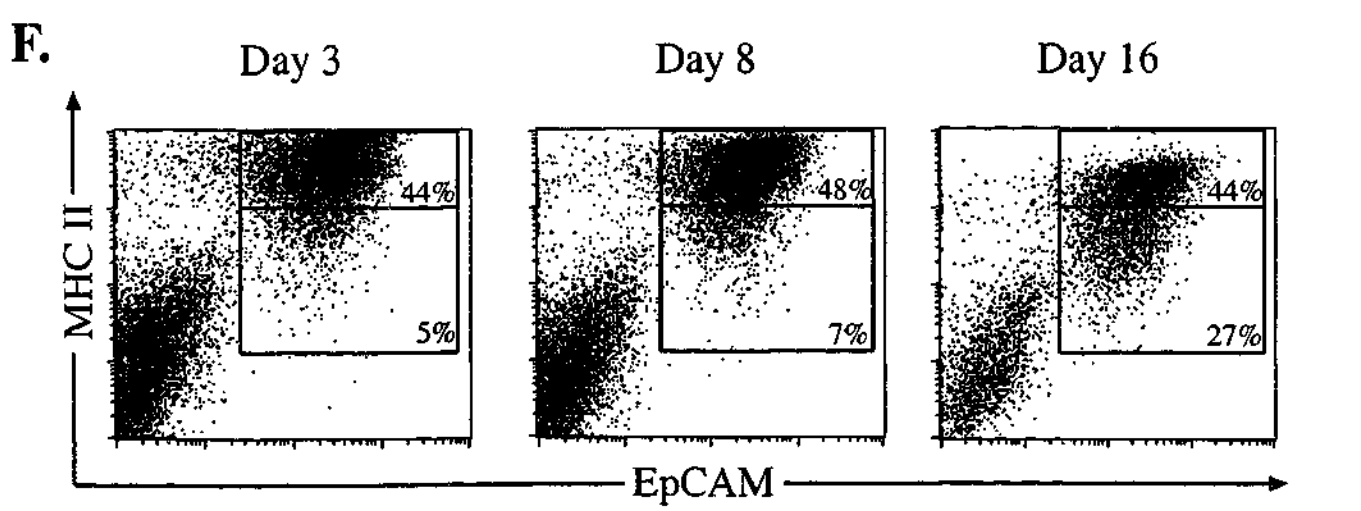
F.
Day 3
Day 8
Day 16
44%
5%
48%
7%
44%
27%
MHC II
EpCAM

At E18, the majority of TECs were MHC II^{hi}, CD40^{+} cortical epithelial cells (Fig 4.3 and Table 4.1). This distribution was maintained in 3 day-old neonatal thymi, however there was an increased MHC II^{hi}, CD40^{+} mTEC compartment. This trend continued through to 4 weeks, where mTECs considerably outnumbered cTECs approximately five-fold (Fig 4.2C, 4.3B and Table 4.1). A MHC II^{lo}, CD40^{-} TEC population also emerged at this time point. In the adult, most cTECs (Ly51^{+}) expressed low levels of MHC II, although a minor MHC II^{hi} cTEC subset was still apparent (Fig 4.3 B). Significant populations of MHC II^{lo} TECs were first detected 2 weeks after birth, proportionally increasing throughout adult life to comprise a major TEC subset in aged mice (Fig. 4.2D, 4.3F and Table 4.1). TEC subsets in the 12 month-old thymus were skewed towards the MHC II^{lo}, cTEC phenotype, compared to 4 week-old mice (Fig 4.2 C and D).

Consistent with previous reports (Nelson et al., 1993; Degermann et al., 1994), CD80 (B7.1) expression was detected on MHC II^{hi} mTECs (Fig 4.3 D and B). CD86 (B7.2) expression was undetectable at all time points (data not shown). Reactivity with the putative precursor TEC marker MTS-24 was predominantly restricted to MHC II^{lo} TECs in the adult (Fig 4.3 E and Gill et al., 2002). Together, these data describe marked phenotypic and compositional alterations of the TEC populations with age.

4.2.4 Influence of thymocyte development upon TEC surface phenotype.

To further investigate TEC maturation, the expression of TEC surface markers was analysed on stromal cells from adult RAG-1$^{-/-}$ and TcR$\alpha^{-/-}$ mice. These mutants have well characterised arrests in thymocyte development at the DN to DP and DP to SP transitions. Corresponding blocks in CD45^{-} EpCAM^{+} TEC maturation were observed in both groups (Fig. 4.4). The predominant phenotype of RAG$^{-/-}$ TECs was Ly51^{hi}/MHC II^{hi}/CD40^{+}, the same cTEC population observed during late embryogenesis (Fig 4.4 and Table 4.2). The presence of DP thymocytes in the TcR$\alpha^{-/-}$ appeared to permit differentiation or expansion of

Figure 4.4 CD45$^-$ thymic stromal cells in RAG-1$^{-/-}$, TcR$\alpha^{-/-}$ and normal mice.

A. TECs gated on CD45$^-$EpCAM$^+$ stromal cells from RAG$^{-/-}$, TcR$\alpha^{-/-}$ and wildtype control mice stained with anti-MHC II and anti-Ly51 demonstrate the blocks in epithelial subsets. **B.** CD31 and MHC II expression on total CD45$^-$ stromal cells from mutant and normal mice. **C.** MHC II expression versus MTS-15 staining on total CD45$^-$ stromal cells from knockout and normal mice. Proportions of CD45$^-$ cells and numbers per thymus are indicated above appropriate regions. The shift of MHC II^{hi} cells observed in plots in **B** and **C** was also observed in the isotype controls, therefore non-specific. Regions were set to minimise background staining (>1%).

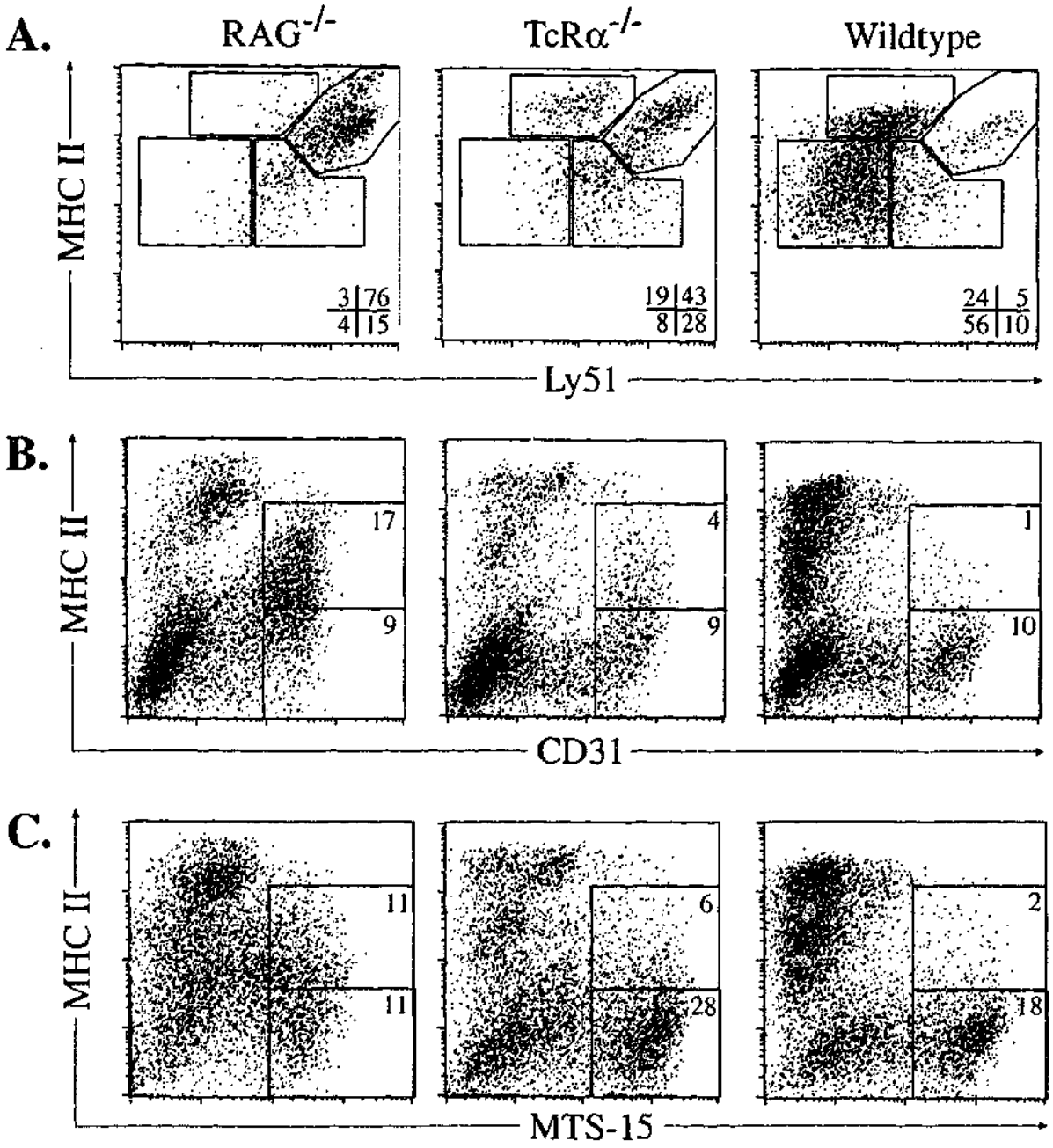
A.
RAG-/-
TcRα-/-
Wildtype
MHC II
3 76
4 15
19 43
8 28
24 5
56 10
Ly51
B.
MHC II
17
9
4
9
1
10
CD31
C.
MHC II
11
11
6
28
2
18
MTS-15

		CD40	CD80	MTS-24
Wildtype	MHC $II^{hi}/Ly51^{hi}$	+	-	-
	MHC $II^{lo}/Ly51^{lo}$	low	-	-
	MHC $II^{hi}/Ly51^{lo/-}$	+	+	-
	MHC $II^{lo}/Ly51^{-}$	low	low	+
$TcR\alpha^{-/-}$	MHC $II^{hi}/Ly51^{hi}$	-/low	-	-
	MHC $II^{lo}/Ly51^{lo}$	-	-	-
	MHC $II^{hi}/Ly51^{lo/-}$	+	+	-
	*MHC $II^{lo}/Ly51^{-}$	-	-	-
$RAG^{-/-}$	MHC $II^{hi}/Ly51^{hi}$	low	-	-
	*MHC $II^{lo}/Ly51^{lo}$	-	-	-
	*MHC $II^{hi}/Ly51^{lo/-}$	-	-	-
	*MHC $II^{lo}/Ly51^{-}$	-	-	-

Table 4.2 TEC phenotypes from wildtype, $TcR\alpha^{-/-}$ and $RAG^{-/-}$mice.

$CD45^{-}$ $EpCAM^{+}$ stromal cells from the mice indicated were divided into subsets (gated as in Figure 4.4) and the expression of CD40, CD80 and the MTS-24 antigen assessed compared to isotype controls. +; positive staining, low; low staining, -; no staining above control, -/+; positive and negative populations present, -/low; low staining and negative populations present. * subset not present.

MHC II^{lo}, Ly51^{lo}, CD40^{-} cTECs and MHC II^{hi}, Ly51$^{lo/-}$ CD40^{+}, CD80^{+} mTECs (Fig 4.4 and Table 4.2). The presence of SP thymocytes in normal mice correlates with a proportional increase in MHC II^{lo} and MHC II^{hi} mTECs. Collectively, these data suggest early differentiation of MHC II^{hi} TEC precursors into MHC II^{hi} mTECs and MHC II^{lo} cTECs requires interactions with DP thymocytes and the development of MHC II^{lo} mTECs is dependent upon the presence of SP thymocytes.

MTS-15^{+} fibroblasts and CD31^{+} endothelial cells were proportionally increased in thymii devoid of mature thymocytes, while TEC frequency was reduced (Fig 4.4). A predominance of MHC II^{lo} endothelial cells compared to MHC II^{-} endothelium in the RAG$^{-/-}$ mouse probably reflects the lack of extensive cortical capillaries in this thymus (Fig 4.4 and Chapter 3).

4.2.5 Proliferative status of thymic stromal subsets.

To investigate a possible link between thymic epithelial development and the skewing of TEC phenotype, the proliferative capacities of the different populations was analysed using expression of the nuclear antigen Ki67 to indicate cell division (Gerdes et al., 1984). Increased division in a particular subset might account for the larger proportions they constitute in downstream time points. This seemed to be the case in the mTEC compartment, where increased expression of Ki67 compared to cTECs at E16 and E17 preceded the proportional expansion of this population (Fig. 4.5 A & Table 4.1). However, Ki67 expression did not partition exclusively into any of the embryonic subsets analysed, demonstrating that division occurred in all major epithelial cell types. In the 4 week old steady-state adult thymus, a much lower proportion of Ki67^{+} TECs was observed among both cortical and medullary TEC subsets (Fig. 4.5 B & C). Most Ki67 TECs were MHC II$^{int/hi}$, although these cells were distributed equally between the cortical and medullary compartments. Short term continuous exposure (3 days) of 4 week old mice to BrdU

Figure 4.5 Proliferation capacities of TEC subsets throughout development.

A. Histograms of Ki67 expression on $CD45^-$ $MTS\text{-}24^+$, $Ly51^+$ (cTECs) and $Ly51^-$ (mTECs) from embryonic mice at E14, E16 and E17 (solid line) versus isotype control staining (dotted line). Markers are set according to minimal (<1%) isotype control staining, with percentages bounded indicated. **B.** Dot plot of MHC II versus Ki67 expression on $CD45^-$ stromal cells from 4wk old thymi, with a region indicating proportion of $Ki67^+$ TECs. Data representative of 7 experiments performed. **C.** Histograms of Ki67 expression on cTECs and mTECs with markers set according to isotype controls. Representative of 3 experiments performed. **D.** MHC II versus Ki67 expression on $CD45^-$ stromal cells from 12 month old thymi, with region indicating proportion of $Ki67^+$ TECs. Data representative of 3 experiments performed. **E.** MHC II expression versus BrdU incorporated into 4 wk old $CD45^-$ stromal cells over a 3 day exposure. The proportion of $BrdU^+$ TECs bounded by set region is indicated.

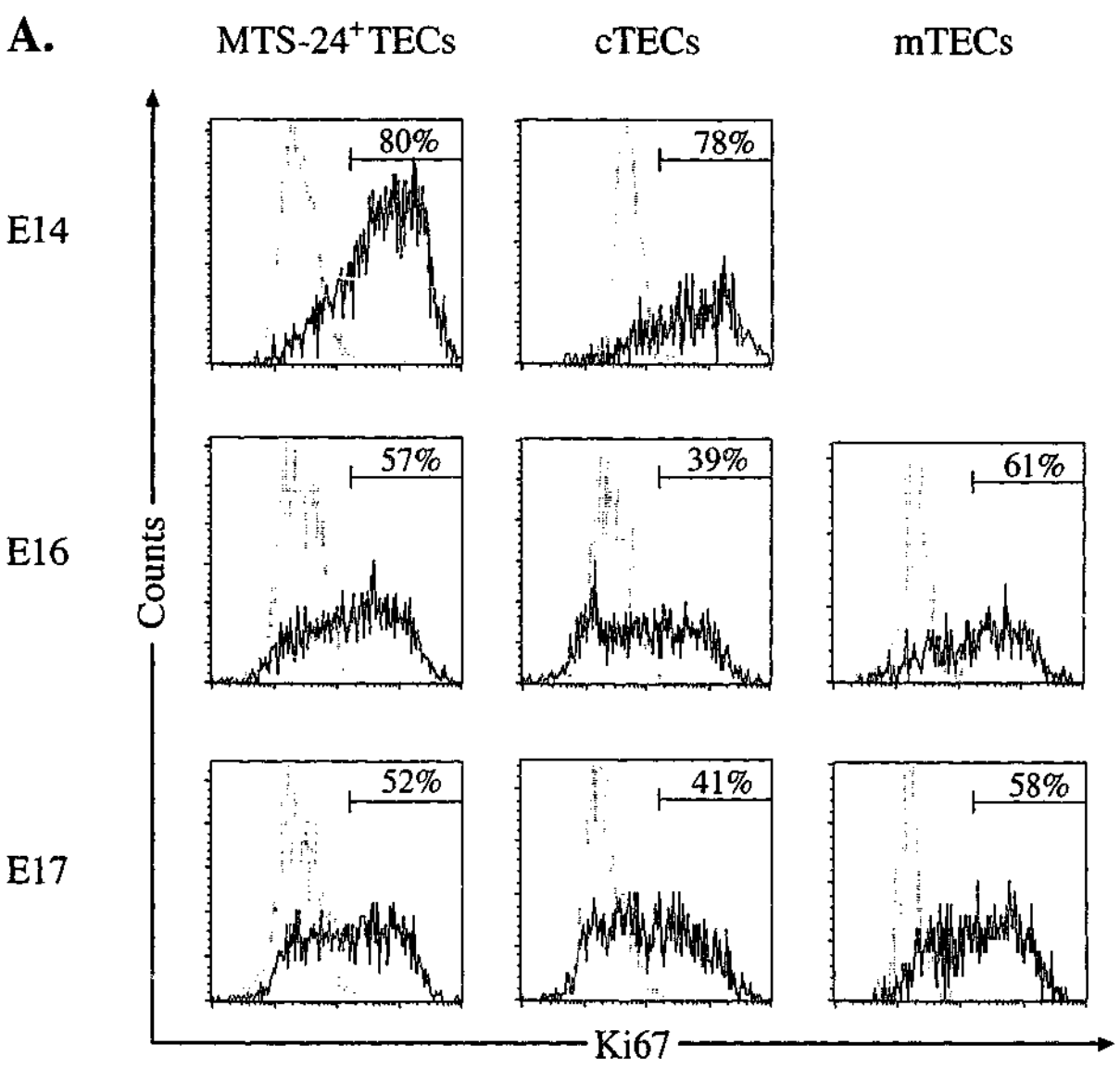
A.
MTS-24+TECs
cTECs
mTECs
E14
E16
E17
80%
78%
57%
39%
61%
52%
41%
58%
Counts
Ki67

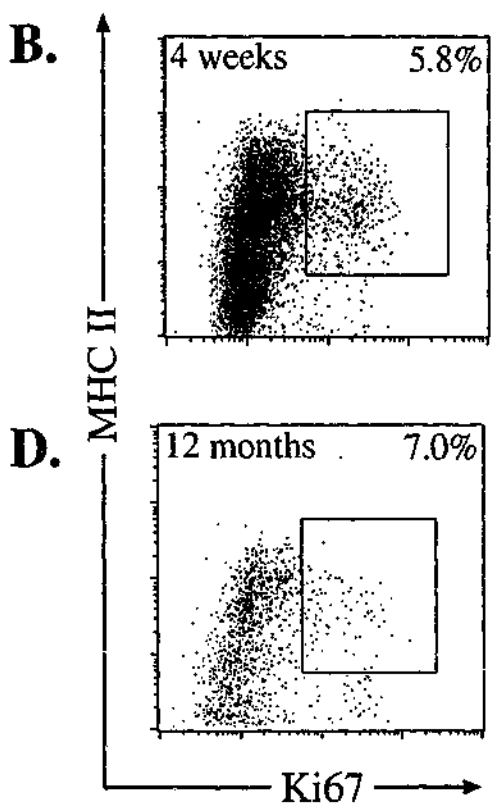
B.
4 weeks
5.8%
MHC II
Ki67
D.
12 months
7.0%
Ki67

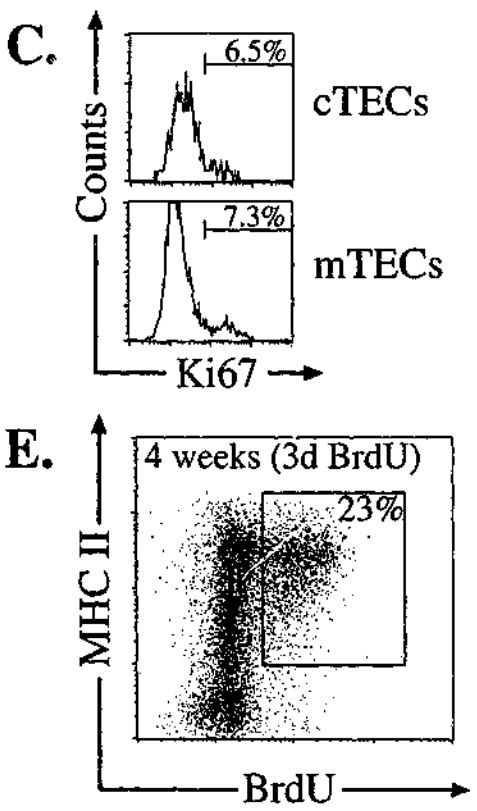
C.
6.5%
cTECs
7.3%
mTECs
Counts
Ki67
E.
4 weeks (3d BrdU)
23%
MHC II
BrdU

revealed a predominantly MHC II^{hi} phenotype of $BrdU^+$ TECs (Fig. 4.5 E). The proportion of cells labelled in this period and the frequency of $Ki67^+$ TECs was consistent with roughly three divisions of a stably dividing population. The aged thymus exhibited a comparable proportion and phenotype of $Ki67^+$ TECs to the 4 week old thymus, suggesting a similar level of epithelial cell division (Fig. 4.5 D).

4.2.6 Castration induced regeneration of thymic stroma in aged mice.

To further test the ability of stromal cells to remodel, aged mice were castrated and the stroma analysed. Surgical castration has been shown to reverse sex steroid induced thymic involution, causing regeneration of the thymus in aged mice by acting on thymic stromal cells (Olsen et al., 2001). While this expansion resembles that in the neonatal and young adult thymus, whether the aged stroma undergoes a similar expansion remains unknown.

A series of three experiments analysing thymic stromal cells of aged mice at various time points after castration were performed, with the kinetics of regeneration shown in Figure 4.6. Two of these time courses showed the greatest increase in thymic cellularity between days 7 and 14, in accordance with previous studies (Sutherland, 2001). However, Experiment 2 showed a more rapid recovery, with thymic cellularity almost tripling between days 3 and 7 (Fig. 4.6). TECs showed a similar trend to thymic recovery, although after a delay of 7 to 14 days following increases in total thymic cellularity (Fig. 4.7). These data demonstrate that the aged thymic epithelium is capable of expansion during thymic regeneration induced by castration.

The phenotype of TECs was assessed to determine whether compositional changes accompanied thymic regeneration. While sham-castrated TEC ratios remained relatively constant, the ratio of MHC II^{hi}:MHC II^{lo} TECs had increased to beyond young levels (0.8, Fig 4.2D) by days 14 to 28 in castrated mice (Fig. 4.8). This distribution was maintained at least 2 months after surgery (Fig. 4.8 B). A similar remodelling of TECs was observed in

Figure 4.6 Kinetics of thymic regeneration following surgical castration of aged mice. Three thymi from each of the groups indicated were pooled and digested in collagenase/Dispase and the total thymic cellularity per thymus calculated. **A.** Bar graph of data from the first time course performed, with an untreated control group of 12 month old C57BL-6 mice. **B.** The second experiment performed included a sham castrated group and analysed mice up to 2 months after surgery. **C.** A third experiment re-analysed the first four time points with a sham castrated group. C57BL-6 mice at 12 months of age were used in all experiments.

A.

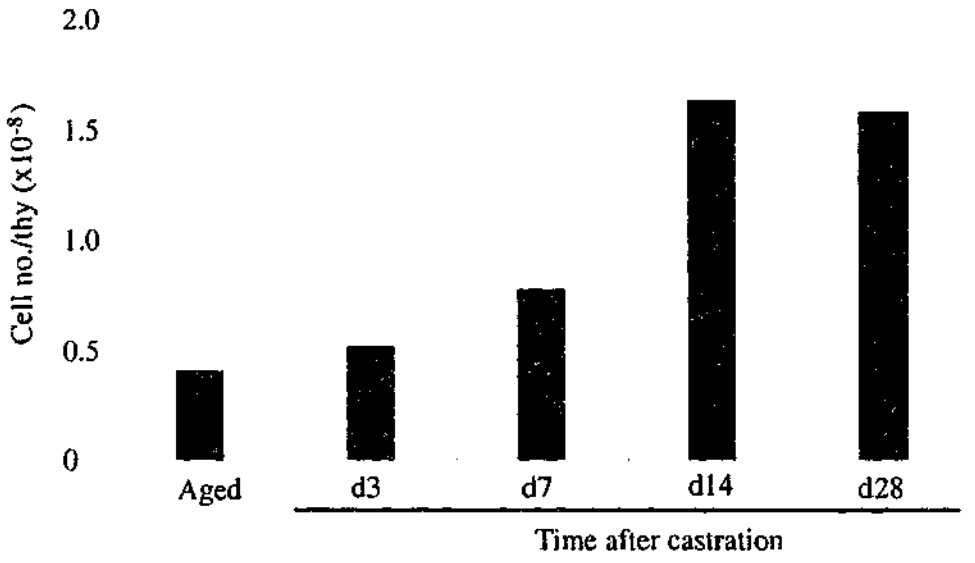
2.0
1.5
1.0
0.5
0
Cell no./thy (x10-8)
Aged
d3
d7
d14
d28
Time after castration

B.

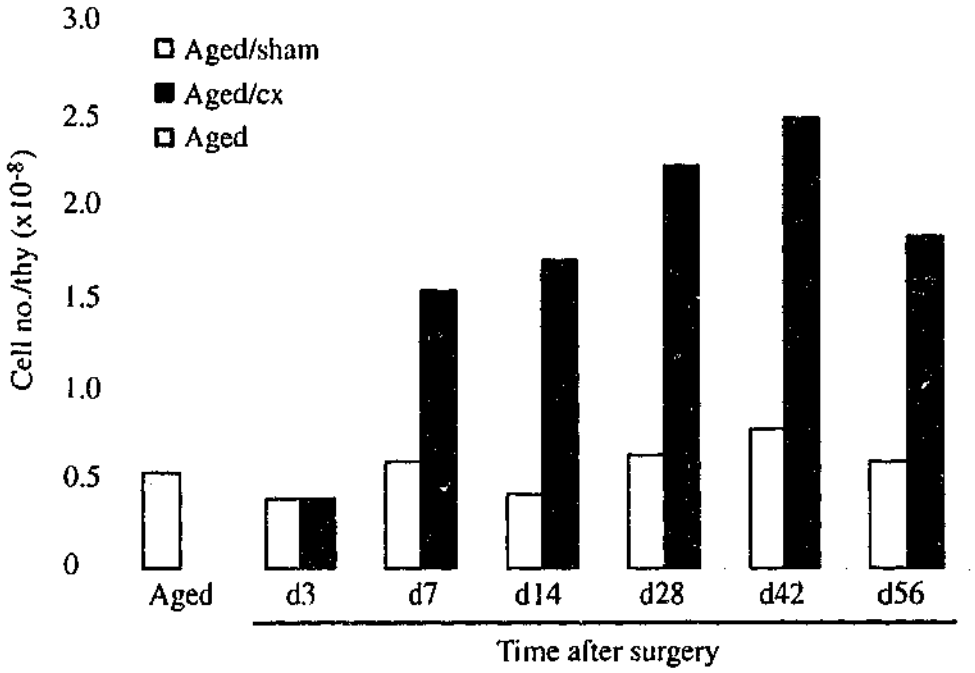
3.0
2.5
2.0
1.5
1.0
0.5
0
Cell no./thy (x10-8)
Aged/sham
Aged/cx
Aged
Aged
d3
d7
d14
d28
d42
d56
Time after surgery

C.

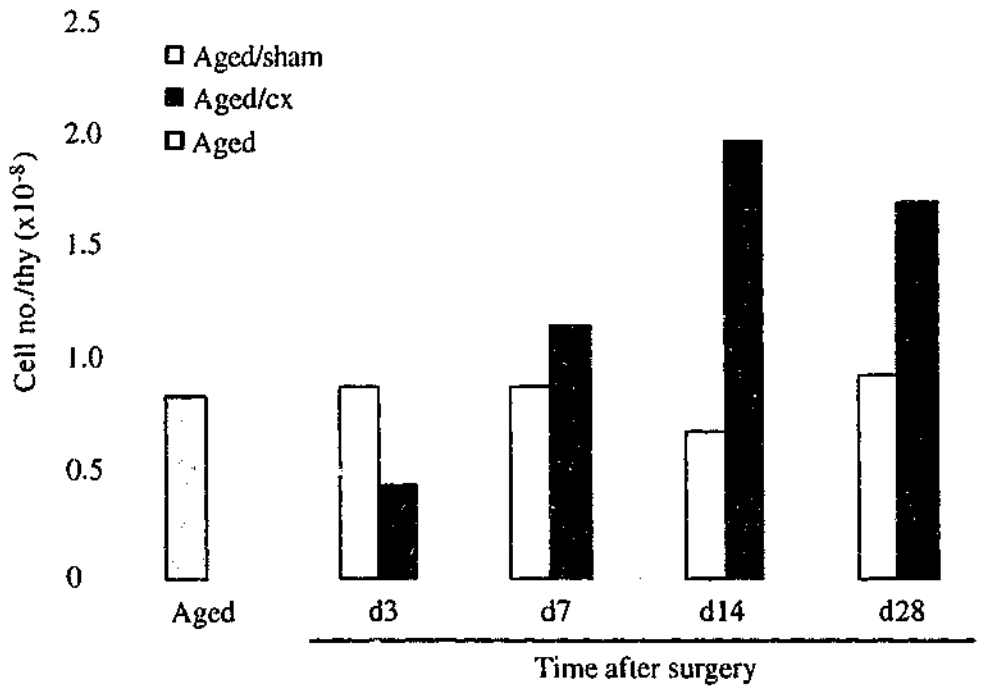
2.5
2.0
1.5
1.0
0.5
0
Cell no./thy (x10-8)
Aged/sham
Aged/cx
Aged
Aged
d3
d7
d14
d28
Time after surgery

Figure 4.7 Kinetics of TEC regeneration following surgical castration of aged mice.

Bar graphs of the total number of TECs per thymus in each group are shown. TEC numbers were determined by flow cytometric analysis gating on $CD45^-$ MHC II^+ stromal cells from each collagenase/Dispase digestion. Data from three independent time course experiments (**A**, **B**, and **C**) are shown.

A.

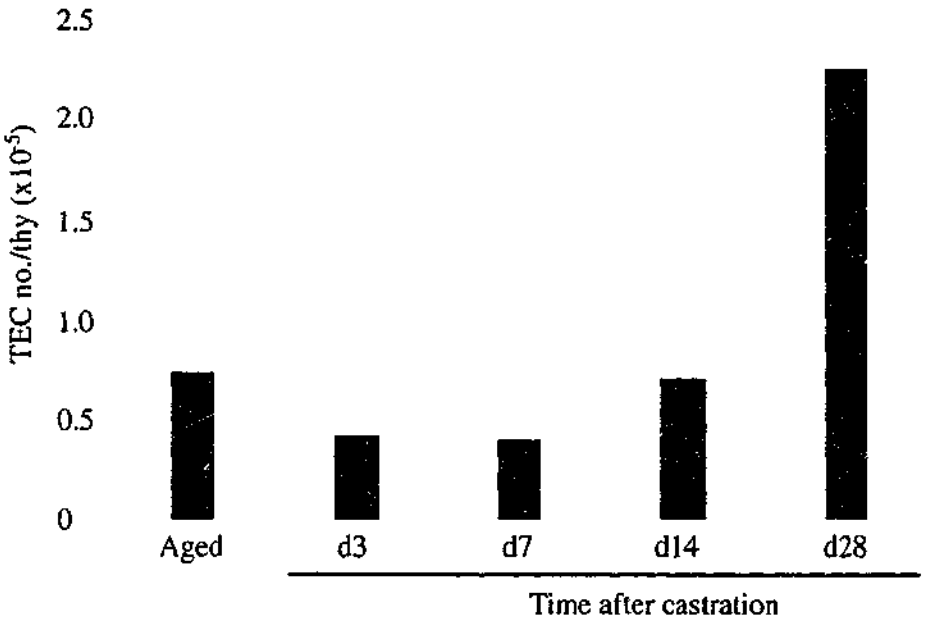
2.5
2.0
1.5
1.0
0.5
0
TEC no./thy (x10-5)
Aged
d3
d7
d14
d28
Time after castration

B.

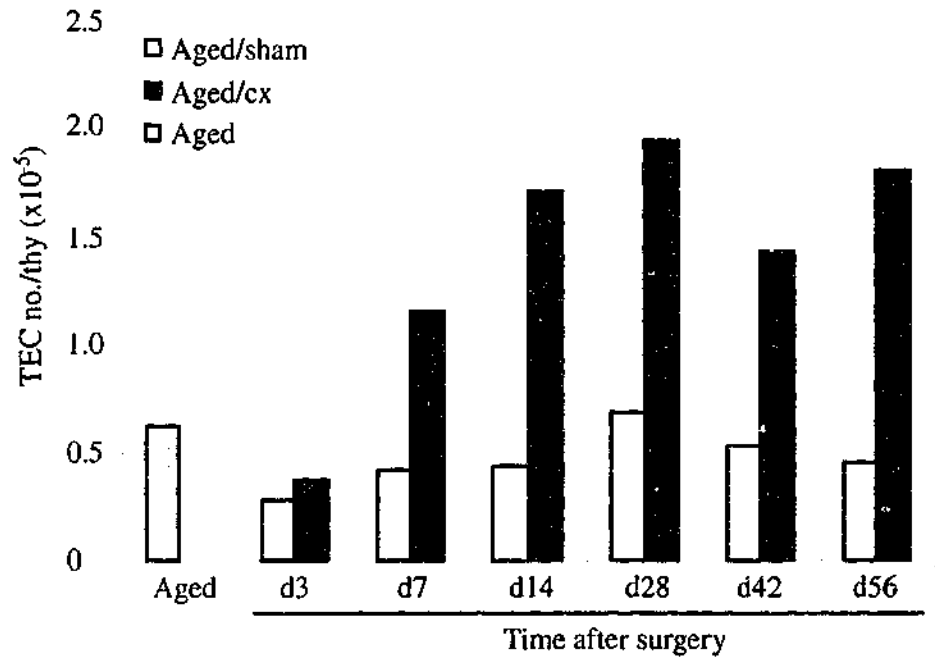
Aged/sham
Aged/cx
Aged
2.5
2.0
1.5
1.0
0.5
0
TEC no./thy (x10-5)
Aged
d3
d7
d14
d28
d42
d56
Time after surgery

C.

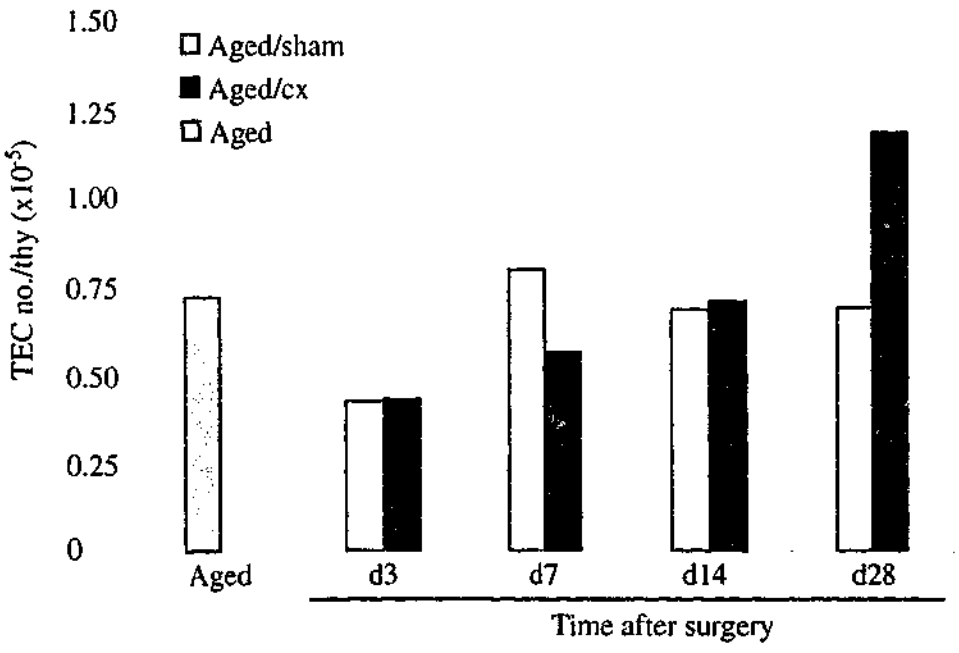
Aged/sham
Aged/cx
Aged
1.50
1.25
1.00
0.75
0.50
0.25
0
TEC no./thy (x10-5)
Aged
d3
d7
d14
d28
Time after surgery

Figure 4.8 Ratio of MHC II^{hi}:MHC II^{lo} TECs following surgical castration of aged mice.

Bar graphs of the ratio of MHC II^{hi}:MHC II^{lo} TECs are shown for each of the groups indicated from three independent time course experiments (**A**, **B**, and **C**).

A.

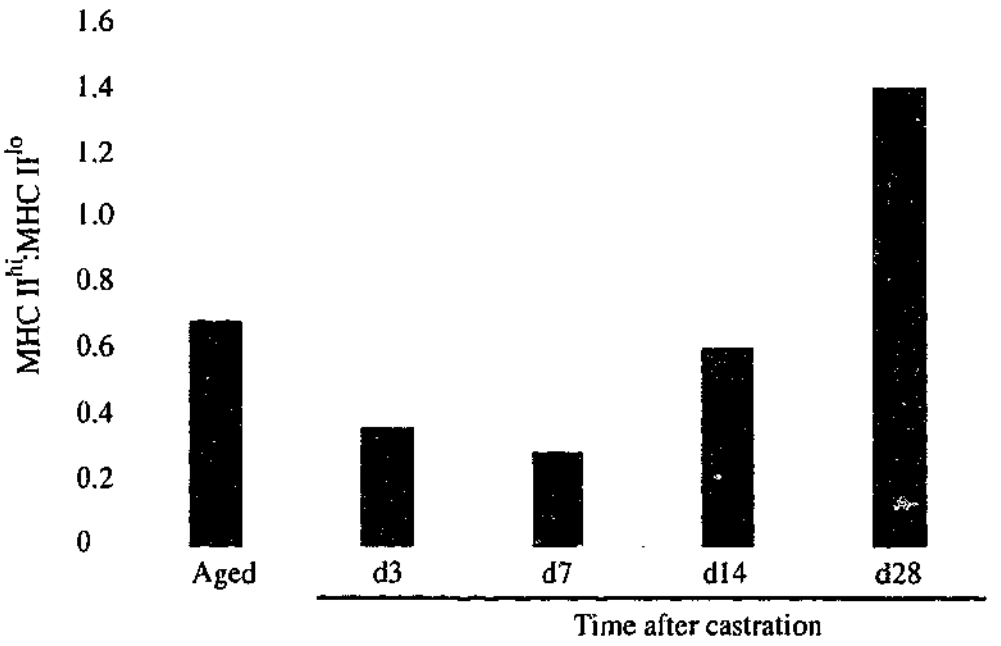
MHC II^hi:MHC II^lo
1.6
1.4
1.2
1.0
0.8
0.6
0.4
0.2
0
Aged
d3
d7
d14
d28
Time after castration

B.

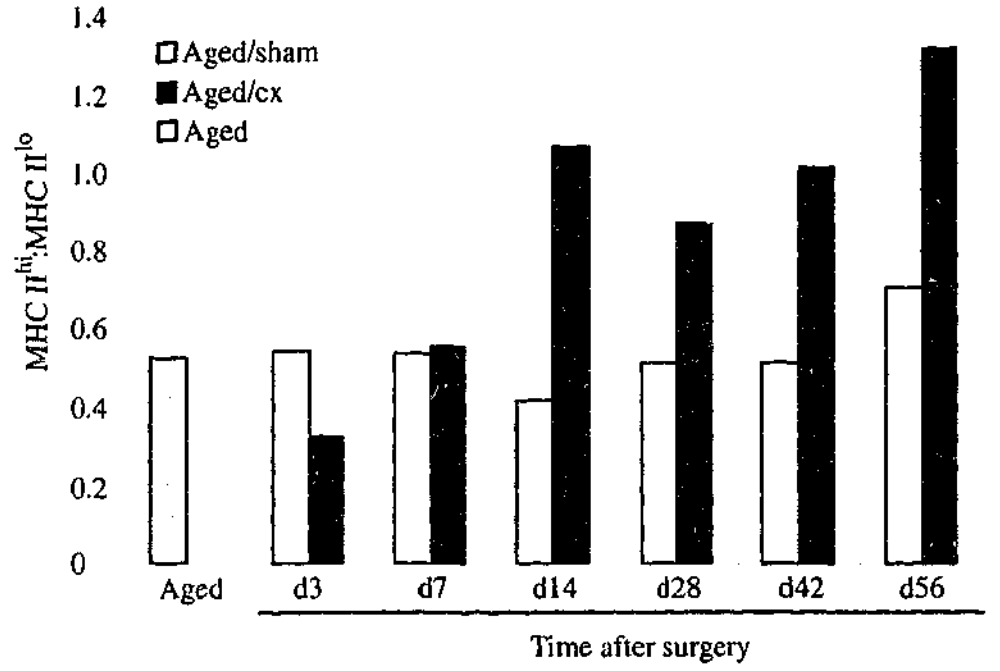
Aged/sham
Aged/cx
Aged
MHC II^hi:MHC II^lo
1.4
1.2
1.0
0.8
0.6
0.4
0.2
0
Aged
d3
d7
d14
d28
d42
d56
Time after surgery

C.

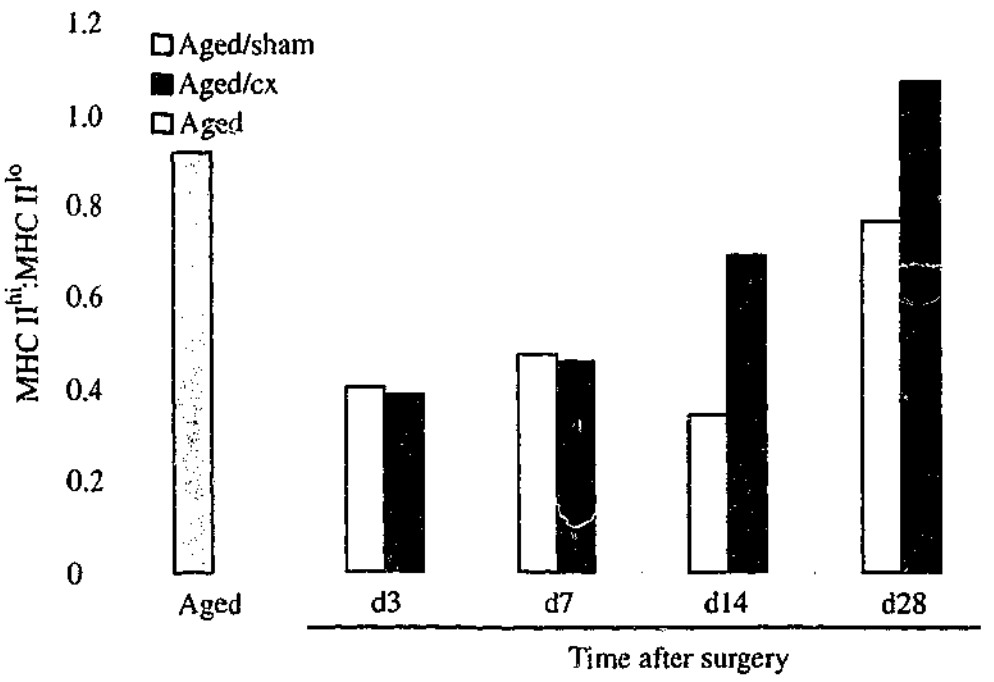
Aged/sham
Aged/cx
Aged
MHC II^hi:MHC II^lo
1.2
1.0
0.8
0.6
0.4
0.2
0
Aged
d3
d7
d14
d28
Time after surgery

the cortical and medullary compartments. In all experiments, mTECs preferentially expanded, skewing the ratio of mTECs to cTECs 4 weeks after castration to beyond normal young levels (5.5, Fig 4.2C). Interestingly, the results of experiment 2 indicated these return to normal young levels after 6 weeks (Fig 4.9 B).

Figure 4.10 A exhibits the proportional decrease observed in both MHC II^{hi} and MHC II^{lo} cTECs in castrated mice after 2 weeks. In terms of other major thymic stromal cell subsets, there was no clear phenotypic changes in MTS-24^+ or MTS-15^+ stromal cells (Figs. 4.10 B & C). Interestingly, fibroblasts appeared to decrease in proportion at day 28 in castrated mice, but not sham-castrated controls. However, this did not translate to a significant difference in TEC:fibroblast ratios in castrated mice.

4.2.7 Castration induced regeneration of thymic stroma in immunodepleted mice.

Similar trends in thymic stromal cell recovery were found in young, castrated mice following immunodepletion with cyclophosphamide (Fig. 4.11). While thymic cellularity fell to aged levels after treatment with cyclophosphamide, thymic regeneration began within 7 days, peaking in castrated and sham-castrated groups at days 42 and 56 respectively (Fig. 4.11A). These trends were also seen with TEC numbers, although a delay in involution and regeneration was apparent at early time points (Fig. 4.11B). TEC recovery was accompanied by similar phenotypic changes to those observed in the aged regeneration experiments. Cyclophosphamide treatment initially reduced both MHC II^{hi}:MHC II^{lo} and mTEC:cTEC ratios to aged levels (Fig 4.2C & D), but these were restored to normal young levels within 4 weeks (Fig. 4.11C & D). Interestingly, thymic regeneration produced the same trends in stromal cells recovery in both groups, however the castrated thymi showed enhanced regeneration in all indices.

Figure 4.9 Ratio of mTECs:cTECs following surgical castration of aged mice.

Bar graphs of the ratio of mTEC:cTECs, determined by Ly51 expression on $CD45^-$ $MHC\ II^+$ stromal cells, for each of the groups indicated in three independent time course experiments (**A**, **B**, and **C**).

A.

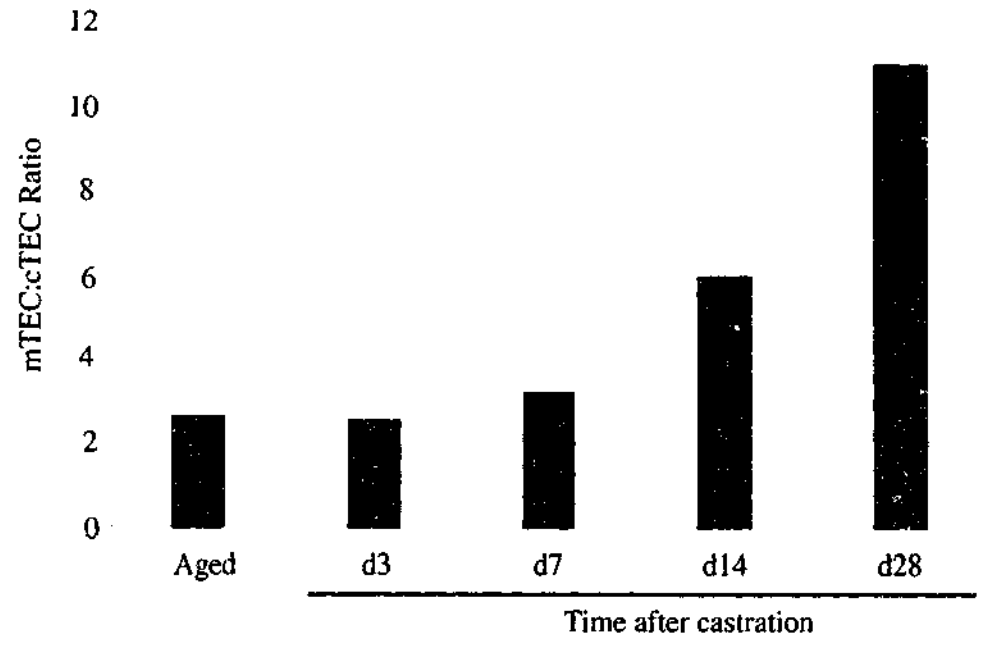
12
10
8
6
4
2
0
mTEC:cTEC Ratio
Aged
d3
d7
d14
d28
Time after castration

B.

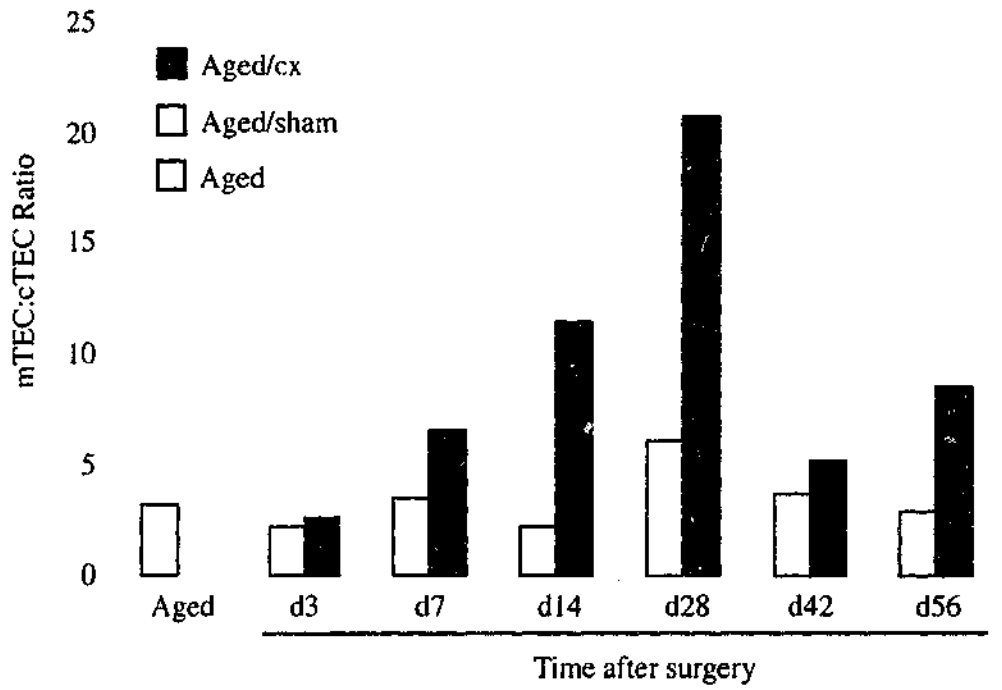
25
20
15
10
5
0
mTEC:cTEC Ratio
Aged/cx
Aged/sham
Aged
Aged
d3
d7
d14
d28
d42
d56
Time after surgery

C.

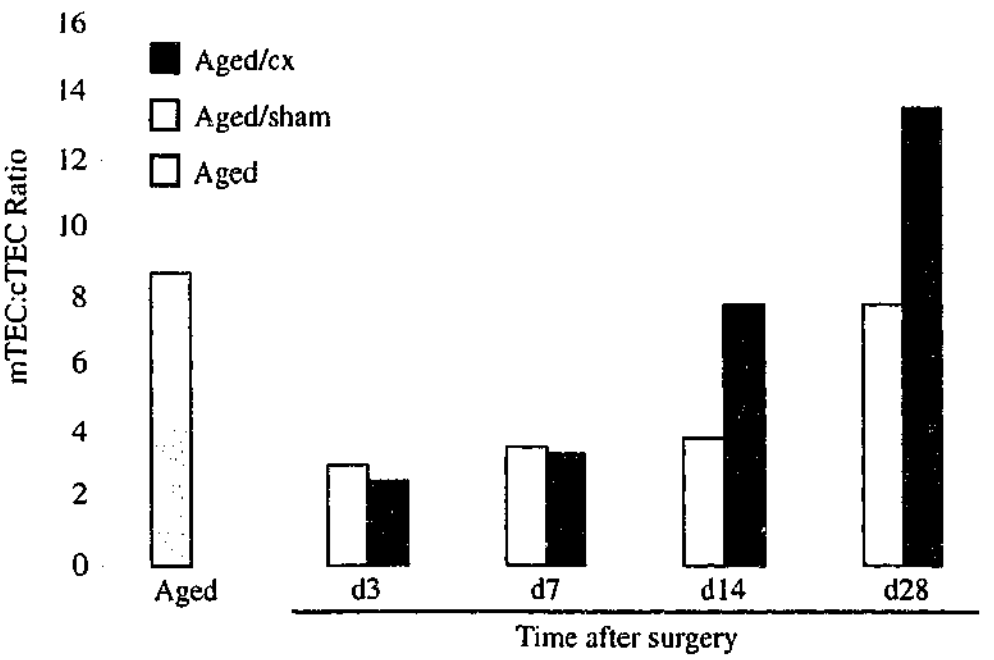
16
14
12
10
8
6
4
2
0
mTEC:cTEC Ratio
Aged/cx
Aged/sham
Aged
Aged
d3
d7
d14
d28
Time after surgery

Figure 4.10 Thymic stromal cell phenotypes at various time points following surgical castration of aged mice.

All dot plots are gated on $CD45^-$ thymic stromal cells and are representative of 3 experiments. **A.** MHC II versus Ly51 expression allowed discrimination of cTEC (MHC II^+ $Ly51^+$) and mTEC (MHC II^+ $Ly51^-$) populations in castrated and sham castrated mice at various time points following surgery. The proportion of total TECs these populations constituted is indicated within the regions. **B.** Dot plots of MHC II versus MTS-24 staining with regions indicating the proportion of total TECs comprised by $MTS\text{-}24^+$ cells at the various time points following surgery. **C.** Dot plots of MHC II versus MTS-15 staining with regions indicating the total proportion of $CD45^-$ thymic stromal cells comprised by $MTS\text{-}15^+$ cells at various time points following surgery.

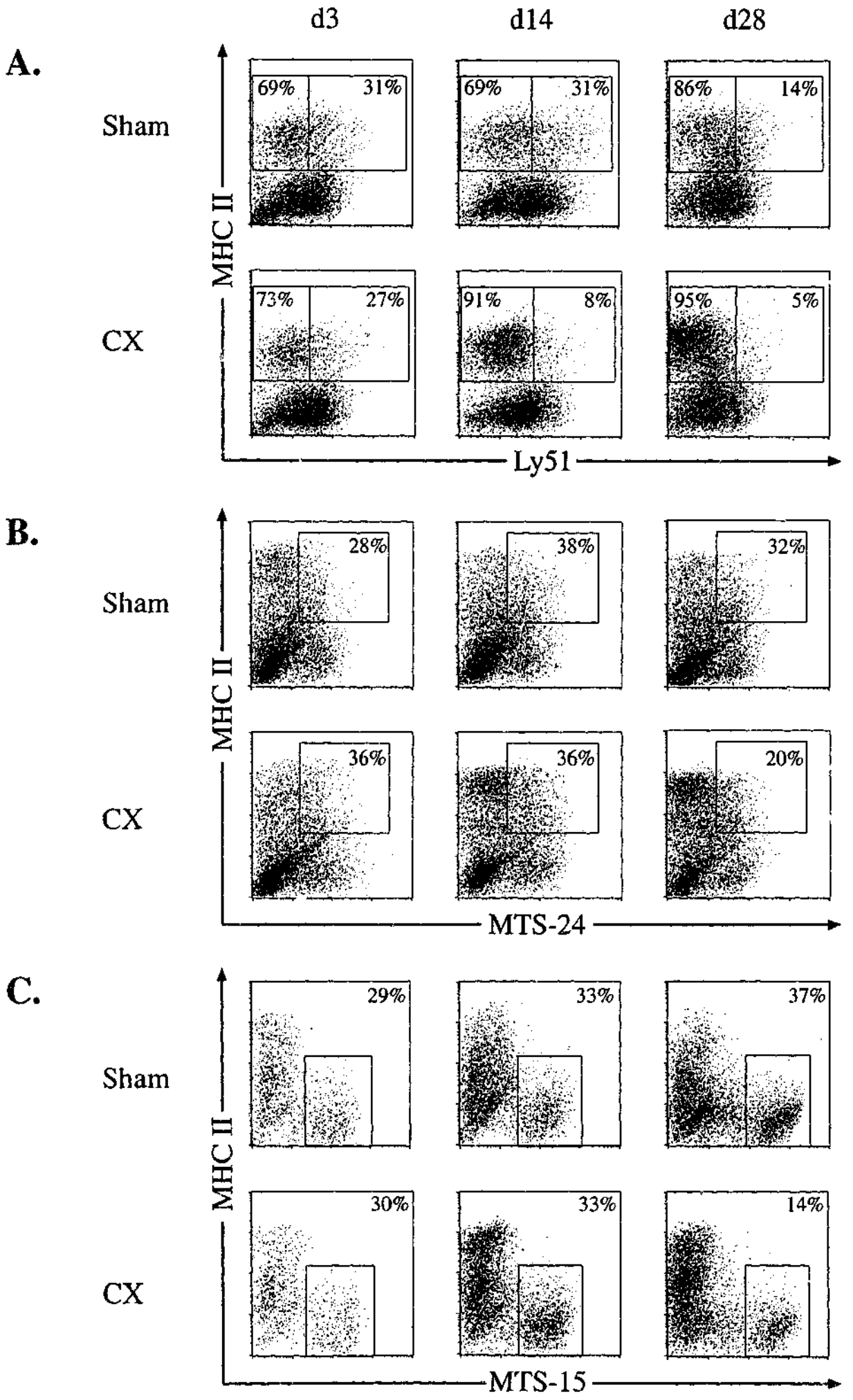
A.
d3
d14
d28
Sham
CX
69%
31%
69%
31%
86%
14%
73%
27%
91%
8%
95%
5%
MHC II
Ly51
B.
Sham
CX
28%
38%
32%
36%
36%
20%
MHC II
MTS-24
C.
Sham
CX
29%
33%
37%
30%
33%
14%
MHC II
MTS-15

Figure 4.11 Kinetics of thymic stromal cell regeneration following surgical castration of cyclophosphamide treated mice.

Bar graphs of cell numbers and phenotypes derived from collagenase/Dispase digestions of pools of 3 thymi from the experimental groups indicated. **A.** Total thymic cellularity increased in both castrated and sham castrated mice following cyclophosphamide treatment, both surpassing untreated control levels. **B.** A similar trend was observed in TEC numbers per thymus. **C.** Bar graph of the ratio of MHC II^{hi}:MHC II^{lo} TECs at various time points following castration and sham castration of cyclophosphamide treated mice. **D.** Bar graph of the ratio of mTECs:cTECs at various time points following castration and sham castration of cyclophosphamide treated mice.

A.

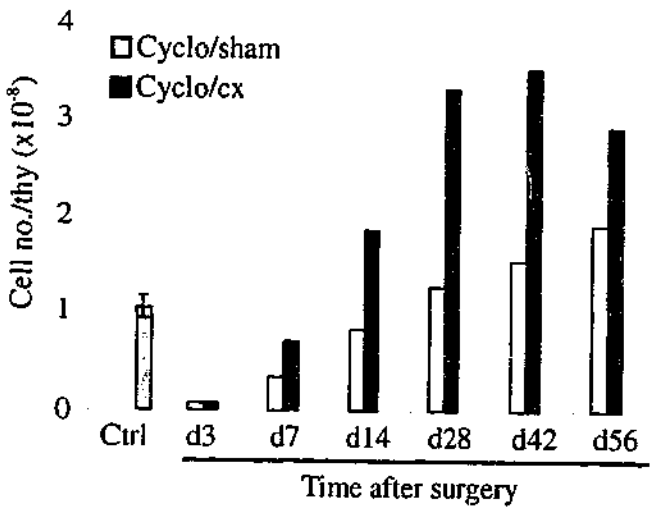
Cyclo/sham
Cyclo/cx
Cell no./thy (x10⁻⁸)
0
1
2
3
4
Ctrl
d3
d7
d14
d28
d42
d56
Time after surgery

B.

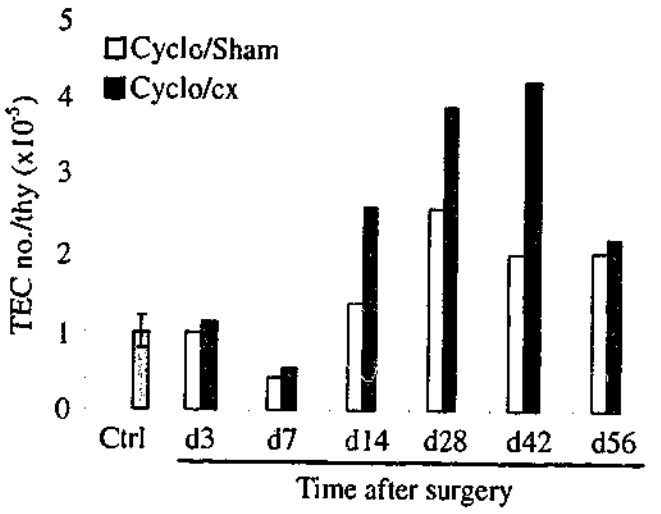
Cyclo/Sham
Cyclo/cx
TEC no./thy (x10⁻⁵)
0
1
2
3
4
5
Ctrl
d3
d7
d14
d28
d42
d56
Time after surgery

C.

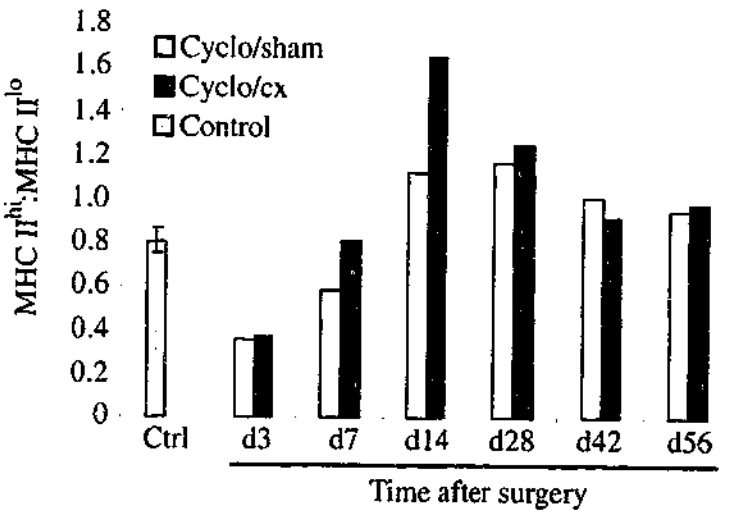
Cyclo/sham
Cyclo/cx
Control
MHC II^hi:MHC II^lo
0
0.2
0.4
0.6
0.8
1.0
1.2
1.4
1.6
1.8
Ctrl
d3
d7
d14
d28
d42
d56
Time after surgery

D.

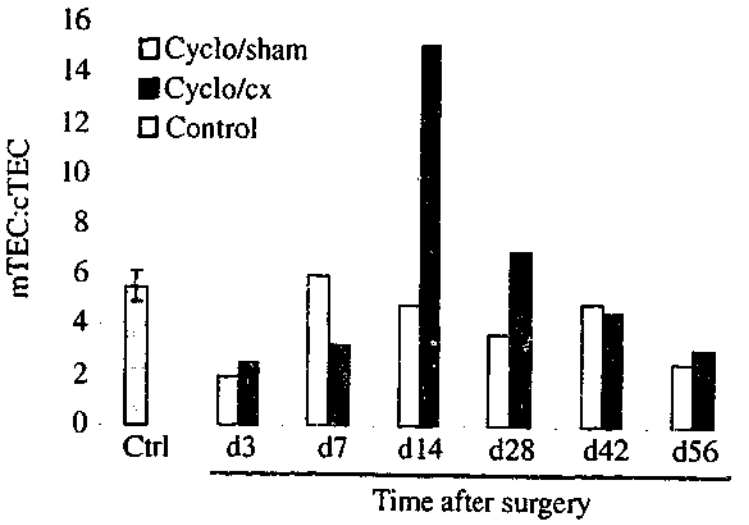
Cyclo/sham
Cyclo/cx
Control
mTEC:cTEC
0
2
4
6
8
10
12
14
16
Ctrl
d3
d7
d14
d28
d42
d56
Time after surgery

4.3 DISCUSSION

Despite the central role of thymic stromal cells in T-cell development, the understanding of this heterogeneous population has been relatively poor. This study defines fundamental parameters of stromal cell biology, demonstrating that these cells are a far more dynamic cell population than previously thought. Marked changes in the composition and the size of the stromal compartment associated with age indicate extensive remodelling during changing thymic states. Alterations in TEC phenotype with age revealed novel TEC subsets defined by MHC II and Ly51 expression. The arrested epithelial development in RAG-$1^{-/-}$ and TcR$\alpha^{-/-}$ mice defines control points in TEC differentiation dependent upon thymocyte/TEC crosstalk. Proliferation of MHC II^{int} cTEC and mTEC populations showed both subsets proliferate independently with a relatively fast turnover. Despite compositional changes in aged stromal cells, the compartment regenerated to resemble normal young thymii in response to sex steroid withdrawal. This confirms the comprehensive thymic regeneration induced by sex steroid ablation and demonstrates the capacity of stromal cells for rapid expansion and remodelling.

The refinement of flow cytometric analysis of stromal cells enabled the acquisition of quantitative data that other techniques cannot assess directly (Chapter 3). This was applied in the current study to enumerate $CD45^-$ stromal cells during thymic ontogeny, steady-state expansion and age-related atrophy. Assessment of overall thymic cellularity with age described the kinetics of expansion and atrophy, showing similar adult trends to that reported previously (Ortman et al., 2002). The finding that stromal cells follow these trends demonstrated their ability to expand and contract with changing thymocyte numbers. Marked differences in the thymocyte to stromal cell ratio over time show that this is a highly dynamic relationship. The low ratios observed during embryogenesis (between 5 to 100) compared to adult ranges (250-480), would be very likely to have a major impact on the

kinetics of thymocyte development. Sustained contact provided by higher proportions of stromal cells observed during embryogenesis may facilitate the accelerated T-cell developmental kinetics of this period.

The consequences of thymic atrophy were evident in the reduced numbers and altered composition of stromal compartment of 12 month old mice. The significant reduction in epithelial content and corresponding increase in fibroblasts reflects the collapse of the thymus during involution. Reduced TEC content was accompanied by proportional increases in cTECs and MHC II^{lo} subsets. While MHC II^{hi} and MHC II^{lo} medullary epithelial subsets have been observed previously in histological studies (Surh et al., 1992b), the functional differences between these subsets remain unknown. This study demonstrates this heterogeneity extends into the cortical compartment and is reflected in differential expression of costimulatory markers. Expression of CD40 (on both cTECs and mTECs) and CD80 (on mTECs) may implicate MHC II^{hi} TECs in distinct roles via the provision of cytokines and costimulation (Galy and Spits, 1992; Degermann et al., 1994; Ruggiero et al., 1996). The induction of increased expression of MHC II and CD40 *in vitro* by IFNγ stimulation of TECs supports the notion that MHC II^{hi} TECs are "activated" epithelial cells (Galy and Spits, 1992; Naquet et al., 1999). The predominance of "resting" TECs in the involuted thymus may reduce the overall efficiency of thymocyte development.

The apparent phenotypic maturation of TEC subsets throughout life was supported by studies of mutant mice. Expansion of significant populations of adult MHC II^{lo} cTECs and MHC II^{hi} mTECs only occurred in the presence of DP thymocytes. The development of MHC II^{lo} mTECs appeared to require signals from SP thymocytes. Whether these populations arise from earlier subsets or the expansion of pre-existing populations of the same phenotype awaits direct lineage analysis (Fig 4.12). Definition of TEC surface phenotypes throughout life provides a means to directly test these relationships.

Figure 4.12 Proposed thymic epithelial lineage relationships.

Mesenchymal interactions with endoderm from the 3rd pharyngeal pouch give rise to $K5^+$, $K8^+$, MTS-24^+ precursor TECs by E12.5. These are capable of differentiating into early MHC II^{hi} cortical and medullary TEC subsets under the influence of DN and DP thymocytes, respectively. In young adult mice, MHC II^{lo} cTEC and mTEC subsets emerge, requiring signals from DP and SP thymocytes, respectively.

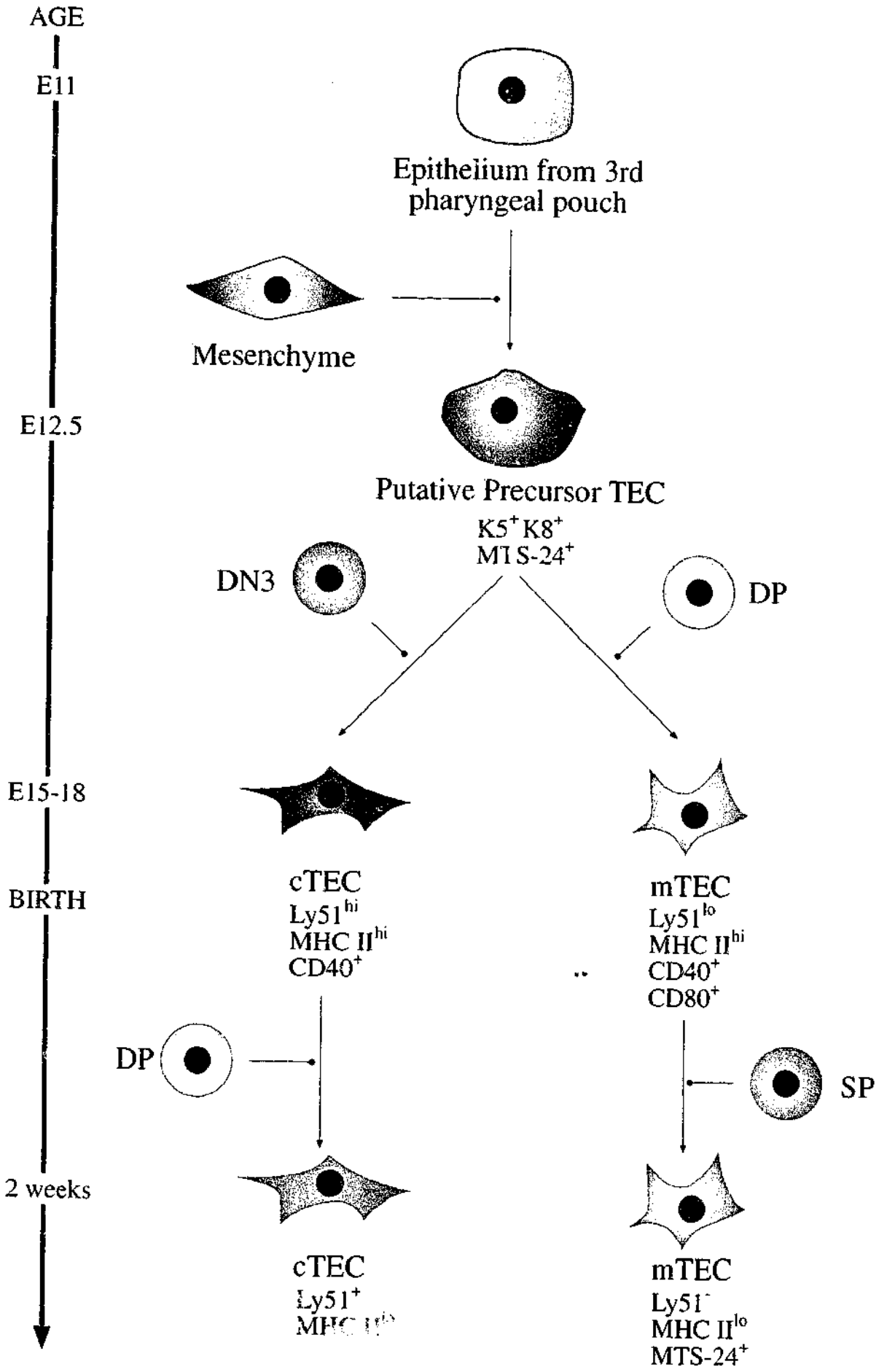
AGE
E11
E12.5
E15-18
BIRTH
2 weeks
Epithelium from 3rd pharyngeal pouch
Mesenchyme
Putative Precursor TEC
K5+ K8+
MTS-24+
DN3
DP
cTEC
Ly51hi
MHC IIhi
CD40+
mTEC
Ly51lo
MHC IIhi
CD40+
CD80+
DP
SP
cTEC
Ly51+
mTEC
Ly51-
MHC IIlo
MTS-24+

The putative TEC precursor marker MTS-24 was expressed by a subset of MHC II^{hi} embryonic and neonatal TECs, similar to the distribution reported previously at E15 (Gill et al., 2002). In the adult, MTS-24 was predominantly expressed by MHC II^{lo} mTECs, with a minor MHC II^{hi}, MTS-24^{+} population. The expression of a precursor marker on the adult, possibly end-stage MHC II^{lo} mTEC population appears contradictory. However, the finding that adult MTS-24^{+} TECs cannot reconstitute the thymic microenvironment (Gill, pers. comm.) may indicate this is not an exclusive marker of adult TEC precursors. Purification, *in vitro* reaggregation and grafting of the adult TEC subsets reported in this study may identify such a precursor population.

Central to the question of TEC differentiation and maintenance of the thymic stromal microenvironment are the proliferative capacities of the various subsets. Expression of the proliferation marker, Ki67, was found in subsets of MHC II^{int} cTECs and mTECs in the embryonic, young and aged thymus. The higher frequency of Ki67^{+} TECs in the embryonic thymus compared to the young adult reflected the greater expansion of epithelium during this phase. Likewise, higher cell division in the medulla compared to the cortical compartment, lead to the proportional increase in this subset during late embryogenesis. This suggests that while early mTECs arise from clonal precursor cells (Rodewald et al., 2001), the majority of normal mTEC expansion is derived from proliferation within this subset.

In the young adult thymus, cell division of Ki67^{+} MHC II^{int} TECs was confirmed by BrdU incorporation. Most BrdU incorporation was detected within the MHC II^{hi} subset, suggesting upregulation of MHC II following cell division of MHC II^{int} TECs. Certainly, there was relatively little proliferation evident in the MHC II^{lo} TEC subset. The frequency of Ki67^{+} TECs and the proportion of cells incorporating BrdU over three days were consistent with a 24 hour division time of a stably dividing population. This relatively rapid turnover is

compatible with the notion that TECs are a cell population capable of continuous remodelling and regeneration.

The regenerative potential of the atrophic thymic stroma was demonstrated following sex-steroid ablation. Expansion of the thymic stromal compartment followed a similar trend to that of thymocytes, albeit delayed by up to two weeks. The faster kinetics observed in Experiment 2 were likely to be due to variability between aged mice that were used in the study. In all experiments, stromal cell regeneration was accompanied by a normalisation of TEC subset ratios back to young adult levels due to a proportional increase in mTECs. These results suggest that stromal proliferation and differentiation is driven by or intimately linked to thymocyte expansion and development in the regenerating thymus. The factors controlling thymic regeneration appear to be closely linked to thymocyte/stromal cross-talk.

Treatment of young mice with cyclophosphamide caused the loss of most thymocytes, but the total number of TECs was not affected after 3 days in both sham and castrated mice. However, disruption of the ratios of mTEC:cTECs and MHC II^{hi}:MHC II^{lo} was evident, closely resembling the subset distribution in the involuted thymus. Despite some thymocyte regeneration after 7 days in both groups, TEC numbers fell by half, either due to a direct effect of the cyclophosphamide or secondary to the initial loss of thymocytes. By day 14 expansion was observed in TECs of both groups, concomitant with a normalisation of TEC subset ratios. The decrease and subsequent increase in TEC numbers resembled that of thymocytes, following a lag of 4 to 7 days. This relationship is consistent with a functional synergy between thymocytes and stromal cells that results in similar trends in population kinetics to those observed in the regenerating aged thymus. It was notable that sham castrated mice also exhibited some thymic regeneration following immunodepletion. with cell numbers exceeding untreated controls by 6-8 weeks. Castrated mice demonstrated a higher and more rapid increase in stromal and overall thymic cellularity compared to sham

castrates. These results support those found in the aged model of regeneration, highlighting the relationship between thymocytes and stromal cells.

In summary, this study reveals many fundamental characteristics of thymic stromal cells and their relationship to thymocytes. The former are a more dynamic cell population than previously thought, with a rapid turnover and the capacity to remodel. Regeneration of atrophic stroma demonstrates the continued functional competence of this population and is of significance to therapeutic manipulation of the thymus in immunodeficient states. These data also have implications for many aspects of thymus biology, providing the basis for direct lineage analysis of thymic epithelial subsets.

CHAPTER 5

A novel thymic fibroblast glycolipid recognised by the mAb MTS-15.

5.1 INTRODUCTION.

The thymus is the exclusive site of development of mainstream αβT-cells that are required for virtually all adaptive immune responses. The complexity of T-cell development is reflected in the heterogeneity of specialised thymic microenvironments which are formed through interactions ("crosstalk") between thymocytes and the various types of thymic stromal cells (Boyd et al., 1993; Ritter and Boyd, 1993; van Ewijk et al., 1994). The stromal compartment includes populations of epithelium. fibroblasts, endothelium, macrophages, and dendritic cells, each of which has distinct roles in T-cell development (reviewed in Anderson et al, 2001).

The diversity of the cellular and molecular components of thymic stroma has been demonstrated by panels of monoclonal antibodies (mAbs) specific for a variety of mouse thymic stromal cell antigens (for example, van Vliet et al., 1984; de Maagd et al., 1985; Lobach et al., 1985; Godfrey et al. 1988, reviewed in Boyd et al, 1993). These reagents have been useful in defining the heterogeneity within and amongst these populations, in particular the thymic epithelium. However, as few of these antibodies recognise determinants expressed specifically by thymic mesenchymal fibroblasts, our knowledge of the heterogeneity and function of this stromal compartment is less comprehensive.

The essential role of mesenchyme in thymic organogenesis has most recently been demonstrated by Suniara et al., 2000, providing poorly defined signals that influence epithelial cell development (Anderson and Jenkinson, 2001). A role for fibroblasts in T-cell

development beyond the $CD4^-CD8^-CD25^+CD44^+$ stage has been shown to be dependent upon extracellular matrix (ECM) components produced by these cells (Anderson et al., 1997). Fibroblasts also form a large component of the perivascular spaces that surround the sites of precursor entry and mature thymocyte export, implicating them in functions such as chemoattraction and early T-cell commitment. A major obstacle in defining the precise role of thymic fibroblasts in epithelial and T-cell development is the lack of specific surface markers enabling their purification for further functional and molecular analysis.

Within the mouse thymic stromal (MTS) panel of mAbs (Godfrey et al., 1990), MTS-15 was distinguished by a unique, restricted expression pattern at the blood/thymus barrier. The antigen bound by MTS-15 is primarily expressed on the surface of the thymic fibroblasts that line the capsule, trabeculae and large blood vessels found at the cortico-medullary junction. This study explores in detail the expression profile and molecular characteristics of the MTS-15 antigen, as well as the potential relevance of fibroblasts to the thymic microenvironment.

5.2 RESULTS

5.2.1 Lymphoid tissue distribution of MTS-15

Immunohistological analysis of adult mouse thymus sections with MTS-15 exhibited specific staining of fibroblasts lining the subcapsule and large blood vessels of the cortico-medullary junction (Figs. 5.1A, B & Chapter 3). At high magnification, MTS-15 staining appeared granular and exhibited apparent diffusion around cells adjacent to areas of expression (Fig. 5.1C & D). Compared to markers of thymic epithelium (anti-keratin) and vasculature (anti-CD31), it was found that MTS-15 reactivity colocalised with the endothelium and perivascular spaces, but not epithelial structures. The extension of staining beyond the endothelium and perivascular space was suggestive of a soluble or shed antigen.

The cellular distribution was analysed further by comparing MTS-15 staining to that of the established thymic fibroblast marker ER-TR-7 (Van Vliet et al., 1986). Staining of serial thymic sections revealed overlapping expression at the subcapsule (Fig. 5.1E & F) and around the large blood vessels of the cortico-medullary junction (Fig. 5.1G & H). This strongly suggests the MTS-15 antigen is expressed by fibroblasts in these areas.

These findings were supported by flow cytometric analysis of freshly isolated thymic stromal cell preparations. MTS-15 surface staining of a major subset of EpCAM$^-$, MHC II$^-$ stromal cells demonstrated the non-epithelial distribution of the antigen (Fig. 5.2 & Chapter 3). Four colour labelling comparing CD31, MHC II and MTS-15 staining on CD45$^-$ stromal cells revealed a novel subset of MHC II^{lo}/MTS-15$^+$ endothelium (Fig. 5.2). Together, these data define the first cell surface marker for thymic fibroblasts lining the subcapsule and perivascular spaces, and identifies a novel subset of MHC II expressing endothelial cells.

The strong association of MTS-15 with vasculature was also observed in the spleen by immunohistology, with prominent staining in the red pulp and surrounding central arterioles (Figs. 5.3A & B). The extension of this granular reactivity around cells adjacent

Figure 5.1 Immunohistological analysis of MTS-15 on 4 week old thymus.

A. MTS-15 staining of 4 week old thymus was detected throughout the subcapsule and thymic vasculature. **B.** Triple staining of a large cortico-medullary junction blood vessel from 4 week old thymus with MTS-15 (green), MTS-12 (anti-CD31; red) and anti-keratin (blue). Extensive colocalisation was observed between the MTS-15 determinant and CD31 on endothelium (yellow), with extension of MTS-15 staining around adjacent thymocytes. **C.** MTS-15 (green) and anti-keratin (red) staining of 4 week old thymus revealed discrete foci of MTS-15 reactivity along the subcapsule, trabeculum and some thymic blood vessels. **D.** A serial section stained with ER-TR-7 (green) and anti-keratin (red) revealed continuous ER-TR-7 reactivity along the subcapsule, trabeculum and around thymic vasculature. **E.** large blood cortico-medullary blood vessel exhibiting the typical granular MTS-15 staining (green) with a similar distribution to ER-TR-7 (green; **F**) on a serial section (anti-keratin; red).

A.

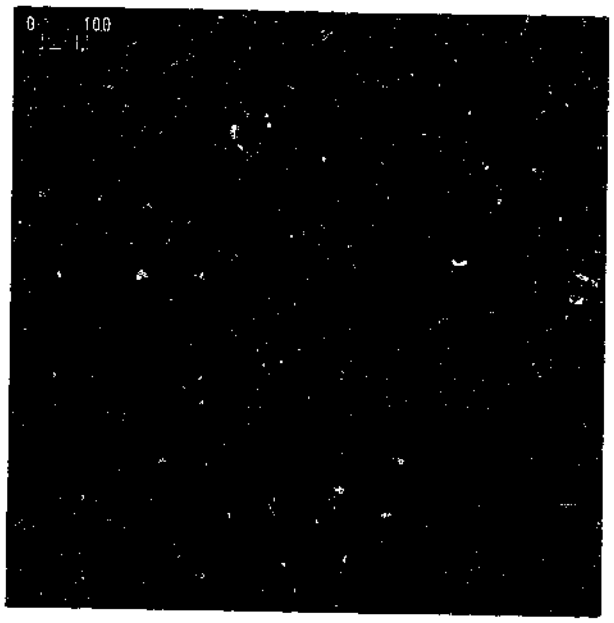

B.

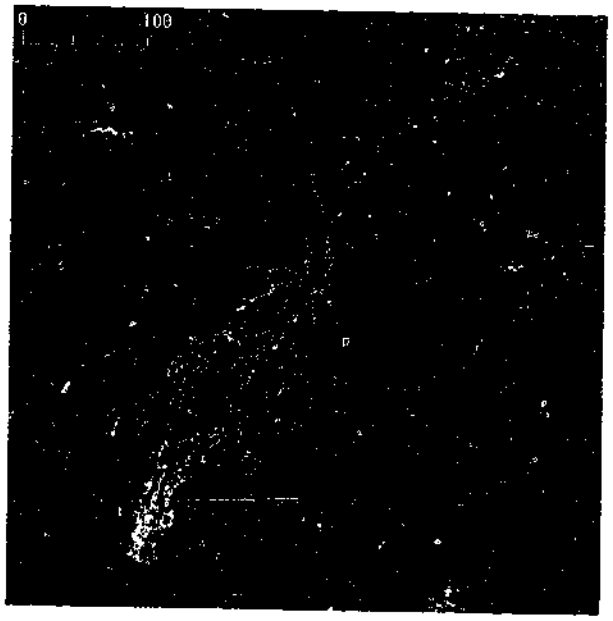

C.

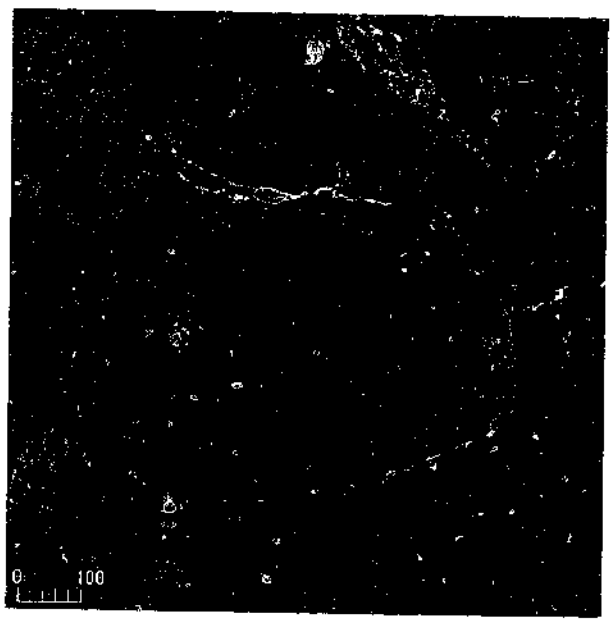

D.

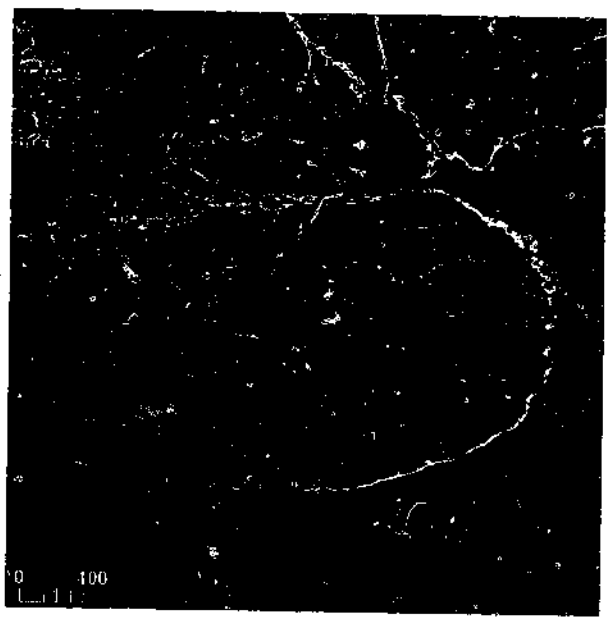

E.

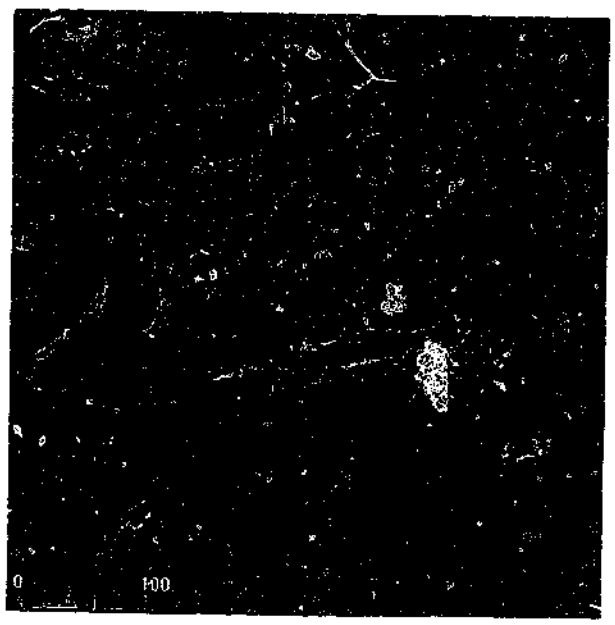

F.

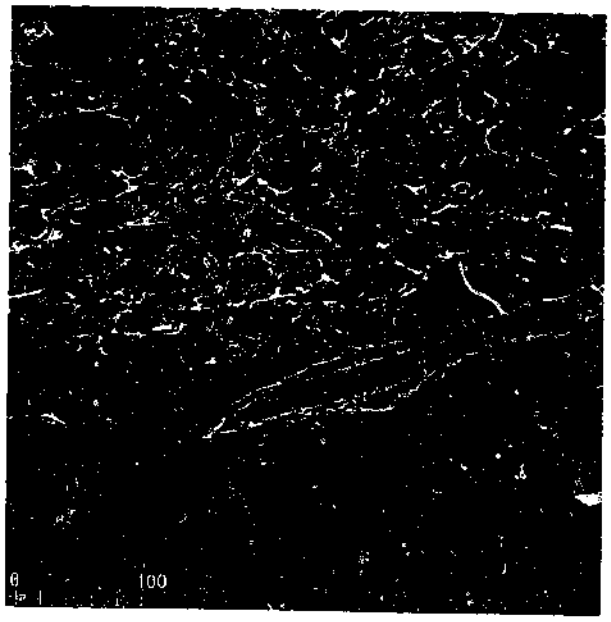

Figure 5.2 Four colour flow cytometric analysis of MTS-15 staining on thymic stromal cells.

A. Histogram showing the region gating of $CD45^-$ thymic stromal cells from 4 week old C57BL-6 mice. **B.** MHC II expression versus MTS-15 staining on CD45- stromal cells, showing a large population of MHC II^- $MTS\text{-}15^+$ cells. A small population of MHC II^{lo} $MTS\text{-}15^+$ is also apparent. **C.** Dot plot of MTS-15 staining versus CD31 expression, showing the percentages of $CD45^-$ stroma that $MTS\text{-}15^+$ $CD31^-$ and $MTS\text{-}15^+$ $CD31^+$ populations constitute. **D.** Histogram showing higher MHC II expression on $MTS\text{-}15^+$ $CD31^+$ (thick line) than $MTS\text{-}15^+$ $CD31^-$ (shaded) thymic stromal cells. Profiles are representative of 3 independent experiments.

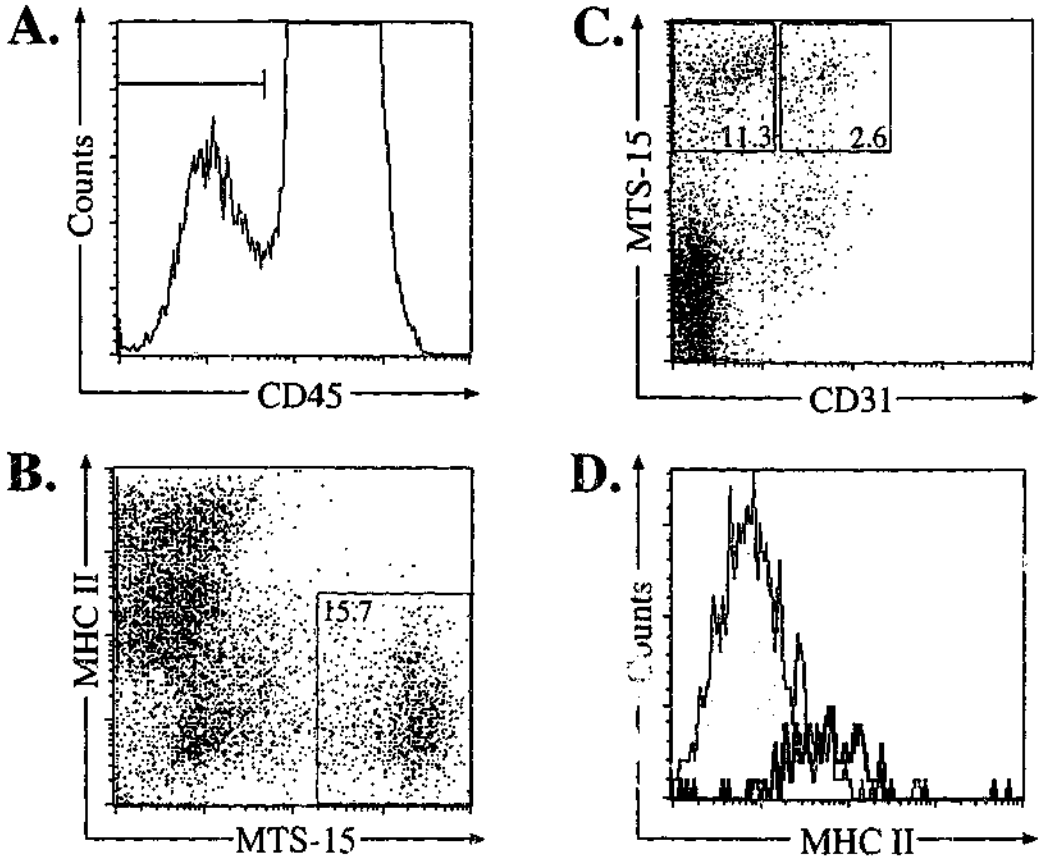
A.
Counts
CD45
C.
MTS-15
11.3
2.6
CD31
B.
MHC II
15.7
MTS-15
D.
Counts
MHC II

Figure 5.3 Immunohistological analysis of MTS-15 on extrathymic tissues.

Tissue sections were taken from 4 week old CBA mice. **A.** Spleen section stained with MTS-15 (green) and anti-CD31 (red). Extensive MTS-15 reactivity was observed throughout the red pulp regions and surrounding central arterioles. **B.** Higher power examination of MTS-15 (green), anti-CD31 (red) and anti-CD45 (blue) staining of a splenic central arteriole revealed colocalisation with endothelium (yellow) and adjacent leukocytes (cyan). **C.** Extensive MTS-15 reactivity (green) was also observed in the connective tissue areas of the small intestine. Anti-CD31 (red) and anti-CD45 (blue) staining defined GIT vasculature and leukocytes. **D.** Small intestine stained with MTS-15 (green), anti-CD45 (red) and anti-keratin (blue) exhibited colocalisation between MTS-15 and intestinal leukocytes (yellow).

A.

B.

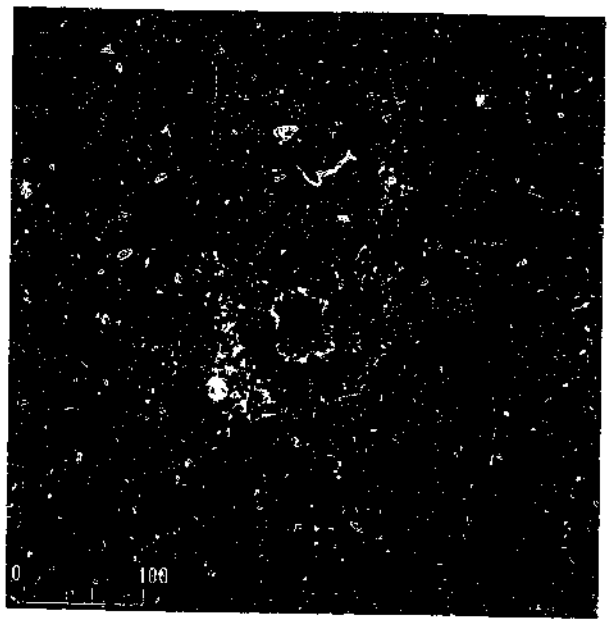

C.

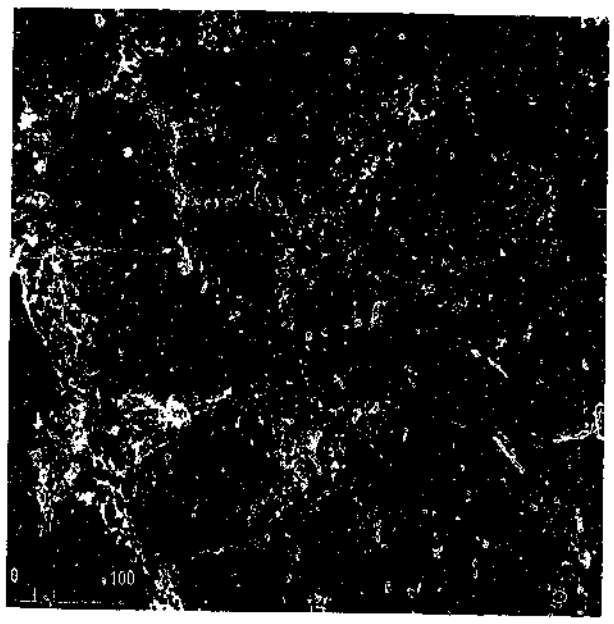

D.

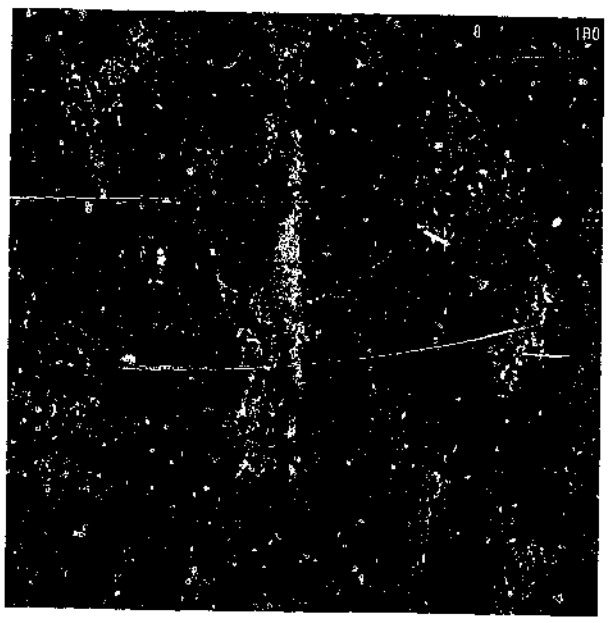

to the central arterioles is similar to the pattern observed around thymic endothelium, suggesting shedding or diffusion from areas adjacent to leukocytes.

5.2.2 Non-lymphoid tissue distribution of MTS-15.

A different distribution pattern to that observed in lymphoid tissues was found in the gastro-intestinal tract (GIT) and female reproductive organs. In these areas, broad, intense MTS-15 staining of the connective tissue areas of the GIT showed no clear association with the vasculature (Figs. 5.3C, D & Table 5.1). Comparison of this reactivity with CD45 and keratin demonstrated colocalisation with MTS-15 on some GIT leukocytes, but not epithelium (Figs. 5.3C & D).

Analysis of MTS-15 reactivity throughout embryogenesis first demonstrated staining at E14 on scattered cells along the middle part of the central midbrain. This association with central nervous tissue continued throughout late embryogenesis and was still evident at the blood-brain barrier in the adult (Figs. 5.4A, D, F, G & Table 5.1). At E15, reactivity was also detected in some cells of the umbilical hernia, however, only by E16 was connective tissue staining apparent in the oesophagus (Figs. 5.4B, C & E). By E16, intense MTS-15 staining was exhibited in scattered cells below the epithelial layers of the skin and other tissues (Fig. 5.4E). MTS-15 expression was first observed in the connective tissue of the small intestine at E17 and persisted thereon (Table 5.1). Interestingly, only low levels of MTS-15 staining were detected on thymic fibroblasts by flow cytometry after E15, with adult levels expressed after E16 (data not shown).

Figure 5.4 Immunohistological analysis of MTS-15 during late embryogenesis.

All sections were taken from whole C57BL-6 embryos and stained with MTS-15 (green) and anti-keratin (red) to define epithelial structures. **A.** Strong MTS-15 reactivity was detected in scattered cells of the middle part of the ventral midbrain. Keratin staining defines the Rathke's Pouch epithelial structure. **B.** Some cells in the connective tissue of the E15 umbilical hernia also expressed high levels of the MTS-15 antigen. **C.** After E16, MTS-15 reactivity could be detected around the oesophagus and scattered cells near the developing thymus. **D.** MTS-15 staining could also be detected along the E17 midbrain and brain stem. **E.** MTS-15 staining did not extend into the small intestine of the E16 embryo, but scattered cells below the epithelial layers of the skin expressed the determinant. **F.** Continuous MTS-15 staining was detected along the lateral border of the left cerebral hemisphere in the E17 embryo. **G.** The borders of E17 vertebrae near the lungs also expressed the determinant.

A.

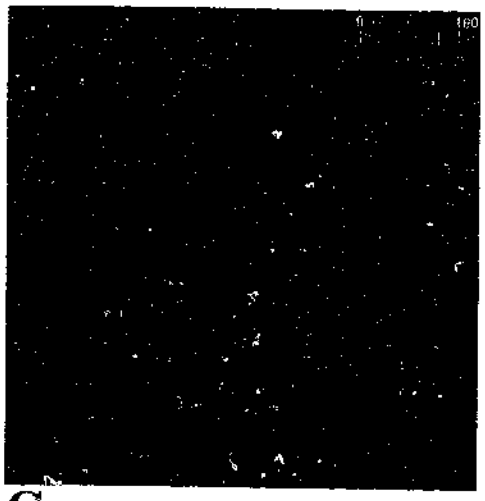

B.

C.

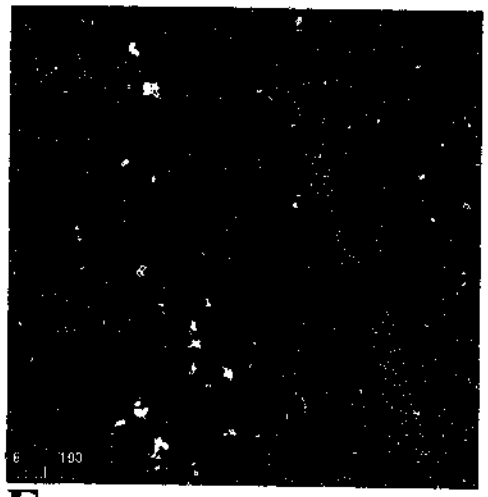

D.

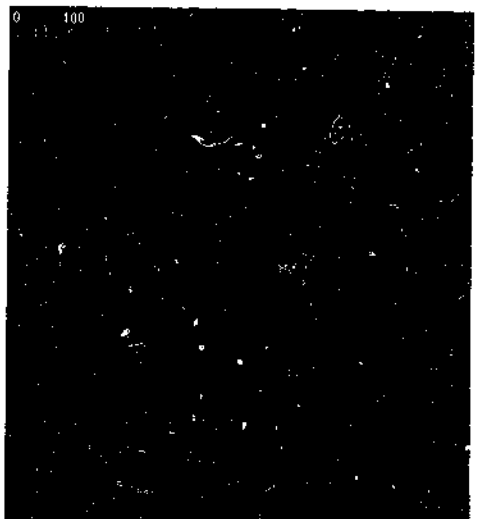

E.

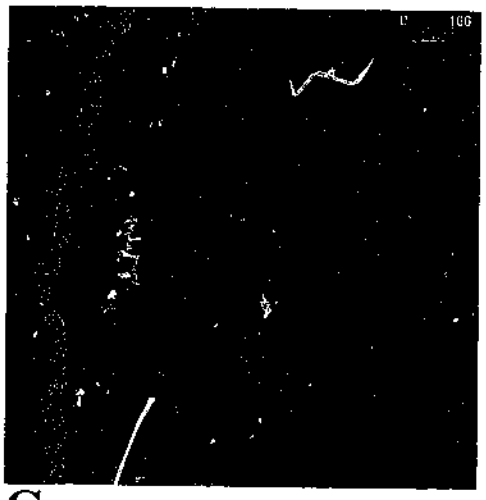

F.

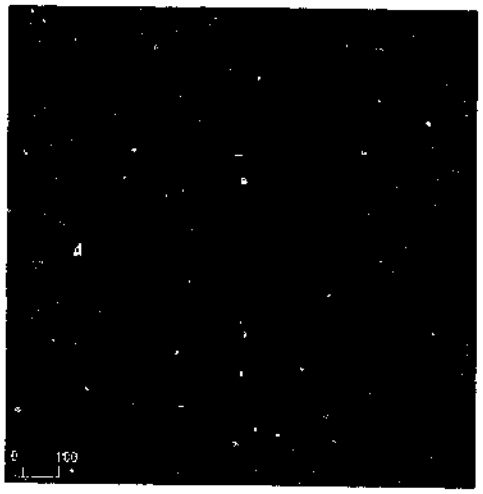

G.

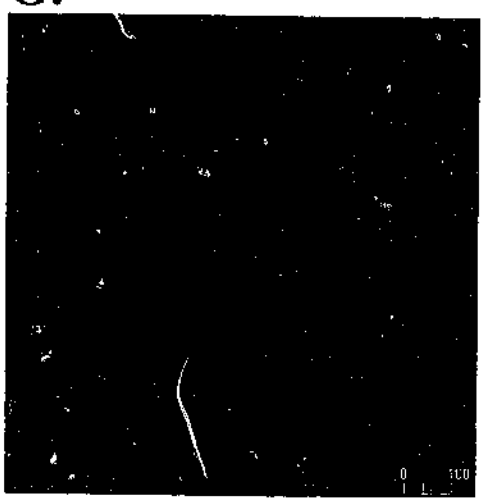

Adult Tissue	**MTS-15 Reactivity**
Thymus	Blood/thymus barrier
Spleen	Red pulp & central arterioles
Lymph Node	Subcapsule
Stomach	Connective tissue, smooth muscle
Small intestine	Connective tissue, smooth muscle
Large intestine	Connective tissue, smooth muscle
Uterus	Connective tissue
Fallopian Tube	Connective tissue
Heart	Connective tissue
Liver	Negative
Kidney	Negative
Brain	Blood/brain barrier
Salivary Gland	Negative
Tongue	Negative
Skeletal muscle	Negative
Embryonic Stage	**MTS-15 Tissue Reactivity**
E14	Discrete neural structures, ventral midbrain marginal layer, umbilical hernia
E15/16	Oesophagus, duodenum, choroid plexus
E17	Submandibular gland, gastro-intestinal tract, olfactory epithelium

Table 5.1 Tissue distribution of the antigen recognised by MTS-15.

5.2.3 Passive acquisition of the MTS-15 antigen by leukocytes.

The surface expression of the MTS-15 antigen coupled with the apparent shedding onto adjacent cells prompted extensive flow cytometric analysis of leukocytes from central and peripheral lymphoid organs. Low levels of MTS-15 staining were detected by flow cytometry on subsets of leukocytes from the thymus, spleen and lymph nodes, but not the blood (Fig. 5.5A). Almost 20% of thymocytes bore the antigen on their surface at low levels, as did lymph node leukocytes (Fig. 5.5A). Higher proportions and intensities of MTS-15 staining were observed on splenocytes (Fig. 5.5A).

A subset analysis of thymocytes indicated the MTS-15 antigen was predominantly found on immature DN (16%) and DP (19%) cells, while mature CD4 and CD8 SPs were almost negative (6% and 5% respectively) (Fig. 5.5B). The slight overall shift in the DP population may suggest broad low level staining with MTS-15. MTS-15 staining was similar in all DN subsets, but undetectable on recent thymic emigrants assessed 24 hours following intrathymic FITC injection (data not shown). MTS-15 labelling of splenocytes distinguished three populations, with high levels of staining observed on half of the non-lymphoid splenocytes (predominantly macrophages, granulocytes and dendritic cells) (Fig. 5.5C). Almost 70% of splenic B-cells were MTS-15$^{lo/hi}$, while MTS-15 staining of splenic T-cells resembled that of total thymocytes (Fig. 5.5C).

This tissue-dependent differential staining of lymphocytes with MTS-15 prompted investigations into the possible transfer of this antigen from stromal cells to lymphocytes. To address this, an MTS-15^{+} TEC line (MTE-1D, Naquet et al., 1989) or an MTS-15^{-} TEC line (3B6) was co-cultured with PBLs (MTS-15^{-}) and flow cytometric analysis used to detect leukocyte MTS-15 staining (Fig. 5.6A). It was found that after 1 day of co-culture with MTE-1D cells, PBLs acquired low levels of the MTS-15 antigen on their surface, while PBLs co-cultured with 3B6 cells remained negative (Fig. 5.6B).

Figure 5.5 MTS-15 staining of leukocyte subsets.

A. Histograms showing MTS-15 staining (solid line) and isotype control staining (dotted line) on leukocytes from the tissues indicated. Proportions of cells bounded by markers set according to staining intensity are indicated. **B.** Histograms of MTS-15 staining of various thymocyte developmental subsets (gated as shown in dot plot regions). Markers set according to minimal staining (<1%) of isotype controls indicate proportions of cells stained. **C.** Histograms of MTS-15 staining on major splenocyte subsets (gated according to dot plot regions) with markers set to bound MTS-15^{int} and MTS-15^{hi} leukocytes (background staining <1%). Representative profiles from 3 independent experiments are shown.

A.

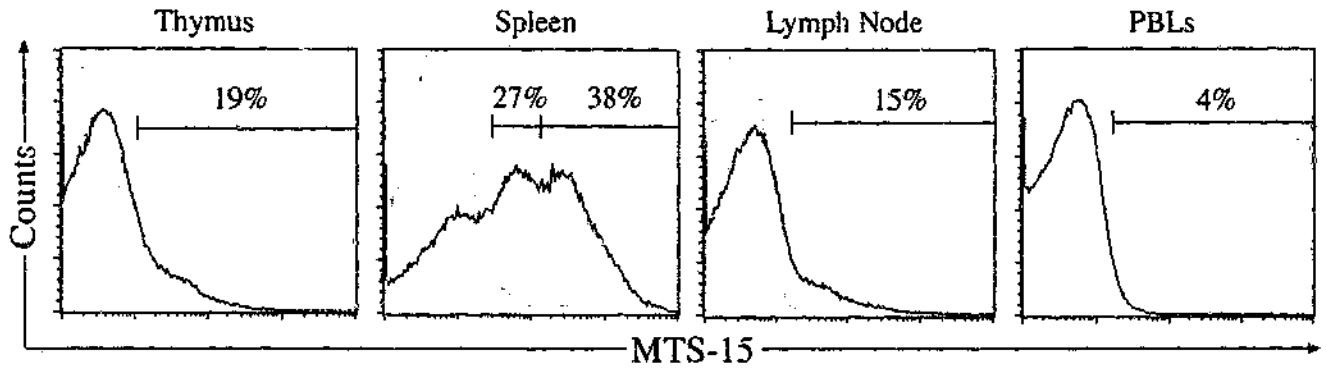
Thymus
Spleen
Lymph Node
PBLs
19%
27%
38%
15%
4%
Counts
MTS-15

B.

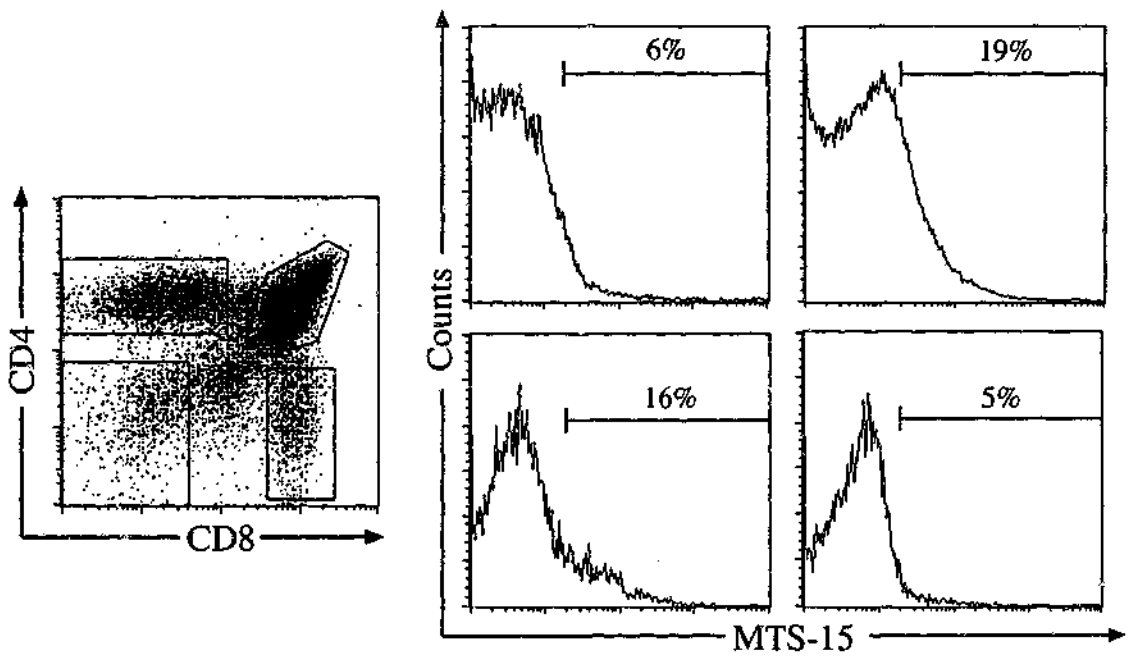
CD4
CD8
Counts
6%
19%
16%
5%
MTS-15

C.

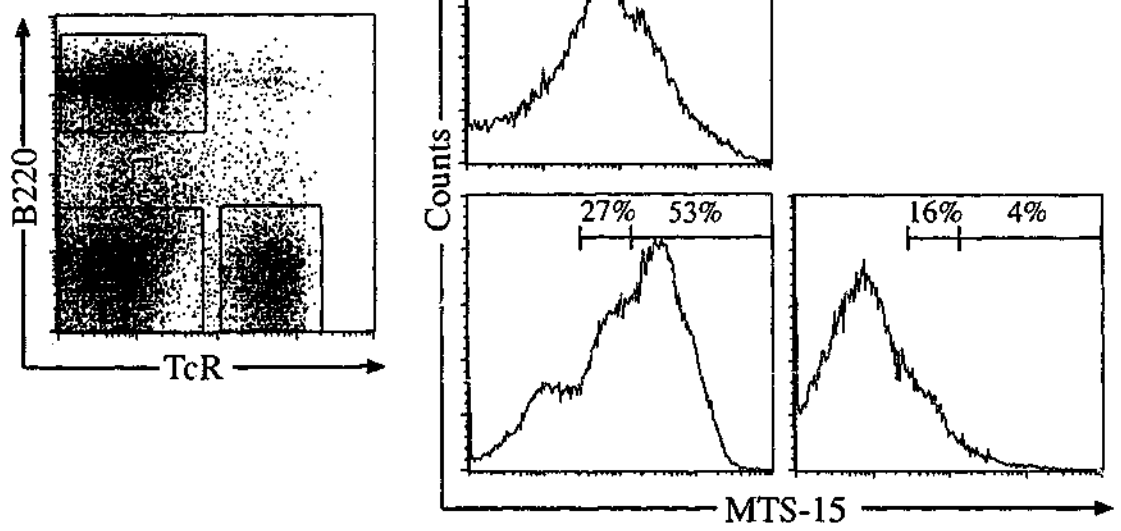
B220
TcR
Counts
35%
32%
27%
53%
16%
4%
MTS-15

Figure 5.6 Transfer of the MTS-15 antigen onto peripheral blood leukocytes.

PBLs were cultured alone or with either MTE-1D or 3B6 cells and analysed for MTS-15 staining 1, 2 and 3 days after the culture was established. **A.** CD45 expression was used to discriminate leukocytes ($CD45^+$) from cell lines ($CD45^-$) and MTS-15 expression analysed. Proportions of total viable cells are indicated in regions shown. **B.** Histograms of MTS-15 staining (solid line) on peripheral blood T-cells ($CD45^+$ TcR^+) and B-cells ($CD45^+$ $B220^+$) at the time points indicated show a greater proportion of MTS-15^+ B-cells than T-cells within markers set according to minimal background staining (<1%) of PBLs cultured alone (dotted line). Profiles are representative of 3 experiments.

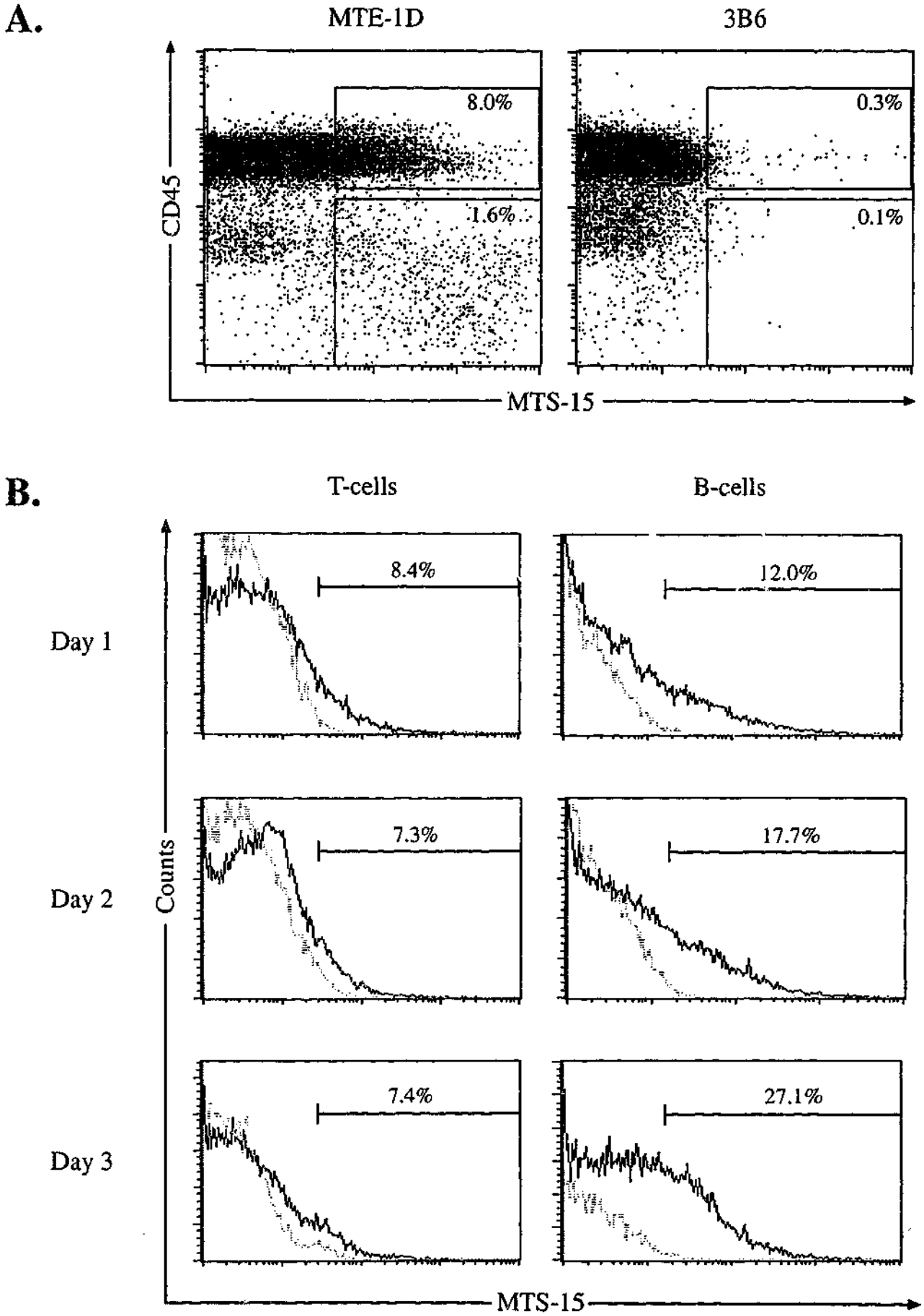
A.
MTE-1D
3B6
8.0%
1.6%
0.3%
0.1%
CD45
MTS-15
B.
T-cells
B-cells
Day 1
8.4%
12.0%
Day 2
7.3%
17.7%
Day 3
7.4%
27.1%
Counts
MTS-15

With respect to lymphocytes, a higher proportion of B-cells acquired or retained the antigen over time (from 12% to 27%), while only very few T-cells became MTS-15 positive (from 8% to 7%).

The transfer of antigen between cells could reflect either the interaction of a soluble antigen with a surface receptor or acquisition of surface antigen via membrane shedding or flipping. These possibilities were investigated by biochemical analysis of the antigen recognised by MTS-15.

5.2.4 Biochemical characterisation of the antigen bound by MTS-15.

Immunoblotting of membrane preparations from various tissues was performed with the MTS-15 mAb. Tricine SDS-PAGE was employed to better resolve low molecular weight species, revealing the antigen to have an extremely low molecular weight (4-5kDa), a high intrinsic negative charge or that it was insoluble in SDS (Fig. 5.7A). To address the latter issue, ultracentrifugal fractionation of antigenic activity from membrane preparations solubilised in various detergents was assayed using dot blots. These experiments suggested that the molecule detected by MTS-15 was extremely hydrophobic, as nearly all activity was consistently detected in the insoluble pellets of all detergents tested, including SDS (data not shown). Together, these data indicated biochemical behaviour consistent with a glycolipid.

To further investigate this possibility, a total lipid extract of an intestinal membrane fraction was analysed by HPTLC and probed with MTS-15. A single orcinol-reactive band was recognised by the mAb, in both the crude mixture and after extensive purification by HTPLC (Fig. 5.7B). Resistance of the determinant to mild base hydrolysis suggested that the antigen contained a ceramide group (ie. a glycosphingolipid) (Fig. 5.7B). However, it was also resistant to EGCase II (Fig. 5.8A), a lipase that hydrolyses many sphingolipids except those belonging to the globo-glycosphinglolipid family (Ito and Yamagata, 1989).

Figure 5.7 MTS-15 recognises a glycosphingolipid.

A. MTS-15 immunoblot of Tween-40 membrane preparations from intestine (int.), spleen (spl.), uterus (ute.), kidney (kid.), thymus (thy.) and MTE-1D cells (MTE), either reduced (R) or non-reduced (NR), separated on tricine SDS-PAGE. **B.** Orcinol staining and an MTS-15 immunoblot of HPTLC plates loaded with membrane (memb.) and chloroform:methanol (C.M.) extracts from intestine (Int.) and kidney (Kid.). Base treatment (B.T.) did not effect the mobility of the MTS-15 antigen.

A.

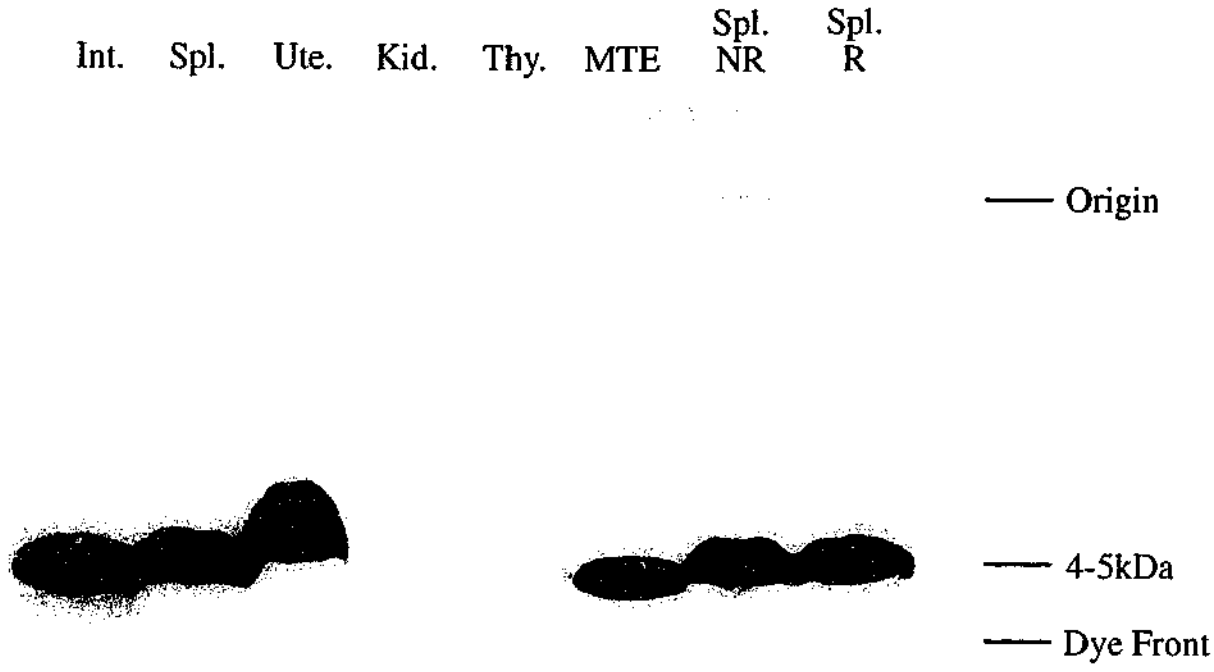
Int.
Spl.
Ute.
Kid.
Thy.
MTE
Spl. NR
Spl. R
Origin
4-5kDa
Dye Front

B.

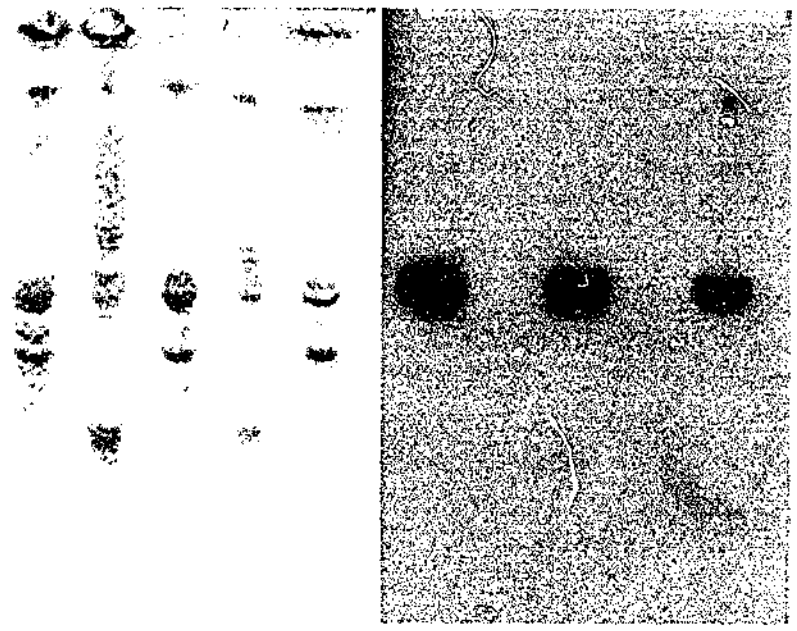
Orcinol stained
MTS-15 IB
Int. Kid. Int. Kid. Int. Int. Kid. Int. Kid.
Memb. C.M. B.T. Memb. C.M. B.T.

Figure 5.8 ECGase resistance and MALDI-TOF mass spectrum of MTS-15 antigen.

A. HPTLC-purified MTS-15 antigen and GM1 (control) were treated with ECGase II and the reaction products detected by orcinol and MTS-15 staining. **B.** MALDI-TOF mass spectrum of purified MTS-15 antigen.

Contributed by Tull, D. and McConville, M.

A.

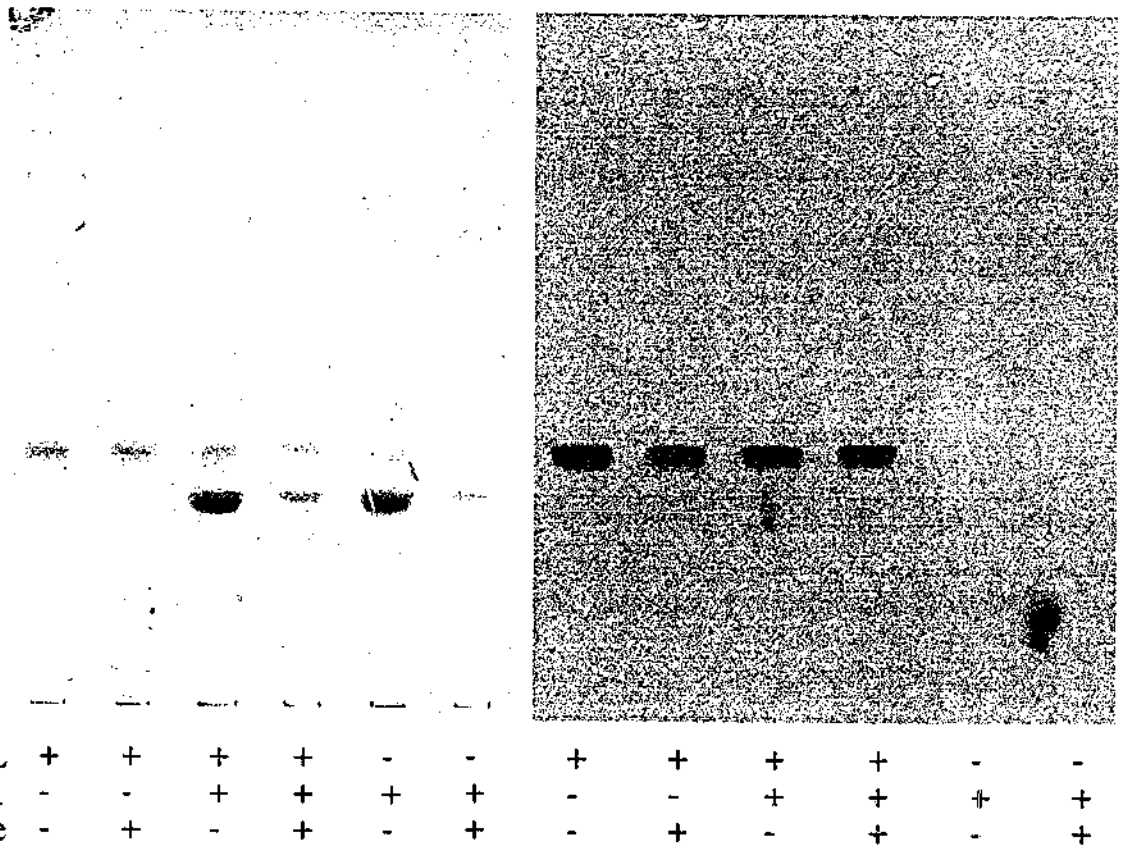
Orcinol stained
MTS-15 IB
M-GSL + + + + - - + + + + - -
GM1 - - + + + + - - + + + +
EGCase - + - + - + - + - + - +

B.

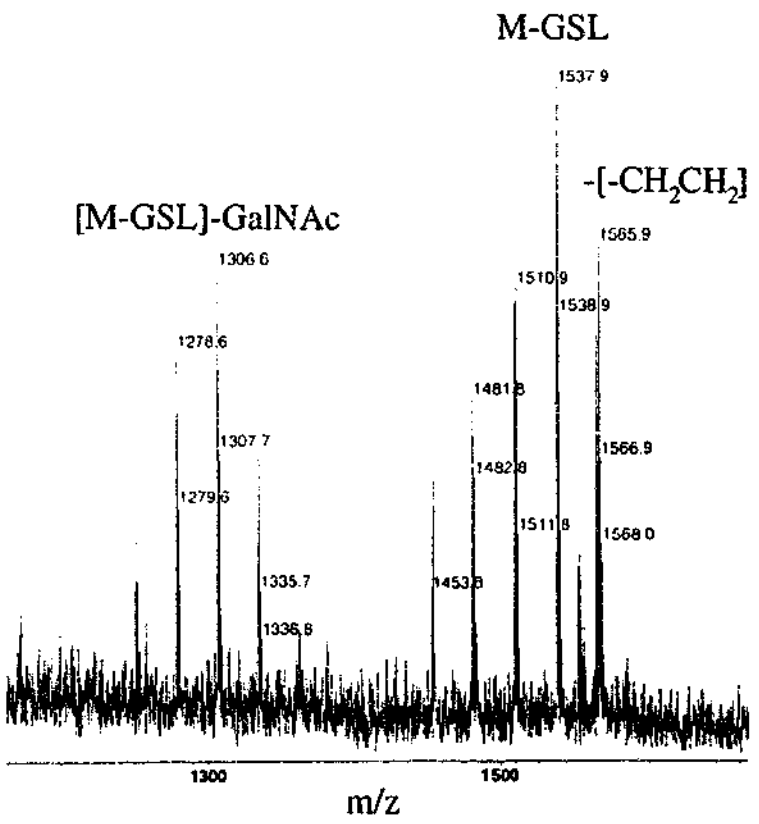
M-GSL
1537.9
-[-CH2CH2]
[M-GSL]-GalNAc
1565.9
1306.6
1510.9
1538.9
1278.6
1481.8
1307.7
1566.9
1482.8
1279.6
1511.8
1568.0
1335.7
1453.8
1336.8
1300
1500
m/z

Gas chromatographic mass spectrometry (GC-MS) compositional analysis of this species revealed stoichiometric amounts of N-acetylgalactosamine, galactose and glucose, also characteristic of a globo-glycosphingolipid. This was further supported by MALDI-TOF analysis of the underivatised band that revealed a cluster of putative $[M+H]^+$ molecular ions at m/z 1453.8, 1481.8, 1509.8, 1537.8 and 1565.8 (Fig 5.8B). Together with the compositional data, this information is consistent with the MTS-15 antigen having the glycan headgroup, $HexNAc_2Hex_3$ and a heterogeneous ceramide moiety.

A second cluster of ions was observed between m/z 250.6 and 1334.7, corresponding to the putative MTS-15 antigen minus a HexNAc residue. As similar loss was observed with a standard glycosphingolipid, GM1, these data suggest that the MTS-15 antigen is capped with a GalNac. These results, taken with the finding that the purified glycolipid was completely resistant to α- and β-galactosidase digestion (data not shown), indicate that the antigen detected by MTS-15 is likely to correspond to the globo-glycosphingolipid, $GalNAc_2Gal_2GlcCer$ (Makita & Tanaguchi, 1985).

To determine whether the terminal GalNAc is a major determinant for binding of the MTS-15 antibody, the purified glycolipid was subjected to partial acid hydrolysis and reanalysed by HPTLC. This treatment generated a number of additional glycolipid species with faster HPTLC mobility, consistent with the loss of one or more sugars (data not shown). However, none of these glycolipids were recognised by MTS-15, suggesting that the terminal GalNAc was essential for antibody recognition.

5.3 DISCUSSION

The lack of specific surface markers for thymic fibroblasts has hindered their purification for functional and genetic analysis. As a consequence, their roles in epithelial and T-cell development remain poorly defined. MTS-15 provided a promising candidate for such a marker, given its restricted expression by stromal cells around the thymic subcapsule and perivascular spaces. In this study, MTS-15 staining was compared to established markers of thymic epithelium and fibroblasts defined specific MTS-15. The antigen was found to be expressed by a subset of lining fibroblasts and a novel population of MHC II^{lo}, $CD31^{+}$ endothelial cells lining the large blood vessels of the corticomedullary junction. The association of MTS-15 staining with the vasculature was also found around splenic central arterioles and red pulp. Given their location, $MTS\text{-}15^{+}$ fibroblasts and endothelial cells are likely candidates for roles in lymphocyte entry and exit from these organs. This surface marker will enable new approaches for investigating the cellular and molecular control of these processes.

In contrast, MTS-15 staining of connective tissue areas was found in the gastro-intestinal tract and uterus. The different expression patterns in lymphoid and non-lymphoid tissues may suggest distinct roles for this antigen at these sites. Furthermore, changes in distribution throughout embryogenesis also point to unique functions in the development of the various central nervous system elements and the gastro-intestinal tract.

The immunohistology of MTS-15 in all tissues was distinguished by granular staining that extended to cells adjacent to $MTS\text{-}15^{hi}$ areas. Transfer of the antigen between cells was confirmed by *in vitro* cocultures of peripheral blood leukocytes with an $MTS\text{-}15^{+}$ cell line. The differences in the extent of acquisition between B and T lymphocytes may reflect differences in the surface compositions of these cell types (either cellular receptor

expression or the plasma membrane itself). The low level of MTS-15 staining on leukocytes analysed *ex vivo* is likely to be due to acquisition of the antigen from MTS-15$^+$ structures, as the intensity of staining correlated well with the proximity of these cells to the areas of high antigen expression (eg. DN thymocytes at the thymic subcapsule and B-cells of the splenic marginal zone adjacent to the red pulp). The absence of MTS-15 antigen on peripheral blood leukocytes suggests the antigen is shed or internalised during, or after, exit from these organs.

Shedding is a characteristic of many glycosphingolipids, occurring as membrane vesicles, micelles or monomers that can be incorporated into the lipid bilayer of nearby cells (Saqr et al., 1993; Kong et al., 1998). The mobility of the MTS-15 reactive band by tricine SDS-PAGE further implicated the antigen as being a glycolipid. This was confirmed by biochemical analyses using enzyme treatments, thin layer chromatography and gas chromatographic mass spectrometry. These data were consistent with a globo-glycosphingolipid bearing the glycan headgroup $GalNAc_2Gal_2Glc$. This corresponds to the reported structure of the Forssman antigenic determinant (Siddiqui and Hakomori, 1971; Stellner et al., 1973), detected on various glycolipid species (Willison et al., 1982). Previous murine distribution studies employing antibodies to this determinant have characterised expression in a variety of tissues, including the splenic red pulp and thymic cortical epithelium (Sadahira et al., 1988). Further work comparing the reactivities of MTS-15 and Forssman antibodies will test this candidate as the MTS-15 antigen and analyse any discrepancies in distribution.

As a surface marker of thymic perivascular fibroblasts, MTS-15 enables their purification for further studies into the role of this stromal cell subset in thymocyte migration. The spatial arrangement of these cells around the sites of precursor entry and mature thymocyte exit from the thymus implicates this subset as mediators of these processes. Given the emerging role for chemokines in thymic migration (Wilkinson et al.,

1999; Norment and Bevan, 2000; Ueno et al., 2002), MTS-15$^+$ thymic stromal cell chemokine expression profiles may shed light on the molecular mechanisms governing immigration and emigration. In addition, tethering of chemokines to perivascular fibroblast-derived ECM components may provide a solid-phase gradient to facilitate thymocyte chemotaxis (Savino et al., 2002a). The MTS-15 mAb provides an important reagent for investigations of these processes in the context of this thymic stromal cell subset.

CHAPTER 6

The role of chemokines and stromal cells in thymic emigration.

6.1 INTRODUCTION.

The thymus has the unique capacity to generate mainstream αβT-cells that are involved in virtually all adaptive immune responses. Thymocytes are ultimately derived from multipotential hematopoietic stem cells in the fetal liver or adult bone marrow that enter the thymus via arterioles (Cantor and Weissman, 1976; Kyewski, 1987; Penit and Vasseur, 1988; Lind et al., 2001). Immature thymocytes ($CD3^-CD4^-CD8^-$ triple negative (TN) cells) migrate through the cortex towards the subcapsule as they progress through the early stages of differentiation (Lind et al., 2001). Upon further development, they express CD4 and CD8 to become double positive (DP) thymocytes that traverse back through the cortex. If these cells survive thymic selection processes, they progress into the thymic medulla as $CD4^+$ or $CD8^+$ single positive (SP) thymocytes (van Ewijk, 1991). Medullary thymocytes are subject to further screening for self-tolerance as they mature sufficiently in this microenvironment to permit export to the periphery (Scollay and Godfrey, 1995; Anderson et al., 1996).

Extensive migration of thymocytes between stromal cells of different thymic microenvironments is essential for T-cell developmental events. The molecular control of thymocyte traffic in the thymus is poorly defined, however a prominent role for chemokines is emerging (Norment and Bevan, 2000). Chemokines are a family of small, basic polypeptides that direct the chemoattraction of cells via G-protein coupled seven-transmembrane receptors (Murphy, 1994; Rossi and Zlotnik, 2000). Differential expression of chemokines by thymic stromal cells and chemokine receptors by thymocytes suggests

various phases of thymic migration are influenced by distinct, but probably overlapping, gradients of these chemoattractants (Norment and Bevan, 2000). In particular, precursor immigration and T-cell emigration appear to involve active signalling processes that probably involve chemokines, in light of the findings that pertussis toxin inhibition of G-protein signalling impinges upon these processes (Chaffin and Perlmutter, 1991; Wilkinson et al., 1999).

The CXCL12 chemokine (also called stromal-cell derived factor-1, or SDF-1) is produced by stromal cells of the outer cortex and is thought to influence the migration of DN thymocytes, which express the CXCL12 receptor CXCR4 (Kim et al., 1998; Aiuti et al., 1999; Suzuki et al., 1999). While CXCR4 deficient thymocytes showed no gross defects in development (Zou et al., 1998), several studies indicate this interaction is important in early T-cell development. The trafficking of DP thymocytes through the cortex seems to be mediated in part by CCL25 (also called thymus-expressed chemokine, or TECK), produced by cortical epithelium (Wurbel et al., 2000). The CCR9 receptor for CCL25 is upregulated following signalling through the pre-T-cell receptor (Norment et al., 2000), although its ablation causes only mild impairment of early thymocyte development (Wurbel et al., 2001). Beyond this stage, the chemokine CCL22 (also called macrophage-derived chemokine, MDC) selectively attracts thymocytes during the transition from DP to SP by ligation of CCR4 (Campbell et al., 1999). Mature $CD4^+$ and $CD8^+$ SP thymocytes avidly respond to the CCR7 ligands, CCL19 (ELC, MIP3β or Exodus-3) (Rossi et al., 1997; Yoshida et al., 1997) and CCL21 (secondary lymphoid chemokine, SLC or 6Ckine) (Hedrick and Zlotnik, 1997; Nagira et al., 1997; Tanabe et al., 1997) chemokines, which are present in the thymic medulla (Annunziato et al., 2000; Bleul and Boehm, 2000). The differential expression of these ligands and receptors is suggestive of involvement in the export of thymocytes, but their precise role remains unclear.

The role of chemokines in lymphocyte trafficking into and through secondary lymphoid organs is better established (Cyster, 2000). CCL19 and CCL21 play particularly important roles in T-cell entry and localisation within lymph nodes and Peyer's Patches (Gunn et al., 1998; Forster et al., 1999; Stein et al., 2000; Warnock et al., 2000). CCL21 primarily promotes the homing of $CCR7^+$ T-cells to these organs through high endothelial venules (Stein et al., 2000). CCL19 also contributes to this process via solid phase presentation on the luminal surface of endothelial cells (Baekkevold et al., 2001), however, its main role is in promoting interactions between T-cells, dendritic cells and activated B-cells (Ngo and Tang, 1998).

The present study examined the role of chemokines in the emigration of mature thymocytes from the thymus. A novel fetal thymic organ culture (FTOC) system was devised to visualise thymocytes elicited from thymic lobes by various chemokines. In this system, CCL19 was the only chemokine capable of mediating mature thymocyte export. Analysis of thymic stromal cell expression of CCL19 and CCL21 demonstrated medullary thymic epithelial cells (mTECs) and perivascular fibroblasts to be the major source of these chemokines. However, these chemokines were presented on the surface of cortical epithelial cells (cTECs), $MTS\text{-}15^+$ perivascular fibroblasts and endothelial cells *ex vivo*. High levels of CCL19, but not CCL21 presentation by perivascular fibroblasts and endothelial cells may account for the differential roles in thymic emigration. While the receptors CCR7 and CCXCKR seem to mediate the presentation of these chemokines by epithelial cells, neither was expressed by perivascular fibroblasts. This work describes a unique role for CCL19 and stromal cells of the thymic vascular microenvironments in thymocyte emigration.

6.2 RESULTS

6.2.1 Role of CCL19 and CCL21 in thymic emigration.

To investigate the roles of various chemokines in the emigration of mature thymocytes from the thymus, a fetal thymic organ culture (FTOC) system was employed. Thymic lobes were cultured in medium containing one of a panel of candidate chemokines, and the numbers of mature thymocytes found outside the organ assessed after two days. Of the chemokines tested, only CCL19 induced the emigration of significant numbers of thymocytes from the lobes (Fig. 6.1A). CCL1, CCL2, CCL3, CCL4, CCL8, CCL11, CCL20, CCL27, XCL1, and CX3CL1 in addition to the other chemokines in Figure 6.1A failed to increase cell numbers outside the lobes (data not shown). It was particularly notable that CCL21, which shares the same receptor specificity as CCL19, did not mediate significant thymocyte emigration.

These results were investigated further using a novel time-lapse visualisation system to monitor directional cell movement from thymic lobes towards a spot of chemokine in a semi-solid medium (Fig 6.1B). Within 1 day of culture, many cells from the thymus were observed moving to a spot of CCL19 (Fig. 6.1C). This emigration was specific for CCL19 as no cells were detected from the opposite side of the lobe, nor towards a spot of CCL21. Cells recovered from these and the previous experiments had a mature thymocyte phenotype, being mostly $CD4^+CD8^-$ or $CD4^-CD8^+$ single positive (SP) TcR^{hi} T-cells, demonstrating the selective retention of the more numerous immature cells (Fig 6.1D). Exported cells were small, quiescent $CD25^-CD69^-$ T-cells, with increased expression of Ly6A and low incorporation of bromodeoxyuridine, therefore resembling recent thymic emigrants, rather than a small subset of artifactually released cells that have expanded in culture (data not shown).

Figure 6.1 CCL19 promotes the emigration of T-cells out of thymus lobes.

A. Numbers of cells recovered outside of FTOC in media supplemented with various chemokines. Listed are means and standard errors (n=4-9) of viable cell numbers found outside of the thymus lobes two days after adding the chemokines. Significance (p-value) of the cell numbers over the culture conditions in the absence of chemokines was evaluated by Student's t test. **B.** Schematic diagram of the time-lapse visualisation system employed to monitor cellular movement out of the thymus. An FTOC lobe was placed in a transparent collagen gel and cultured in medium under high oxygen conditions. Either 10μM CCL19 or 10μM CCL21 (5μl) was spotted into the collagen gel and the area within the rectangular box time-lapse monitored under a microscope with a CCD camera for 24 hours. **C.** FTOC visualised at indicated time points after spotting CCL19 or CCL21. Where indicated, the thymus lobe was monitored on the opposite side of the CCL19 spot. Bar = 250μm. Representative results of 4 experiments. **D.** Flow cytometric analysis of cells elicited from FTOC in the absence or presence of CCL19. Cells were stained with anti-CD4, anti-CD8 and anti-TcRβ. Numbers indicate the frequency of cells within each area. Data are representative of 10 experiments. Contributed by Ueno, T. and Takahama, Y. from (Ueno et al., 2002).

A.

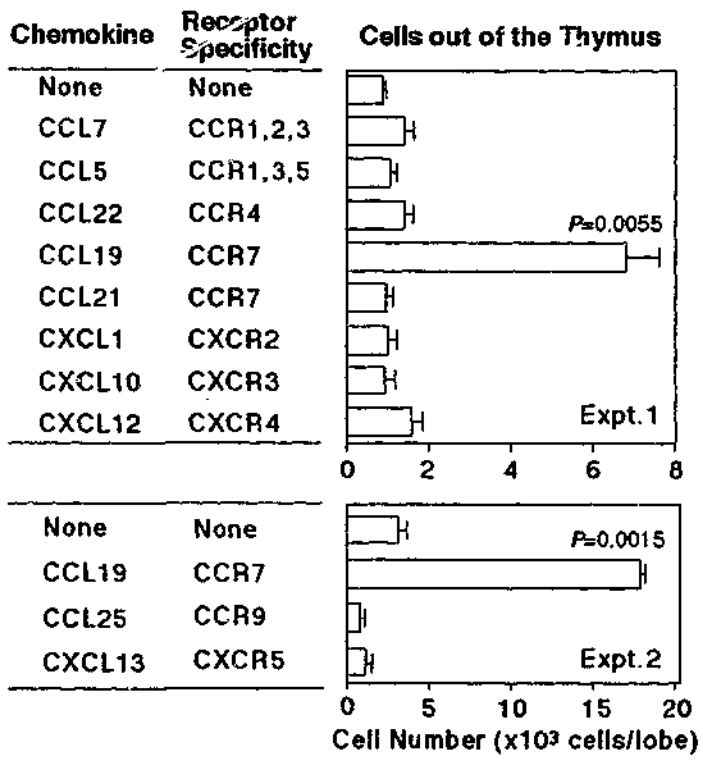
Chemokine
Receptor Specificity
Cells out of the Thymus
None None
CCL7 CCR1,2,3
CCL5 CCR1,3,5
CCL22 CCR4
CCL19 CCR7
CCL21 CCR7
CXCL1 CXCR2
CXCL10 CXCR3
CXCL12 CXCR4
P=0.0055
Expt.1
0 2 4 6 8
None None
CCL19 CCR7
CCL25 CCR9
CXCL13 CXCR5
P=0.0015
Expt.2
0 5 10 15 20
Cell Number (x10³ cells/lobe)

B.

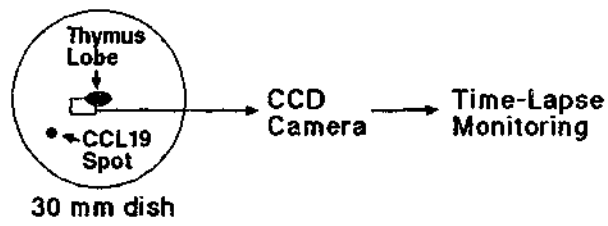
Thymus Lobe
CCL19 Spot
30 mm dish
CCD Camera
Time-Lapse Monitoring

C.

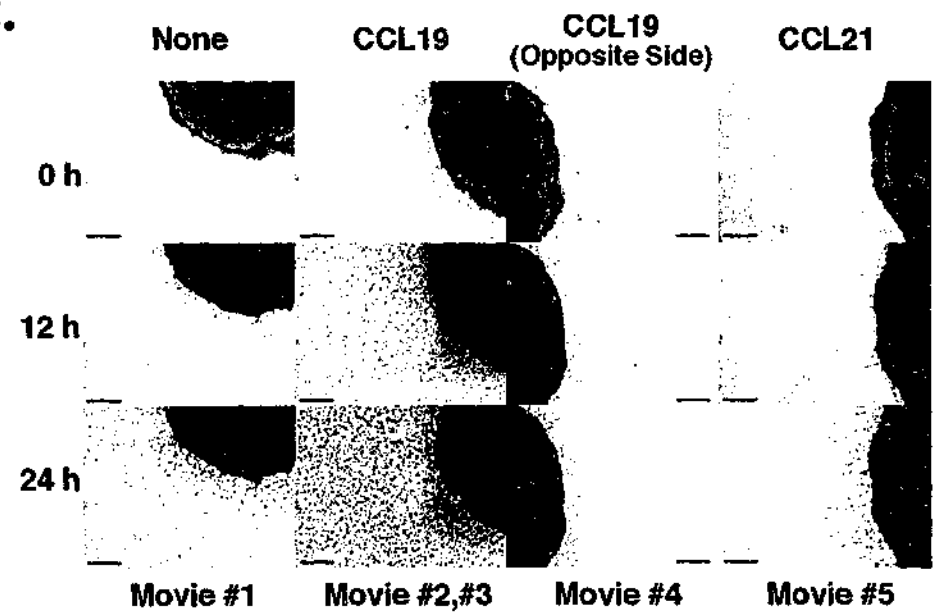
None
CCL19
CCL19 (Opposite Side)
CCL21
0 h
12 h
24 h
Movie #1
Movie #2,#3
Movie #4
Movie #5

D.

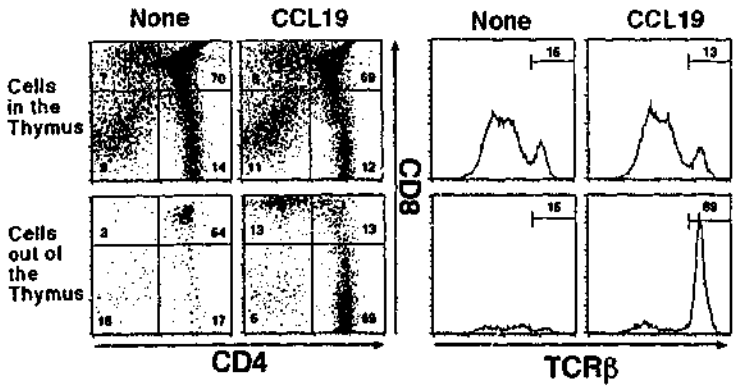
None
CCL19
None
CCL19
Cells in the Thymus
Cells out of the Thymus
CD8
CD4
TCRβ

The apparently specific effect of CCL19 in FTOC emigration, compared to CCL21, may have been due to a CCL19 specific signalling pathway that fails to transduce CCL21 derived signals, and/or the reduced accessibility of CCL21 to thymocytes under the culture conditions. Relating to this, it was found by Ueno et al., (2002) that CCL21 was as efficient at mediating the chemotaxis of CCR-7$^+$ mature T-cells in suspension culture as CCL19. This suggests the failure of CCL21 to attract thymocytes from FTOC was not due to a lack of CCR7 or other signalling molecules to transmit CCL21-induced chemotaxis. Furthermore, Ueno et al. (2002) found that removal of a unique C-terminal extension of positively charged residues from CCL21 enabled this protein to mediate emigration of thymocytes from FTOC. These data suggested the limited diffusion of CCL21 into the organ may have been responsible for the reduced efficiency of this molecule in mediating thymocyte emigration. Defective thymic emigration in neonatal CCR7-deficient and anti-CCL19 neutralised mice confirmed the selective role for CCL19 in this process (Ueno et al., 2002).

6.2.2 CCL19 and CCL21 expression by thymic stromal cells.

Central to the question of how CCL19 mediates neonatal thymocyte emigration is the expression pattern of this molecule in the thymus. While immunohistological experiments showed the localisation of this chemokine in the medulla (Annunziato et al., 2000; Bleul and Boehm, 2000), the cells expressing or presenting CCL19 were not defined. FACS purification of the major thymic stromal cell populations enabled PCR analysis of CCL19 and CCL21 mRNA transcripts. The high expression levels of CCL19 and CCL21 by medullary epithelial cells and MTS-15$^+$ perivascular fibroblasts suggest a requirement for high local concentrations of these chemokines at the sites of export (Fig. 6.2A & B).

Figure 6.2 CCL19 and CCL21 expression by thymic stromal cell subsets.

A. CCL19 and CCL21 expression by purified subsets of thymic stromal cells was assessed by PCR normalised using HPRT levels. CCL19 and CCL21 were found to be most highly expressed by mTECs. **B.** CCL19 and CCL21 expression on purified whole thymic epithelium and MTS-15$^+$ lining fibroblasts. **C.** CD45$^-$ thymic stromal cells stained with anti-EpCAM and anti-CCL21 demonstrated populations of CCL21$^+$ TECs and non-epithelial cells. **D.** Similar proportions of total cells were observed when CD45$^-$ thymic stromal cells were stained with anti-CCL19. **E.** Histogram of cTECs stained with CCL19 (solid line) and an isotype control (dotted line). A marker set according to minimal background staining (<1%) indicates the proportion of cTECs stained with CCL19. **F.** Histogram of mTECs stained with CCL21 (solid line) and an isotype control (dotted line). The proportion of CCL21$^+$ mTECs bound by the marker is indicated. **G.** CD45$^-$ thymic stromal cells stained with MTS-15 and anti-CCL19 demonstrated a distinct population of CCL19$^+$ fibroblasts. Quadrant proportions are indicated in the top right of the profile. **H.** Anti-CD31 and anti-CCL19 stained CD45$^-$ thymic stromal cells revealed a population of CCL19$^+$ endothelial cells. **I.** CD45$^-$ thymic stromal cells stained with MTS-15 and anti-CCL21 exhibited a minor population of CCL21$^+$ fibroblasts. **J.** Similarly, a small population of CCL-21$^+$ endothelial cells was observed with anti-CD31 and anti-CCL21 stained CD45$^-$ thymic stromal cells.

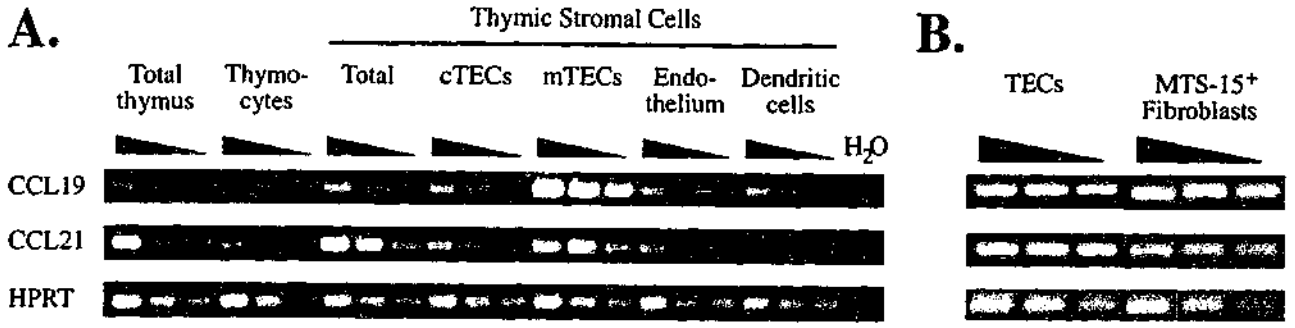
A.
Thymic Stromal Cells
Total thymus
Thymo-cytes
Total
cTECs
mTECs
Endo-thelium
Dendritic cells
H_2O
CCL19
CCL21
HPRT
B.
TECs
MTS-15+ Fibroblasts

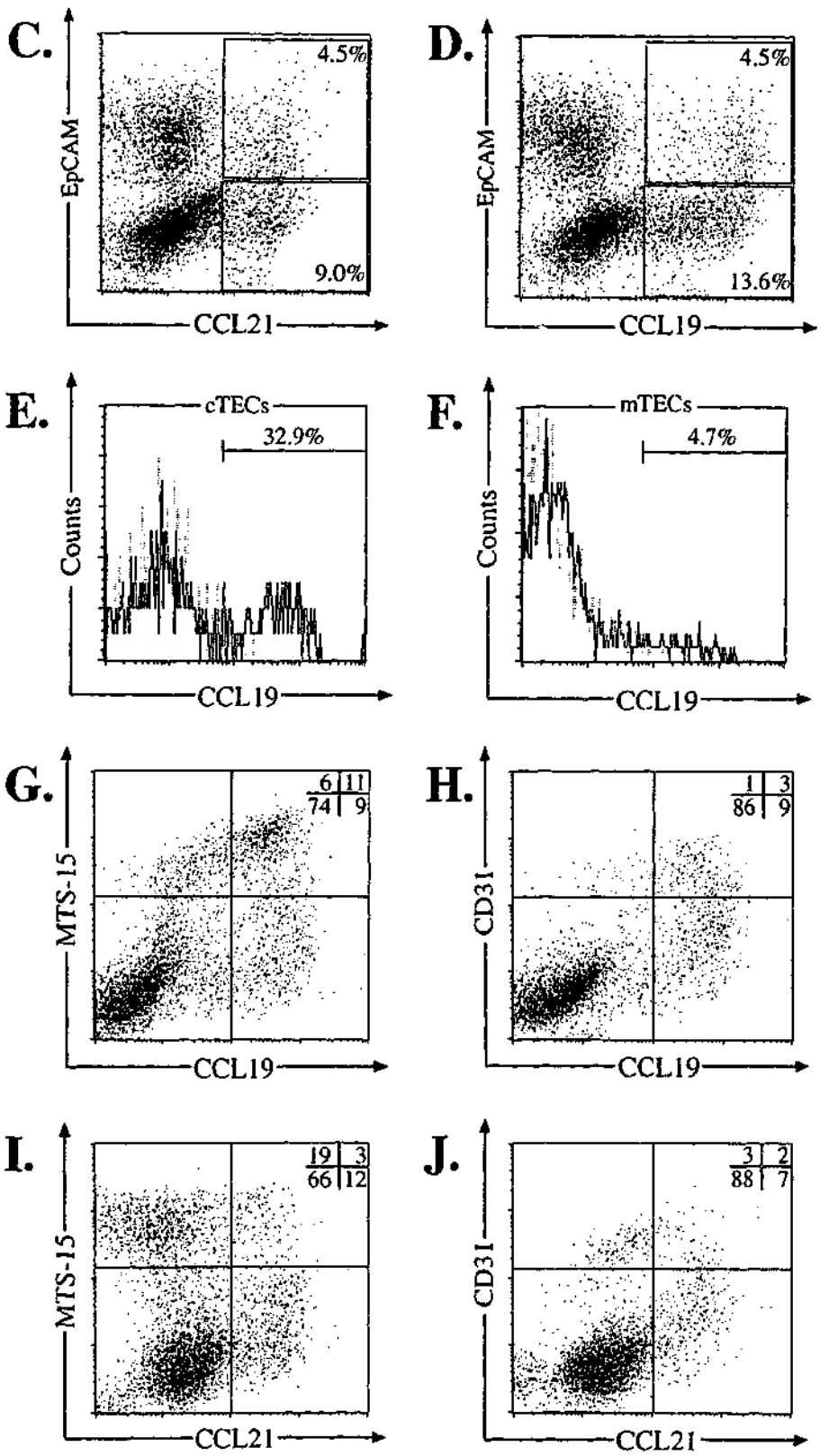
C.
4.5%
9.0%
EpCAM
CCL21
D.
4.5%
13.6%
EpCAM
CCL19
E.
cTECs
32.9%
Counts
CCL19
F.
mTECs
4.7%
Counts
CCL19
G.
6 11
74 9
MTS-15
CCL19
H.
1 3
86 9
CD31
CCL19
I.
19 3
66 12
MTS-15
CCL21
J.
3 2
88 7
CD31
CCL21

In contrast with the PCR results, flow cytometric analysis of thymic stromal populations with anti-CCL19 and anti-CCL21 (Figs. 6.2C & D) revealed a higher proportion of cTECs than mTECs bore surface CCL19 (Figs. 6.2E & F). The majority of perivascular fibroblasts and thymic endothelial cells presented CCL19, while only minor proportions were $CCL21^+$ (Figs. 6.2G-J). The apparent selectivity in fibroblast and endothelial cell presentation may relate to the ability of CCL19, but not CCL21, to mediate neonatal thymocyte export.

To determine the extent to which thymic stromal cells were capable of presenting surface CCL19, cells were preincubated with varying concentrations of recombinant CCL19 and CCL21. The intensity and proportion of anti-CCL19 staining of $CD45^-$ stromal cells specifically increased upon recombinant CCL19, but not recombinant CCL21 preincubation (Fig. 6.3A). This was reflected in all major stromal cell populations, in particular endothelial cells (all of which became $CCL19^+$) and perivascular fibroblasts (data not shown). These data suggest that the receptors responsible for presenting CCL19 on the surface of $CD45^-$ stromal cells were not saturated *ex vivo*.

This was also found to be the case for neonatal and adult thymocytes. Very low proportions of thymocytes were $CCL19^+$, with the highest levels on thymic B-cells (Fig. 6.3B and data not shown). Following preincubation with recombinant CCL19, this staining was markedly increased on TcR^{hi} SP thymocytes, although some $CD4^+$ $CD8^+$ double positive (DP) cells were also $CCL19^+$ (Fig. 6.3C). More detailed analysis showed that anti-CCL19 stained nearly all mature (HSA^{lo}) $CD8^+$ SP cells, whereas only two thirds of the less mature HSA^{hi} $CD8^+$ SP thymocytes bore the chemokine after recombinant CCL19 amplification (Fig. 6.3D). This trend was also observed on $HSA^{hi/lo}$ $CD4^+$ SP thymocytes (data not shown).

Figure 6.3 Amplification of anti-CCL19 staining on CD45$^-$ thymic stromal cells and thymocytes.

A. CD45$^-$ thymic stromal cells were stained with anti-CCL19 in the presence of varying molar excesses of either recombinant CCL19 (squares), CCL21 (triangles) or an irrelevant protein (soluble Ly6; diamonds). The proportions of CD45$^-$ cells bounded by the marker indicated on the inset plot are shown. **B.** Freshly isolated thymocytes were stained with anti-TcRβ and either a control antibody or anti-CCL19. Thymocytes pre-incubated with recombinant CCL19 and subsequently stained with anti-CCL19 are shown on the right dot plot. **C.** Dot plot of anti-CD4 and anti-CD8 staining on TcR^{hi} CCL19$^+$ region gated events in **B**. Percentages bound by regions are indicated. **D.** Histograms of anti-CCL19 staining on TcR^{hi} CD8$^+$ HSA^{hi} and TcR^{hi} CD8$^+$ HSA^{lo} pre-incubated with recombinant CCL19. Markers were set according to minimal background staining (<1%) and the percentage of CCL19$^+$ events shown.

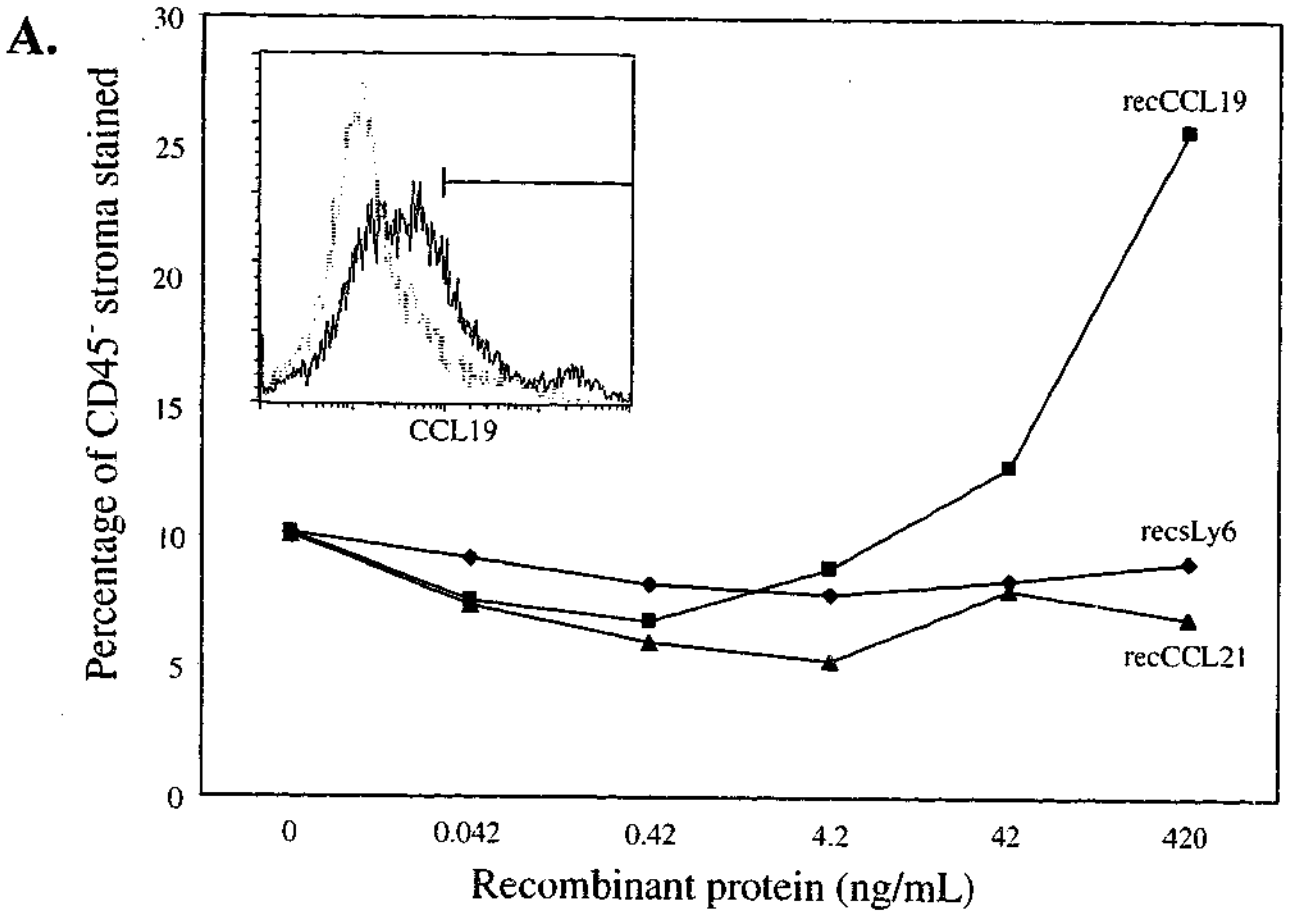
A.
Percentage of CD45⁻ stroma stained
30
25
20
15
10
5
0
CCL19
recCCL19
recsLy6
recCCL21
0
0.042
0.42
4.2
42
420
Recombinant protein (ng/mL)
B.
TcRβ
0.1%
0.6%
7.0%
Control
CCL19
CCL19 (amp.)
C.
CD4
61%
8%
27%
CD8
D.
HSA^hi
HSA^lo
Counts
66%
90%
CCL19

6.2.3 CCL19 and CCL21 receptor expression in the thymus.

The finding that both thymocytes and thymic stromal cells displayed surface CCL19 and CCL21 prompted analysis of chemokine receptors on these cell populations. It has been established that mature thymocytes express CCR7, the main receptor for these chemokines (Campbell et al., 1999), but a distinct chemokine receptor (CCXCKR) capable of binding these molecules has recently been described (Townson and Nibbs, 2002). Unlike most other chemokine receptors, CCXCKR does not mediate calcium fluxes upon ligand binding (Townson and Nibbs, 2002). CCR7 and CCXCKR expression by thymic stromal cells and thymocytes was assessed by reverse transcriptase PCR of FACS purified populations. CCXCKR expression could not be detected in thymocytes, suggesting that CCR7 is the most likely candidate receptor binding CCL19 and CCL21 detected on these cells. In contrast, CCXCKR transcripts were detected in cTECs, but not other stromal cell populations by conventional and real-time PCR (Fig. 6.4A & B). Therefore, cTECs appear to be the only major cell type expressing this receptor in the thymus, which is likely to mediate at least some CCL19 presentation by these cells (Fig. 6.2E). It was also found that total thymic epithelial cells express low levels of the functional receptor CCR7, which may also be involved in CCL19 presentation (Fig. 6.2C). Interestingly, MTS-15^{+} lining fibroblasts that preferentially present CCL19 over CCL21, did not express either receptor at detectable levels.

To further investigate the nature of CCL19 interaction with thymocytes and stromal cells, the effect of various enzyme treatments on CCL19 presentation was assessed. Thymocyte or stromal cell suspensions were incubated with collagenase, dispase or trypsin, followed by recombinant CCL19 incubation and staining. Figure 6.5A shows that CCL19 binding to TcR^{hi} thymocytes (CCR7 dependent) is sensitive to trypsin digestion, but not dispase, collagenase or heparinase treatment. CCL19 binding to thymic stromal cells was

Figure 6.4 Chemokine receptor expression by thymic stromal cells.

A. Expression of CCXCKR was assessed in purified stromal cell subsets by PCR normalised by HPRT levels. **B.** Real-time PCR was employed to confirm the levels of CCXCKR expression in purified stromal cell subsets. A bar graph of amounts of CCXCKR relative to whole thymus expression (equals 1) is shown. **C.** CCR7 and CCXCKR expression was determined in purified TECs and MTS-15$^+$ fibroblasts by PCR normalised using HPRT levels.

A.

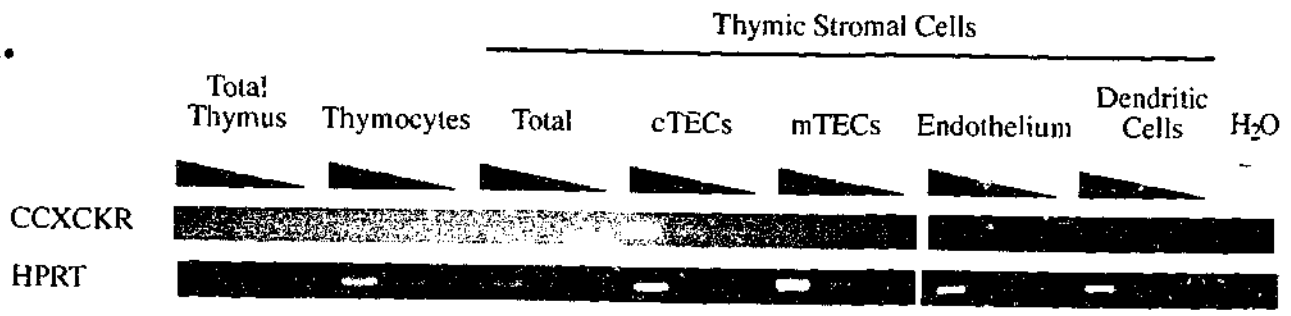
Thymic Stromal Cells
Total Thymus
Thymocytes
Total
cTECs
mTECs
Endothelium
Dendritic Cells
H_2O
CCXCKR
HPRT

B.

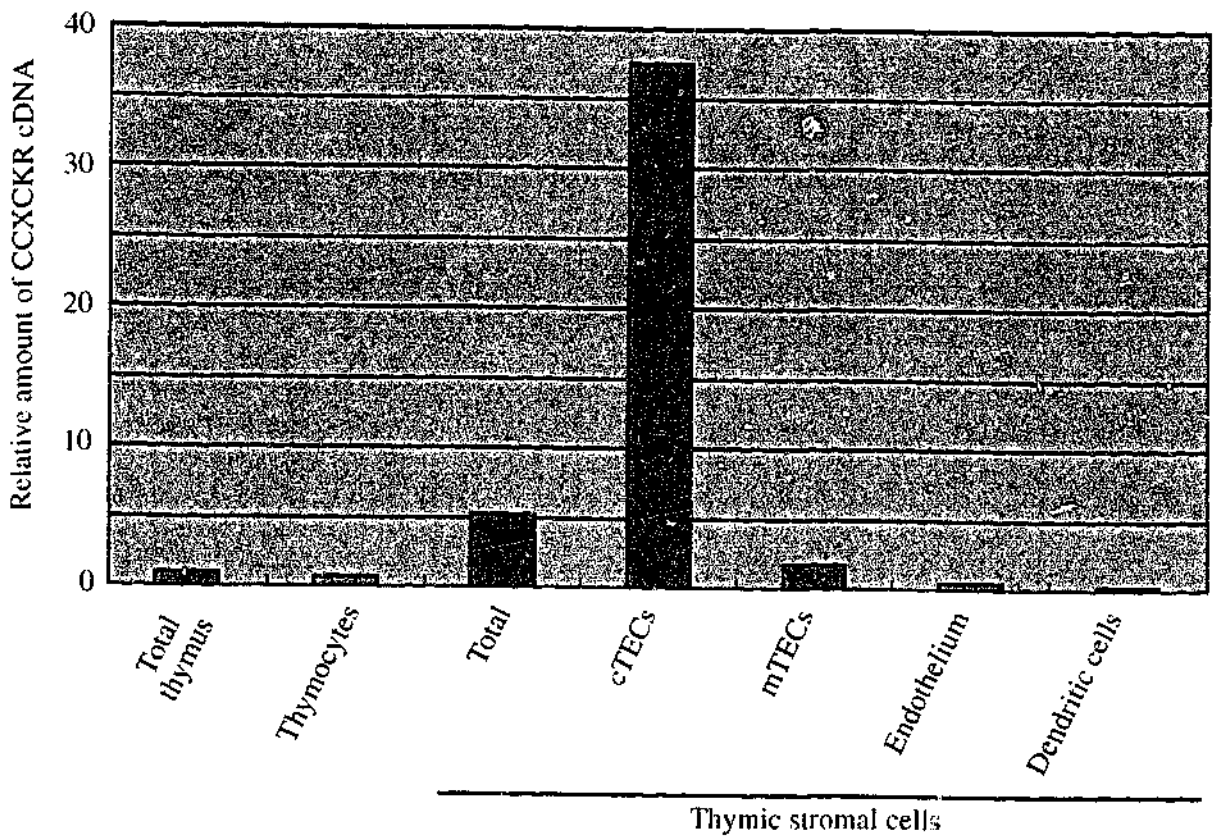
Relative amount of CCXCKR cDNA
40
30
20
10
0
Total thymus
Thymocytes
Total
cTECs
mTECs
Endothelium
Dendritic cells
Thymic stromal cells

C.

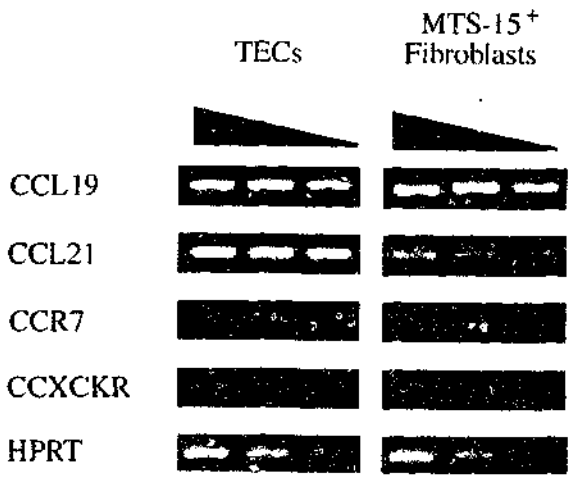
TECs
MTS-15+ Fibroblasts
CCL19
CCL21
CCR7
CCXCKR
HPRT

Figure 6.5 Enzyme sensitivity of CCL19 receptors on thymocytes and CD45$^-$ thymic stromal cells.

A. Thymocytes incubated in collagenase, dispase, trypsin or heparinase were treated with recombinant CCL19 and anti-CCL19 staining examined on TcR^{hi} thymocytes. Histograms with markers set according to minimal control staining (dashed lines) show the almost complete loss of CCL19 staining (solid line) after trypsin treatment. **B.** Dot plots of CCL19 and MHC II expression gated on CD45$^-$ stromal cells following enzyme treatment and recombinant CCL19 incubation. The proportion of CCL19$^+$ stromal cells (indicated on plots) decreases with dispase and trypsin treatment.

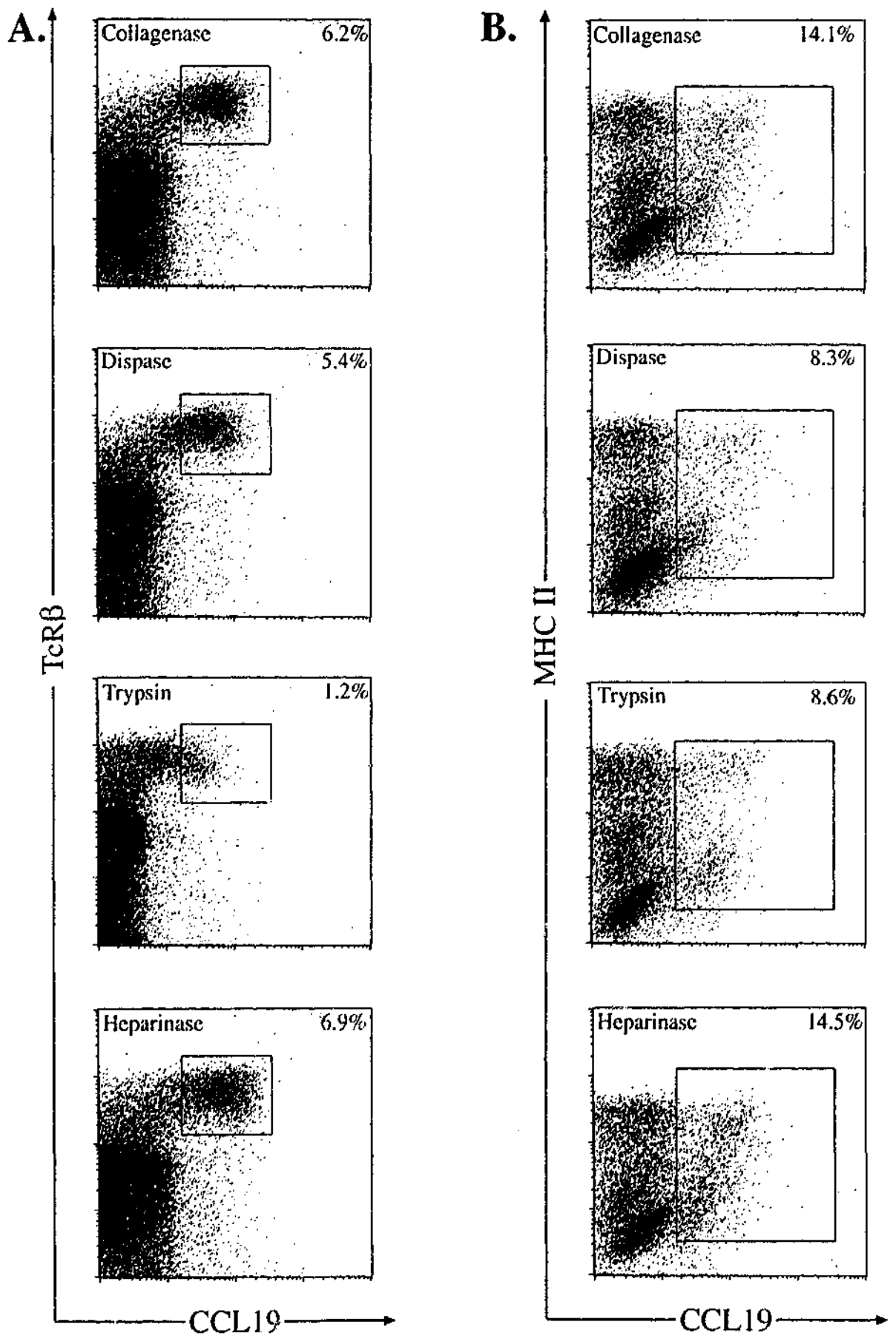
A.
Collagenase
6.2%
Dispase
5.4%
Trypsin
1.2%
Heparinase
6.9%
TcRβ
CCL19
B.
Collagenase
14.1%
Dispase
8.3%
Trypsin
8.6%
Heparinase
14.5%
MHC II
CCL19

partially susceptible to dispase digestion, however some TECs and non-epithelial cells still exhibited surface CCL19. These populations retained this activity after trypsin digestion also, suggesting the expression of CCL19 receptors other then CCR7 on these cells.

6.3 DISCUSSION

The disruption of thymic export in mice with a defect in G-protein signalling first implicated active, possibly chemokine, receptor signalling in this process. Of the chemokines tested in this study, only CCL19 affected the export of cells that phenotypically resembled recent thymic emigrants from FTOC. CCL21, which binds to the CCR7 receptor with CCL19, did not mediate export, primarily due to retention of this chemokine by thymic ECM components (Ueno et al., 2002). These findings were supported by *in vivo* experiments demonstrating CCR7 deficient and anti-CCL19 (but not anti-CCL21) neutralised neonatal mice had export defects (Ueno et al., 2002).

CCL19 and CCL21 mRNA were detected mainly in mTECs (supporting Bleul and Boehm, 2000) and perivascular fibroblasts. CCL19 (and to a lesser extent, CCL21) protein was detected on the surface of cTECs, perivascular fibroblasts and endothelial cells, but not mTECs. Since CCL19 mRNA levels were very low in endothelial cells and cTECs, it is likely that the surface CCL19 presented by these cells is derived from soluble chemokine expressed by nearby perivascular fibroblasts and mTECs, respectively. The presentation of chemokine on the surface of these cells presumably facilitates interactions with thymocytes, in a similar manner to that reported for T-cell interactions with high endothelial venules (Baekkevold et al., 2001), and dendritic cells within lymph nodes by CCL19 (Ngo and Tang, 1998). The selective presentation of CCL19 compared to CCL21 by endothelial cells and perivascular fibroblasts may explain the predominant role for this chemokine in neonatal thymic export. An important question regarding the endothelial presentation of CCL19 is

whether this occurs on the luminal, abluminal or both sides of the cells (Rot, 2003). Endothelial presentation influencing thymic export would be expected to occur on the abluminal surface.

Chemokines could potentially be tethered to the cell surface in several ways. Non-specific presentation by endothelial cells has been shown to be predominantly mediated by glycosaminoglycans (GAGs) and the Duffy antigen/receptor for chemokines (DARC) (Middleton et al., 2002). However, it has been reported that DARC does not bind CCL19 (Baekkevold et al., 2001) and the persistence of stromal cell CCL19 presentation after heparinase treatment argues against a role for the GAGs, heparin and heparin sulfate. Another way these chemokines may be tethered to cells is via specific cell surface receptors such as CCR7 or CCXCKR. For instance, the likely involvement of a protein cell surface receptor in binding CCL19 to the surface of thymocytes was demonstrated by trypsin ablation of anti-CCL19 staining. In the absence of CCXCKR expression, this interaction is likely to be solely mediated by CCR7 expression.

Restricted CCXCKR expression by $CCL19^{+}$ cTECs suggests this receptor mediates some CCL19 presentation by this cell type, although a role for CCR7 cannot be ruled out. A non-signalling receptor such as CCXCKR may have a role as a reservoir for soluble CCL19 emerging from the medulla, either to facilitate interactions between late DP thymocytes and cTECs, or to reduce the amount of soluble CCL19 in this microenvironment. The detection of CCL19 binding capacity on a small population of TcR^{hi} DP thymocytes supports earlier studies showing chemotaxis of mature DP and SP thymocytes to CCL19 (Kim et al., 1998; Ngo and Tang, 1998; Campbell et al., 1999). This is consistent with a proposed role for CCL19 and CCL21 in attracting cells into and through the medullary microenvironment (Ansel and Cyster, 2001). Once in the medulla, SP thymocytes are likely to influenced predominantly by soluble CCL19 and CCL21 (along with other chemokines), given that nearly all mTECs were $CCL19^{-}$. The preferential surface presentation of CCL19 by

perivascular fibroblasts and endothelial cells may facilitate interactions with thymocytes to enable those at the appropriate stage of maturation to extravasate. The nature of CCL19 and CCL21 tethering to these cell types remains to be characterised. Unlike epithelial cells or thymocytes, these cells do not express CCR7 or CCXCKR and surface CCL19 interaction displays different enzyme sensitivity. This suggests either non-specific tethering or an as yet uncharacterised surface receptor mediates this interaction.

In summary, we propose a two-step role for CCL19 and CCL21 in thymocyte migration (Fig 6.6). Initially, these chemokines influence the movement of mature DP and SP thymocytes towards the medullary microenvironment following positive selection (Ansel and Cyster, 2001). This may involve cellular interactions with cTECs facilitated by CCL19 presentation. Maturation within the medulla leads to further expression of CCR7 by SP thymocytes, potentiating interactions with $CCL19^{+}$ perivascular fibroblasts and thymic endothelial cells and facilitating the export of mature thymocytes from the thymus. The fact that CCR7 deficient and anti-CCL19 neutralised mice demonstrate only partial blocks in thymic export point to roles for other chemokines or cell adhesion molecules in this process. These different, but overlapping roles for CCL19 and CCL21 in thymic emigration mirror those observed in secondary lymphoid organs.

Figure 6.6 Two step model for CCL19 and CCL21 in thymocyte migration.

CCL19 and CCL21 expression by mTECs creates a soluble gradient that mediates the chemotaxis of mature, TcR^{hi} DP and SP thymocytes from the cortex (1). CCXCKR on cTECs acts as a reservoir receptor for CCL19 and CCL21, to either facilitate interactions with cTECs or prevent chemokines penetrating further into the cortex. Following maturation of SP thymocytes in the medulla, CCL19 presentation by perivascular fibroblasts and endothelial cells facilitates the extravasation of T-cells eligible for export (2).

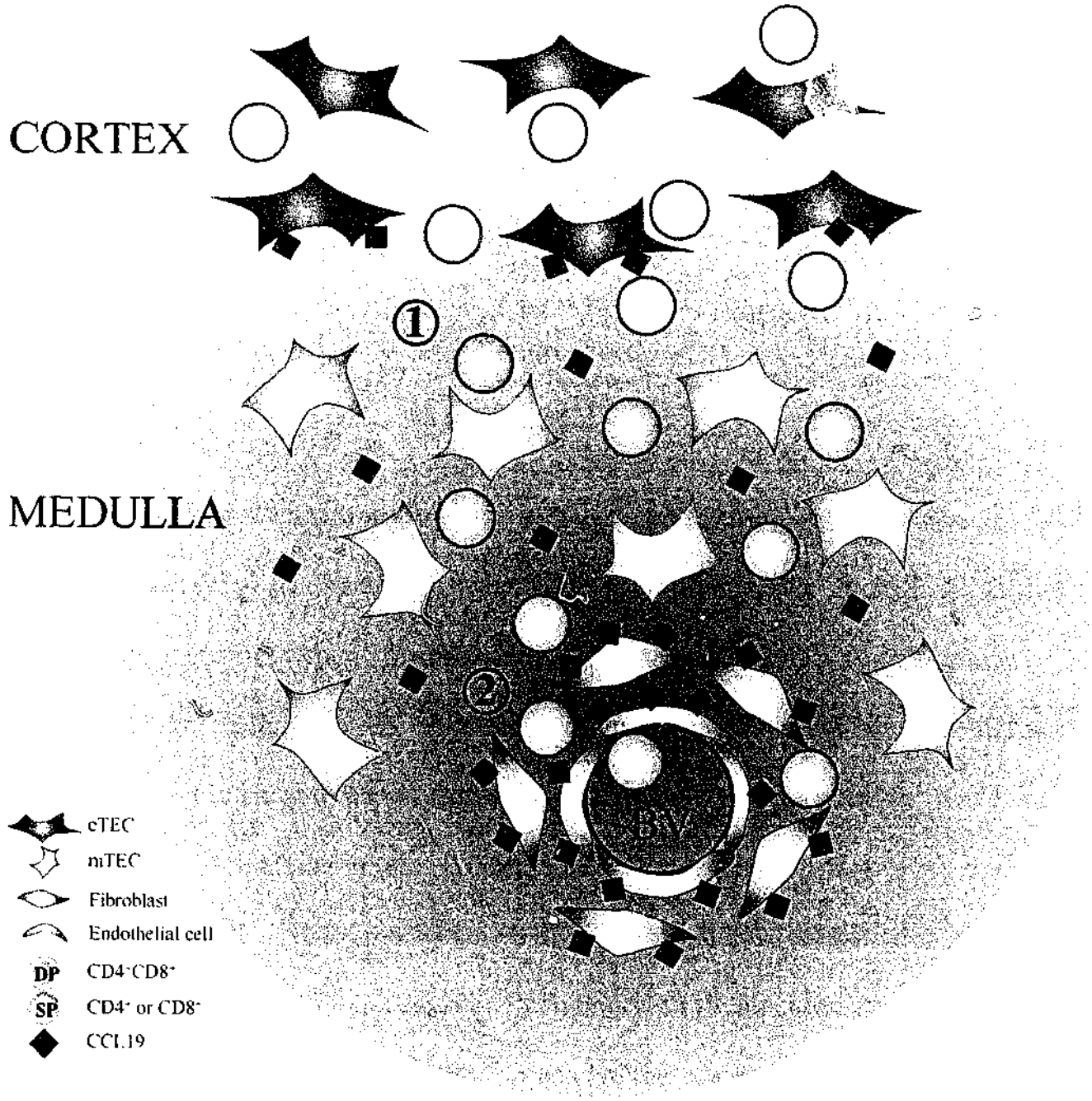
CORTEX
MEDULLA
①
②
③
BV
cTEC
mTEC
Fibroblast
Endothelial cell
DP CD4⁺CD8⁺
SP CD4⁺ or CD8⁺
CCL19

CHAPTER 7

General Discussion: Stromal cells in thymic homeostasis.

Despite the importance of thymic stromal cells to T-cell development, little is known regarding the local or systemic factors controlling their function. Improving our understanding of these factors will not only shed light on aspects of T cell development, but will be important for the development of strategies that manipulate thymic homeostasis to re-establish immunity following immunodepletion regimes (eg. chemotherapy, AIDS or bone marrow transplants).

Under normal conditions, the rate of T-cell production is closely linked to overall thymic cellularity, so the marked changes observed in thymus size throughout life directly impinge upon thymic output. Stromal cells have been shown to play critical roles in all parameters that might govern thymic size, namely, precursor import, thymocyte proliferation, deletion and export (for example, Wilkinson et al., (1999); Anderson and Jenkinson, (2001); Ueno et al., (2002), see Chapter One). However, the current understanding of the mechanisms by which thymic stromal cells mediate these processes is poor. Given that stroma functions in co-operation with thymocytes, the maintenance and alteration of thymic homeostasis is likely to involve the modulation of these lymphostromal interactions. Our understanding of these interactions has been limited due to the difficulty in studying the heterogeneous stromal populations.

This thesis developed the reagents and technologies required to study thymic stromal cells by flow cytometry, and employed them to define fundamental relationships between stromal cells and thymocytes at the quantitative and phenotypic levels. In addition,

investigations of the role of stromal cells in mediating the export of mature thymocytes gave some insight into possible mechanisms of this process.

7.1 QUANTITATIVE AND PHENOTYPIC ASPECTS OF THE LYMPHO-STROMAL INTERPLAY.

To date, most thymic stromal research has relied heavily upon immunohistology to describe the phenotypic heterogeneity of this population. This approach has provided valuable information regarding the distribution of various stromal subsets, but has only limited power to reliably analyse this compartment at the single cell and population level. Hence, there has been little or no assessment of quantitative aspects of the lymphostromal relationship. The refinement of stromal cell isolation techniques and correlation surface markers described in Chapter Three enable flow cytometric analysis of thymic stromal cells, permitting the enumeration and purification of this heterogeneous population. This was highlighted in subsequent chapters of this thesis where key questions regarding the stromal cell population dynamics, phenotype and their role in thymic export were addressed. The focus on these technically challenging questions revealed important parameters of thymic homeostasis.

Chapter Four shows that stromal cells are a more dynamic cell population than previously thought. Rather than providing a static scaffold through which thymocytes differentiate, stromal microenvironments appear to constantly turnover and remodel throughout life. Following birth, the ratio of thymocytes to stromal cells is relatively constant within a narrow range, which raises the question of what influences and maintains this relationship. Do thymocytes simply expand to fill available stromal cell niches, or is there an active homeostatic feedback loop between the two cell types? In light of the association between enhanced stromal cell contact and accelerated thymocyte development during embryogenesis, the answers to these questions will have direct implications on

thymic function. A major determinant of this relationship is likely to be the nature of lympho-stromal crosstalk. This thesis and previous studies have demonstrated that reciprocal interaction between stromal cells and thymocytes are intimately linked to their differentiation. Chapter Four extends our understanding of this synergy, characterising the thymocyte dependency of novel adult TEC subsets. The definition of TEC subsets using surface markers enables the FACS purification of these subpopulations for direct assessment of their lineage potential. These studies will be important in determining whether a population of adult thymic epithelial stem cells exist. If this were the case, it would represent an ideal target for therapeutic strategies aimed at restoring thymic function.

Chapters 3 and 4 also provide a framework for further investigations into situations where stromal cell and thymocyte homeostasis is disrupted. Given the polygenic complexities of thymus organogenesis, the aetiology of the thymic microenvironmental defects observed in many autoimmune models may be multifactorial, but one likely possibility is disturbances in thymic "crosstalk". A greater understanding of how these defects arise in turn should provide insight into how central tolerance can be broken. Conversely, cyclin D1 transgenic mice exhibit severe thymic hyperplasia, while maintaining a normal thymic microenvironment and T-cell development (Robles et al., 1996). Investigations into the thymocyte and stromal cell relationships in this model should reveal more about quantitative aspects of thymic homeostasis and how they may be influenced.

7.2 THYMIC STROMAL CELLS AND THYMIC MIGRATION

Thymic stromal cells may affect alterations in thymus size in four main ways; by changing thymic import or export rates, or by modulating thymocyte expansion or deletion (Fig. 7.1). While thymic stromal cells are known to be critical for the processes of immigration and emigration, the subsets involved and their precise roles are unknown.

Figure 7.1 Possible stromal cell control points of thymic homeostasis.

Thymic stromal cells may maintain or alter thymic cellularity by influencing thymic import, intrathymic proliferation or thymic export. Increased precursor recruitment may lead to a large downstream increase in overall thymic cell numbers, as each precursor gives rise to many thymocytes (**A**). Alterations of stromal-derived growth factors such as IL-7 may induce thymocyte proliferation to increase thymic cellularity. Thymocyte expansion may in turn increase the provision of TEC growth factors like KGF, enhancing the potential for further thymic growth (**B**). Stromal cell regulation of thymic export could retain mature thymocytes or accelerate their release into the periphery, thereby causing slight changes in thymic cellularity (**C**).

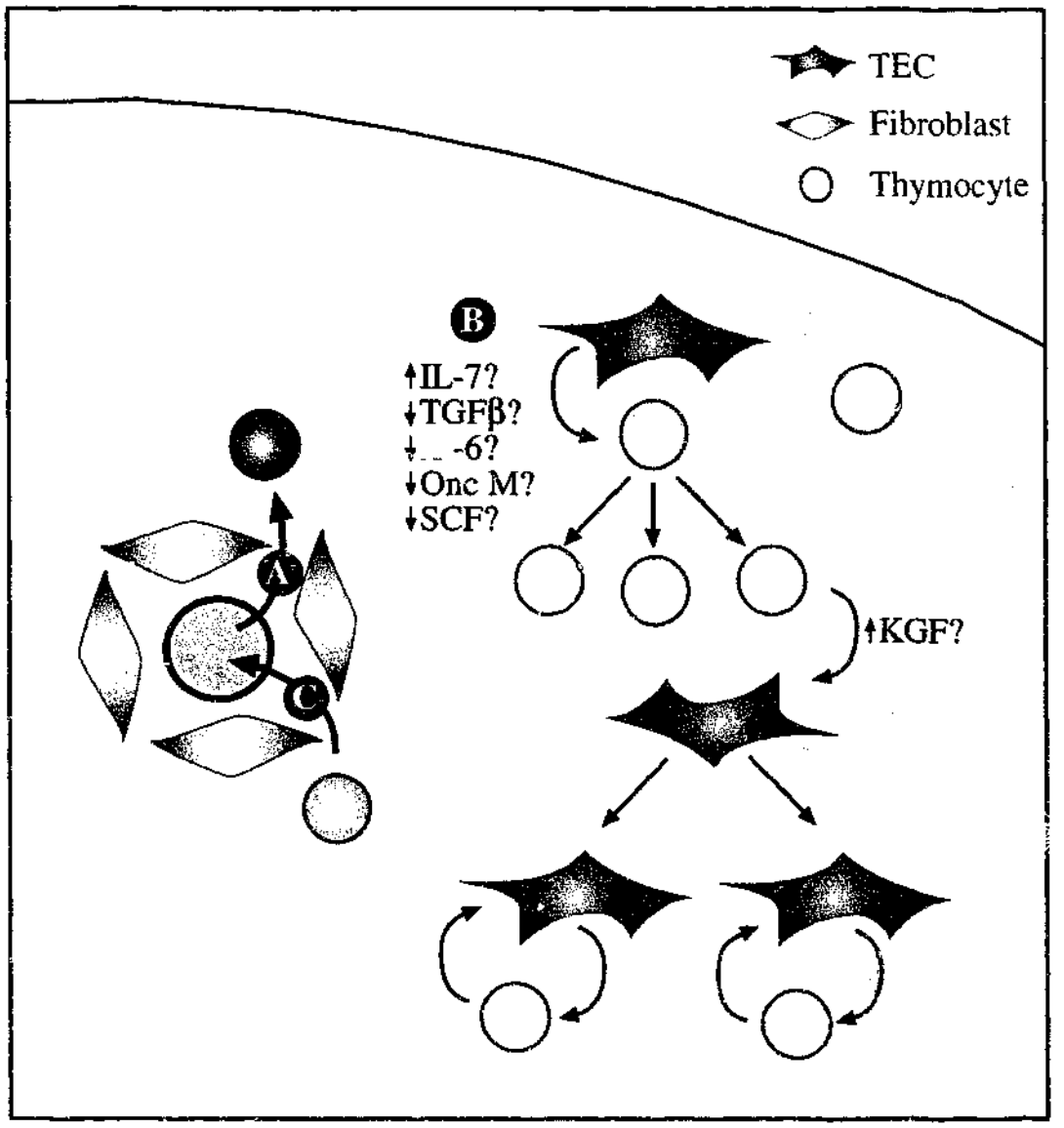
TEC
Fibroblast
Thymocyte
B
↑IL-7?
↓TGFβ?
↓...-6?
↓Onc M?
↓SCF?
A
C
↑KGF?

A logical stromal cell subset to be involved in the immigration of thymocyte precursors and the export of mature T-cells are the perivascular fibroblasts (pericytes). Residing in the first microenvironment encountered by immigrants, pericytes may influence thymic import via the provision of directional cues or adhesion factors. The characterisation of the MTS-15 mAb in Chapter Five shows that it detects a glycolipid antigen specifically expressed by these cells, providing an invaluable tool for their analysis. Purification of MTS-15$^+$ pericytes for functional and molecular analysis should not only define the precise role for these cells in this process, but also contribute to our understanding of how thymic import is regulated. Such studies will be important since a slight increase in thymic HSC import, for example, could translate into large differences in overall numbers due to thymocyte expansion. However currently, this is a difficult process to investigate. While the uptake of HSCs with congenic markers in different thymic states might indicate changes in "permeability" to precursors, the possibility of rapid expansion or death of precursors immediately following import could not be ruled out. Experiments involving the intrathymic injection of varying numbers of congenically marked HSCs into mice could reveal whether increased HSC supply to the thymus alone alters thymic homeostasis. These studies must then be related to physiological control of thymic import, perhaps involving MTS-15$^+$ stromal cells.

Chapter Six examined the role of the stroma in thymic export. Following demonstration of the involvement of CCL19 and CCL21 in mature T-cell export from the thymus using an elegant culture system, characterisation of stromal expression patterns was a key progression to defining the mechanisms mediating export. Flow cytometric purification of the various subsets identified medullary epithelium and MTS-15$^+$ pericytes as the main producers of these chemokines in the thymus. The finding that pericytes and endothelium predominantly present CCL19, but not CCL21 on their surface provided the cellular context for a hypothesis addressing why these chemokines have differential effects

on neonatal export. Further testing of this hypothesis by disrupting or augmenting chemokine presentation by these cells will enhance our understanding of thymic export and how it may be manipulated. The transgenic expression of high levels of CCL19 under control of a mTEC specific promoter (eg. K14 promoter construct in Capone et al., (2001) may increase thymocyte migration into this microenvironment and subsequent export.

Intuitively, it may seem beneficial to enhance thymic export in immunodepleted states to improve immunity. However, the constant rate of thymic export, autonomous of changes in the periphery or supply (Gabor et al., 1997b; Berzins et al., 1998), suggests this is a tightly regulated process in thymocyte maturation, which ensures appropriate interaction of developing T cells with the microenvironment. Disturbances in this would be likely to predispose to pathological conditions, the most obvious of which would be the by-passing of tolerance mechanisms to induce autoimmunity. It would thus be important to assess the functional competence and self-tolerance of T-cells generated by increasing the rate of T-cell development and export, since this may compromise thymic selection processes. In the context of the global problem of enhancing thymic export in atrophic or immunodepleted states, care must be taken to abide by "thymic rules" to prevent the escape of potentially pathological T-cells.

7.3 THE THYMIC STROMA IN REGENERATION

Another means by which stromal cells may mediate changes in thymic cellularity is by inducing thymocyte proliferation or death via modulation of growth factors. Systemic factors such as hormones have trophic (eg. growth hormone Savino et al., (2002b)) and atrophic (eg. sex steroids Olsen et al., (1991a)) influence on thymic size via stromal cells (Staples et al., 1999; Tibbetts et al., 1999; Olsen et al., 2001). Thymic regeneration following sex steroid ablation is an example of how thymic homeostasis can be altered (via

the stroma (Olsen et al., 2001)) to affect broad improvements of immunity in the aged (Sutherland, 2001). Blocking sex steroids induced rapid expansion of all major thymocyte subsets, resulting in greatly increased thymus size (Sutherland, 2001). This suggests regeneration stems from an overall trophic effect in addition to, or rather than, increased precursor recruitment. However, the phenotypic and numerical relationships between thymocytes and stromal cells during this process are central to any understanding of how thymic homeostasis is influenced.

The data presented in Chapter Four shows that while stromal cells also change during thymic regeneration to resemble normal young composition and numbers, the kinetics of their regeneration are delayed compared to thymocytes. This may indicate that following the initial stromal-derived stimulus for thymocyte growth, it takes some time for crosstalk to feed back on stromal cells to induce their proliferation. Although the factors involved in the lympho-stromal crosstalk during thymic regeneration are yet to be characterised, sex steroid blockade demonstrates how alteration of a systemic factor can affect stromal cells and change thymic homeostasis. More work characterising how the stroma mediates this effect will be important to improve our understanding of how these changes occur naturally and may be induced therapeutically.

Several stromal-derived cytokines linked to thymic homeostasis are candidates to provide the initial regenerative stimulus. For example, IL-7 stimulation causes extensive proliferation of early thymocytes and systemic administration enhances thymic regeneration following immunodepletion (Bolotin et al., 1996; Mackall et al., 2001). On the other hand, elevated levels of IL-6, Oncostatin M, Leukaemia Inhibitory Factor (LIF) and Stem Cell Factor (SCF) have been shown to cause and be upregulated during thymic atrophy (Sempowski et al., 2000). Decreased production of these cytokines and/or increased production of IL-7 by stromal cells in response to ablation of sex steroid signalling is likely drive the general thymocyte expansion observed.

Enhancement of thymopoiesis would in turn lead to an increased provision of keratinocyte growth factor (KGF or FGF-7) by mature thymocytes. KGF is a potent stimulator of TEC proliferation and like IL-7, systemic administration causes thymic regeneration (Erickson et al., 2002; Min et al., 2002; Rossi et al., 2002). Such cytokines represent key molecular candidates in the crosstalk promoting thymic regeneration. Genetic analysis of FACS purified thymic stromal subsets following sex steroid withdrawal will reveal which of these factors are involved in thymic regeneration. This modulation of lymphostromal interactions is likely to be the predominant mechanism by which stromal cells influence adult thymic homeostasis.

The influence of stromal cells on thymic homeostasis has important implications for therapeutic interventions that focus on manipulating thymic function. However, approaches to improving thymopoiesis must take care to obey "thymic rules" to prevent the generation of pathological T-cells. This thesis defines fundamental parameters of thymic stromal cell biology, broadening our understanding of this population within the context of the whole organ. In addition, the definition of new techniques and reagents described here provides invaluable tools for further research into how the stroma maintains thymic homeostasis and function

BIBLIOGRAPHY

Aiuti, A., Tavian, M., Cipponi, A., Ficara, F., Zappone, E., Hoxie, J., Peault, B. and Bordignon, C. (1999) Expression of CXCR4, the receptor for stromal cell-derived factor-1 on fetal and adult human lympho-hematopoietic progenitors. *Eur J Immunol* **29**, 1823-1831.

Alam, S.M., Travers, P.J., Wung, J.L., Nasholds, W., Redpath, S., Jameson, S.C. and Gascoigne, N.R.J. (1996) T-cell-receptor affinity and thymocyte positive selection. *Nature* **381**, 616-620.

Allman, D., Sambandam, A., Kim, S., Miller, J.P., Pagan, A., Well, D., Meraz, A. and Bhandoola, A. (2003) Thymopoiesis independent of common lymphoid progenitors. *Nat Immunol* **4**, 168-174.

Anderson, G., Anderson, K.L., Tchilian, E.Z., Owen, J.J. and Jenkinson, E.J. (1997) Fibroblast dependency during early thymocyte development maps to the CD25+ CD44+ stage and involves interactions with fibroblast matrix molecules. *Eur J Immunol* **27**, 1200-1206.

Anderson, G. and Jenkinson, E.J. (2001) Lymphostromal interactions in thymic development and function. *Nature Reviews Immunology* **1**, 31-40.

Anderson, G., Jenkinson, E.J., Moore, N.C. and Owen, J.J. (1993) MHC class II-positive epithelium and mesenchyme cells are both required for T-cell development in the thymus. *Nature* **362**, 70-3.

Anderson, G., Moore, N.C., Owen, J.J.T. and Jenkinson, E.J. (1996) Cellular interactions in thymocyte development. *Annu. Rev. Immunol.* **14**, 73-99.

Anderson, G., Owen, J.J., Moore, N.C. and Jenkinson, E.J. (1994) Thymic epithelial cell provide unique signals for positive selection of CD4+CD8+ thymocytes in vitro. *J Exp Med* **179**, 2027-2031.

Anderson, G., Partington, K.M. and Jenkinson, E.J. (1998) Differential effects of peptide diversity and stromal cell type in positive and negative selection in the thymus. *J Immunol* **161**, 6599-603.

Anderson, M., Anderson, S.K. and Farr, A.G. (2000) Thymic vasculature: organiser of the medullary epithelial compartment? *Int Immunol* **12**, 1105-1110.

Anderson, M.S., Venanzi, E.S., Klein, L., Chen, Z., Berzins, S.P., Turley, S.J., von Boehmer, H., Bronson, R., Dierich, A., Benoist, C. and Mathis, D. (2002) Projection of an immunological self shadow within the thymus by the aire protein. *Science* **298**, 1395-13401.

Annunziato, F., Romagnani, P., Cosmi, L., Beltrame, C., Steiner, B.H., Lazzeri, E., Raport, C.J., Galli, G., Manetti, R., Mavilia, C., Vanini, V., Chantry, D., Maggi, E. and Romagnani, S. (2000) Macrophage-derived chemokine and EBI-1-ligand chemokine attract human thymocytes in different stages of development and are produced by distinct subsets of

medullary epithelial cells: possible implications for negative selection. *J Immunol* **165**, 238-246.

Ansel, K.M. and Cyster, J.G. (2001) Chemokines in lymphopoiesis and lymphoid organ development. *Curr Opin Immunol* **13**, 172-179.

Artavanis-Tsakonas, S., Rand, M.D. and Lake, R.J. (1999) Notch signaling: cell fate control and signal integration in development. *Science* **284**, 770-776.

Asano, M., Toda, M., Sakaguchi, N. and Sakaguchi, S. (1996) Autoimmune disease is a consequence of developmental abnormality of a T cell population. *J Exp Med* **184**, 387-396.

Ashton-Rickardt, P.G., Bandeira, A., Delaney, J.R., Van Kaer, L., Pircher, H., Zinkernagel, R.M. and Tonegawa, S. (1994) Evidence for a differential avidity model of T cell selection in the thymus. *Cell* **76**, 593-596.

Ashton-Rickardt, P.G. and Tonegawa, S. (1994) A differential-avidity model for T-cell selection. *Immunol Today* **15**, 362-6.

Aspinall, R. (1997) Age-Associated Thymic Atrophy in the Mouse is Due to a Deficiency Affecting Rearrangement of the TCR During Intrathymic T Cell Development. *J. Immunology* **158**, 3037-3045.

Aspinall, R. and Andrew, D. (2000) Thymic involution in aging. *J Clin Immunol* **20**, 250-6.

Atlan-Gepner, C., Naspetti, M., Valero, R., Barad, M., Lepault, F., Vialettes, B. and Naquet, P. (1999) Disorganization of thymic medulla precedes evolution towards diabetes in female NOD mice. *Autoimmunity* **31**, 249-260.

Baekkevold, E.S., Yamanaka, T., Palframan, R.T., Carlsen, H.S., Reinholt, F.P., von Andrian, U.H., Brandtzaeg, P. and Haraldsen, G. (2001) The CCR7 ligand ELC (CCL19) is transcytosed in high endothelial venules and mediates T cell recruitment. *J Exp Med* **193**, 1105-1111.

Balciunaite, G., Keller, M., Balciunaite, E., Piali, L., Zuklys, S., Mathieu, Y.D., Gill, J., Boyd, R., Sussman, D.J. and Hollander, G. (2002) Wnt glycoproteins regulate the expression of FoxN1, the gene defective in nude mice. *Nat Immunol* **3**, 1102-1108.

Bennett, A.R., Farley, A., Blair, N.F., Gordon, J., Sharp, L. and Blackburn, C.C. (2002) Identification and characterization of thymic epithelial progenitor cells. *Immunity* **16**, 803-14.

Benoist, C. and Mathis, D. (1989) Positive selection of the T cell repertoire: where and when does it occur? *Cell* **58**, 1027-1033.

Bertho, J.-M., Demarquay, C., Moulian, N., Van Der Meeren, A., Berrih-Aknin, S. and Gourmelon, P. (1997) phenotypic and immunohistological analyses of the human adult thymus: evidence for an active thymus during adult life. *Cell. Immunol.* **179**, 30-40.

Berzins, S.P., Boyd, R.L. and Miller, J.F. (1998) The role of the thymus and recent thymic migrants in the maintenance of the adult peripheral lymphocyte pool. *J Exp Med* **187**, 1839-48.

Berzins, S.P., Uldrich, A.P., Sutherland, J.S., Gill, J., Miller, J.F., Godfrey, D.I. and Boyd, R.L. (2002) Thymic regeneration: teaching an old immune system new tricks. *Trends Mol Med* **8**, 469-476.

Bill, J. and Palmer, E. (1989) Positive selection of CD4+ T cells mediated by MHC class II-bearing stromal cells in the cortex. *Nature* **341**, 1989.

Blackburn, C.C., Augustine, C.L., Harvey, R.P., Malin, M.A., Boyd, R.L., Miller, J.F.A.P. and Morahan, G. (1996) The *nu* gene acts cell-autonomously and is required for differentiation of thymic epithelial progenitors. *Proc. Natl. Acad. Sci. USA* **93**, 5742-5746.

Blackburn, C.C., Manley, N., Palmer, D.B., Boyd, R.L., Anderson, G. and Ritter, M.A. (2002) One for all and all for one: thymic epithelial stem cells and regeneration. *Trends Immunol* **23**, 391-395.

Bleul, C.C. and Boehm, T. (2000) Chemokines define distinct microenvironments in the developing thymus. *Eur J Immunol* **30**, 3371-3379.

Bockman, D.E. and Kirby, M.L. (1984) Dependence of thymus development on derivatives of the neural crest. *Science* **223**, 498-500.

Bolotin, E., Smogorzewska, M., Smith, S., Widmer, M. and Weinberg, K. (1996) Enhancement of thymopoiesis after bone marrow transplant by in vivo interleukin-7. *Blood* **88**, 1887-94.

Bonifer, C., Faust, N., Geiger, H. and Muller, A.M. (1998) Developmental changes in the differentiation capacity of haematopoietic stem cells. *Immunol Today* **19**, 236-41.

Boyd, R.L. and Hugo, P. (1991) Towards an integrated view of thymopoiesis. *Immunol. Today* **12**, 71-79.

Boyd, R.L., Tucek, C.L., Godfrey, D.I., Wilson, T.J., Davidson, N.J., Bean, A.G.D., Ladyman, H.M., Ritter, M.A. and Hugo, P. (1993) The thymic microenvironment. *Immunology Today* **14**, 445-459.

Brabb, T., Huseby, E.S., Morgan, T.M., Sant'Angelo, D.B., Kirchner, J., Farr, A.G. and Goverman, J. (1997) Thymic stromal organization is regulated by the specificity of T cell receptor/major histocompatibility complex interactions. *Eur J Immunol* **27**, 136-46.

Buer, J., Aifantis, I., DiSanto, J.P., Fehling, H.J. and von Boehmer, H. (1997) Role of different T cell receptors in the development of pre-T cells. *J Immunol* **185**, 1541-1547.

Burkly, L., Hession, C., Ogata, L., Reilly, C., Marconi, L.A., Olson, D., Tizard, R., Cate, R. and Lo, D. (1995) Expression of RelB is required for the development of thymic medulla and dendritic cells. *Nature* **373**, 531-536.

Campbell, J.J., Pan, J. and Butcher, E.C. (1999) Cutting Edge: developmental switches in chemokine responses during T-cell maturation. *J Immunol* **163**, 2353-2357.

Cantor, H. and Weissman, I. (1976) Development and function of subpopulations of thymocytes and T lymphocytes. *Prog Allergy* **20**, 1-64.

Capone, M., Romagnoli, P., Beermann, F., MacDonald, H.R. and van Meerwijk, J.P. (2001) Dissociation of thymic positive and negative selection in transgenic mice expressing major histocompatibility complex class I molecules exclusively on thymic cortical epithelial cells. *Blood* **97**, 1336-42.

Carlyle, J.R. and Zuniga-Pflucker, J.C. (1998a) Lineage commitment and differentiation of T and natural killer lymphocytes in the fetal mouse. *Immunol Rev* **165**, 63-74.

Carlyle, J.R. and Zuniga-Pflucker, J.C. (1998b) Requirement for the thymus in alphabeta T lymphocyte lineage commitment. *Immunity* **9**, 187-197.

Chaffin, K.E. and Perlmutter, R.M. (1991) A pertussis toxin-sensitive process controls thymocyte emigration. *Eur J Immunol* **21**, 2565-73.

Champion, S., Imhof, B.A., Savagner, P. and Thiery, J.P. (1986) The embryonic thymus produces chemotactic peptides involved in the homing of hemopoietic precursors. *Cell* **44**, 781-90.

Chantry, D., Romagnani, P., Raport, C.J., Wood, C.L., Epp, A., Romagnani, S. and Gray, P.W. (1999) Macrophage-derived chemokine is localized to thymic medullary epithelial cells and is a chemoattractant for CD3+, CD4+, CD8low thymocytes. *Blood* **94**, 1890-1898.

Chidgey, A. and Boyd, R.L. (2001) Thymic stromal cells and positive selection. *APMIS* **109**, 481-492.

Chidgey, A.P., Pircher, H., MacDonald, H.R. and Boyd, R.L. (1998) An adult thymic stromal-cell suspension model for in vitro positive selection. *Dev Immunol* **6**, 157-170.

Conway, S.J., Henderson, D.J. and Copp, A.J. (1997) Pax3 is required for cardiac neural crest migration in the mouse: evidence from the splotch (Sp2H) mutant. *Development* **124**, 505-14.

Cordier, A.C. and Haumond, S.M. (1980) Development of thymus, parathyroids, and ultimobranchial bodies in NMRI and nude mice. *American Journal of Anatomy* **157**, 227-254.

Cordier, A.C. and Heremans, J.F. (1975) Nude mouse embryo: ectodermal nature of the primordial thymic defect. *Scand J Immunol* **4**, 193-6.

Cosgrove, D., Chan, S.H., Waltzinger, C., Benoist, C. and Mathis, D. (1992) The thymic compartment responsible for positive selection of CD4+ T cells. *Int Immunol* **4**, 707-10.

Cyster, J.G. (2000) Leukocyte migration: Scent of the T zone. *Curr Biol* **10**, R30-R33.

de Maagd, R.A., MacKenzie, W.A., Schuurman, H.-J., Ritter, M.A., Price, K.M., Broekhuizen, R. and Kater, L. (1985) The human thymus microenvironment: heterogeneity detected by monoclonal anti-epithelial cell antibodies. *Immunology* **54**, 745-754.

de Vries, P., Brasel, K.A., McKenna, H.J., Williams, D.E. and Watson, J.D. (1992) Thymus reconstitution by c-kit-expressing hematopoietic stem cells purified from adult mouse bone marrow. *J Exp Med* **176**, 1503-1509.

Deftos, M.L., Huang, E., Ojala, E.W., Forbush, K.A. and Bevan, M.J. (2000) Notch1 signaling promotes the maturation of CD4 and CD8 SP thymocytes. *Immunity* **13**, 73-84.

Degermann, S., Surh, C.D., Glimcher, L.H., Sprent, J. and Lo, D. (1994) B7 expression on thymic medullary epithelium correlates with epithelium-mediated deletion of Vbeta5+ thymocytes. *J Immunol* **152**, 3254-3263.

Derbinski, J., Schulte, A., Kyewski, B. and Klein, L. (2001) Promiscuous gene expression in medullary thymic epithelial cells mirrors the peripheral self. *Nat Immunol* **2**, 1032-9.

Di Santo, J.P. and Rodewald, H.-R. (1998) *In vivo* roles of receptor tyrosine kinases and cytokine receptors in early thymocyte development. *Curr. Opin. Immunol.* **10**, 196-207.

Douek, D.C. and Koup, R.A. (2000) Evidence for thymic function in the elderly. *Vaccine* **18**, 1638-41.

Douek, D.C., Vescio, R.A., Betts, M.R., Brenchley, J.M., Hill, B.J., Zhang, L., Berenson, J.R., Collins, R.H. and Koup, R.A. (2000) Assessment of thymic output in adults after haematopoietic stem-cell transplantation and prediction of T-cell reconstitution. *Lancet* **355**, 1875-1881.

Dudley, E.C., Petrie, H.T., Shah, L.M., Owen, M.J. and Hayday, A.C. (1994) T cell receptor beta chain gene rearrangement and selection during thymocyte development in adult mice. *Immunity* **1**, 83-93.

Dyall, R. and Nikolic-Zugic, J. (1995) The majority of postselection CD4+ single-positive thymocytes requires the thymus to produce long-lived, functional T cells. *J Exp Med* **181**, 235-45.

Erickson, M., Morkowski, S., Lehar, S., Gillard, G., Beers, C., Dooley, J., Rubin, J.S., Rudensky, A. and Farr, A. (2002) Regulation of thymic epithelium by keratinocyte growth factor. *Blood* **100**, 3269-3278.

Farr, A.G. and Anderson, S.K. (1985) Epithelial heterogeneity in the murine thymus: fucose-specific lectins bind medullary epithelial cells. *J Immunol* **134**, 2971-2777.

Farr, A.G., Dooley, J.L. and Erickson, M. (2002) Organization of thymic medullary epithelial heterogeneity: implications for mechanisms of epithelial differentiation. *Immunol Rev* **189**, 20-27.

Farr, A.G. and Rudensky, A. (1998) Medullary thymic epithelium: a mosaic of epithelial "self"? *J Exp Med* **188**, 1-4.

Farr, A.G. and Sidman, C.L. (1984) Reduced expression of Ia antigens by thymic epithelial cells of aged mice. *J. Immunol.* **133**, 98-103.

Fehling, H.J., Krotkova, A., Saint-Ruf, C. and von Boehmer, H. (1995) Crucial role of the pre-T-cell receptor alpha gene in development of alpha beta but not gamma delta T cells. *Nature* **375**, 795-8.

Ferrick, D.A., Sambhara, S.R., Ballhausen, W., Iwamoto, A., Pircher, H., Walker, C.L., Yokoyama, W.M., Miller, R.G. and Mak, T.W. (1989) T cell function and expression are dramatically altered in T cell receptor V gamma 1.1J gamma 4C gamma 4 transgenic mice. *Cell* **57**, 483-492.

Forster, R., Schubel, A., Breitfeld, D., Kremmer, E., Renner-Muller, I., Wolf, E. and Lipp, M. (1999) CCR7 coordinates the primary immune response by establishing functional microenvironments in secondary lymphoid organs. *Cell* **99**.

Foss, D.L., Donskoy, E. and Goldschneider, I. (2001) The importation of hematogenous precursors by the thymus is a gated phenomenon in normal adult mice. *J Exp Med* **193**, 365-374.

Frank, J., Pignata, C., Panteleyev, A.A., Prowse, D.M., Baden, H.P., Weiner, L., Gaetaniello, L., Ahmad, W., Pozzi, N., Cserhalmi-Friedman, P.B., Aita, V.M., Uyttendaele, H., Gordon, D., Ott, J., Brissette, J.L. and Christiano, A.M. (1999) Exposing the human nude phenotype. *Nature* **398**, 473-474.

Fridkis-Hareli, M., Abel, L. and Globerson, A. (1992) Patterns of dual lymphocyte development in co-cultures of foetal thymus and lymphohaemopoietic cells from young and old mice. *Immunology* **77**, 185-188.

Gabor, M.J., Godfrey, D.I. and Scollay, R. (1997a) Recent thymic emigrants are distinct from most medullary thymocytes. *Eur J Immunol* **27**, 2010-5.

Gabor, M.J., Scollay, R. and Godfrey, D.I. (1997b) Thymic T cell export is not influenced by the peripheral T cell pool. *Eur J Immunol* **27**, 2986-93.

Galy, A.H.M. and Spits, H. (1992) CD40 is functionally expressed on human thymic epithelial cells. *J Immunol* **149**, 775-782.

Gerdes, J., Lemke, H., Baisch, H., Wacker, H.H., Schwab, U. and Stein, H. (1984) Cell cycle analysis of a cell proliferation-associated human nuclear antigen defined by the monoclonal antibody Ki-67. *J Immunol* **133**, 1710-5.

Gill, J. (2002) Progenitor cells of the thymic epithelium and factors influencing thymic development. In: Department of Pathology and Immunology. Monash University, Melbourne, p. 191.

Gill, J., Malin, M., Hollander, G.A. and Boyd, R. (2002) Generation of a complete thymic microenvironment by MTS24(+) thymic epithelial cells. *Nat Immunol* **3**, 635-42.

Globerson, A., Sharp, A., Fridkis-Hareli, M., Kukulansky, T., Abel, L., Knyszynski, A. and Eren, R. (1992) Aging in the T lymphocyte compartment. A developmental view. *Ann N Y Acad Sci* **673**, 240-251.

Godfrey, D.I., Izon, D.J., Tucek, C.L., Wilson, T.J. and Boyd, R.L. (1990) The phenotypic heterogeneity of mouse thymic stromal cells. *Immunology* **70**, 66-74.

Godfrey, D.I., Izon, D.J., Wilson, T.J., Tucek, C.L. and Boyd, R.L. (1988) Thymic stromal elements defined by mAbs: ontogeny and modulation in vivo by immunosuppression. *Adv Exp Med Biol* **237**, 269-275.

Godfrey, D.I., Kennedy, J., Mombaerts, P., Tonegawa, S. and Zlotnik, A. (1994) Onset of TCR-β gene rearrangement and role of TCR-β expression during $CD3^-CD4^-CD8^-$ thymocyte differentiation. *J. Immunol.* **152**, 4783-4792.

Godfrey, D.I., Kennedy, J., Suda, T. and Zlotnik, A. (1993) A developmental pathway involving four phenotypically and functionally distinct subsets of $CD3^-CD4^-CD8^-$ triple-negative adult mouse thymocytes defined by CD44 and CD25 expression. *J. Immunol.* **150**, 4244-4252.

Godfrey, D.I. and Zlotnik, A. (1993) Control points in early T-cell development. *Immunology Today* **14**, 547-553.

Gounari, F., Aifantis, I., Martin, C., Fehling, H.J., Hoeflinger, S., Leder, P., von Boehmer, H. and Reizis, B. (2002) Tracing lymphopoiesis with the aid of a pTalpha-controlled reporter gene. *Nat Immunol* **3**, 489-96.

Groettrup, M., Ungewiss, K., Azogui, O., Palacios, R., Owen, M.J., Hayday, A.C. and von Boehmer, H. (1993) A novel disulfide-linked heterodimer on pre-T cells consists of the T cell receptor beta chain and a 33 kd glycoprotein. *Cell* **75**, 283-94.

Gunn, M.D., Kyuwa, S., Tam, C., Kakiuchi, T., Matsuzawa, A., Williams, L.T. and Nakano, H. (1999) Mice lacking expression of secondary lymphoid organ chemokine have defects in lymphocyte homing and dendritic cell localization. *J Exp Med* **189**, 451-460.

Gunn, M.D., Tangemann, K., Tam, C., Cyster, J.G., Rosen, S.D. and Williams, L.T. (1998) A chemokine expressed in lymphoid high endothelial venules promotes the adhesion and chemotaxis of naive T lymphocytes. *PNAS* **95**, 258-263.

Hare, K.J., Jenkinson, E.J. and Anderson, G. (2001) Specialisation of thymic epithelial cells for positive selection of CD4+8+ thymocytes. *Cell Mol Biol (Noisy-le-grand)* **47**, 119-27.

Harman, B.C., Jenkinson, E. and Anderson, G. (2003) Entry into the thymic microenvironment triggers Notch activation in the earliest migrant T cell precursors. *J Immunol* **170**, 1299-1303.

Haynes, B.F., Markert, M.L., Sempowski, G.D., Patel, D.D. and Hale, L.P. (2000a) The role of the thymus in immune reconstitution in aging, bone marrow transplantation, and HIV-1 infection. *Annu Rev Immunol* **18**, 529-60.

Haynes, B.F., Sempowski, G.D., Wells, A.F. and Hale, L.P. (2000b) The human thymus during aging. *Immunol Res* **22**, 253-261.

Hedrick, J.A. and Zlotnik, A. (1997) Identification and characterisation of a novel beta chemokine containing six conserved cysteines. *J Immunol* **159**, 1589-1593.

Hernandez-Lopez, C., Varas, A., Sacedon, R., Jimenez, E., Munoz, J.J., Zapata, A.G. and Vicente, A. (2002) Stroma cell-derived factor-1/CXCR4 signaling is critical for early human T-cell development. *Blood* **99**, 546-554.

Hetzer-Egger, C., Schorpp, M., Haas-Assenbaum, A., Balling, R., Peters, H. and Boehm, T. (2002) Thymopoiesis requires Pax9 function in thymic epithelial cells. *Eur J Immunol* **32**, 1175-1181.

Hirokawa, K., Utsuyama, M., Kasai, M. and Kurashima, C. (1992) Aging and immunity. *Acta Pathol Jpn* **42**, 537-548.

Hoffmann, M.W., Allison, J. and Miller, J.F. (1992) Tolerance induction by thymic medullary epithelium. *Proc Natl Acad Sci U S A* **89**, 2526-30.

Hoffmann, M.W., Heath, W.R., Ruschmeyer, D. and Miller, J.F. (1995) Deletion of high-avidity T cells by thymic epithelium. *Proc Natl Acad Sci U S A* **92**, 9851-5.

Hoffmann-Fezer, G., Antica, M., Schuh, R. and Thierfelder, S. (1989) Distribution of injected anti-Thy-1 monoclonal antibodies in mouse lymphatic organs: evidence for penetration of the cortical blood-thymus barrier, and for intravascular antibody-binding onto lymphocytes. *Hybridoma* **8**, 517-27.

Hogquist, K.A., Jameson, S.C., Heath, W., Howard, M., Bevan, M.J. and Carbone, F.R. (1994) T cell receptor antagonist peptides induce positive selection. *Cell* **76**, 17-27.

Hollander, G.A., Simpson, S.J., Mizoguchi, E., Nichogiannopoulou, A., She, J., Gutierrez-Ramos, J.C., Bhan, A.K., Burakoff, S.J., Wang, B. and Terhorst, C. (1995a) Severe colitis in mice with aberrant thymic selection. *Immunity* **3**, 27-38.

Hollander, G.A., Wang, B., Nichogiannopoulou, A., Platenburg, P.P., van Ewijk, W., Burakoff, S.J., Gutierrez-Ramos, J.-C. and Terhorst, C. (1995b) Developmental control point in induction of thymic cortex regulated by a subpopulation of prothymocytes. *Nature* **373**, 350-353.

Huesmann, M., Scott, B., Kisielow, P. and von Boehmer, H. (1991) Kinetics and efficacy of positive selection in the thymus of normal and T cell receptor transgenic mice. *Cell* **66**, 533-40.

Hugo, P., Waanders, G.A., Scollay, R., Shortman, K. and Boyd, R.L. (1990) Ontogeny of a novel CD4+CD8-CD3- thymocyte subpopulation: a comparison with CD4- CD8+ CD3- thymocytes. *Int Immunol* **2**, 209-18.

Ignatowicz, L., Kappler, J. and Marrack, P. (1996) The repertoire of T cells shaped by a single MHC/peptide ligand. *Cell* **84**, 521-529.

Ito, M. and Yamagata, T. (1989) Purification and characterisation of glycosphingolipid-specific endoglycosidases (endoglycoceramidases) from a mutant strain of Rhodococcus sp. Evidence for three molecular species of endoglycoceramidase with different specificities. *J Biol Chem* **264**, 9510-9519.

Itoh, M., Takahashi, T., Sakaguchi, N., Kuniyasu, Y., Shimizu, J., Otsuka, F. and Sakaguchi, S. (1999) Thymus and autoimmunity: production of CD25+CD4+ naturally anergic and suppressive T cells as a key function of the thymus in maintaining immunologic self-tolerance. *J Immunol* **162**, 5317-5126.

Izon, D.J., Nieland, J.D., Godfrey, D.I., Boyd, R.L. and Kruisbeek, A.M. (1994) Flow cytometric analysis reveals unexpected shared antigens between histologically defined populations of thymic stromal cells. *Int. Immunol.* **6**, 31.

Jameson, S.C. and Bevan, M.J. (1998) T-cell selection. *Curr Opin Immunol* **10**, 214-9.

Jameson, S.C., Hogquist, K.A. and Bevan, M.J. (1994) Specificity and flexibility in thymic selection. *Nature* **369**, 750-752.

Jameson, S.C., Hogquist, K.A. and Bevan, M.J. (1995) Positive selection of thymocytes. *Annu Rev Immunol* **13**, 93-126.

Jenkinson, E.J., Anderson, G. and Owen, J.J. (1992) Studies on T cell maturation on defined thymic stromal cell populations in vitro. *J Exp Med* **176**, 845-853.

Jiang, X., Rowitch, D.H., Soriano, P., McMahon, A.P. and Sucov, H.M. (2000) Fate of the mammalian cardiac neural crest. *Development* **127**, 1607-16.

Kampinga, J., Berges, S., Boyd, R.L., Brekelmans, P., Colic, M., van Ewijk, W., Kendall, M.D., Ladyman, H., Nieuwenhuis, P., Ritter, M.A., Schuurman, H.J. and Tournefier, A. (1989) Thymic epithelial antibodies: immunohistological analysis and introduction of nomenclature. *Thymus* **13**, 165-173.

Kato, S. (1997) Thymic microvascular system. *Microsc Res Tech* **38**, 287-299.

Kato, S. (1989) Microvasculature of normal and involuted mouse thymus. Light- and electron-microscopic study. *Acta Anat (Basel)* **135**, 1-11.

Katsura, Y. and Kawamoto, H. (2001) Stepwise lineage restriction of progenitors in lympho-myelopoiesis. *Int Rev Immunol* **20**, 1-20.

Kawabata, K., Ujikawa, M., Egawa, T., Kawamoto, H., Tachibana, K., Iizasa, H., Katsura, Y., Kishimoto, T. and Nagasawa, T. (1999) A cell-autonomous requirement for CXCR4 in long-term lymphoid and myeloid reconstitution. *P.N.A.S.* **96**, 5663-5667.

Kawamoto, H., Ohmura, K. and Katsura, Y. (1998) Presence of progenitors restricted to T, B, or myeloid lineage, but absence of multipotent stem cells, in the murine thymus. *J Immunol* **161**, 3799-3802.

Kendall, M.D. (1991) Functional anatomy of the thymic microenvironment. *J Anat* **177**, 1-29.

Kendall, M.D., Fitzpatrick, F.T.A., Greenstein, B.D., Khoylou, F., Safieh, B. and Hamblin, A. (1990) Reversal of ageing changes in the thymus of rats by chemical or surgical castration. *Cell and Tissue Res* **261**, 555-564.

Kim, C.H., Pelus, L.M., White, J.R. and Broxmeyer, H.E. (1998) Differential chemotactic behavior of developing T-cells in response to thymic chemokines. *Blood* **91**, 4434-4443.

Kishimoto, H. and Sprent, J. (1997) Negative selection in the thymus includes semimature T cells. *J Exp Med* **185**, 263-271.

Kishimoto, H. and Sprent, J. (1999) Several different cell surface molecules control negative selection of medullary thymocytes. *J Exp Med* **190**, 65-73.

Kishimoto, H. and Sprent, J. (2000) The thymus and central tolerance. *Clin Immunol* **95**, S3-S7.

Kishimoto, H. and Sprent, J. (2001) A defect in central tolerance in NOD mice. *Nat Immunol* **2**, 1025-1031.

Kishimoto, T.K., Larson, R.S., Corbi, A.L., Dustin, M.L., Staunton, D.E. and A., S.T. (1989) The leukocyte integrins. *Adv. Immunol.* **46**, 149.

Klein, L., Klein, T., Ruther, U. and Kyewski, B. (1998) CD4 T cell tolerance to human C-reactive protein, an inducible serum protein, is mediated by medullary thymic epithelium. *J Exp Med* **188**, 5-16.

Klein, L. and Kyewski, B. (2000) Self-antigen presentation by thymic stromal cells: a subtle division of labor. *Curr. Opin. Immunol.* **12**, 179-186.

Klein, L., Roettinger, B. and Kyewski, B. (2001) Sampling of complementing self-antigen pools by thymic stromal cells maximizes the scope of central T cell tolerance. *Eur J Immunol* **31**, 2476-86.

Klug, D.B., Carter, C., Crouch, E., Roop, D., Conti, C.J. and Richie, E.R. (1998) Interdependence of cortical thymic epithelial cell differentiation and T-lineage commitment. *Proc Natl Acad Sci U S A* **95**, 11822-7.

Klug, D.B., Carter, C., Gimenez-Conti, I.B. and Richie, E.R. (2002) Cutting edge: thymocyte-independent and thymocyte-dependent phases of epithelial patterning in the fetal thymus. *J Immunol* **169**, 2842-5.

Kojima, A., Taguchi, O. and Nishizuka, Y. (1980) Experimental production of possible autoiommune gastritis followed by macrocytic anaemia in athymic nude mice. *Lab Invest* **42**, 387-395.

Kojima, A., Tanaka-Kojima, Y., Sakakura, T. and Nishizuka, Y. (1976) Spontaneous development of autoimmune thyroiditis in neonatally thymectomized mice. *Lab Invest* **34**, 550-557.

Kong, Y., Li, R. and Ladisch, S. (1998) Natural forms of shed tumor gangliosides. *Biochim Biophys Acta* **1394**, 43-56.

Kyewski, B., Derbinski, J., Gotter, J. and Klein, L. (2002) Promiscuous gene expression and central T-cell tolerance: more than meets the eye. *Trends Immunol* **23**, 364-71.

Kyewski, B.A. (1987) Seeding of thymic microenvironments defined by distinct thymocyte-stromal cell interactions is developmentally controlled. *J. Exp. Med.* **166**, 520-538.

Laufer, T.M., DeKoning, J., Markowitz, J.S., Lo, D. and Glimcher, L.H. (1996) Unopposed positive selection and autoreactivity in mice expressing class II MHC only on thymic cortex. *Nature* **383**, 81-85.

Le Campion, A., Lucas, B., Dautigny, N., Leaument, S., Vasseur, F. and Penit, C. (2002) Quantitative and qualitative adjustment of thymic T cell production by clonal expansion of premigrant thymocytes. *J Immunol* **168**, 1664-1671.

Le Douarin, N.M. and Jotereau, F.V. (1975) Tracing of cells of the avian thymus through embryonic life in interspecific chimeras. *J Exp Med* **142**, 17-40.

Le Lievre, C.S. and Le Douarin, N.M. (1975) Mesenchymal derivatives of the neural crest: analysis of chimaeric quail and chick embryos. *J Embryol Exp Morphol* **34**, 125-154.

Lin, Q., Taniuchi, I., Kitamura, D., Wang, J., Kearney, J.F., Watanabe, T. and Cooper, M.D. (1998) T and B cell development in BP-1/6C3/Aminopeptidase-A deficient mice. *J Immunol* **160**, 4681-4687.

Lind, E.F., Prockop, S.E., E., P.H. and Petrie, H.T. (2001) Mapping precursor movement through the postnatal thymus reveals specific microenvironments supporting defined stages of early lymphoid development. *J Exp Med* **194**, 127-134.

Liston, A., Lesage, S., Wilson, J., Peltonen, L. and Goodnow, C.C. (2003) Aire regulates negative selection of organ-specific T cells. *Nat Immunol*, 1-5.

Lobach, D.F., Scearce, R.M. and Haynes, B.F. (1985) The human thymic microenvironment. Phenotypic characterisation of Hassall's bodies with the use of monoclonal antibodies. *J Immunol* **134**, 250-257.

Lucas, B., Vasseur, F. and Penit, C. (1994) Production, selection and maturation of thymocytes with high surface density of TcR. *J Immunol* **153**, 53-62.

MacDonald, H.R., Wilson, A. and Radtke, F. (2001) Notch1 and T-cell development: insights from conditional knockout mice. *Trends Immunol* **22**, 155-160.

Mackall, C.L., Fleisher, T.A., Brown, M.R., Andrich, M.P., Chen, C.C., Feuerstein, I.M., Horowitz, M.E., Magrath, I.T., Shad, A.T., Steinberg, S.M. and et al. (1995) Age, thymopoiesis, and CD4+ T-lymphocyte regeneration after intensive chemotherapy. *N Engl J Med* **332**, 143-9.

Mackall, C.L., Fry, T.J., Bare, C., Morgan, P., Galbraith, A. and Gress, R.E. (2001) IL-7 increases both thymic-dependent and thymic-independent T-cell regeneration after bone marrow transplantation. *Blood* **97**, 1491-1497.

Mackall, C.L. and Gress, R.E. (1997) Thymic aging and T-cell regeneration. *Immunological Reviews* **160**, 91-102.

Mackall, C.L., Punt, J.A., Morgan, P., Farr, A.G. and Gress, R.E. (1998) Thymic function in young/old chimeras: substantial thymic T cell regenerative capacity despite irreversible age-associated thymic involution.
Eur. J. Immunol. **28**, 1886-1893.

Madrenas, J., Wange, R.L., Wang, J.L., Isakov, N., Samelson, L.E. and Germain, R.N. (1995) Zeta phosphorylation without ZAP-70 activation induced by TcR antagonists or partial agonists. *Science* **267**, 515-518.

Mallick, C.A., Dudley, E.C., Viney, J.L., Owen, M.J. and Hayday, A.C. (1993) Rearrangement and diversity of T cell receptor beta chain genes in thymocytes: critical role for the beta chain in development. *Cell* **73**, 513-519.

Manley, N. and Blackburn, C.C. (2003) A developmental look at thymus organogenesis: where do the non-hematopoietic cells in the thymus come from? *Curr Opin Immunol* **15**, 225-232.

Manley, N.R. (2000) Thymus organogenesis and molecular mechanisms of thymic epithelial cell differentiation. *Semin Immunol* **12**, 421-428.

Manley, N.R. and Capecchi, M.R. (1995) The role of Hoxa-3 in mouse thymus and thyroid development. *Development* **121**, 1989-2003.

Marshall, A.H.E. and White, R.G. (1961) The immunological reactivity of the thymus. *Br. J. Exp. Pathol.* **42**, 379-385.

Merkenschlager, M., Power, M.O., Pircher, H. and Fisher, A.G. (1999) Intrathymic deletion of MHC class I-restricted cytotoxic T cell precursors by constitutive cross-presentation of exogenous antigen. *Eur. J. Immunol.* **29**, 1477.

Middleton, J., Patterson, A.M., Gardner, L., Schmutz, C. and Ashton, B.A. (2002) Leukocyte extravasation: chemokine transport and presentation by the endothelium. *Blood* **100**, 3853-3860.

Min, D., Taylor, P.A., Panoskaltsis-Mortari, A., Chung, B., Danilenko, D.M., Farrell, C., Lacey, D.L., Blazar, B.R. and Weinberg, K.I. (2002) Protection from thymic epithelial cell injury by keratinocyte growth factor: a new approach to improve thymic and peripheral T-cell reconstitution after bone marrow transplantation. *Blood* **99**, 4592-600.

Mombaerts, P., Iacomini, J., Johnson, R.S., Herrup, K., Tonegawa, S. and Papaioannou, V.E. (1992) RAG-1-deficient mice have no mature B and T lymphocytes. *Cell* **68**, 869-877.

Murphy, P.M. (1994) The molecular biology of leukocyte chemoattractant receptors. *Annu Rev Immunol* **12**, 593-533.

Nagira, M., Imai, T., Hieshima, K., Kusuda, J., Ridanpaa, M., Takagi, S., Nishimura, M., Kakizaki, M., Nomiyama, H. and Yoshie, O. (1997) Molecular cloning of a novel human CC chemokine secondary lymphoid-tissue chemokine that is a potent chemoattractant for lymphocytes and mapped to chromosome 9p13. *J Biol Chem* **272**, 19518-19524.

Nakano, H., Mori, S., Yonekawa, H., Nariuchi, H., Matsuzawa, A. and Kakiuchi, T. (1998) A novel mutant gene involved in T-lymphocyte-specific homing into peripheral lymphoid organs on mouse chromosome 4. *Blood* **91**, 2886-2895.

Naquet, P., Naspetti, M. and Boyd, R. (1999) Development, organization and function of the thymic medulla in normal, immunodeficient or autoimmune mice. *Sem. Immunol.* **11**, 47-55.

Naspetti, M., Aurrand-Lions, M., DeKoning, J., Malissen, M., Galland, F., Lo, D. and Naquet, P. (1997) Thymocytes and RelB-dependent medullary epithelial cells provide growth- promoting and organization signals, respectively, to thymic medullary stromal cells. *Eur J Immunol* **27**, 1392-7.

Nehls, M., Kyewski, B., Messerle, M., Waldschutz, R., Schuddekopf, K., Smith, A.J. and Boehm, T. (1996) Two genetically separable steps in the differentiation of thymic epithelium. *Science* **272**, 886-9.

Nehls, M., Pfeifer, D., Schorpp, M., Hedrich, H. and Boehm, T. (1994) New member of the winged-helix protein family disrupted in mouse and rat nude mutations. *Nature* **372**, 103-7.

Nelson, A.J., Dunn, R.J., Peach, R., Aruffo, A. and Farr, A.G. (1996) The murine homolog of human Ep-CAM, a homotypic adhesion molecule, is expressed by thymocytes and thymic epithelial cells. *Eur. J. Immunol.* **26**, 401.

Nelson, A.J., Hosier, S., Brady, W., Linsley, P.S. and Farr, A.G. (1993) Medullary thymic epithelium expresses a ligand for CTLA4 in situ and in vitro. *J Immunol* **151**, 2453-2461.

Ngo, V.N. and Tang, H.L. (1998) Epstein-Barr virus-induced molecule 1 ligand chemokine is expressed by dendritic cells in lymphoid tissues and strongly attracts naive T cells and activated B cells. *J Exp Med* **188**, 181-191.

Nieuwenhuis, P., J., S.R., P., W.J., S., W.A., Kampinga, J. and A., K. (1988) The transcapsular route: a new way for (self-) antigens to by-pass the blood-thymus barrier? *Immunol Today* **9**, 372-375.

Nikolic-Zugic, J. (1991) Phenotypic and functional stages in the intrathymic development of αβ T cells. *Immunol. Today* **12**, 65-70.

Nishizuka, Y. and Sakakura, T. (1969) Thymus and reproduction: sex-linked dysgenesia of the gonad after neonatal thymectomy in mice. *Science* **166**, 753-755.

Norment, A.M. and Bevan, M.J. (2000) Role of chemokines in thymocyte development. *Semin Immunol* **12**, 445-455.

Norment, A.M., Bogatzki, L.Y., Gantner, B.N. and Bevan, M.J. (2000) Murine CCR9, a chemokine receptor for thymus-expressed chemokine that is up-regulated following pre-TCR signaling. *J Immunol* **164**, 639-48.

Ohmura, K., Kawamoto, H., Fujimoto, S., Ozaki, S., Nakao, K. and Katsura, Y. (1999) Emergence of T, B, and myeloid lineage-committed as well as multipotent hemopoietic progenitors in the aorta-gonad-mesonephros region of the day 10 fetuses. *J Immunol* **163**, 4788-4795.

Ohnemus, S., Kanzler, B., Jerome-Majewska, L.A., Papaioannou, V.E., Boehm, T. and Mallo, M. (2002) Aortic arch and pharyngeal phenotype in the absence of BMP-dependent neural crest in the mouse. *Mech Dev* **119**, 127-135.

Olsen, N.J. and Kovacs, W.J. (1996) Gonadal steroids and immunity. *Endocr Rev* **17**, 369-84.

Olsen, N.J., Olson, G., Viselli, S.M., Gu, X. and Kovacs, W.J. (2001) Androgen receptors in thymic epithelium modulate thymus size and thymocyte development. *Endocrinology* **142**, 1278-83.

Olsen, N.J., Watson, M.B., Henderson, G.S. and Kovacs, W.J. (1991a) Androgen deprivation induces phenotypic and functional changes in the thymus of adult mice. *Endocrinology* **129**, 2471-2476.

Olsen, N.J., Watson, M.B. and Kovacs, W.J. (1991b) Studies of immunological function in mice with defective androgen action. Distinction between alterations in immune function due to hormonal insensitivity and alterations due to other genetic factors. *Immunology* **73**, 52-57.

Onai, N., Zhang, Y., Yoneyama, H., Kitamura, T., Ishikawa, S. and Matsushima, K. (2000) Impairment of lymphopoeisis and myelopoiesis in mice reconstituted with bone marrow-hematopoietic progenitor cells expressing SDF-1-intrakine. *Blood* **96**, 2074-2080.

Oosterwegel, M.A., Haks, M.C., Jeffry, U., Murray, R. and Kruisbeek, A.M. (1997) Induction of TCR gene rearrangements in uncommitted stem cells by a subset of IL-7 producing MHC Class-II-expressing thymic stromal cells. *Immunity* **6**, 351-360.

Ortman, C.L., Dittmar, K.A., Witte, P.L. and Le, P.T. (2002) Molecular characterization of the mouse involuted thymus: aberrations in expression of transcription regulators in thymocyte and epithelial compartments. *Int Immunol* **14**, 813-22.

Palmer, D.B., Viney, J.L., Ritter, M.A., Hayday, A.C. and Owen, M.J. (1993) Expression of the alpha/beta T-cell receptor is necessary for the generation of the thymic medulla. *Dev. Immunol.* **3**, 175-179.

Penit, C., Lucas, B. and Vasseur, F. (1995) Cell expansion and growth arrest phases during the transition from precursor ($CD4^-CD8^-$) to immature ($CD4^+CD8^+$) thymocytes in normal and genetically modified mice. *J. Immunol.* **154**, 5103-5113.

Penit, C., Lucas, B., Vasseur, F., Rieker, T. and Boyd, R.L. (1996) Thymic medulla epithelial cells acquire specific markers by post-mitotic maturation. *Dev. Immunology* **5**, 25-36.

Penit, C. and Vasseur, F. (1988) Sequential events in thymocyte differentiation and thymus regeneration revealed by a combination of bromodeoxyuridine DNA labeling and antimitotic drug treatment. *Journal of Immunology* **140**, 3315-3323.

Penit, C. and Vasseur, F. (1997) Expansion of mature thymocyte subsets before emigration to the periphery. *J Immunol* **159**, 4848-56.

Penit, C., Vasseur, F. and Papiernik, M. (1988) *In vivo* dynamics of $CD4^-CD8^-$ thymocytes. Proliferation, renewal and differentiation of different cell subsets studied by DNA biosynthetic labeling and surface antigen detection. *Eur. J. Immunol.* **18**, 1343-1350.

Peters, H., Neubüser, A., Kratochwil, K. and Balling, R. (1998) Pax9-deficient mice lack pharyngeal pouch derivatives and teeth and exhibit craniofacial and limb abnormalities. *Genes Dev* **12**, 2735-47.

Petrie, H.T., Livak, F., Schatz, D.G., Strasser, A., Crispe, I.N. and Shortman, K. (1993) Multiple rearrangements in T cell receptor alpha chain genes maximize the production of useful thymocytes. *J Exp Med* **178**, 615-622.

Philpott, K.L., Viney, J.L., Kay, G., Rastan, S., Gardiner, E.M., Chae, S., Hayday, A.C. and Owen, M.J. (1992) Lymphoid development in mice congenitally lacking T cell receptor alpha beta-expressing cells. *Science* **256**, 1448-1452.

Pircher, H., K., B., U., S., M., K., T., M., Zinkernagel, R.M., Hengartner, H., Kyewski, B. and P., M.K. (1993) Tolerance induction by clonal deletion of CD4+CD8+ thymocytes in vitro does not require dedicated antigen-presenting cells. *Eur. J. Immunol.* **23**, 669.

Pui, J.C., Allman, D., Xu, L., DeRocco, S., karnell, F.G., Bakkour, S., Lee, J.Y., kadesch, T., Hardy, R.R., Aster, J.C. and Pear, W.S. (1999) Notch1 expression in early lymphopoiesis influences B versus T lineage determination. *Immunity* **11**, 299-308.

Pyke, K.W. and Bach, J.F. (1979) The in vitro migration of murine fetal liver cells to thymic rudiments. *Eur J Immunol* **9**, 317-323.

Radtke, F., Wilson, A., Stark, G., Bauer, M., van Meerwijk, J.P., MacDonald, H.R. and Aguet, M. (1999) Deficient T cell fate specification in mice with an induced inactivation of Notch1. *Immunity* **10**, 547-558.

Reizis, B. and Leder, P. (2002) Direct induction of T lymphocyte-specific gene expression by the mammalian Notch signaling pathway. *Genes Dev* **16**, 295-300.

Revest, J.M., Suniara, R.K., Kerr, K., Owen, J.J. and Dickson, C. (2001) Development of the thymus requires signaling through the fibroblast growth factor receptor r2-iiib. *J Immunol* **167**, 1954-61.

Ritter, M.A. and Boyd, R.L. (1993) Development in the thymus: it takes two to tango. *Immunology Today* **14**, 1993.

Robles, A.I., Larcher, F., Whalin, R.B., Murillas, R., Richie, E., Gimenez-Conti, I.B., Jorcano, J.L. and Conti, C.J. (1996) Expression of cyclin D1 in epithelial tissues of transgenic mice results in epidermal hyperproliferation and severe thymic hyperplasia. *Proc Natl Acad Sci U S A* **93**, 7634-8.

Rodewald, H.-R., Kretschmar, K., Takeda, S., Hohl, C. and Dessing, M. (1994) Identification of pro-thymocytes in murine fetal blood: T lineage commitment can precede thymus colonization. *The EMBO Journal* **13**, 4229-4240.

Rodewald, H.-R., Ogawa, M., Haller, C., Waskow, C. and DiSanto, J.P. (1997) Pro-Thymocyte Expansion by c-kit and the Common Cytokine Receptor γ Chain Is Essential for Repertoire Formation. *Immunity* **6**, 265-272.

Rodewald, H.R., Paul, S., Haller, C., Bluethmann, H. and Blum, C. (2001) Thymus medulla consisting of epithelial islets each derived from a single progenitor. *Nature* **414**, 763-8.

Ropke, C., Van Soest, P., Platenburg, P.P. and Van Ewijk, W. (1995) A common stem cell for murine cortical and medullary thymic epithelial cells? *Dev Immunol* **4**, 149-56.

Rossi, D. and Zlotnik, A. (2000) The biology of chemokines and their receptors. *Annu Rev Immunol* **18**, 217-42.

Rossi, D.L., Vicari, A.P., Franz-Bacon, K., McClanahan, T.K. and Zlotnik, A. (1997) Identification through bioinformatics of two new macrophage proinflammatory human chemokines: MIP-3alpha and MIP-3beta. *J Immunol* **158**, 1033-1036.

Rossi, S., Blazar, B.R., Farrell, C.L., Danilenko, D.M., Lacey, D.L., Weinberg, K.I., Krenger, W. and Hollander, G.A. (2002) Keratinocyte growth factor preserves normal thymopoiesis and thymic microenvironment during experimental graft-versus-host disease. *Blood* **100**, 682-91.

Rot, A. (2003) In situ binding assay for studying chemokine interactions with endothelial cells. *J Immunol Methods* **273**, 63-71.

Rouse, R.V., Bolin, L.M., Bender, J.R. and Kyewski, B.A. (1988) Monoclonal antibodies reactive with subsets of mouse and human thymic epithelial cells. *J Histochem Cytochem* **36**, 1511-1517.

Rudolph, U., Finegold, M.J., Rich, S.S., Harriman, G.R., Srinivasan, Y., Brabet, P., Boulay, G., Bradley, A. and Birnbaumer, L. (1995) Ulcerative colitis and adenocarcinoma of the colon in G alpha i2-deficient mice. *Nat Genet* **10**, 143-150.

Ruggiero, G., Caceres, E.M., Voordouw, A., Noteboom, E., Graf, D., Kroczek, R.A. and Spits, H. (1996) CD40 expressed on thymic epithelial cells provides costimulation for proliferation but not for apoptosis of human thymocytes. *J Immunol* **156**, 3737-3746.

Sadahira, Y., Mori, M., Awai, M., Watari, S. and Yasuda, T. (1988) Forssman glycosphingolipid as an immunohistochemical marker for mouse stromal macrophages in hematopoietic foci. *Blood* **71**, 42-48.

Saint-Ruf, C., Ungewiss, K., Groettrup, M., Bruno, L., Fehling, H.J. and von Boehmer, H. (1994) Analysis and expression of a cloned pre-T cell receptor gene. *Science* **266**, 1208-1212.

Sakaguchi, S., Sakaguchi, N., Shimizu, J., Yamazaki, S., Sakihama, T., Itoh, M., Kuniyasu, Y., Nomura, T., Toda, M. and Takahashi, T. (2001) Immunologic tolerance maintained by CD25+CD4+ regulatory T cells: their common role in controlling autoimmunity, tumor immunity and transplantation tolerance. *Immunol Rev* **182**, 18-32.

Saqr, H.E., Pearl, D.K. and Yates, A.J. (1993) A review and predictive models of ganglioside uptake by biological membranes. *J Neurochem.* **61**, 395-411.

Savino, W., Mendes-da-Cruz, D.A., Silva, J.S., Dardenne, M. and Cotta-de-Almeida, V. (2002a) Intrathymic T-cell migration: a combinatorial interplay of extracellular matrix and chemokines? *Trends Immunol* **23**, 305-13.

Savino, W., Postel-Vinay, M.C., Smaniotto, S. and Dardenne, M. (2002b) The thymus gland: a target organ for growth hormone. *Scand J Immunol* **55**, 442-452.

Schagger, H. and von Jagow, G. (1987) Tricine-sodium dodecyl sulfate-polyacrylamide gel electrophoresis for the separation of proteins from 1 to 100kDa. *Anal Biochem* **166**, 368.

Schmitt, T.M. and Zuniga-Pflucker, J.C. (2002) Induction of T cell development from hematopoietic progenito cells by Delta-like-1 in vitro. *Immunity* **17**, 749-756.

Schonrich, G., Momburg, F., Hammerling, G.J. and Arnold, B. (1992) Anergy induced by thymic medullary epithelium. *Eur J Immunol* **22**, 1687-91.

Scollay, R. and Godfrey, D.I. (1995) Thymic emigration: conveyor belts or lucky dips? *Immunol Today* **16**, 268-73; discussion 273-4.

Sebzda, E., Mariathasan, S., Ohteki, T., Jones, R., Bachmann, M.F. and Ohashi, P.S. (1999) Selection of the T cell repertoire. *Annu Rev Immunol* **17**, 829-74.

Sebzda, E., Wallace, V.A., Mayer, J., Yeung, R.S., Mak, T.W. and Ohashi, P.S. (1994) Positive and negative selection induced by different concentrations of a single peptide. *Science* **263**, 1615-1618.

Sempowski, G.D., Hale, L.P., Sundy, J.S., Massey, J.M., Koup, R.A., Douek, D.C., Patel, D.D. and Haynes, B.F. (2000) Leukemia Inhibitory Factor, Oncostatin M, IL-6, and Stem Cell Factor mRNA expression in human thymus increases with age and is associated with thymic atrophy. *J. Immunology* **164**, 2180-2187.

Shevach, E.M. (2000) Regulatory T cells in autoimmunity. *Annu Rev Immunol* **18**, 423-449.

Shinohara, T. and Honjo, T. (1997) Studies in vitro on the mechanism of the epithelial/mesenchymal interaction in the early fetal thymus. *Eur J Immunol* **27**, 522-9.

Shores, E.W., van Ewijk, W. and Singer, A. (1991) Disorganisation and restoration of thymic medullary epithelial cells in T cell receptor-negative scid mice: evidence that receptor-bearing lymphocytes influence maturation of the thymic microenvironment. *Eur. J. Immunol.* **21**, 1657-1661.

Shortman, K., Vremec, D., D'Amico, A., Battye, F. and Boyd, R. (1989) Nature of the thymocytes associated with dendritic cells and macrophages in thymic rosettes. *Cell. Immunol.* **119**, 85.

Siddiqui, B. and Hakomori, S. (1971) A revised structure for the Forssman glycolipid hapten. *J Biol Chem* **246**, 5766-5769.

Sloan-Lancaster, J., Shaw, A.S., Rothbard, J.B. and Allen, P.M. (1994) Partial T cell signaling: altered phospho-zeta and lack of zap70 recruitment in APL-induced T cell anergy. *Cell* **79**, 913-922.

Small, T.N., Papdopoulos, E.B., Boulad, F., Black, P., Castro-Malaspina, H., Childs, B.H., Collins, N., Gillio, A., George, D., Jakubowski, A., Heller, G., Fazzari, M., Kernan, N., MacKinnon, S., Szabolcs, P., Young, J.W. and O'Reilly, R.J. (1999) Comparison of immune reconstitution after unrelated and related T-cell-depleted Bone Marrow transplantation: effect of patient age and donor leukocyte infusions. *Blood* **93**, 467-480.

Smith, C. (1965) Studies on the thymus of the mammal XIV: Histology and histochemistry of embryonic and early postnatal thymuses of C57BL-6 and AKR strain mice. *Am J Anat* **116**, 611-630.

Sprent, J. and Webb, S.R. (1995) Intrathymic and extrathymic clonal deletion of T cells. *Curr Opin Immunol* **7**, 196-205.

Standring, R. and Williams, A.F. (1978) Glycoproteins and antigens of membranes prepared from rat thymocytes after lysis by shearing with the detergent Tween-40. *Biochem Biophys Acta* **508**, 85.

Staples, J.E., Gasiewicz, T.A., Fiore, N.C., Lubahn, D.B., Korach, K.S. and Silverstone, A.E. (1999) Estrogen Receptor α is necessary in thymic development and estradiol-induced thymic alterations. *J. Immunol.* **163**, 4168-4174.

Stein, J.V., Rot, A., Luo, Y., Narasimhaswamy, M., Nakano, H., Gunn, M.D., Matsuzawa, A., Quackenbush, E.J., Dorf, M.E. and von Andrian, U.H. (2000) The CC chemokine thymus-derived chemotactic agent 4 (TCA-4, secondary lymphoid tissue chemokine, 6Ckine, exodus-2) triggers lymphocyte function-associated antigen 1-mediated arrest of rolling T lymphocytes in peripheral lymph node high endothelial venules. *J Exp Med* **191**, 61-75.

Stellner, K., Saito, H. and Hakomori, S.I. (1973) Determination of aminosugar linkages by methylation. Aminosugar linkages of ceramide pentasaccharides of rabbit erythrocytes and of Forssman antigen. *Arch Biochem. Biophys.* **155**, 464-472.

Suniara, R.K., Jenkinson, E.J. and Owen, J.J.T. (2000) An essential role for thymic mesenchyme in early T cell development. *J. Exp. Med.* **191**, 1051-1056.

Surh, C.D., Ernst, B. and Sprent, J. (1992a) Growth of epithelial cells in the thymic medulla is under the control of mature T cells. *Journal of Experimental Medicine.* **176**, 611-616.

Surh, C.D., Gao, E.K., Kosaka, H., Lo, D., Ahn, C., Murphy, D.B., Karlsson, L., Peterson, P. and Sprent, J. (1992b) Two subsets of epithelial cells in the thymic medulla. *Journal of Experimental Medicine* **176**, 495-505.

Surh, C.D. and Sprent, J. (1994) T-cell apoptosis detected *in situ* during positive and negative selection in the thymus. *Nature* **372**, 100-103.

Sutherland, J.S. (2001) Enhancement of thymopoiesis and cell-mediated immunity through sex steroid blockade. In: Department of Pathology and Immunology. Monash University, Melbourne, p. 195.

Suzuki, G., Sawa, H., Kobayashi, Y., Nakata, Y., Nakagawa, K., Uzawa, A., Sakiyama, H., Kakinuma, S., Iwabuchi, K. and Nagashima, K. (1999) Pertussis toxin-sensitive signal control the trafficking of thymocytes across the corticomedullary junction in the thymus. *J Immunol* **162**, 5981-5985.

Taguchi, N., Hashimoto, Y., Naiki, M., Farr, A.G., Boyd, R.L., Ansari, A.A., Shultz, L.D., Kotzin, B.L., Dorshkind, K., Ikehara, S. and Gershwin, M.E. (1999) Abnormal thymic expression of Epithelial Cell Adhesion Molecule (EP-CAM) in New Zealand Black (NZB) mice. *J. Autoimmunity* **13**, 393-404.

Takeoka, Y., Chen, S.-Y., Boyd, R.L., Tsuneyama, K., Taguchi, N., Morita, S., Yago, H., Suehiro, S., Ansari, A.A., Shultz, L.D. and Gershwin, M.E. (1997) A comparative analysis of the murine thymic microenvironment in Normal, Autoimmune, and Immunodeficiency States. *Dev. Immunol.* **5**, 79-89.

Takeoka, Y., Chen, S.Y., Yago, H., Boyd, R., Suehiro, S., Shultz, L.D., Ansari, A.A. and Gershwin, M.E. (1996) The murine thymic microenvironment: changes with age. *Int Arch Allergy Immunol* **111**, 5-12.

Takeoka, Y., Whitmer, K.J., Chen, S.Y., Ansari, A.A., Boyd, R.L., Shultz, L.D., Suehiro, S. and Gershwin, M.E. (1995a) Thymic epithelial cell abnormalities in (NZB x H-2u)F1 mice. *Clin Immunol Immunopathol* **76**, 297-307.

Takeoka, Y., Yoshida, S.H., van de Water, J., Boyd, R., Suehiro, S., Ansari, A.A. and Gershwin, M.E. (1995b) Thymic microenvironmental abnormalities in MRL/MP-lpr/lpr, BXSB/MpJ Yaa and C3H HeJ-gld/gld mice. *J Autoimmun* **8**, 145-161.

Tanabe, S., Lu, Z., Luo, Y., Quackenbush, E.J., Berman, M.A., Collins-Racie, L.A., Mi, S., Reilly, C., Lo, D., Jacobs, K.A. and Dorf, M.E. (1997) Identification of a new mouse beta-chemokine, thymus-dependent chemotactic agent 4, with activity on T lymphocytes and mesangial cells. *J Immunol* **159**, 5671-5679.

Tatsumi, Y., Kumanogoh, A., Saitoh, M., Mizushima, Y., kimura, K., Suzuki, S., Yagi, H., Horiuchi, A., Ogata, M., Hamaoka, T. and Fujiwara, H. (1990) Differentiation of thymocytes from $CD3^-CD4^-CD8^-$ through $CD3^-CD4^-CD8^+$ into more mature stages induced by a thymic stromal cell clone. *PNAS* **87**, 2750-2754.

Thomas, M.L. (1989) The leukocyte common antigen family. *Annu. Rev. Immunol.* **7**, 339.

Tibbetts, T.A., DeMayo, F., Rich, S., Conneely, O.M. and O'Malley, B.W. (1999) Progesterone receptors in the thymus are required for thymic involution during pregnancy and for normal fertility. *Proc Natl Acad Sci U S A* **96**, 12021-6.

Townson, J.R. and Nibbs, R.J.B. (2002) Characterization of mouse CCX-CKR, a receptor for the lymphocyte-attracting chemokines TECK/mCCL25, SLC/mCCL21 and MIP-3beta/mCCL19: comparison to human CCX-CKR. *Eur J Immunol* **32**, 1230-1241.

Ueno, T., Hara, K., Willis, M.S., Malin, M.A., Hopken, U.E., Gray, D.H., Matsushima, K., Lipp, M., Springer, T.A., Boyd, R.L., Yoshie, O. and Takahama, Y. (2002) Role for CCR7 ligands in the emigration of newly generated T lymphocytes from the neonatal thymus. *Immunity* **16**, 205-18.

Ushiki, T. and Takeda, M. (1997) Three-dimensional ultrastructure of the perivascular space in the rat thymus. *Arch Histol Cytol* **60**, 89-99.

Utsuyama, M., Hirokawa, K., Mancini, C., Brunelli, R., Leter, G. and Doria, G. (1995) Differential effects of gonadectomy on thymic stromal cells in promoting T cell differentiation in mice. *Mech. Ageing and Dev.* **81**, 107-117.

van de Wijngaert, F.P., Kendall, M.D., Schuurman, H.J., Rademakers, L.H. and Kater, L. (1984) Heterogeneity of epithelial cells in the human thymus. An ultrastructural study. *Cell Tissue Res* **237**, 227-237.

van Ewijk, W. (1991) T-cell differentiation is influenced by thymic microenvironments. *Annu. Rev. Immunol.* **9**, 591-615.

van Ewijk, W., Hollander, G., Terhorst, C. and Wang, B. (2000a) Stepwise development of thymic microenvironments in vivo is regulated by thymocyte subsets. *Development* **127**, 1583-1591.

van Ewijk, W., Kawamoto, H., Germeraad, W.T. and Katsura, Y. (2000b) Developing thymocytes organize thymic microenvironments. *Curr Top Microbiol Immunol* **251**, 125-32.

van Ewijk, W., Shores, E.W. and Singer, A. (1994) Cross talk in the mouse thymus. *Immunology Today* **15**, 214-217.

van Meerwijk, J.P., Marguerat, S., Lees, R.K., Germain, R.N., Fowlkes, B.J. and MacDonald, H.R. (1997) Quantitative impact of thymic clonal deletion on the T cell repertoire. *J Exp Med* **185**, 377-83.

Van Vliet, E., Melis, M., Foidart, J.M. and van Ewijk, W. (1986) Reticular fibroblasts in peripheral lymphoid organs identified by a monoclonal antibody. *J Histochem Cytochem* **34**, 883-890.

Van Vliet, E., Melis, M. and van Ewijk, W. (1984) Monoclonal antibodies to stromal cell types of the mouse thymus. *Eur J Immunol* **14**, 524-529.

Vassileva, G., Soto, H., Zlotnik, A., Nakano, H., Kakiuchi, T., Hedrick, J.A. and Lira, S.A. (1999) The reduced expression of 6Ckine in the plt mouse results from the deletion of one of two 6Ckine genes. *J Exp Med* **190**, 1183-1188.

Vidalain, P.-., Laine, D., Zaffran, Y., Azocar, O., Servet-Delprat, C., Wild, T.F., Rabourdin-Combe, C. and Valentin, H. (2002) Interferons mediate terminal differentiation of human cortical thymic epithelial cells. *J Virol* **76**, 6415-6424.

Vremec, D., Pooley, J., Hochrein, H., Wu, L. and Shortman, K. (2000) CD4 and CD8 expression by dendritic cell subtypes in mouse thymus and spleen. *J. Immunol.* **164**, 2978.

Wallin, J., Eibel, H., Neubuser, A., Wilting, J., Koseki, H. and Balling, R. (1996) Pax1 is expressed during development of the thymus epithelium and is required for normal T-cell maturation. *Development* **122**, 23-30.

Wang, B., Simpson, S.J., Hollander, G. and Terhorst, C. (1997) Development and function of T lymphocytes and natural killer cells after bone marrow transplantation of severely immunodeficient mice. *Immunol Rev* **157**, 53-60.

Warnock, R.A., Campbell, J.J., Dorf, M.E., Matsuzawa, A., McEvoy, L.M. and Butcher, E.C. (2000) The role of chemokines in the micorenvironmental control of T versus B cell arrest in Peyer's patch high endothelial venules. *J Exp Med* **191**, 77-88.

Wilkinson, B., Owen, J.J.T. and Jenkinson, E.J. (1999) Factors regulating stem cell recruitment to the fetal thymus. *J. Immunol.* **162**, 3873-3881.

Wilkinson, R.W., Anderson, G., Owen, J.J. and Jenkinson, E.J. (1995) Positive selection of thymocytes involves sustained interactions with the thymic microenvironment. *J Immunol* **155**, 5234-40.

Williams, O., Tanaka, Y., Tarazona, R. and Kioussis, D. (1997) The agonist-antagonist balance in positive selection. *Immunol Today* **18**, 121-6.

Willison, K.R., Karol, R.A., Suzuki, A., Kundu, S.K. and Marcus, D.M. (1982) Neutral glycolipid antigens as developmental markers of mouse teratocarcinoma and early embryos: an immunologic and chemical analysis. *J Immunol* **129**, 603-609.

Wilson, A., MacDonald, H.R. and Radtke, F. (2001) Notch 1-deficient common lymphoid precursors adopt a B cell fate in the thymus. *J Exp Med* **194**, 1003-12.

Windmill, K.F., Meade, B.J. and Lee, V.W.K. (1993) Effect of prepubertal Gonadectomy and sex steroid treatment on the growth and lymphocyte populations of the rat thymus. *Reprod. Fertil. Dev.* **5**, 73-81.

Wolfer, A., Wilson, A., Nemir, M., MacDonald, H.R. and Radtke, F. (2002) Inactivation of Notch1 impairs VDJbeta rearrangement and allows pre-TCR- independent survival of early alpha beta lineage thymocytes. *Immunity* **16**, 869-79.

Wu, L., Antica, M., Johnson, G.R., Scollay, R. and Shortman, K. (1991a) Development potential of the earliest precursor cells from the adult mouse thymus. *J Exp Med* **174**, 1617-1627.

Wu, L., Scollay, R., Egerton, M., Pearse, M., Spangrude, G.J. and Shortman, K. (1991b) CD4 expressed on earliest T-lineage precursor cells in the adult murine thymus. *Nature* **349**, 71-4.

Wu, L., Vremec, D., Ardavin, C., Winkel, K., Suss, G., Georgiou, H., Maraskovsky, E., Cook, W. and Shortman, K. (1995) Mouse thymus dendritic cells: kinetics of development and changes in surface markers during maturation. *Eur J Immunol* **25**, 418-425.

Wu, Q., Lahti, J.M., Air, G.M., Burrows, P.D. and Cooper, M.D. (1990) Molecular cloning of the murine BP-1/6C3 antigen: a member of the zinc-dependent metallopeptidase family. *Proc. Natl. Acad. Sci. USA* **87**, 993.

Wurbel, M.A., Malissen, M., Guy-Grand, D., Meffre, E., Nussenzweig, M.C., Richelme, M., Carrier, A. and Malissen, B. (2001) Mice lacking the CCR9 CC-chemokine receptor show a mild impairment of early T- and B-cell development and a reduction in T-cell receptor gammadelta(+) gut intraepithelial lymphocytes. *Blood* **98**, 2626-32.

Wurbel, M.A., Philippe, J.M., Nguyen, C., Victorero, G., Freeman, T., Wooding, P., Miazek, A., Mattei, M.G., Malissen, M., Jordan, B.R., Malissen, B., Carrier, A. and Naquet, P. (2000) The chemokine TECK is expressed by thymic and intestinal epithelial cells and attracts double- and single-positive thymocytes expressing the TECK receptor CCR9. *Eur J Immunol* **30**, 262-71.

Yoshida, R., Imai, T., Hieshima, K., Kusuda, J., Baba, M., Kitaura, M., Nishimura, M., Kakizaki, M., Nomiyama, H. and Yoshie, O. (1997) Molecular cloning of a novel human CC chemokine EBI1-ligand chemokine that is a specific functional ligand for EBI1, CCR7. *J Biol Chem* **272**, 13803-13809.

Zerrahn, J., Held, W. and Raulet, D. (1997) The MHC reactivity of the T cell repertoire prior to positive and negative selection. *Cell* **88**, 627-636.

Zou, Y.-R., Kottman, A.H., Kuroda, M., Taniuchi, I. and Littman, D.R. (1998) Function of the chemokine receptor CXCR4 in haematopoiesis and in cerebellar development. *Nature* **393**, 595-599.

ELSEVIER

Journal of Immunological Methods 260 (2002) 15–28

JIM
Journal of Immunological Methods

www.elsevier.com/locate/jim

Analysis of thymic stromal cell populations using flow cytometry

D.H.D. Gray *, A.P. Chidgey, R.L. Boyd

Department of Pathology and Immunology, Monash Medical School, Commercial Road, Prahran, Melbourne 3181, Australia

Received 30 May 2001; received in revised form 13 August 2001; accepted 15 August 2001

Abstract

The complexity of the lymphostromal interplay that is essential to αβT-cell development is reflected by the heterogeneity of both lymphocytes and thymic stromal cells. While panels of monoclonal antibodies have described many of the cellular components of these microenvironments, the means to quantify stromal cell subsets using flow cytometry remains poorly defined. This study refines and compares various stromal cell isolation procedures and determines the effects of various digestion enzymes on important surface molecules. Three- and four-color flow cytometry is used to correlate established and novel stromal cell markers to define thymic fibroblasts, epithelium and a unique subset of thymic endothelium that express MHC class II. This work provides a basis for the purification of thymic stromal cells for further phenotypic, functional and genetic analysis. © 2002 Elsevier Science B.V. All rights reserved.

Keywords: Thymus; Stromal cells; Flow cytometry; Thymic epithelial cells

1. Introduction

The thymus provides a unique microenvironment that efficiently generates αβT-lymphocytes capable of responding to foreign peptide in the context of self-MHC. This microenvironment is established through the interplay of developing thymocytes with a non-lymphocytic component broadly termed the thymic stroma. The latter consists of a phenotypically diverse group of cells, including epithelium, endothelium, reticular fibroblasts, macrophages, dendritic cells and neuroendocrine cells (Boyd et al., 1993). These cells collectively provide cell surface molecules, cytokines and extracellular matrix elements that are essential for various stages of T-cell development (Anderson et al., 1996). While the various subsets of thymocytes in the thymus have been studied in depth, relatively little is known about the stromal cell types that influence their development.

Earlier ultrastructural studies initially demonstrated the diversity of thymic epithelial cells based on morphology and electron lucency, identifying six discrete subsets (types 1–6) (van de Wijngaert et al., 1984). Further investigations into thymic stromal cells (TSC) have involved immunohistological analysis using panels of monoclonal antibodies (mAbs) specific for stromal antigens (for example, van Vliet

Abbreviations: mAb, monoclonal antibody; MHC, major histocompatibility complex; FcR, Fc receptor; FACS, fluorescence-activated cell sorting; PBS, phosphate buffered saline; TSC, thymic stromal cell.

* Corresponding author. Tel.: +61-3-990-302-23; fax: +61-3-990-307-31.

E-mail address: daniel.gray@med.monash.edu.au (D.H.D. Gray).

0022-1759/02/$ - see front matter
PII: S0022-1759(01)00493-8

et al., 1984; de Maagd et al., 1985; Lobach et al., 1985; Godfrey et al., 1988). Such work has defined stromal cells (particularly the epithelial cells) into discrete subsets on the basis of morphology and the expression of intracellular and cell surface markers (Kampinga et al., 1989). However, the coexpression of these various markers and population kinetics of the stromal cell subsets have been difficult to evaluate by histological studies alone. A previous study attempting to resolve some of these issues using flow cytometric analysis of thymic stromal cells found extensive overlap between the distributions of determinants thought to be exclusive in their expression (Izon et al., 1994). Here, we describe the usage of multicolor flow cytometry to distinguish the various thymic stromal populations using mAbs to surface antigens.

The stromal cell yields from various enzymatic digestion methods are compared and the epitope sensitivities of important markers determined. As found previously, flow cytometry reveals a more extensive distribution of some stromal antigens than would have been predicted from immunohistology, highlighting the greater sensitivity of the former technique. However, exclusion of certain contaminating cell types has enabled clearer correlation of TSC reactive mAbs on stromal cell subsets. FACS purification of these stromal subsets will hopefully aid in the determination of the precise functional roles each of these cell types have in T-cell development. Furthermore, genetic and antigenic analysis of individual populations may lead to a better understanding of the molecules that mediate these functions.

2. Materials and methods

2.1. Animals

CBA × C57BL/6 F1 mice at 3 days or 4 weeks of age were used as a source of thymic stromal cells. Mice were bred and maintained by the Monash University Central Animal Services.

2.2. Thymic stromal cell isolation by collagenase digestion

The thymic stromal cell isolation procedure used was based on that described by us previously (Shortman et al., 1989). Two to three thymi were dissected from freshly killed mice and trimmed of fat and connective tissue. Small cuts into the capsules were made with a pair of fine scissors and the thymi were gently agitated in 50 ml of RPMI-1640 with a magnetic stirrer at 4 °C for 30 min to remove the majority of thymocytes. The resulting thymic fragments were transferred into 10 ml of fresh RPMI-1640 and dispersed further with a wide bore glass pipette to free more thymocytes. Medium was changed 2–3 times after agitations, with fragments recovered by settling each time. The thymic fragments were then incubated in 5 ml of 0.125% (w/v) collagenase D with 0.1% (w/v) DNAse I (both from Boehringer Mannheim, Germany) in RPMI-1640 at 37 °C for 15 min, with gentle agitation using a Pasteur pipette every 5 min. Enzyme mixtures with isolated cells were removed after fragments had settled, then replaced with fresh mixture for further incubation. Gentle mechanical agitation was performed with a 3-ml syringe and 26G needle to break up aggregates remaining in final digestions. After 3–4 digestions, cells were pooled and centrifuged at $450g_{max}$ for 5 min, resuspended in 5 mM EDTA in PBS + 1% FCS + 0.02% (w/v) NaN_3 (EDTA/FACS buffer) and allowed to incubate for 10 min at 4 °C to disrupt rosettes (Shortman et al., 1989). Cells were then passed through 100-μm mesh to remove clumps, and viable cells were counted using ethidium bromide/acridine orange staining prior to antibody labeling.

2.3. Thymic stromal cell isolation by collagenase/dispase or trypsin digestion

Thymi were removed and mechanically digested as above. The first enzymatic incubations were performed in collagenase, with final digestion of large aggregates performed in 5 ml of either collagenase, 0.125% (w/v) collagenase/dispase (Boehringer Mannheim) with 0.1% (w/v) DNase I in RPMI or 0.125% (w/v) trypsin (Boehringer Mannheim) in Ca/Mg-free HBSS for 30 min at 37 °C with gentle agitation every 15 min. Five milliliters of 0.1% (w/v) DNase I in RPMI was then added to the trypsin digestion mixture and incubation resumed at 37 °C for a further 15 min, with gentle agitation every 5 min. Cells recovered by centrifugation were resuspended in EDTA/

FACS buffer and incubated at 4 °C for 10 min, then passed through 100-μm mesh before counting and staining.

2.4. Antibodies and immunoconjugates

The panel of surface reactive stromal cell mAbs used for flow cytometric analysis were grown and conjugated in this laboratory unless otherwise stated; MTS-12 (anti-CD31, unpublished), biotinylated MTS-15 (detects a low molecular weight glycolipid expressed on the surface of cells at the blood/thymus barrier; see Section 3), CDR-1 (Rouse et al., 1988), biotinylated UEA-1 lectin (Vector, USA), biotinylated G8.8a and hybridoma supernatant (Nelson et al., 1996) (both generous gifts from Andrew Farr), anti-B7.1 (clone IG10, a generous gift from Dale Godfrey), rabbit anti-mouse keratin (wide screen) (DAKO), biotinylated anti-Ly51 (clone 6C3, Pharmingen, USA), anti-TSA-1 (clone CR-12 (Kosugi et al., 1998)), FITC or PE-conjugated anti-CD45.2 (clone 104, Pharmingen), PE-conjugated anti-I-A^b/I-A^c (clone M5/114.15.2, Pharmingen), purified anti-CD40 (clone 3/23, Pharmingen), anti-ICAM-1 (clone YN1/1.7.4), anti-Fc-receptor (clone 2.4G2), biotinylated CD11c (clone HL3, Pharmingen), APC-conjugated anti-CD11b (clone M1/70, Pharmingen), APC-conjugated anti-CD8 (clone 53-6.7, Pharmingen), PE-conjugated anti-CD4 (clone RM 4-5, Pharmingen), anti-Thy 1.2 (clone 12H12).

Secondary reagents used were PE-conjugated goat polyclonal anti-rat IgG (Southern Biotechnologies, USA), FITC-conjugated goat anti-rat Ig (Silenus, Australia), biotinylated rabbit anti-rat IgG (H + L) (Vector), APC-conjugated goat anti-rat Ig (Caltag, USA), Alexa-568-conjugated goat anti-rabbit IgG (Molecular Probes), PerCP-conjugated Streptavidin (Pharmingen) and CyChrome-conjugated Streptavidin (Pharmingen).

2.5. Immunofluorescent staining and flow cytometry

Cells were washed in cold EDTA/FACS buffer and 3×10^6 cells dispensed into wells of a 96-well round-bottomed plate (an empty well was left between each sample). Primary antibody (30 μl of hybridoma supernatant or purified antibody at a sub-optimal dilution) was incubated with resuspended cells for 20 min at 4 °C, followed by two washes in 200 μl of EDTA/FACS buffer. The secondary antibody was added, incubated and washed, before 5 μl of 10% (v/v) normal rat serum in FACS buffer was added for 5 min at 4 °C to block any remaining reactive sites of the secondary reagent. Biotinylated and direct conjugates were added, incubated and washed, followed by the appropriate streptavidin conjugate. After final incubation, cells were washed, then resuspended in 200 μl of EDTA/FACS buffer for acquisition. Sample data from 1×10^4 $CD45^-$ (non-lymphoid) cells were acquired on a FACScalibur (Becton Dickinson) using up to four fluorescent channels (FL1 for FITC, FL2 for PE, FL3 for CyChrome and PerCP and FL4 for APC) and analysed using CellQuest software (Becton Dickinson). All compensations were performed on single-color labeling of stromal cells. An FcR block (clone 2.4G2 supernatant) was employed before antibody staining of dendritic cells and macrophages.

2.6. Immunohistology

Sections (8 μm) of normal 4-week-old thymus were cut at −20 °C on a cryostat (Miles Laboratories) and air dried for 10 min before fixation in acetone (−20 °C) for 1 min at room temperature. Sections were then washed and incubated with 30 μl of primary mAb for 15 min in a moist container at room temperature, washed three times in PBS with gentle agitation for 5 min, then incubated with 30 μl of appropriate secondary Abs, followed by washing. For three-color immunofluorescence, 10 μl of 10%(v/v) normal rat serum in PBS was applied to sections for 5 min at room temperature to block any remaining reactive sites of the secondary reagent, before incubation of biotinylated reagents for 15 min followed by washing. Sections were then incubated with streptavidin conjugates before final washing and mounting with fluorescent mounting medium (DAKO) using coverslips.

Images were acquired on a BIO-RAD MRC 1024 confocal microscope with a three-line Kr/Ag laser (excitation lines 488, 568 and 647 nm) using the acquisition software BIO-RAD LaserSharp v3.2. Analysis of files obtained was performed using LaserSharp processing software.

3. Results and discussion

3.1. Analysis of thymic stromal cells isolated by collagenase digestion

To determine the enrichment and numbers of thymic stromal cells that could be obtained using collagenase digestion, cells isolated from a series of incubations were analyzed for CD45 expression, which detects all cells derived from haematopoietic stem cells (HSCs) (reviewed by Thomas, 1989). This enabled discrimination of CD45$^-$ epithelium, endothelium, fibroblasts and neuroendocrine cells from all other cells in the thymus.

Table 1 shows that incubation of thymic fragments in a series of three collagenase digestions released increasing levels of CD45$^-$ cells. Very few were released by the initial agitation alone. The highest number and proportion of CD45$^-$ cells was obtained in the final digestion, resulting in an enrichment of these stromal cells of almost 30-fold (Fig. 1A and B). This was verified by microscopic evaluation of the gradual enrichment of the larger of these cells throughout the course of the collagenase digestion (Fig. 1C and D). This characteristic was also apparent with the high forward and side scatter properties of some CD45$^-$ cells, particularly in the final digest (Fig. 1E and F). However, backgating of CD45$^-$ events isolated in these digests revealed that there were also many small stromal cells, necessitating the inclusion of the larger thymocytes in a FSC/SSC stromal gate. Extremely high FSC or SSC events were excluded from the gate to minimize the risk of including doublets in the analysis.

3.2. Comparison of digestion enzymes

Many previous studies into thymic stromal cells have used various isolation procedures that employ enzymes other than collagenase to dissociate the thymic tissue, in particular, collagenase/dispase (Pircher et al., 1993) and trypsin (Jenkinson et al., 1992). In this study, these enzymes were used to gauge how effective each was in digesting the stromal cell aggregates that are normally left after the final collagenase digestion (Table 2).

Trypsin was the most effective, dissociating all thymic fragments and stromal aggregates into a single cell suspension, thereby releasing all remaining stromal cells. The total CD45$^-$ cells isolated from this preparation represented the maximal recovery against which the other enzymes were compared. The recovery of almost 80% of CD45 negatives with collagenase digestion suggests that the undigested aggregates contained many thymic stromal cells (1.56×10^5 per thymus). Collagenase/dispase dissociated some of these aggregates, recovering 94% of available CD45$^-$ stromal cells.

While dispase and trypsin isolated more CD45$^-$ stromal cells, the possibility that these enzymes may cleave potentially important cell surface markers was addressed by incubating suspensions of stromal cells with these enzymes for 1 h at 37 °C, followed by immunofluorescent labeling. The summary of the epitope sensitivities of a variety of thymocyte and stromal antigens in Table 3 shows that collagenase digestion preserves all markers tested. Most of these molecules are also resistant to dispase treatment. However, CD4, CD8 and CD11c profiles did change

Table 1
Yields and viability of total cells and CD45$^-$ cells released from a series of collagenase digestions of thymi

	Total cells per thymus	Proportion of CD45$^-$ cells in digest (%)	CD45$^-$ cells per thymus	Viability (%)
Depletion	1.66×10^8	0.18	8.30×10^4	96
Collagenase 1	1.80×10^7	1.13	5.76×10^4	98
Collagenase 2	3.03×10^7	1.43	1.21×10^5	97
Collagenase 3	1.85×10^7	5.79	3.26×10^5	97
Total/thymus	2.33×10^8	0.25	5.88×10^5	

The number of collagenase digestions required and cell numbers released at each step varied between experiments. However, the trend of CD45$^-$ cell release remained the same. This data is representative of five experiments.

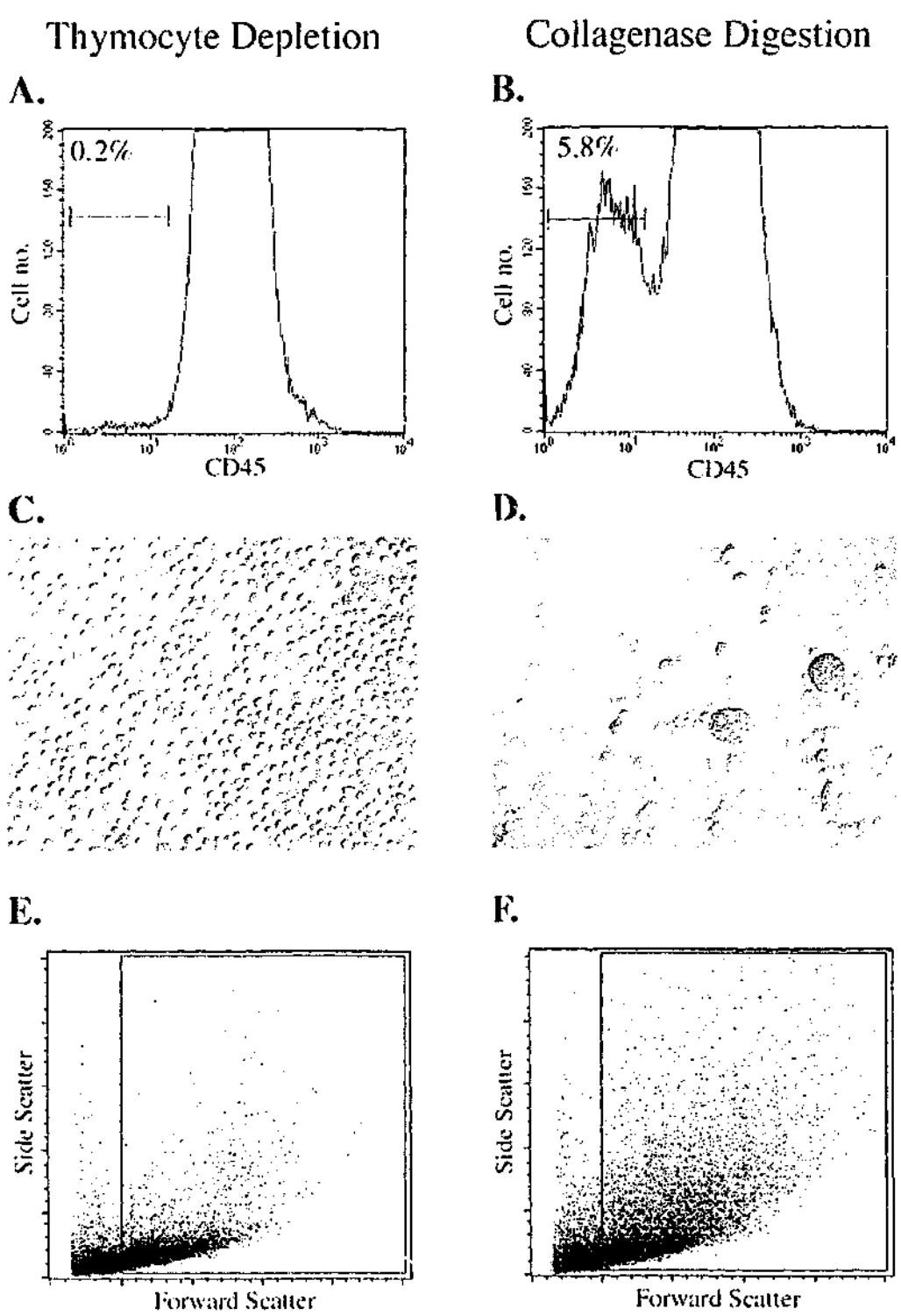

Fig. 1. CD45$^-$ cells are enriched in the final collagenase digestion of 4-week-old thymi. Cells from the thymocyte-depletion step and the final collagenase digestion were analyzed for CD45 expression (A and B). The larger stromal cells were apparent microscopically (C and D). This was reflected in more cells of high forward and side scatter properties being found in the collagenase digestion (E) than the depletion (F). Profiles are representative of five experiments.

Table 2
Comparison of CD45$^-$ cell yields using various digestion enzymes

	CD45$^-$ cells isolated in final digestion per thymus	Total CD45$^-$ cells isolated per thymus	Proportion of maximal recovery of CD45$^-$ (%)
Collagenase	3.26×10^5	5.88×10^5	79
Collagenase/dispase	4.40×10^5	7.02×10^5	94
Trypsin	4.82×10^5	7.44×10^5	100

Thymi were digested in collagenase for two incubations, then the final digestion performed in either collagenase, collagenase/dispase or trypsin (data for previous collagenase digestions shown in Table 1). CD45$^-$ cell yields from the final and overall digestion are determined and the proportion of maximal recovery (trypsin digest) calculated. This data is representative of three experiments performed.

with this enzyme. More than half of the epitopes tested were disrupted or cleaved entirely upon trypsin treatment. However, some important markers (e.g. CD45, MHC II) were resistant.

3.3. Flow cytometric analysis of thymic stromal cell subsets

Pooled collagenase preparations enriched for thymic stromal cells were analyzed further by flow cytometry for their autofluorescence. While these cells alone gave high signals in the FL1, FL2 and FL3 channels (Fig. 2A; Izon et al., 1994), the majority of this background was due to autofluorescence from a population of CD45$^+$ cells (Fig. 2B). These highly autofluorescent, CD45$^+$ cells are probably thymic macrophages, as has been previously reported (Vremec et al., 2000), and are excluded from the analysis when gating on CD45$^-$ thymic stromal cells. Furthermore, it was found that CD45$^-$ cells exhibited little or no background staining due to nonspecific binding of IgG (Fig. 2C) and did not express Fc-receptors (Fig. 2D). A population of thymic MHC^{hi} cells do express FcR and further analysis determined that these were myeloid derived cells and some lymphoid dendritic cells (data not shown), necessitating the use of an FcR block when staining for these cell types.

Further phenotypic analysis of thymic stromal cells was conducted using a panel of surface reactive mAbs. Of particular interest were thymic epithelial cells, which could be defined using the mAb G8.8a that recognizes EpCAM, expressed by thymic epithelium, dendritic cells and some thymocytes (Nelson et al., 1996). By first gating on CD45$^-$ stromal cells, the latter two cell types could be excluded, leaving only the epithelial cells staining positive with this marker.

Under these conditions, EpCAM positive cells comprised about 45–60% of CD45$^-$ cells in the pooled collagenase digestions and could be further divided into cortical and medullary epithelial cells using CDR-1 as a marker of cortical epithelium (Rouse et al., 1988) (Fig. 3A). In normal 4-week-old mice, about half of the epithelium is CDR-1$^+$, the remainder presumably medullary epithelium (see later section).

Table 3
Epitope resistance to various digestion enzymes

Marker	Collagenase	Collagenase/dispase	Trypsin
CD45	+	+	+
CD4	+	±	–
CD8	+	–	–
CD11c	+	±	–
CD11b	+	+	±
MHC II	+	+	+
EpCAM	+	+	–
ICAM-1	+	+	+
PECAM	+	+	–
Thy1	+	+	±
TSA-1	+	+	±
CD40	+	+	±
B7.1	+	+	–
Ly51	+	+	+
CDR-1	+	+	+
MTS-15	+	+	+
UEA-1	+	+	–

Isolated stromal cells were incubated in collagenase, collagenase/dispase or trypsin and immunofluorescent staining with various mAbs analysed by flow cytometry. Epitopes that were resistant (+), partially resistant (±) or sensitive (–) to enzyme treatment were determined using histograms representative of three experiments.

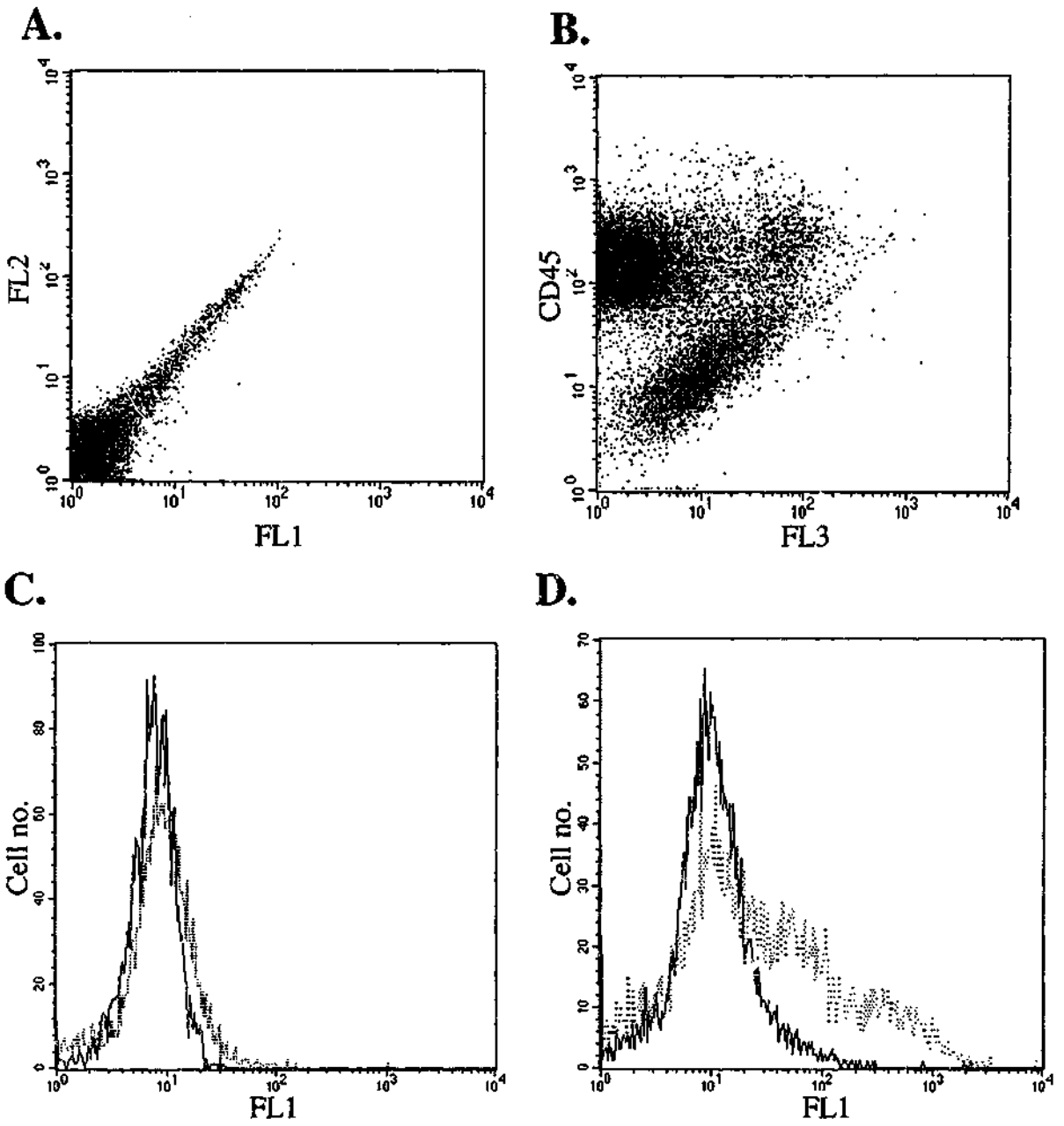

Fig. 2. Autofluorescence and FcR expression in collagenase-digested preparations of 4-week-old thymic stromal cells. Autofluorescence of isolated cells alone extends up to 10^2 in the FL1, FL2 and FL3 channels (A). Analysis of CD45 expression vs. an empty FL3 channel reveals most of the high autofluorescent signals are derived from a population of CD45$^+$ cells, while CD45$^-$ cells display a range of intensities (B). The histogram in (C) plots unlabeled CD45$^-$ cells (solid line) vs. an IgG2b isotype control detected by an anti-rat Ig FITC on CD45$^-$ cells (dotted line). Histogram (D) plots anti-FcR (clone F2.4G2) staining revealed by anti-rat Ig FITC gated on CD45$^-$ cells (solid line) and anti-FcR staining revealed by anti-rat Ig FITC gated on total MHC II^{hi} cells (dotted line). Profiles are representative of three experiments.

Interestingly, all CD45$^-$/EpCAM$^+$ stromal cells expressed MHC class II, although at varying levels (Fig. 3B). This presumably reflects the antigen-presenting role these cells play in selecting developing thymocytes. Certainly, it has been demonstrated by Jenkinson et al. (1992) that embryonic CD45$^-$/MHC class II$^+$ thymic stromal cells can mediate the development of double positive to functional single positive thymocytes. While this fraction includes both cortical and medullary epithelial cells, about half of

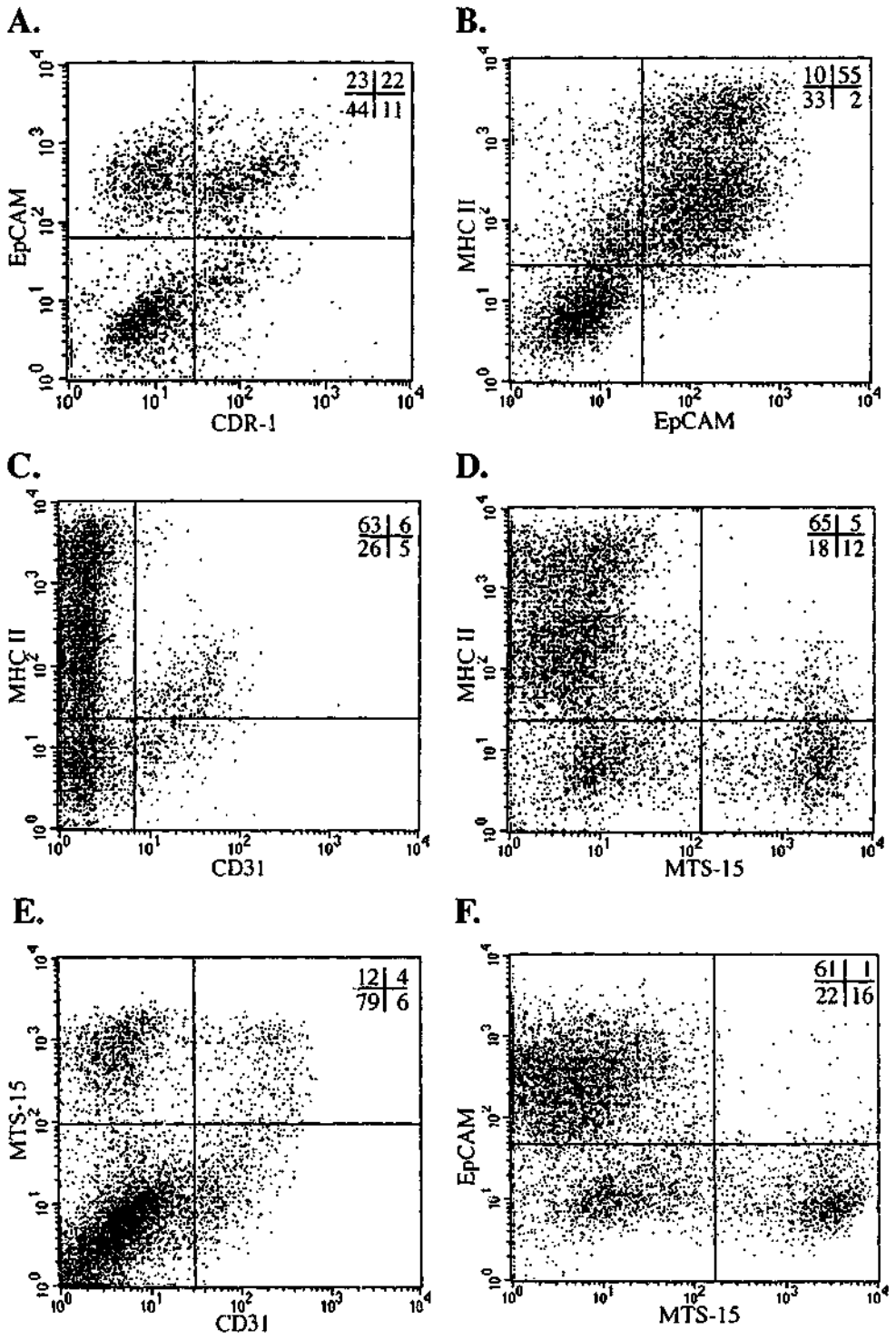

Fig. 3. Phenotypic analysis of CD45$^-$ thymic stromal cell subsets defined by a panel of mAbs. Collagenase digested CD45$^-$ stromal cells from 4-week-old mice were gated and analysed for the expression of certain markers. Expression of EpCAM and CDR-1 allows distinction of cortical and medullary epithelium (A). All EpCAM$^+$ epithelial cells express MHC class II (B). CD31-positive endothelial cells comprise 11% of CD45$^-$ cells, half of which express low levels of MHC class II (C). Most cells expressing the fibroblast marker MTS-15 do not express MHC class II (D). MTS-15 is also expressed on the surface of some endothelial cells (E). As expected, MTS-15$^+$ fibroblasts do not express EpCAM (F). Representative profiles from three experiments shown.

the endothelial cells in the thymus (defined by expression of CD31) also expressed low levels of MHC class II (Fig. 3C). Whether these cells play a role in selection remains to be addressed. It is unlikely that they are primarily involved in positive selection because this appears to be a unique feature of cortical epithelium (Benoist and Mathis, 1989). They could, however, contribute to positive and negative selection by providing MHC/peptide ligands for thymocyte T-cell receptors, acting in cis with differentiating signals from cortical epithelium (Chidgey et al., 1998).

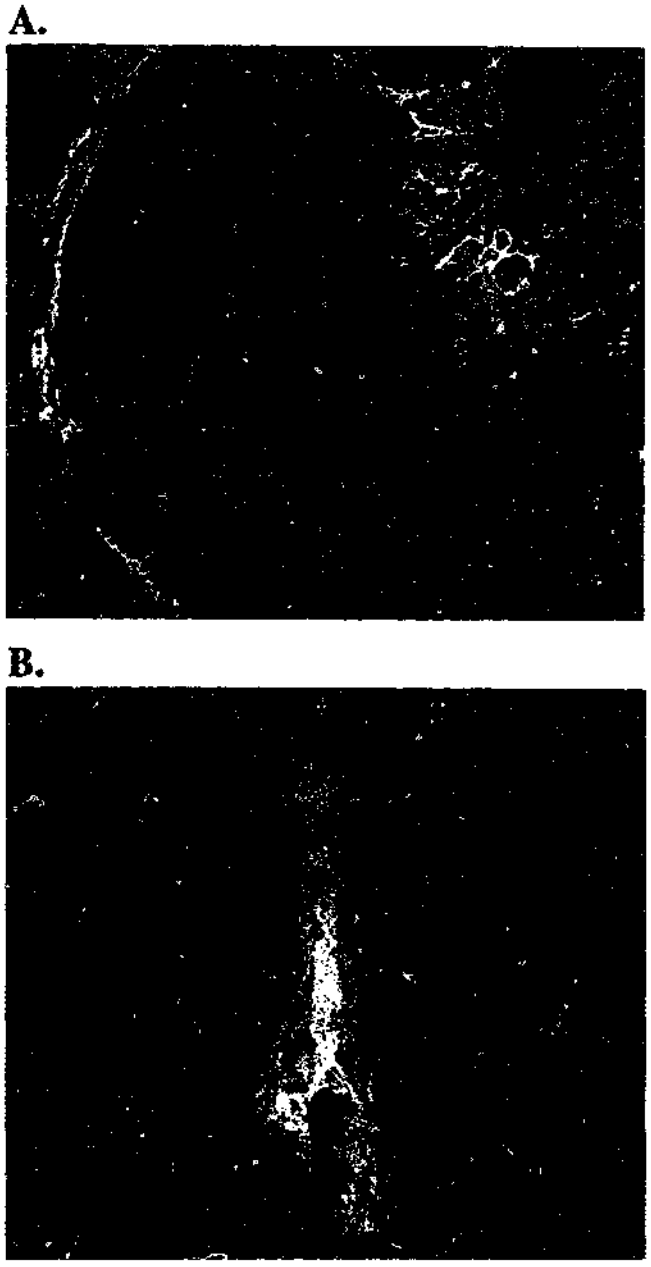

Fig. 4. MTS-15 recognizes an antigen expressed by subcapsular and perivascular fibroblasts in the 4-week-old thymus. MTS-15 antigen can be detected around the subcapsule and large blood vessels of the medulla (green) with little colocalization (yellow) with keratin-positive epithelial cells (red) (A). More extensive colocalization (yellow) is observed upon higher power examination of counterstaining of MTS-15 (green) with anti-CD31 (red) than with anti-keratin (blue) (B).

In addition to thymic epithelial and endothelial cells, fibroblasts constitute a major component of the stromal microenvironment in which thymocytes develop. These cells are important in forming the ECM components essential to CD4$^-$CD8$^-$ thymocyte development (Anderson et al., 1997), although other roles remain to be defined. The mAb MTS-15 recognizes a glycolipid antigen expressed on the surface of MHC class II$^-$ thymic fibroblasts that line the subcapsule and large blood vessels (Figs. 3D and 4A and B). However, this antigen also appears to be present on some MHC class II$^+$ cells (Fig. 3D). Four-color labeling examining MTS-15, MHC II and CD31 expression on CD45$^+$ stromal cells revealed that these MHC II/MTS-15$^+$ events are the MHC II/CD31$^+$ endothelial cells mentioned earlier (Fig 3E and data not shown). Whether the distinct phenotype of these endothelial cells relates to a specialized function within the thymus is an interesting, as yet unanswered, question.

As would be expected, MTS-15 and anti-EpCAM define mutually exclusive populations of CD45$^-$ stromal cells (Fig. 3F). The remaining population of CD45$^-$/EpCAM$^-$/MTS-15$^-$ cells may include more fibroblasts and neuroendocrine cells.

The other major cellular components of the thymic stroma include the CD45$^+$ macrophages and dendritic cells. Thymic dendritic cells can be defined as CD11c^{hi}, MHC class II^{hi} cells (Fig. 5A) (Wu et al., 1995), while myeloid derived cells (predominantly macrophages) are CD11b^{hi}, CD11c^{lo} (Kishimoto et al., 1989) (Fig. 5B). Thymic macrophages appear to be predominantly MHC class II$^-$, although there are some MHC class II high and low macrophages (Fig. 5C). These stromal cells are found to emerge at all stages of the collagenase digestion (including the thymocyte depletion step), although they are enriched in the final few digestions (data not shown).

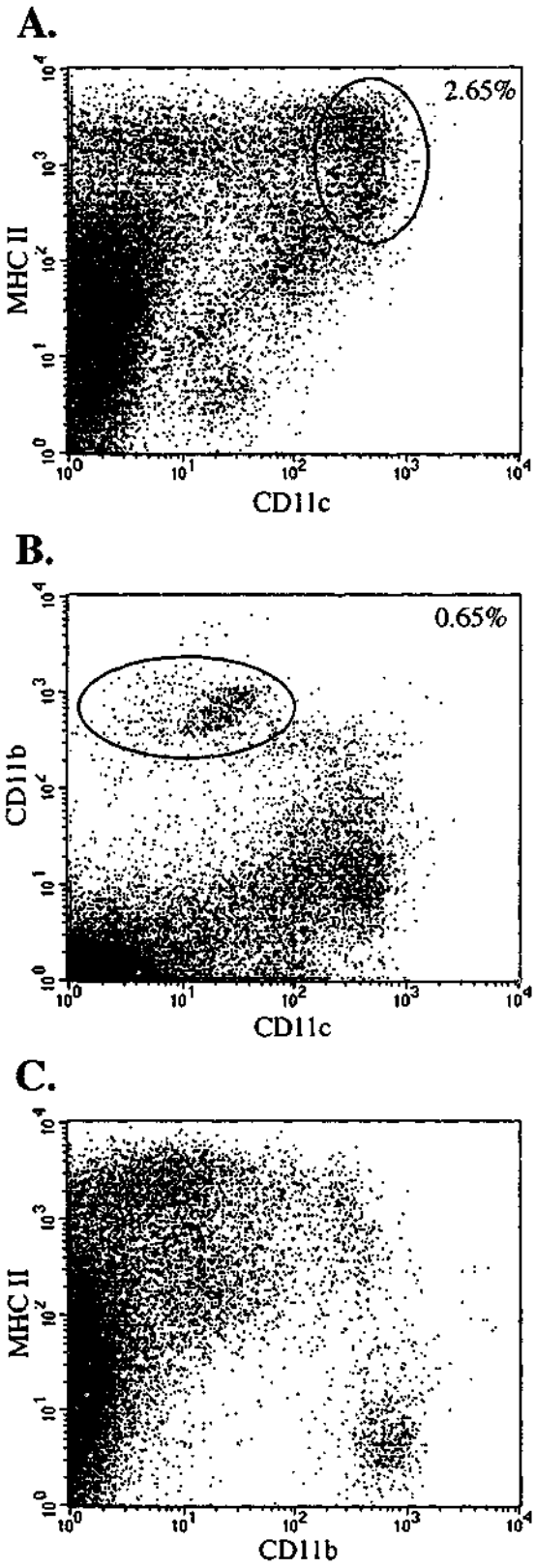

Fig. 5. Thymic dendritic cells and myeloid derived cells in collagenase digested stromal cell preparations of 4-week-old thymi. Thymic dendritic cells can be defined by high expression of CD11c and MHC class II (A). Thymic myeloid derived cells are CD11b^{hi} and CD11c^{lo} (B). The few CD11c^{hi}, CD11b$^+$ events may represent myeloid-derived dendritic cells. The CD11b^{hi} cells can be divided into MHC class II positive and negative populations (C). Representative profiles from three experiments are shown gated on total viable thymic stromal cells (CD45$^-$ and CD45$^+$).

3.4. Cortical and medullary epithelial cell markers

While it has been established that cortical and medullary epithelial cells play distinct roles in thymic selection (Klein and Kyewski, 2000), purification of these cell types will be essential for future functional and molecular studies. The mAbs CDR-1 and 6C3 have previously been used to define thymic cortical epithelial cells histologically (Rouse et al., 1988; Surh et al., 1992). Furthermore, immunomagnetic

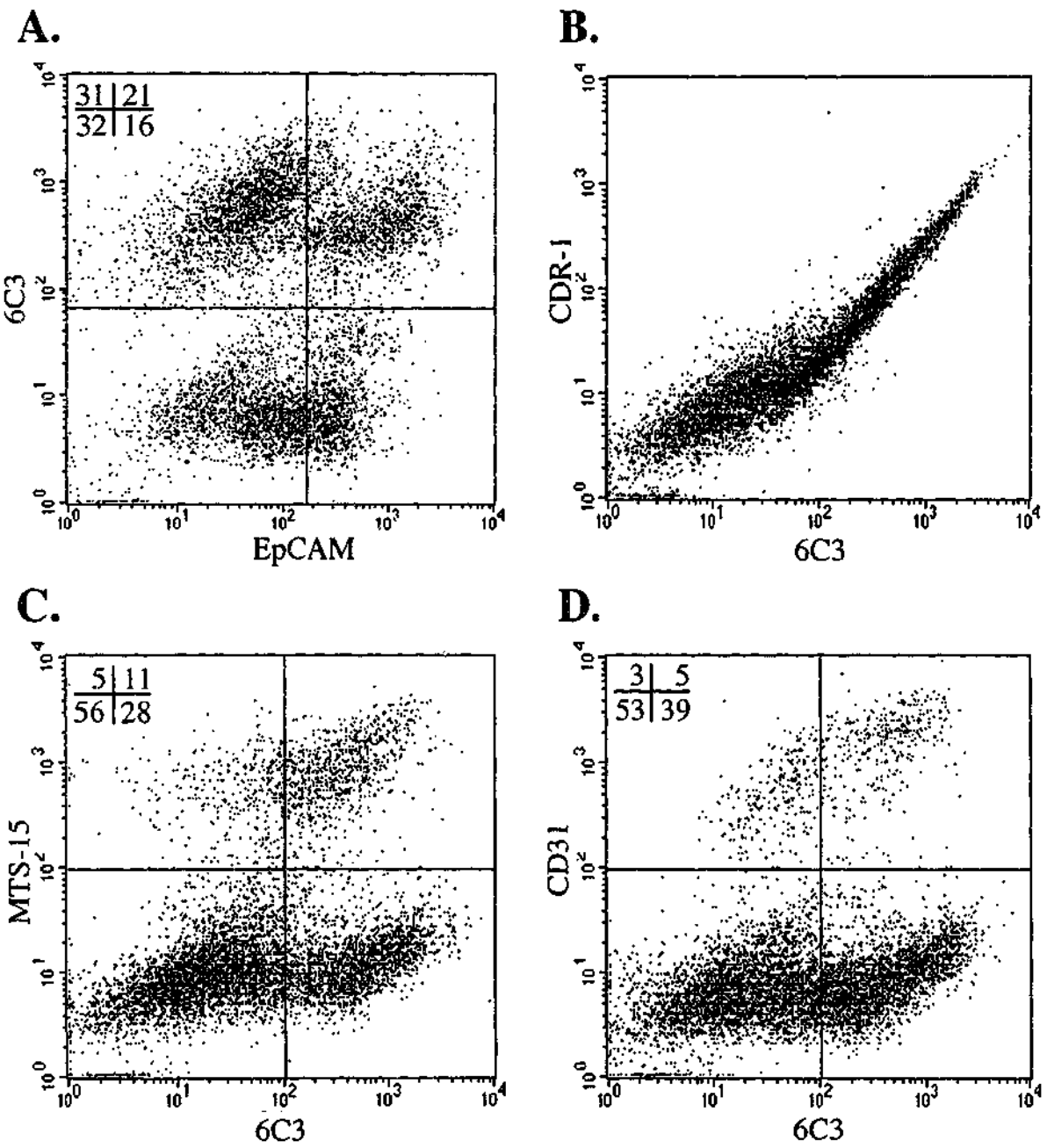

Fig. 6. Cortical epithelial cell markers on neonatal thymic stroma. Representative profiles from three experiments are shown, gated on CD45$^-$ cells. Ly51 is expressed on an EpCAM negative subset of cells, as well as EpCAM-positive cortical epithelial cells (A). CDR-1 and 6C3 (anti-Ly51) bind to the same cells at equivalent levels (B). Most of the EpCAM negative subset of 6C3-positive cells express the fibroblast marker MTS-15 (C) and/or the endothelial marker CD31 (D).

and flow cytometric purification of cortical and medullary epithelial cells using CDR-1 has enabled comparisons of gene expression and antigen processing (Klein et al., 1998; Merkenschlager et al., 1999). Therefore, these markers were used to analyse the surface phenotype of cortical epithelial cells in more detail.

Both CDR-1 and 6C3 label a subset of EpCAM$^+$ cells (Figs. 3A and 6A). However, each also recognizes a determinant expressed by some EpCAM$^-$ cells. The proportion of cortical and medullary epithelial cells tends to be roughly equal at 4 weeks of age. However, it may vary during thymic development (e.g. it appears to favor medullary epithelial cells in neonatal mice).

A direct comparison of the two cortical markers reveals that they label the same cells with similar intensities, suggesting they recognize distinct epitopes of the same molecule or complex (Fig. 6B). The antigen detected by 6C3 has been established as aminopeptidase A (Ly51) (Wu et al., 1990) that is also expressed on subsets of B-cell precursors and thymic dendritic cells (Wu et al., 1995). Studies using Ly51 deficient mice demonstrate that this enzyme is not essential for normal T and B cell development (Lin et al., 1998). By inference, CDR-1 may also recognize this molecule, however further studies will be needed to address this directly.

The non-epithelial reactivity of these two mAbs was further investigated by comparison to MTS-15 and CD31 (Fig. 6C and D), revealing that Ly51 is also expressed on some fibroblasts and endothelial cells.

One of the few reagents specific for a determinant expressed on the surface of medullary epithelial cells that has been reported is the lectin Ulex Europaeus Aglutinin I (UEA-1) (Farr and Anderson, 1985). By immunohistology, it appears to label only a subset of medullary epithelial cells, so its reactivity by flow cytometry was of interest. The profile shown in

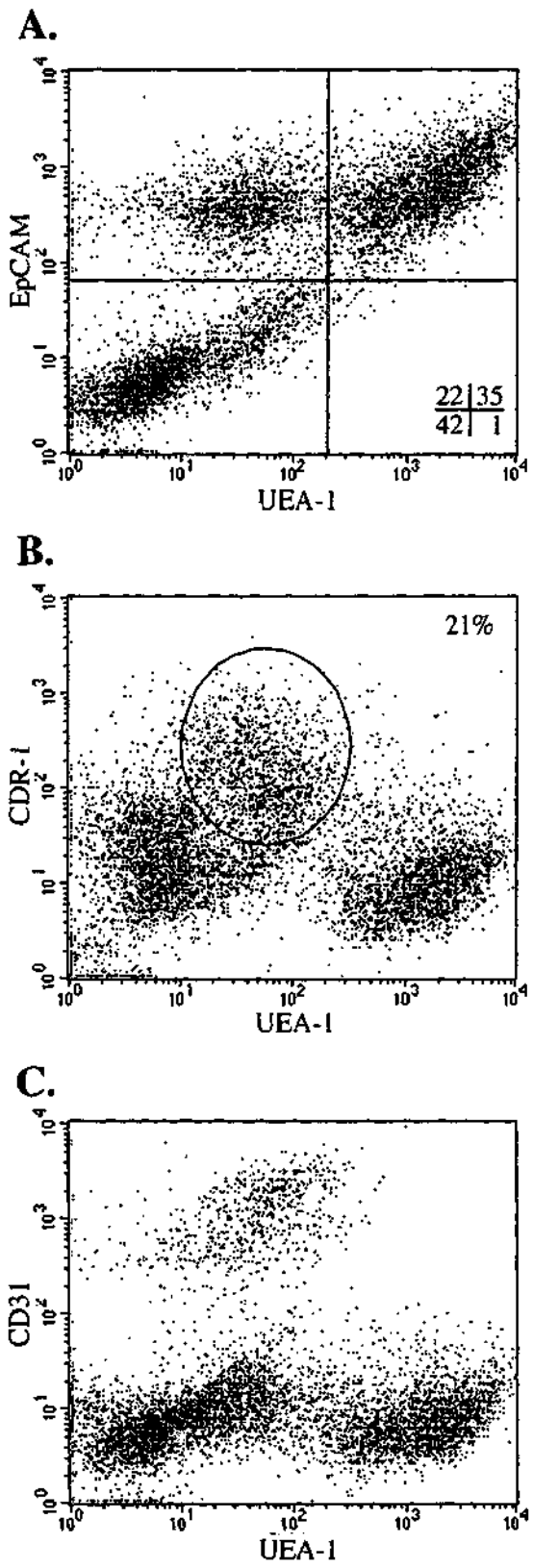

Fig. 7. Medullary epithelial cell markers on the neonatal thymus. All profiles are gated on CD45$^-$ cells. UEA-1 is highly expressed on a subset of EpCAM$^+$ cells (A). The remaining UEA-1 intermediate events coexpress the cortical epithelial cell marker CDR-1 (B). Endothelial cells also express intermediate levels of UEA-1 (C). The remaining CD31$^-$, UEA-1$^-$ events are presumably fibroblasts and neuroendocrine cells. Representative profiles from three experiments are shown.

Table 4
Surface phenotypes of thymic stromal cell subsets

Thymic stromal cell subset	Surface phenotype
Dendritic cells	CD45$^+$, CD11c^{hi}, MHC II^{hi}
Myeloid-derived cells	CD45$^+$, CD11b$^+$, CD11c$^{-/lo}$, MHC II$^{-/+}$
Cortical epithelial cells	CD45$^-$, EpCAM$^+$, MHC II$^+$, CDR-1/Ly51$^+$, UEA – 1^{lo}
Medullary epithelial cells	CD45$^-$, EpCAM$^+$, MHC II$^+$, CDR – 1/Ly51$^-$, UEA – 1^{hi}
Fibroblasts	CD45$^-$, MTS – 15$^+$, EpCAM$^-$, MHC II$^-$
Endothelial cells	CD45$^-$, CD31$^+$, EpCAM$^-$, MHC II$^{-/lo}$, MTS – 15$^{-/+}$

Fig. 7A demonstrates the high expression of UEA-1 found on more than half of the EpCAM$^+$ cells and intermediate expression on the remaining epithelial cells. These UEA-1^{hi} cells are presumably the medullary epithelial cells observed by immunohistology, since only the intermediates colabeled with CDR-1 (Fig. 7B). Endothelial cells were also found to express intermediate levels of UEA-1 (Fig. 7C).

4. Conclusion

This study refines isolation protocols for thymic stromal cells and characterizes the major subsets using a panel of surface reactive mAbs. Collagenase digestion of thymic fragments from 4-week-old and neonatal mice enriched CD45 negative and positive stromal cells appropriate for immunofluorescent labeling and flow cytometry. However, collagenase digestion did not dissociate all CD45$^-$ stromal cells, leaving up to 20% remaining as aggregates. Incubation with trypsin ensures maximal recovery but also cleaves many useful epitopes. The different properties of these enzymes will be an important consideration in the use of stromal cells for phenotypic, genetic and functional analyses.

The various thymic stromal cellular subsets were analysed using a panel of mAbs that had previously been defined using immunohistology. As in the previous study (Izon et al., 1994), a broader distribution of some of these antigens was found, perhaps due to the higher sensitivity of flow cytometry compared to immunohistology. However, the extent of overlap between subsets reported previously was reduced by the exclusion of CD45$^+$ stromal cells from the analysis. Thymic fibroblasts, endothelium, dendritic cells, myeloid cells, cortical and medullary epithelium can be defined into discrete populations using combinations of mAbs to provide quantitative data about the stromal microenvironment (summarized in Table 4). Future studies will focus on phenotypic and functional changes to these populations accompanying different thymic states.

Acknowledgements

The authors wish to thank Dr. A Farr for kindly providing mAbs. This work was supported by grants from the Australian NH&MRC.

References

Anderson, G., Moore, N.C., Owen, J.J., Jenkinson, E.J., 1996. Cellular interactions in thymocyte development. Annu. Rev. Immunol. 14, 73.

Anderson, G., Anderson, K.L., Tchilian, E.Z., Owen, J.J.T., Jenkinson, E.J., 1997. Fibroblast dependency during early thymocyte development maps to the CD25$^+$CD44$^+$ stage and involves interactions with fibroblast matrix molecules. Eur. J. Immunol. 27, 1200.

Benoist, C., Mathis, D., 1989. Positive selection of the T-cell repertoire: where and when does it occur? Cell 58, 1027.

Boyd, R.L., Tucek, C.L., Godfrey, D.I., Izon, D.J., Wilson, T.J., Davidson, N.J., Bean, A.G.D., Ladyman, H.M., Ritter, M.A., Hugo, P., 1993. The thymic microenvironment. Immunol. Today 14, 445.

Chidgey, A.P., Pircher, H., MacDonald, R., Boyd, R.L., 1998. An adult thymic stromal-cell suspension model for in vitro positive selection. Dev. Immunol. 6, 157.

de Maagd, R.A., MacKenzie, W.A., Schuurman, H.J., Ritter, M.A., Price, K.M., Broekhuizen, R., Kater, L., 1985. The human thymic microenvironment: heterogeneity detected by monoclonal anti-epithelial cell antibodies. Immunology 54, 745.

Farr, A.G., Anderson, S.K., 1985. Epithelial heterogeneity in the murine thymus: fucose-specific lectins bind medullary epithelial cells. J. Immunol. 134, 2971.

Godfrey, D.I., Izon, D.J., Wilson, T.J., Tucek, C.L., Boyd, R.L., 1988. Thymic stromal elements defined by mAbs: ontogeny and modulation in vivo by immunosuppression. Adv. Exp. Med. Biol. 237, 269.

Izon, D.J., Nieland, J.D., Godfrey, D.I., Boyd, R.L., Kruisbeek, A.M., 1994. Flow cytometric analysis reveals unexpected shared antigens between histologically defined populations of thymic stromal cells. Int. Immunol. 6, 31.

Jenkinson, E.J., Anderson, G., Owen, J.J.T., 1992. Studies on T cell

maturation on defined thymic stromal cell populations in vitro. J. Exp. Med. 176, 845.

Kampinga, J., Berges, S., Boyd, R.L., Brekelmans, P., Colic, M., van Ewijk, W., Kendall, M.D., Ladyman, H., Nieuwenhuis, P., Ritter, M.A., Schuurman, H.J., Tournefier, A., 1989. Thymic epithelial antibodies: immunohistological analysis and introduction of CTES nomenclature. Thymus 13, 165.

Kishimoto, T.K., Larson, R.S., Corbi, A.L., Dustin, M.L., Staunton, D.E., Springer, T.A., 1989. The leukocyte integrins. Adv. Immunol. 46, 149.

Klein, L., Kyewski, B., 2000. Self-antigen presentation by thymic stromal cells: a subtle division of labor. Curr. Opin. Immunol. 12, 179.

Klein, L., Klein, T., Ruther, U., Kyewski, B., 1998. CD4 cell tolerance to human C-reactive protein, an inducible serum protein, is mediated by medullary thymic epithelium. J. Exp. Med. 188, 5.

Kosugi, A., Saitoh, H., Noda, S., Miyake, K., Yamashita, Y., Kimoto, M., Ogata, M., Hamaoka, T., 1998. Physical and functional association between Thymic Shared Antigen-1/Stem Cell Antigen-2 and the T-cell receptor complex. J. Biol. Chem. 273, 12301.

Lin, Q., Taniuchi, I., Kitamura, D., Wang, J., Kearney, J.F., Watanabe, T., Cooper, M.D., 1998. T and B cell development in BP-1/6C3/Aminopeptidase-A deficient mice. J. Immunol. 160, 4681–4687.

Lobach, D.F., Scearce, R.M., Haynes, B.F., 1985. The human thymic microenvironment. Phenotypic characterization of Hassall's bodies with the use of monoclonal antibodies. J. Immunol. 134, 250.

Merkenschlager, M., Power, M.O., Pircher, H., Fisher, A.G., 1999. Intrathymic deletion of MHC class I-restricted cytotoxic T cell precursors by constitutive cross-presentation of exogenous antigen. Eur. J. Immunol. 29, 1477.

Nelson, A.J., Dunn, R.J., Peach, R., Aruffo, A., Farr, A.G., 1996. The murine homolog of human Ep-CAM, a homotypic adhesion molecule, is expressed by thymocytes and thymic epithelial cells. Eur. J. Immunol. 26, 401.

Pircher, H., Bruduscha, K., Steinhoff, U., Kasai, M., Mizuochi, T., Zinkernagel, R.M., Hengartner, H., Kyewski, B., Muller, K.P., 1993. Tolerance induction by clonal deletion of CD4+CD8+ thymocytes in vitro does not require dedicated antigen-presenting cells. Eur. J. Immunol. 23, 669.

Rouse, R.V., Bolin, L.M., Bender, J.R., Kyewski, B.A., 1988. Monoclonal antibodies reactive with subsets of mouse and humans thymic epithelial cells. J. Histochem. Cytochem. 36, 1511.

Shortman, K., Vremec, K., D'Amico, A., Battye, F., Boyd, R., 1989. Nature of the thymocytes associated with dendritic cells and macrophages in thymic rosettes. Cell. Immunol. 119, 85.

Surh, C.D., Gao, E., Kosaka, H., Lo, D., Ahn, C., Murphy, D.B., Karlsson, L., Peterson, P., Sprent, J., 1992. Two subsets of epithelial cells in the thymic medulla. J. Exp. Med. 176, 495.

Thomas, M.L., 1989. The leukocyte common antigen family. Annu. Rev. Immunol. 7, 339.

van de Wijngaert, F.P., Kendall, M.D., Schuurman, H.J., Rademakers, L.H., Kater, L., 1984. Heterogeneity of epithelial cells in the human thymus. An ultrastructural study. Cell Tissue Res. 237, 227.

van Vliet, E., Melis, M., van Ewijk, W., 1984. Monoclonal antibodies to stromal cell types of the thymus. Eur. J. Immunol. 14, 524.

Vremec, D., Pooley, J., Hochrein, H., Wu, L., Shortman, K., 2000. CD4 and CD8 expression by dendritic cell subtypes in mouse thymus and spleen. J. Immunol. 164, 2978.

Wu, Q., Lahti, J.M., Air, G.M., Burrows, P.D., Cooper, M.D., 1990. Molecular cloning of the murine BP-1/6C3 antigen: a member of the zinc-dependent metallopeptidase family. Proc. Natl. Acad. Sci. U. S. A. 87, 993.

Wu, L., Vremec, D., Ardavin, C., Winkel, K., Suss, G., Georgiou, H., Maraskovsky, E., Cook, W., Shortman, K., 1995. Mouse thymus dendritic cells: kinetics of development and changes in surface markers during maturation. Eur. J. Immunol. 25, 418.

Immunity, Vol. 16, 205–218, February, 2002, Copyright ©2002 by Cell Press

Role for CCR7 Ligands in the Emigration of Newly Generated T Lymphocytes from the Neonatal Thymus

Tomoo Ueno,[1] Kyoko Hara,[1]
Melissa Swope Willis,[2] Mark A. Malin,[3]
Uta E. Höpken,[4] Daniel H.D. Gray,[3]
Kouji Matsushima,[5] Martin Lipp,[4]
Timothy A. Springer,[2] Richard L. Boyd,[3]
Osamu Yoshie,[6] and Yousuke Takahama[1,7]
[1]Division of Experimental Immunology
Institute for Genome Research
The University of Tokushima and
Laboratory of Immune System Development
RIKEN Research Center for Allergy and Immunology
3-18-15 Kuramoto, Tokushima 770-8503
Japan
[2]Center for Blood Research
Harvard Medical School
200 Longwood Avenue
Boston, Massachusetts 02115
[3]Department of Pathology and Immunology
Monash University Medical School
Commercial Road
Prahran 3181, Victoria
Australia
[4]Department of Molecular Tumorgenetics
and Immunogenetics
Max-Delbrueck-Center for Molecular Medicine
Robert-Roessle-Strasse 10
Berlin
Germany
[5]Department of Molecular Preventive Medicine
School of Medicine
The University of Tokyo, 7-3-1 Hongo
Tokyo 113-0033
[6]Department of Microbiology
Kinki University Medical School
Osaka 589-0014
Japan

Summary

Most T lymphocytes are generated within the thymus. It is unclear, however, how newly generated T cells relocate out of the thymus to the circulation. The present study shows that a CC chemokine CCL19 attracts mature T cells out of the fetal thymus organ culture. Another CC chemokine CCL21, which shares CCR7 with CCL19 but has a unique C-terminal extension containing positively charged amino acids, failed to show involvement in thymic emigration. Neonatal appearance of circulating T cells was defective in CCL19-neutralized mice as well as in CCR7-deficient mice but not in CCL21-neutralized mice. In the thymus, CCL19 is predominantly localized in the medulla including endothelial venules. These results indicate a CCL19- and CCR7-dependent pathway of thymic emigration, which represents a major pathway of neonatal T cell export.

[7]Correspondence: takahama@genome.tokushima-u.ac.jp

Introduction

The development of T lymphocytes involves dynamic cellular movement of developing lymphocytes through the thymus. Lymphoid precursor cells that are capable of generating T cells immigrate into the thymus from hematopoietic organs such as fetal liver and bone marrow (Fontaine-Perus et al., 1981; Scollay et al., 1986; Jotereau et al., 1987; Dunon and Imhof, 1993; Wilkinson et al., 1999). Within the thymus, developing thymocytes migrate through the cortex to the medulla (van Ewijk, 1991; Picker and Siegelman, 1999). Newly matured T cells emigrate out of the thymus to peripheral lymphoid tissues (Scollay et al., 1980; Scollay and Godfrey, 1995).

Recent studies have shown that chemokine signals may control T cell migration through the thymus. For example, a CXC chemokine CXCL12 (also called stromal cell-derived factor-1, or SDF-1) predominantly attracts immature $CD4^-CD8^-$ and $CD4^+CD8^+$ thymocytes that express the CXCL12 receptor, CXCR4 (Kim et al., 1998; Suzuki et al., 1998). A CC chemokine CCL25 (thymus-expressed chemokine, or TECK) predominantly attracts $CD4^+CD8^+$ thymocytes by binding the receptor CCR9 (Wurbel et al., 2000; Norment et al., 2000). Another CC chemokine CCL22 (macrophage-derived chemokine, or MDC) selectively attracts transitional thymocytes between the $CD4^+CD8^+$ and $CD4^+CD8^-/CD4^-CD8^+$ single-positive (SP) stages by binding CCR4 (Campbell et al., 1999). Mature $CD4^+CD8^-/CD4^-CD8^+$ SP thymocytes efficiently respond to the CCR7 ligands (Kim et al., 1998; Campbell et al., 1999), CCL19 (also known as ELC, MIP-3β, and Exodus-3) (Yoshida et al., 1997; Rossi et al., 1997; Rossi and Zlotnik, 2000) and CCL21 (also known as 6Ckine, Exodus-2, TCA-4, and secondary lymphoid chemokine, or SLC) (Nagira et al., 1997; Tanabe et al., 1997; Hedrick and Zlotnik, 1997). These results indicate that the responsiveness of developing thymocytes to various chemokines sequentially changes during T cell differentiation. However, it is unclear whether and how these chemokines are involved in physiological movement of developing thymocytes through the thymus.

It is interesting to note that transgenic mice expressing the catalytic subunit of pertussis toxin in thymocytes exhibited accumulation of mature T cells in the thymus and failure of T cells to populate peripheral lymphoid organs (Chaffin and Perlmutter, 1991). These results suggested that a pertussis toxin-sensitive G protein-mediated signal is essential for the emigration of mature T cells from the thymus. Since chemokine signals are mediated through pertussis toxin-sensitive G protein-coupled receptors (Murphy, 1994; Cyster and Goodnow, 1995; Premack and Schall, 1996; Cyster, 1999), it is possible that G protein-mediated chemokine signals may be required for thymocyte emigration.

The present study has examined the role of chemokines in the emigration of newly matured T cells out of the thymus. To do so, we have devised a novel technique in which fetal thymus organ culture (FTOC) can be time-lapse visualized under a microscope. We find that, among various chemokines, CCL19 attracts mature

T cells out of the FTOC. In contrast, CCL21, which shares CCR7 with CCL19 (Cyster, 1999; Birkenbach et al., 1993; Yoshida et al., 1998), failed to promote thymocyte emigration. Importantly, either targeted disruption of CCR7 gene or antibody neutralization of CCL19, but not neutralization of CCL21, caused a significant decrease of peripheral circulating T cells in newborn mice, while these mice exhibited an elevation in thymocyte numbers, suggesting that CCR7 and its ligand CCL19, rather than CCL21, are essential for neonatal emigration of most T cells from the thymus in vivo. Confocal immunofluorescence analysis, in situ hybridization analysis, and mRNA analysis of isolated thymic stromal cells indicated that CCL19 is present at higher levels in the medulla than in the cortex, and that most endothelial venules in the medulla are positive for CCL19, suggesting that CCL19 in the medulla attracts mature T cells generated within the thymus, guiding thymic emigration through the venules. These results show that CCL19, rather than CCL21, plays a major role in the emigration of mature thymocytes in newborn mice.

Results

CCL19 Promotes the Emigration of Mature T Cells from Fetal Thymus Organ Cultures

To analyze the role of chemokines in influencing T cell migration through the thymus, we initially tested the effects of adding various chemokines into fetal thymus organ cultures. Among the chemokines tested, we found that addition of the CC chemokine CCL19 (also known as ELC, MIP-3β, and Exodus-3) significantly increased the number of cells found outside of the thymus lobes in the culture medium (Figure 1A). In addition to the chemokines listed in Figure 1A, CCL1, CCL2, CCL3, CCL4, CCL8, CCL11, CCL20, CCL27, XCL1, and CX3CL1 failed to increase the cell number outside of the lobes (data not shown). The extrathymic cells in CCL19-treated cultures were mostly $CD4^+CD8^-$ or $CD4^-CD8^+$ single-positive (SP) TCR-β^{high} mature T cells (Figure 1B), indicating that the cell increase was not due to nonspecific leakage of thymocytes. Most extrathymic T cells were small and $CD25^-CD69^-$, with increased expression of Ly-6A and decreased ability to incorporate bromodeoxyuridine (Figure 1C), therefore resembling physiological, noncycling recent thymic emigrants (Tough and Sprent, 1994; Berzins et al., 1998) rather than extensively proliferating T cells derived from small numbers of artifactually released thymocytes. Thus, the CCL19-induced increase of T cells outside of FTOC lobes was likely due to selective emigration of mature T cells from the thymus.

To directly examine whether CCL19 induces the emigration of mature T cells out of the thymus, we devised a time-lapse FTOC visualization system in which cell movement was directly monitored under the microscope and recorded using a digital CCD camera (Figure 1D). To perform FTOC in transparent culture condition, thymus lobes were submerged in culture medium and maintained in 75% O_2 and 5% CO_2. Thymus cultures were placed in a collagen gel to minimize liquid swirling during culture. An aliquot of CCL19 was spotted into the gel, and the cultures were monitored under the microscope by time-lapse digital recording for 1 day (Figure 1D). As shown in Figure 1E and attached Supplemental Movies (S1 [http://www.immunity.com/cgi/content/full/16/2/205/DC1] versus S2 [http://www.immunity.com/cgi/content/full/16/2/205/DC1] and S3 [http://www.immunity.com/cgi/content/full/16/2/205/DC1]), many cells in the thymus were attracted toward the spot of CCL19 within 1 day in culture. The thymus emigrants in this culture condition were mostly mature T cells (data not shown). Emigrating cells moved specifically toward the CCL19 spot, since no cell migration was observed toward the opposite side of the thymus (Figure 1E; Supplemental Movie S4 at http://www.immunity.com/cgi/content/full/16/2/205/DC1). These results directly indicate that CCL19 attracts mature T cells out of the fetal thymus organ culture.

CCL21 Fails to Mediate the Emigration of Mature T Cells out of the Thymus Culture

Both CCL19 and its CC chemokine family member CCL21 (also known as SLC, 6Ckine, TCA-4, and Exodus-2) interact with the cellular receptor CCR7 (Yoshida et al., 1997, 1998). Unlike CCL19, however, CCL21 failed to mediate the emigration of mature T cells out of the thymus lobes (Figures 1A and 1E; Supplemental Movie S5 at http://www.immunity.com/cgi/content/full/16/2/205/DC1). Titration of CCL19 and CCL21 confirmed that CCL21 is markedly less effective than CCL19 in attracting T cells from the thymus culture (Figure 2A). The selective activity of CCL19 in attracting T cells out of the thymus was also observed in the thymus culture without a collagen-sponge or collagen-gel (data not shown), ruling out the possibility that the selective inefficiency of CCL21 might be due to its adherence to collagen in culture. Thus, the selective emigration-stimulating activity by CCL19 could have been caused by (1) a CCL19-specific signaling pathway that fails to transduce CCL21-derived signals in thymic T cells, and/or (2) a CCL19-specific accessibility to T cells in the fetal thymus lobes. RT-PCR analysis indicated that CCL19-induced thymus emigrants expressed CCR7 (Figure 2B). We also found that CCL19 and CCL21 equivalently induced the chemotaxis of mature SP thymocytes in suspension cultures (Figure 2A). Thus, the failure of CCL21 to attract T cells out of the thymus is apparently not due to a lack of CCR7 or other signaling molecules that transmit CCL21-induced chemotaxis in newly generated T cells. On the other hand, unlike CCL19, CCL21 contains a unique C-terminal extension of amino acids with two cysteine residues and a net positive charge (Nagira et al., 1997; Tanabe et al., 1997; Hedrick and Zlotnik, 1997) (Figure 2C), so that CCL21 may better adhere to negatively charged extracellular matrix components such as heparin-like glycosaminoglycans, rendering CCL21 incapable of entering the thymus organ. Indeed, CCL21 but not CCL19 efficiently bound to heparin, while truncation of the C-terminal extension from CCL21 markedly reduced the heparin binding activity (Figure 2C). The truncated CCL21 considerably gained the ability to attract T cell emigrants out of the thymus (Figure 2D; Supplemental Movie S6 [http://www.immunity.com/cgi/content/full/16/2/205/DC1] versus S7 [http://www.immunity.com/cgi/content/full/16/2/205/DC1]), even

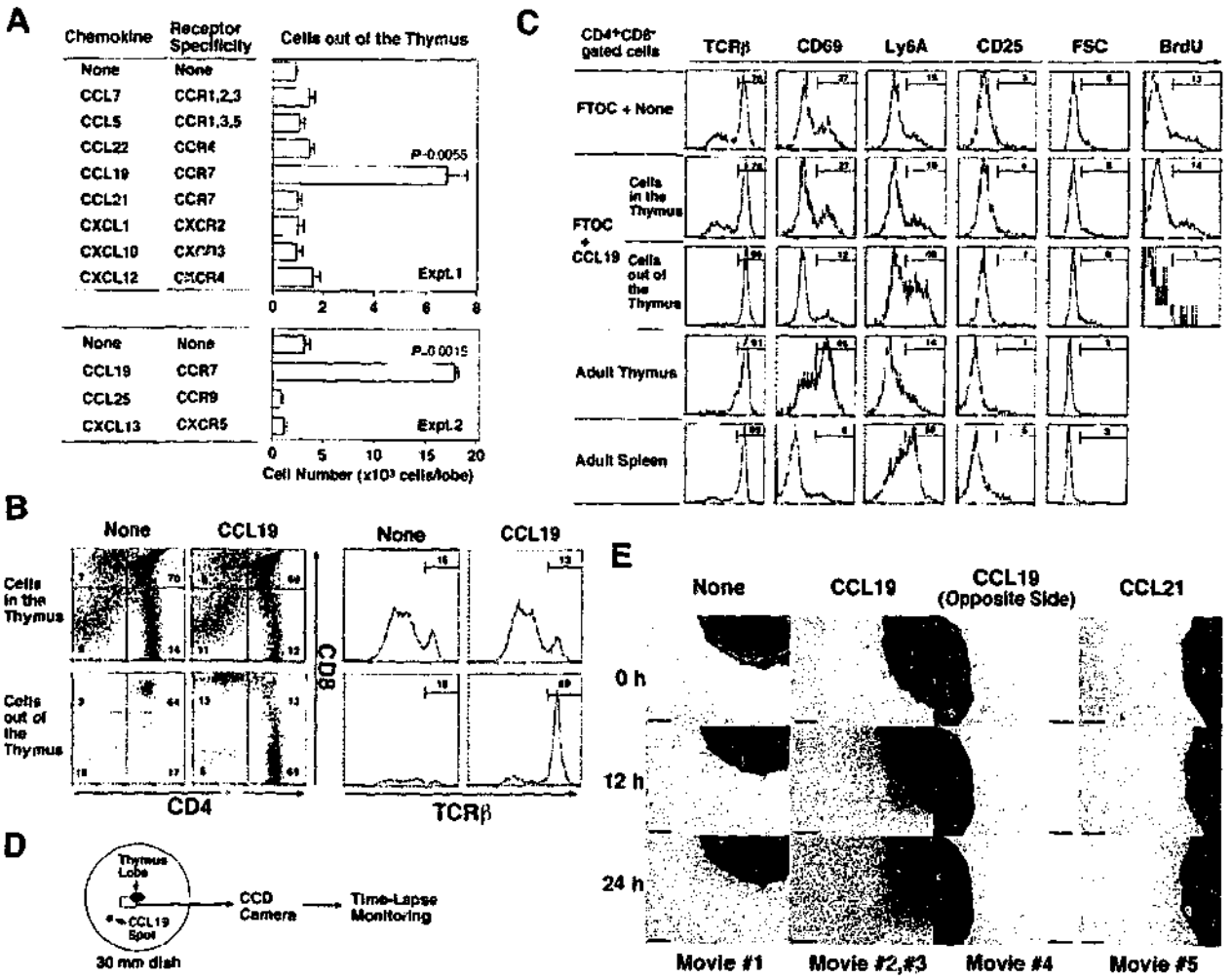

Figure 1. CCL19 Promotes the Emigration of T Cells out of Thymus Lobes

(A) Numbers of cells outside of thymus lobes in culture media supplemented with various chemokines. Mouse fetal thymus lobes were precultured for 5 to 10 days, so that the thymus organs contained thymocytes in a broad range of developmental stages, resembling the distribution of mature adult thymus. FTOC thymus lobes were washed and cultured for an additional 2 days in the absence or presence of indicated chemokines at 100 nM. Listed are means and standard errors (n = 4–9) of viable cell numbers found outside of the thymus lobes 2 days after adding chemokines. Significance (P-value) of the cell numbers over the culture condition in the absence of chemokines was evaluated by Student's t test using StatView software (SAS Institute Inc., Cary, NC).

(B) Flow cytometric analysis of cells in FTOC cultures in the absence or presence of CCL19. Cells were 3-color stained for CD4, CD8, and TCR-β. Numbers within each area indicate the frequency of cells within that area.

(C) Flow cytometric analysis of $CD4^+CD8^-$ cells in the FTOC cultures containing CCL19. Cells were 3-color stained for CD4, CD8, and indicated molecules. Surface levels of indicated molecules and forward light scatter (FSC) intensity, which estimates cell size, were measured for the $CD4^+CD8^-$ gated cells. FTOC cells were also assessed for DNA synthesis during the last 4 hr of culture by intracellular staining of bromodeoxyuridine (BrdU) incorporation.

(D) A diagram of the time-lapse FTOC visualization system employed to monitor cellular movement out of the thymus. An FTOC lobe was placed in a transparent collagen gel and cultured in medium under high oxygen conditions. Either 10 μM CCL19 or 10 μM CCL21 (5 μl) was spotted into a collagen gel approximately 10 mm outside of the thymus lobe. The culture within the rectangular box was time-lapse monitored under the microscope with a CCD camera for 24 hr.

(E) FTOC visualized at indicated time points after spotting CCL19 or CCL21. Where indicated, the thymus lobe was monitored on the opposite side of the CCL19 spot, indicating that cell emigration was directed toward the CCL19 spot. Bar, 250 μm. Animated versions of the pictures are shown as QuickTime files (Supplemental Movies S1–S5 at http://www.immunity.com/cgi/content/full/16/2/205/DC1). Representative results of ≥10 (B), 2–3 (C), and ≥4 (E) independent experiments are shown.

though truncated CCL21 in suspension culture exhibited a slightly decreased chemotactic activity (Figure 2D). Moreover, binding assay of ^{125}I-labeled proteins directly showed that CCL19 exhibited better access to T cells in the intact thymus organ rather than CCL21 (Figure 2E). These results suggest that the inefficient activity of CCL21 to attract T cells from the thymus is at least in part due to the limited ability of CCL21 to diffuse into the organ. Thus, unlike CCL19, CCL21 is inefficient in stimulating thymic emigration in fetal thymus organ culture.

Defective Thymic Emigration in CCR7-Deficient Newborn Mice

We then wished to examine the in vivo roles for CCL19 and CCL21 in thymic emigration. In newborn mice, thy-

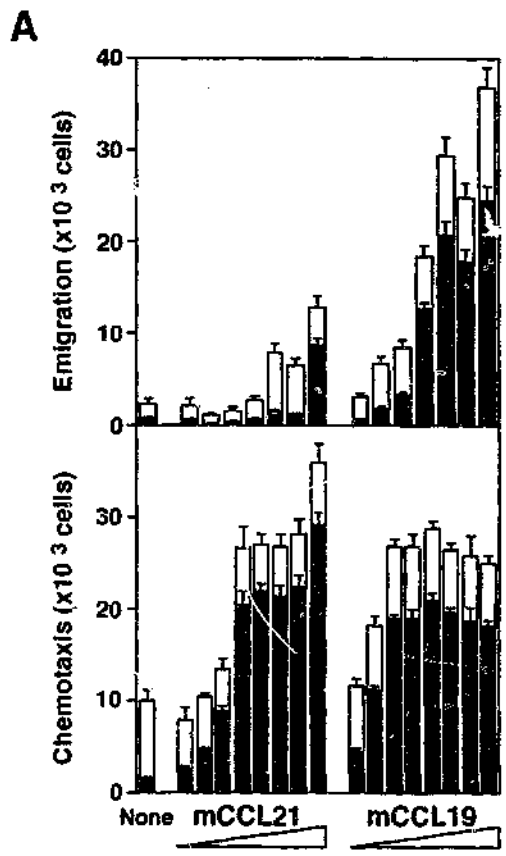

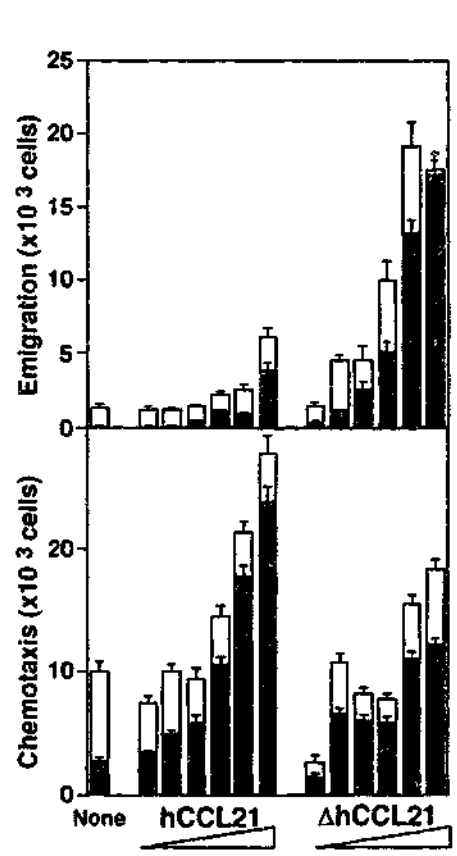

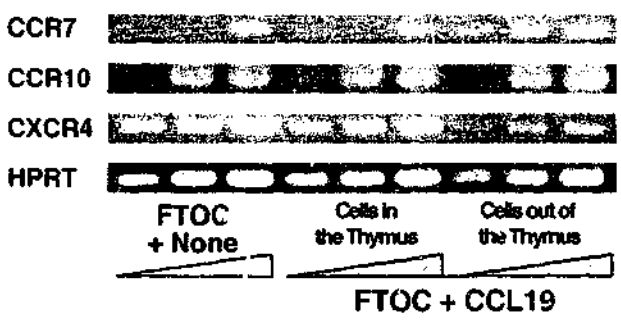

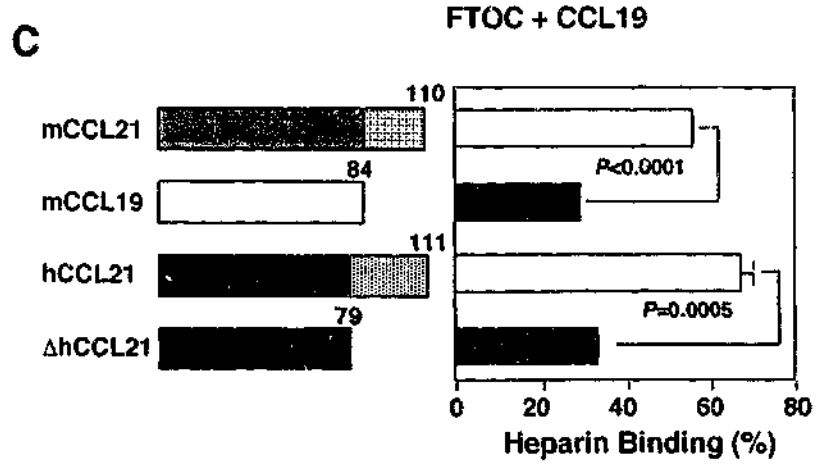

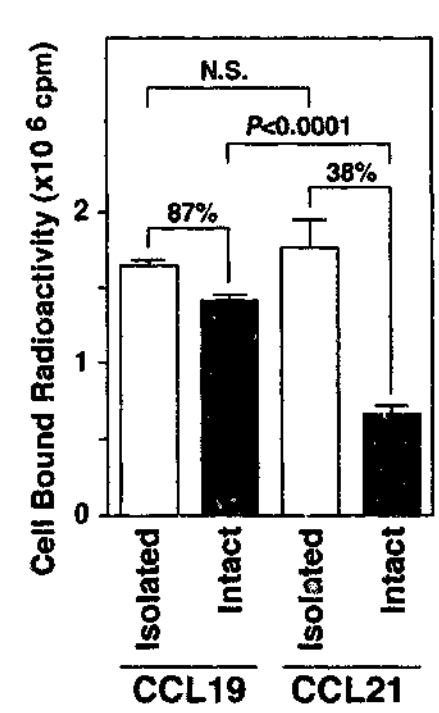

Figure 2. The Role of CCL19 and CCL21 in the Thymic Emigration and T Cell Chemotaxis In Vitro

(A) CCL19 and CCL21 were examined for their ability to attract mature thymocytes out of thymus lobe (upper panel) (as in Figure 1) and for their chemotaxis activity to attract mature thymocytes in suspension culture (lower panel). Two-fold serial dilutions (in the range of 1.56 nM to 200 nM) of recombinant mouse CCL21 and CCL19 proteins (R&D Systems) were examined. Means and standard errors (n = 4–8) of viable cell numbers of total migrated cells (total height of the bars) and TCR-β^{high} mature T cells (filled bars) are indicated.

(B) Reverse transcriptase-PCR analysis for mRNA levels of CCR7 in CCL19-reactive thymus emigrants. Serial dilutions of cDNA from indicated

mic emigrants of mature T cells begin to populate peripheral lymphoid organs including the spleen (Figure 3A). Neonatal supply of spleen T cells detected by 5 days old is completely absent in *nu/nu* mice lacking the thymus (Figure 3A), suggesting that neonatal T cells in the spleen are derived from the thymus, representing recent thymic emigrants. Interestingly, we found that newborn T cells in the spleen of CCR7-deficient mice (Förster et al., 1999) were markedly lower in number than those of wild-type mice (Figure 3A). T cell number in CCR7-deficient mice was lower not only in the white pulp area but also in the red pulp area of the spleen (Figures 3B and 3C), into which lymphocytes enter along the blood flow without active migration through pertussis-toxin-sensitive chemokine signals (Cyster and Goodnow, 1995), suggesting that T cell number in open blood circulation is lower in CCR7-deficient neonates than wild-type neonates. On the other hand, thymocytes in neonatal CCR7-deficient mice were slightly but significantly higher in number than those in age-matched wild-type mice (Figure 3A). These results suggest that the neonatal supply of T cells from the thymus to the circulation is greatly reduced in CCR7-deficient mice, and that CCR7 is essential for neonatal emigration of most T cells from the thymus.

It should be noted that, in the absence of CCR7, a small number of T cells were found in newborn spleen (Figure 3A) and T cell number in adult spleen was even higher in CCR7-knockout mice than in control mice (Figure 3D), suggesting that thymic emigration can occur independently of CCR7 as a minor pathway during the neonatal period. It is possible that the CCR7-independent thymic emigration becomes a major pathway in adult mice, or that a small number of CCR7-independent thymic emigrants expands during postnatal period to saturate the peripheral tissues in adult mice.

CCL19 Neutralization Impairs Thymic Emigration of Neonatal T Cells In Vivo

To further examine the role of CCL19 and CCL21 in thymic emigration in vivo, normal newborn mice were injected daily with either anti-CCL19 or anti-CCL21 neutralizing antibodies, which specifically blocked the chemotaxis of thymocytes toward CCL19 and CCL21, respectively (Figure 4A). We found that administration of anti-CCL19 neutralizing antibody significantly inhibited the supply of spleen T cells as well as circulating peripheral blood T cells (Figures 4B–4D). At 3 days old, the number of thymocytes in anti-CCL19-treated mice was slightly but significantly higher than in the control antibody-treated mice (Figure 4B). On the other hand, the injection of anti-CCL21 neutralizing antibody did not significantly affect the numbers of spleen T cells or thymocytes in neonatal mice (Figures 4B–4D). Anti-CCL21 antibody, however, significantly inhibited the supply of T cells to lymph nodes (Figure 4D) as expected from previous studies (Gunn et al., 1998; Stein et al., 2000), suggesting that the injected anti-CCL21 antibody maintained its in vivo neutralizing activity to CCL21, inhibiting T cell migration to lymph nodes. These results suggest that in vivo neutralization of CCL19, but not CCL21, impaired thymic emigration of T cells to peripheral circulation. Thus, our results suggest that CCL19 rather than CCL21 plays a major role in neonatal emigration of mature T cells out of the thymus in vivo.

Although it was possible that mature single-positive thymocytes might accumulate in either CCR7-deficient or CCL19-neutralized mice, we have so far detected no difference in expression profiles of CD4, CD8, and TCR in neonatal thymocytes among normal, CCR7-deficient, and CCL19-neutralized mice (data not shown).

Expression of CCL19 in the Mouse Thymus

Finally, we have examined the localization of CCL19 within the thymus by immunofluorescence analysis. In secondary lymphoid organs, CCL19 is mainly produced by dendritic cells as well as T zone stromal cells (Ngo et al., 1998; Luther et al., 2000). Consistent with previous reports (Annunziato et al., 2000), CCL19 in the adult thymus was predominantly detected in the MTS10$^+$ medulla rather than in the CDR1$^+$ cortex (Figures 5A–5F). In the medulla, CCL19 was localized to MTS10$^+$ epithelial cells, CD11c$^+$ dendritic cells, as well as CD31$^+$ endothelial venular cells (Figures 5D–5L). Importantly, most CD31$^+$ venules in the medulla were positive for CCL19 (Figures 5J–5O). Also in the newborn thymus, CCL19 immunofluorescence signals were predominantly detected within the G8.8^{high} medullary area (Figures 6A–6C),

---

cells were PCR-amplified for CCR7, CCR10, and CXCR4. The thymic emigrants expressed CCR7 at levels higher than the cells that remained in the thymus, whereas the expression of CXCR4 was lower in the emigrants than in the thymocytes. Housekeeping HPRT levels and other chemokine receptor CCR10 levels were approximately equivalent among the cells. Representative results of ≥2 independent experiments are shown.

(C) Heparin binding abilities of mouse CCL21 (mCCL21), mouse CCL19 (mCCL19), human CCL21 (hCCL21), and a truncated mutant form of hCCL21 (ΔhCCL21). Numbers above the schematic representation of the chemokines indicate amino acid numbers of indicated proteins. Dotted regions of CCL21 indicate the C-terminal extension with a net positive charge. An equal amount of ^{125}I-labeled proteins was incubated with either heparin-agarose gel or control agarose gel, and the gel-bound radioactivity was measured. Means and standard errors (n = 4) of radioactivity specifically bound to heparin are shown.

(D) Recombinant hCCL21 and ΔhCCL21 were examined for their ability in the thymic emigration assay (upper panel) and for the chemotaxis assay in suspension culture (lower panel) as in (A). Two-fold serial dilutions of proteins were made in the range of 100 nM to 3200 nM for the thymic emigration assay and 12.5 nM to 400 nM for the chemotaxis assay. Means and standard errors (n = 4–8) of viable cell numbers are indicated. Animated versions of the pictures can be found as supplementary results (Supplemental Movie S6 [at http://www.immunity.com/cgi/content/full/16/2/205/DC1] for hCCL21 and Supplemental Movie S7 [at http://www.immunity.com/cgi/content/full/16/2/205/DC1] for ΔhCCL21).

(E) Equal amount of ^{125}I-labeled CCL19 or CCL21 was incubated with either an intact FTOC lobe or isolated thymocytes from an FTOC lobe. Thymocytes were isolated, washed, and measured for the bound radioactivity. Means and standard errors (n = 3–5) of radioactivity per thymocytes in one FTOC lobe are indicated

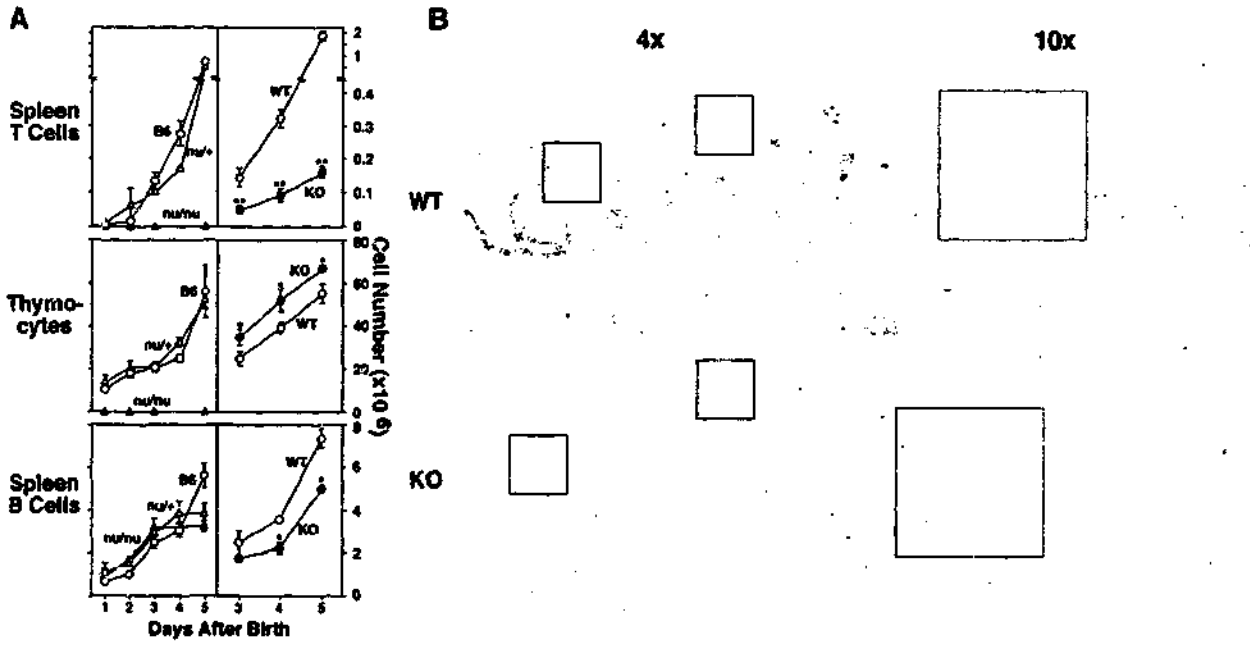

Figure 3. Defective Supply of Peripheral T Cells in CCR7-Deficient Newborn Mice In Vivo

(A) Ontogeny of spleen T cells and B cells in newborn mice at indicated age of days after birth. T and B cells in the spleen were identified as TCR-β$^+$CD3$^+$ and B220$^+$CD3$^-$ cells, respectively, using flow cytometry. Numbers of total thymocytes are also shown. Results from normal mice (B6, open circles; BALB/c-*nu*/+ mice, open triangles) and thymus-deficient *nu/nu* mice (BALB/c-*nu/nu*, closed triangles) show that spleen T cells during the neonatal period are virtually all thymus-derived (left panels). Numbers of spleen T cells and thymocytes in CCR7-deficient (KO, closed circles) and wild-type mice (WT, open circles) show that numbers of spleen T cells and thymocytes are significantly (*$P < 0.05$; **$P \leq 0.005$) lower and higher in CCR7-deficient mice than in wild-type mice, respectively (right panels).

(B and C) Immunohistochemical analysis of 5-day-old spleens from CCR7-deficient and wild-type mice. Representative sections stained for T cells (Thy-1.2) are shown. Boxes indicate 0.25 mm^2 red pulp areas identified by the Thy-1 and B220 staining profiles of serial sections. Indicated in (C) are means and standard errors of T cell numbers in the red pulp area (n = 10) and of the numbers of white pulp areas (n = 5) per 1 mm^2 of the section. In addition to the loss of T cell areas in the white pulp, the number of T cells in the red pulp area was significantly lower in CCR7-deficient mice than wild-type mice.

(D) Distribution of lymphocytes in adult CCR7-KO and WT mice (9 weeks old). Shown are means and standard errors (n = 3–8 in [A], n = 4–8 in [D]) of viable cell numbers in the spleen, thymus, and inguinal lymph nodes.

and were found in most CD31$^+$ endothelial venular cells but not in MTS15$^+$ fibroblasts (Figures 6D–6F). In situ hybridization analysis of newborn thymus also showed that CCL19 transcripts were weakly detected within the medullary area (Figures 7A–7C), as has been reported (Bleul and Boehm, 2000). Further analysis involved isolation of thymic stromal cell subsets for RT-PCR analysis of CCL19 mRNA expression. As shown in Figure 7E, CCL19 mRNA in the thymus was most highly detected in medullary epithelial cells, rather than endothelial cells, dendritic cells, cortical epithelial cells, or thymocytes. CCL21 mRNA was also mainly expressed by medullary epithelial cells among the four kinds of sorted cell populations. Given the strong signals of CCL21 mRNA in total thymic stromal samples, however, cells other than these four populations might also express CCL21 mRNA. Together, these results indicate that CCL19 in the thymus is predominantly produced by medullary epithelial cells and localized to epithelial cells, dendritic cells, and endothelial cells within the medulla. It is interesting to note that, in double immunofluorescence analysis (Figures 6G–6I), in situ hybridization analysis (Figures 7C and 7D), or RT-PCR analysis (Figure 7E), CCL21 signals were detected in an overlapping population of cells with CCL19 signals but detected in a broader population of cells than CCL19 signals, suggesting that CCL19 and CCL21 may play different, though possibly overlapping, roles in the thymus. These results are consistent with

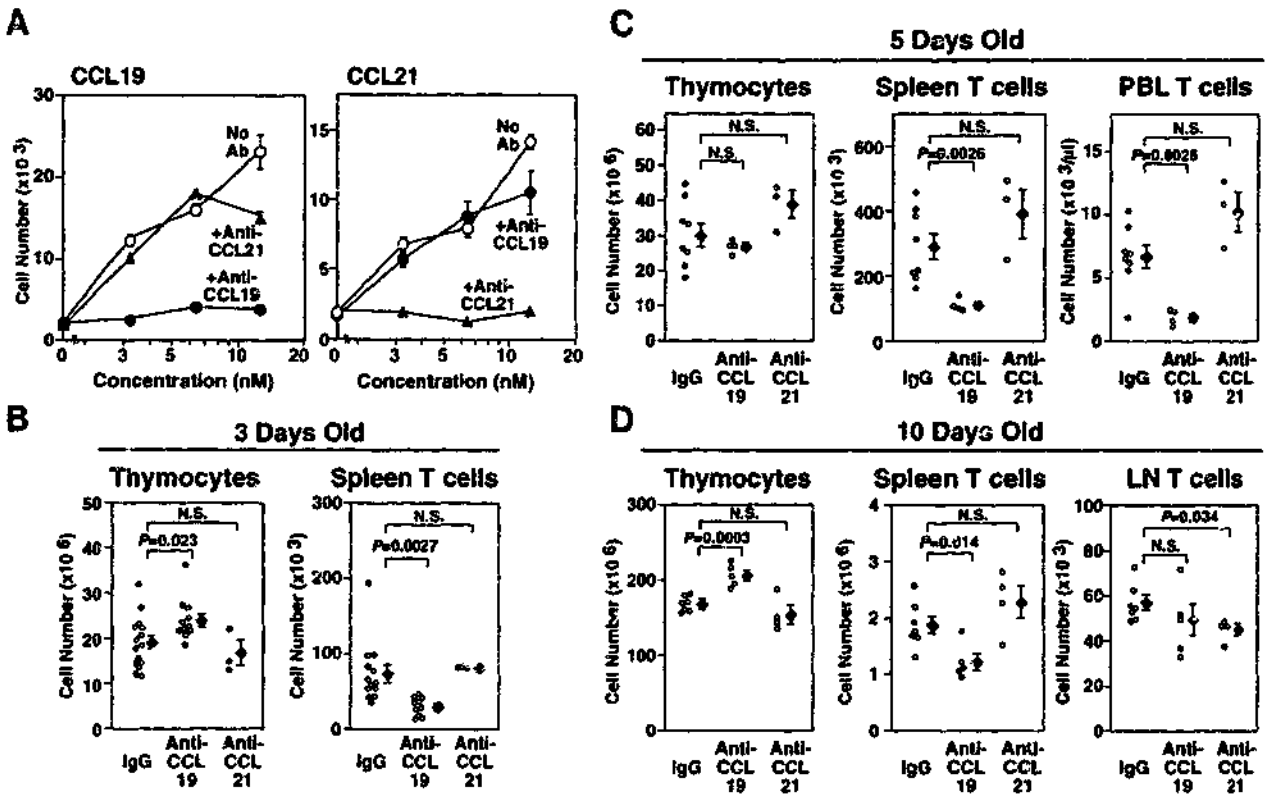

Figure 4. The Effects of Anti-CCL19 and Anti-CCL21 on the Peripheral T Cell Supply in Newborn Mice In Vivo

(A) The specificity of anti-CCL19 and anti-CCL21 neutralizing antibody. Anti-CCL19 or anti-CCL21 goat IgG antibody (10 μg/ml) was added to the chemotaxis assay of thymocytes for CCL19 (left panel) and CCL21 (right panel) in suspension cultures.

(B–D) The effects of in vivo injection of anti-CCL19 antibody or anti-CCL21 antibody in normal newborn mice. Goat antibodies were injected daily, and indicated cells were analyzed on 3 days old (B), 5 days old (C), and 10 days old (D). Independent preparation of rabbit anti-CCL21 antibody similarly affected to the goat anti-CCL21 antibody, in which the numbers of thymocytes and spleen T cells were not affected on day 3, 5, or 10 but the number of lymph node T cells examined on day 10 was reduced (data not shown). Means and standard errors (n = 4 in [A]) of viable cell numbers are indicated. In (B)–(D), open circles represent cell numbers of individual mice examined (n = 3–15).

the possibility that CCL19 in the medulla attracts mature T cells generated within the thymus, guiding thymic emigration through endothelial venules in the medulla.

Discussion

Thymic emigration of newly generated T cells is an essential process for seeding circulating T cells. The present study examined the role of chemokines in the emigration of T cells from the thymus, utilizing a modified fetal thymus organ culture to directly visualize and evaluate the thymocyte emigration. We have found that, among various chemokines tested, only one chemokine, CCL19, attracted mature T cells out of fetal thymus organ cultures. The CCL19-attracted T cells phenotypically resembled recent thymic emigrants. Interestingly, CCL21, which shares a common receptor CCR7 with CCL19, failed to cause thymocyte emigration. Using truncated CCL21, we have found that the failure of CCL21 to mediate thymocyte emigration was at least in part due to its unique C-terminal extension containing positively charged amino acids. By this C-terminal extension, CCL21 efficiently adheres to negatively charged extracellular matrix components such as heparin-like glycosaminoglycans, thereby being inefficient in accessing T cells in the thymus organ. The selective role for CCL19, rather than CCL21, in attracting T cells out of the thymus was further supported by in vivo experiments in which antibody-mediated neutralization of CCL19 but not CCL21 in newborn mice impaired thymic emigration of T cells to the peripheral circulation. In CCL19-neutralized mice and CCR7-deficient mice, but not in CCL21-neutralized mice, circulating T cells were reduced and thymocytes accumulated in the neonates. Our results indicate that CCL19, rather than CCL21, plays a major role in the emigration of mature T cells out of the thymus in newborn mice.

Analysis of CCL19 distribution in adult and newborn mice showed that CCL19 in the thymus is predominantly localized within the medulla. Consistent with a previous report (Bleul and Boehm, 2000), our results show that CCL19 mRNA in the thymus was primarily detected in medullary epithelial cells rather than other stromal cells, including dendritic cells, endothelial cells, and cortical epithelial cells. In the medullary area, however, CCL19 protein was localized to dendritic cells and endothelial cells as well as epithelial cells. Since CCL19 mRNA levels were low in dendritic cells and endothelial cells, it is possible that a fraction of CCL19 localized on these cells may be derived from nearby medullary epithelial cells, a possibility consistent with a recent finding that CCL19 generated in the perivascular stroma is translo-

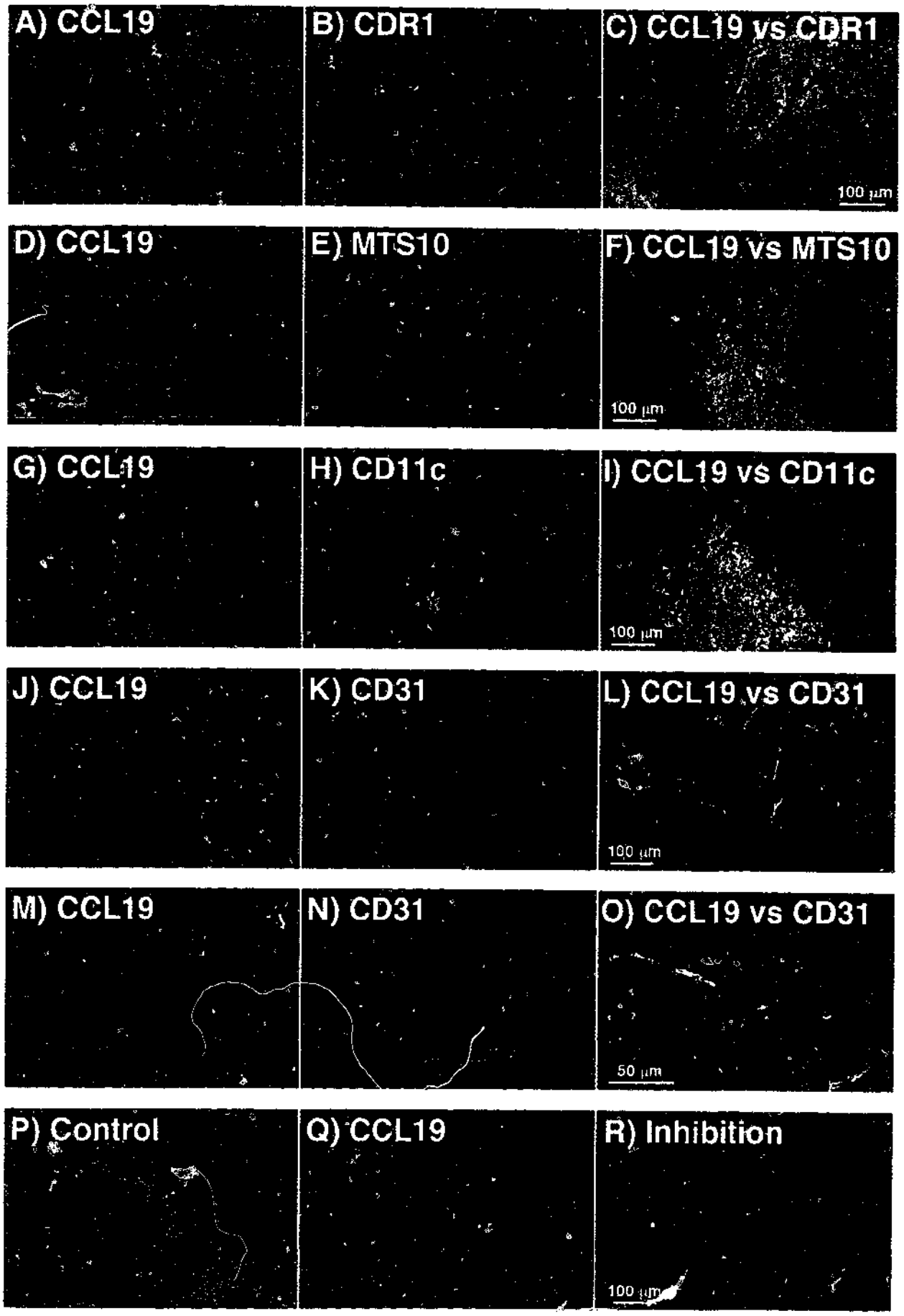
A) CCL19
B) CDR1
C) CCL19 vs CDR1
100 µm
D) CCL19
E) MTS10
F) CCL19 vs MTS10
100 µm
G) CCL19
H) CD11c
I) CCL19 vs CD11c
100 µm
J) CCL19
K) CD31
L) CCL19 vs CD31
100 µm
M) CCL19
N) CD31
O) CCL19 vs CD31
50 µm
P) Control
Q) CCL19
R) Inhibition
100 µm

cated to the high endothelial venules of the secondary lymphoid tissues (Baekkevold et al., 2001). It is further possible that a fraction of CCL19 localized in the thymus may be derived from remote organs, i.e., parathymic lymph nodes, since the thymus organ is highly accessible to CCL19 (Figures 2A and 2E). Nonetheless, it is important to note that CCL19 was found on most endothelial venules in the medulla. A recent report on the analysis of human thymus sections also showed that CCL19 immunoreactivity in the thymus, which was primarily localized to medullary epithelial cells, was often found in cells surrounding medullary vessels (Annunziato et al., 2000). Thus, it is possible that CCL19 may direct mature thymocytes not only to the medullary area but also to endothelial venules within the medulla, through which mature thymocytes may emigrate to the blood circulation. Further mechanisms of thymic emigration, including the mechanism of possible T cell relocation from the tissue side to the lumen side of the vessels, are still unclear.

Our results suggest that, unlike CCL19, CCL21 fails to show a role in thymic emigration. However, like CCL19, CCL21 in the thymus was localized predominantly in the medulla, as has been previously described (Tanabe et al., 1997; Bleul and Boehm, 2000). Our results further show that CCL21 in the thymus is localized in an area that overlaps with CCL19 but is localized in a broader area than CCL19, suggesting that CCL21 in the thymus may play a role that is similar to but is different from CCL19 that is involved in thymic emigration. It is possible that CCL21 may be involved in attracting maturing thymocytes from the cortex to the medulla and that CCL19 may also be involved in this process.

The present results using CCR7-deficient mice clearly document a major involvement of CCR7 in the neonatal seeding of the peripheral T cell pool in vivo. In CCR7-deficient newborn mice, the number of peripheral T cells including the open circulating red pulp T cells was significantly reduced, whereas the number of thymocytes was significantly increased. Antibody-mediated neutralization of CCL19, but not CCL21, caused essentially the same effect on T cell distribution in normal newborn mice, i.e., increased in thymocytes and reduced in peripheral T cells including blood circulating T cells. These results strongly suggest that the chemokine signal through CCR7, most likely mediated by CCL19, plays a key role in the emigration of T cells from the thymus in newborn mice. The greater effect of CCR7 deficiency than the anti-CCL19 treatment in newborn mice could be due to incomplete neutralization of CCL19-CCR7 interaction by the antibody injection, and/or the involvement of unidentified ligands for CCR7 other than CCL19 or CCL21. Importantly, our data along with previous results (Förster et al., 1999) indicate that the number of circulating T cells in adult CCR7-deficient mice is not reduced. Thus, it is logical to assume that thymic emigration can occur via a CCR7-independent pathway in addition to the CCR7-dependent pathway. It is not clear whether the CCR7-independent thymic emigration may represent a major pathway in adult mice, or whether a small number of CCR7-independent neonatal thymic emigrants (as seen in Figure 3) may subsequently expand to saturate the peripheral tissues in adult mice. However, it has been recently shown that there is a continuous supply of thymic emigrants in adult mice (Berzins et al., 1998, 1999) and in adult humans (Douek et al., 1998; Poulin et al., 1999), and that these recent thymic emigrants in adult are involved in maintaining a peripheral pool of T cells with a diverse repertoire (Berzins et al., 1998; Poulin et al., 1999). It is possible that thymic emigration in adult may largely occur via a CCR7-independent pathway, unlike neonatal thymic emigration that is largely CCR7 dependent. It has been also reported in sheep (Miyasaka et al., 1990) and in guinea pig (Kotani et al., 1966) that thymic emigration also occurs via lymphatic drainage in addition to the emigration via blood vessels (Miyasaka et al., 1990). It is thus possible that the CCR7-dependent and CCR7-independent emigration processes may represent either one of the pathways via lymphatic or blood vessels. Interestingly, adult transgenic mice expressing the catalytic subunit of pertussis toxin in thymocytes exhibited accumulation of T cells in the thymus and failure of T cells to populate peripheral lymphoid organs (Chaffin and Perlmutter, 1991). Thus, the CCR7-independent pathway of thymic emigration may still be dependent on pertussis toxin-sensitive signals through G protein-coupled chemokine receptors.

The present study suggests that CCL19 and CCL21, even though they share CCR7, are functionally different in relocating T lymphocytes from the primary lymphoid organ to secondary lymphoid organs. In secondary lymphoid organs, locally produced CCL21 mainly participates in promoting the homing of $CCR7^+$ lymphocytes into the organ through high endothelial venules (Stein et al., 2000; also supported by the results in Figure 4). CCL21 may additionally exhibit a unique role through the CXCR3 receptor, which interacts with CCL21 but does not interact with CCL19 (Soto et al., 1998; Lu et al., 1999). On the other hand, CCL19 in secondary lymphoid organs, which is also involved in homing of $CCR7^+$ lymphocytes via the high endothelial venules (Baekkevold et al., 2001), is suggested to be involved in promoting encounters between recirculating T cells and dendritic cells and in the migration of activated B cells into the T cell zone (Ngo et al., 1998). Our results suggest an

Figure 5. Distribution of CCL19 in the Adult Thymus

Thymus sections from adult B6 mice were stained with biotin-conjugated anti-CCL19 antibody and streptavidin-Alexa-568 (red) and indicated antibodies visualized with Alexa-488 (green). White signals in right panels show colocalization of Alexa-568 signals with Alexa-488 signals. Bars, 100 μm for (A)–(L) and (P)–(R), and 50 μm for (M)–(O). Note that CCL19, enriched in $MTS10^+$ medulla rather than $CDR1^+$ cortex, is colocalized with $MTS10^+$ epithelial cells, $CD11c^{int+}$ dendritic cells, as well as $CD31^+$ endothelial venules. (L) and (O) indicate that most endothelial venules express CCL19. The CCL19 signals were specific, though not very strong, since (i) the signals were specifically detected by multiple batches of anti-CCL19 antibodies (A)–(C) and (Q) but not by control antibodies (P), (ii) the signals were specifically reduced by preabsorption of the antibody with CCL19 but not with CCL21 (data not shown), and (iii) the signals were specifically reduced by preincubation of the staining reaction with CCL19 (R).

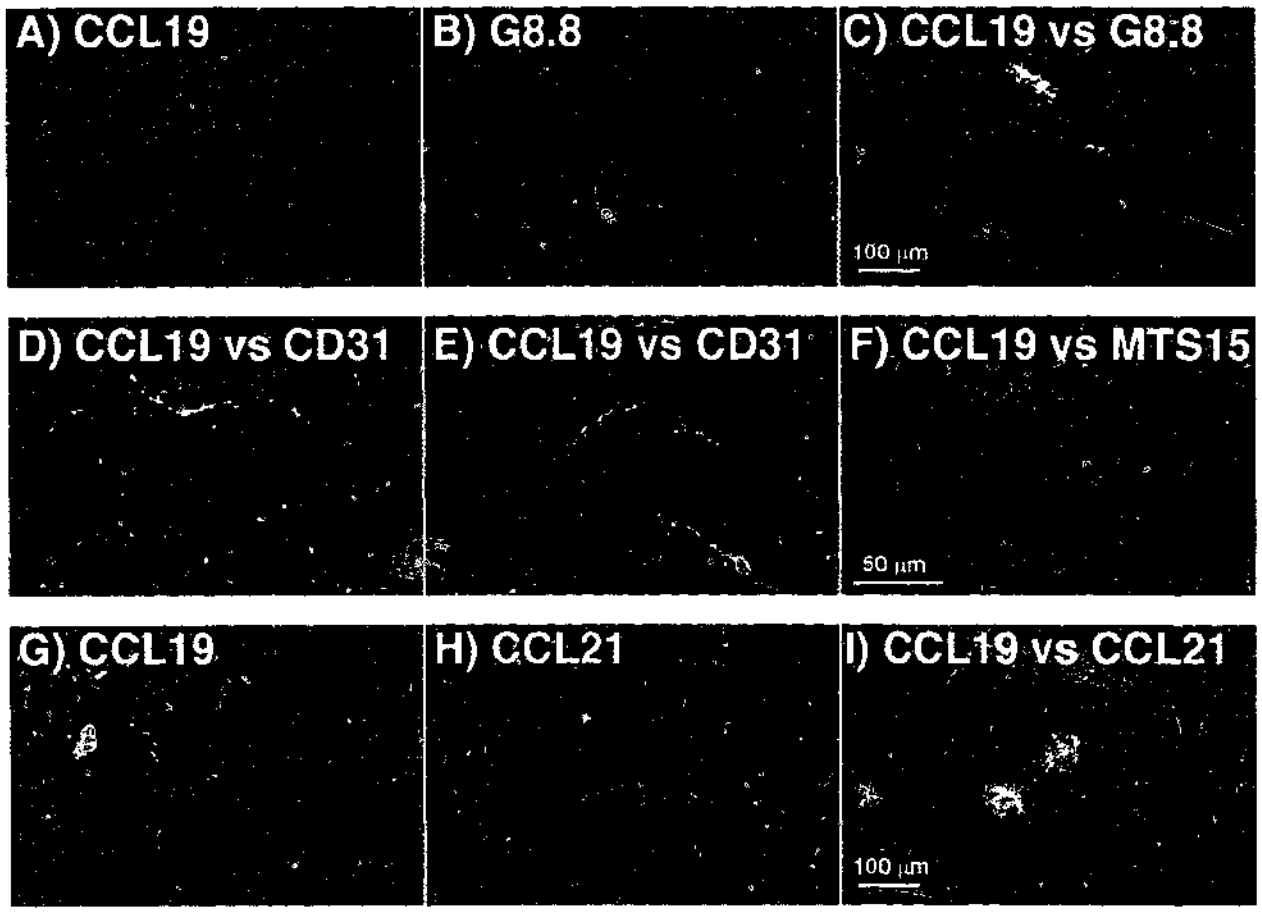

Figure 6. Distribution of CCL19 in the Newborn Thymus

Thymus sections from 3 day old B6 mice were stained with biotin-conjugated anti-CCL19 antibody and streptavidin-Alexa-568 (red) and indicated antibodies visualized with Alexa-488 (green). White signals in (C), (D), (E), (F), and (I) indicate colocalization of Alexa-568 signals with Alexa-488 signals. Bars, 100 μm for (A)–(C) and (G)–(I) and 50 μm for (D)–(F). In the thymus, G8.8^{high} areas identify the medulla (Nelson et al., 1996) and MTS15 expression identifies fibroblasts (Gray et al., 2002).

additional role of CCL19 in lymphocyte traffic, in which CCL19 in the thymic medulla may attract newly generated T lymphocytes by binding to CCR7 receptor and may play a previously unidentified role of chemokine in promoting the emigration of thymus-generated T cells into the circulation. Thus, CCL19 and CCL21 may cooperate in attracting CCR7$^+$ T cells from the thymus to peripheral lymphoid organs, by guiding the emigration of newly generated thymocytes to the circulation and directing the immigration of circulating naive T cells to the secondary lymphoid organs.

Experimental Procedures

Chemokines

Recombinant proteins of mouse CCL1 (TCA3), CCL2 (JE), CCL3 (MIP-1α), CCL4 (MIP-1β), CCL11 (eotaxin), CCL19 (ELC), CCL20 (LARC), CCL21 (SLC), CCL22 (MDC), CCL25 (TECK), CCL27 (CTACK), CXCL12 (SDF1), CXCL13 (BLC), XCL1 (lymphotactin), and CX3CL1 (fractalkine) were obtained from R&D Systems, Minneapolis, MN. Recombinant proteins of mouse CCL5 (RANTES), CCL7 (MCP3), CCL8 (MCP-2), CXCL1 (KC), and CXCL10 (IP10) were obtained from PeproTech, Rocky Hill, NJ.

Truncated CCL21 Protein

Recombinant human CCL21 and truncated CCL21 (amino acids 1-79) were produced using the Pichia pastoris yeast expression system (invitrogen) following the manufacturer's protocol. The coding sequence of wild-type CCL21 was generated by PCR using the sense primer 5′-GAA**CTCGAG***AAAAGA*AGTGATGGAGGGGCT-3′ containing an XhoI restriction site (in bold), yeast α-secretion factor sequence prior to the Kex2 cleavage site (in italic) and the codons of the first 5 amino acids of human CCL21 (underlined). The antisense primer 5′-ATTTCTAGA*TGA*GCCCTGGGCTGGTTTCTG-3′ annealed to codons corresponding to amino acids 74-79 (underlined), a stop codon (italic), and an XbaI restriction site (bold). The template for each PCR reaction was PCRII/huSLC (kindly provided by Dr. K. Hieshima). The PCR products were cloned into pPicZαA, transfected into *E. coli* DH5α, and recombinant colonies were selected on plates containing 25 μg/ml zeocin. Plasmid from a single colony of each construct was purified and the sequence of the insert confirmed. Plasmid (10 μg) containing the correct sequence was linearized using PmeI and transfected into GS115 Pichia pastoris using electroporation. Colonies were selected on YPDS plates containing 100 μg/ml zeocin at 30°C for 2–3 days. For large-scale growth and purification, the highest expressing colony was used to inoculate 25 ml of BMGY in a baffle flask and incubated in a 30°C shaking incubator overnight. One liter of BMGY was inoculated with the overnight culture and grown 2 days to an OD_{600} of 10-20. Protein production was initiated by spinning down the culture and resuspending the pellet in 200 ml BMMY containing 1% methanol. Cultures were put back on the 30°C shaker and methanol was added every 24 hr to a final concentration of 1%. After 72 hr, the supernatant was collected, filtered with a 0.22 μm filter, and purified using cation exchange chromatography. Wild-type and mutant CCL21 were ~98% pure as determined by SDS-PAGE and Coomassie staining.

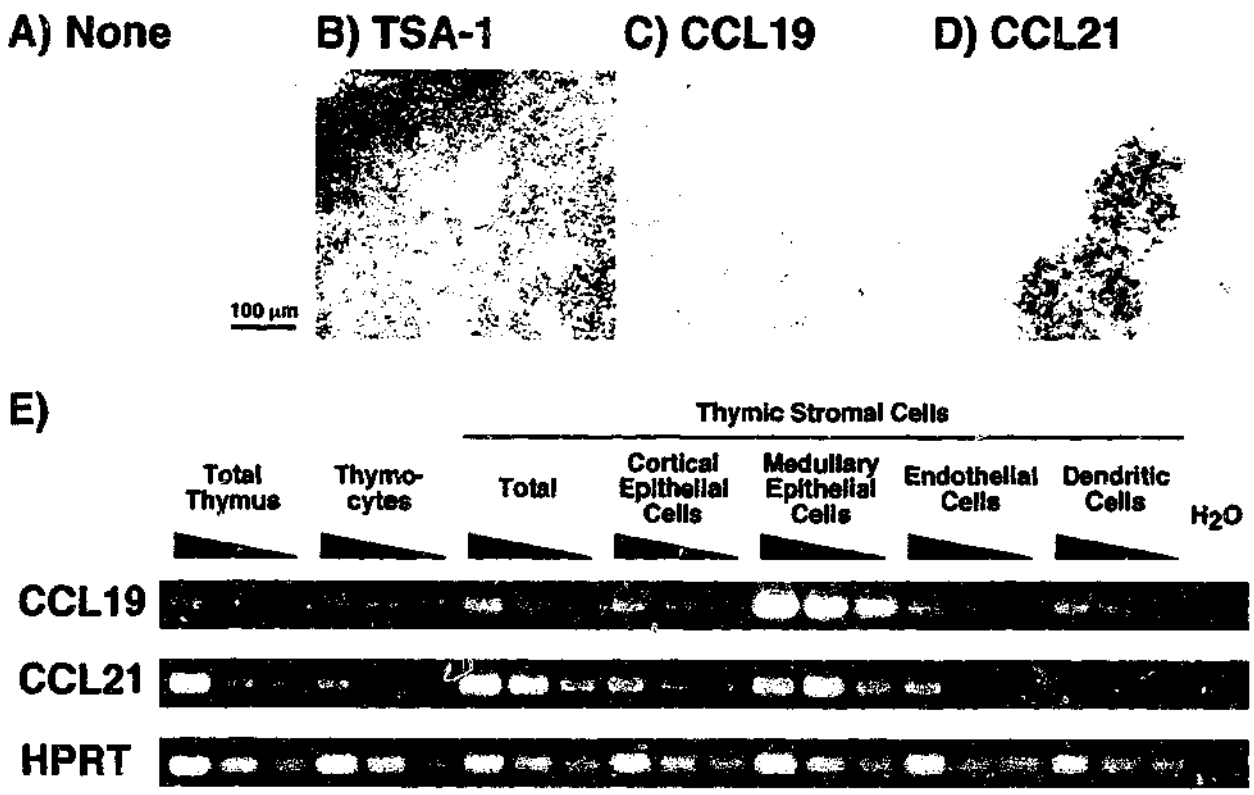

Figure 7. Expression of CCL19 Transcripts in the Thymus

(A–D) In situ hybridization analysis of the thymus from 3 day old B6 mice. Thymus sections were hybridized with indicated antisense RNA probe. Note that CCL19 signals and CCL21 signals were primarily present in the medullary areas, while the cortical and subcapsular areas were high for TSA-1 signals. The RNA probes for CCL19 and CCL21 were synthesized for the antisense sequences corresponding to the nucleotide 267-636 of GenBank AF059208 and the nucleotide 92-385 of GenBank AF001980, respectively.

(E) RT-PCR analysis of isolated thymic stromal cells. Thymus cells from newborn B6 mice were fractionated into thymocytes and thymic stromal cells. Thymic stromal cells were then sorted into cortical epithelial cells (CD45$^-$ class II MHC$^+$ UEA-1^{low}), medulary epithelial cells (CD45$^-$ class II MHC$^+$ UEA-1^{high}), endothelial cells (CD45$^-$ CD31$^+$), and dendritic cells (CD45$^+$ CD11c^{high}). Serial dilutions of cDNA from indicated cells were PCR-amplified for CCL19, CCL21, and housekeeping HPRT. Representative results of two independent experiments are shown.

CCR7-Deficient Mice

CCR7-knockout mice have been described (Förster et al., 1999). The CCR7$^{-/-}$ and wild-type littermates used in the present study were in a mixed background of 129S6/SvEv and BALB/c.

In Vivo Administration of the Antibodies

Goat polyclonal IgG antibody specific for either mouse CCL19 (MIP-3β) or mouse CCL21 (6Ckine) were obtained from R&D Systems. Rabbit anti-CCL21 polyclonal antibody (N. Onai and K.M., unpublished data) was purified over a Protein A affinity column. Control goat anti-hamster IgG polyclonal antibody and normal rabbit IgG were purchased from Jackson Immunoresearch Laboratories (West Grove, PA). 10 μg per day was injected daily into the peritoneum of newborn C57BL/6 mice from the day of birth.

Fetal Thymus Organ Cultures

Thymus lobes obtained from C57BL/6 mouse fetuses at 15.5 days postcoitum were cultured on sponge-supported filter membranes at an interface between 5% CO_2-humidified air and RPMI1640-based culture medium containing 10% fetal bovine serum, 50 μM 2-mercaptoethanol, 2 mM L-glutamine, 1× nonessential amino acids, 10 mM HEPES, 1 mM sodium pyruvate, 100 U/ml penicillin, and 100 μg/ml streptomycin (Life Technologies, Gaithersburg, MD). Details have been described (Takahama, 2000).

Transparent Fetal Thymus Organ Cultures

Thymus lobes from 15.5 dpc C57BL/6 fetal mice were cultured for 5 days in standard FTOC conditions. Thymus lobes were washed, placed in a 30 mm dish, and submerged in 1.08 mg/ml Cellmatrix collagen gel (Type I-A, Nitta Gelatin, Osaka, Japan). The dish was filled with culture medium and was cultured at 37°C in 75% O_2 and 5% CO_2 atmosphere under an Axiovert S-100 microscope (Carl Zeiss, Jena, Germany). The culture was monitored by a time-lapse visualization system equipped with C4742-95 digital CCD camera (Hamamatsu Photonics, Hamamatsu, Japan) and Openlab software (Improvision Inc., Lexington, MA).

Immunofluorescence Staining and Flow Cytometric Analysis

Single cell suspensions were washed in phosphate-buffered saline (pH 7.2) containing 0.2% bovine serum albumin and 0.1% NaN_3. Cells were first incubated with 2.4G2 anti-FcγR monoclonal antibody (Unkeless, 1979) to block binding of labeled antibodies to FcγR. Cells were then stained with fluorescein isothiocyanate (FITC)-labeled antibody and phycoerythrin (PE)-labeled antibody, and allophycoerythrin (APC)-labeled antibody. Labeled monoclonal antibodies as well as normal IgG controls were obtained from Pharmingen, San Diego, CA. Multicolor flow cytometry analysis was performed using 2-laser FACS-Calibur (Becton-Dickinson, San Jose, CA). Data were obtained using Cell Quest software on viable cells as determined by forward light scatter intensity and propidium iodide exclusion.

Bromodeoxyuridine Staining of the Cells

Bromodeoxyuridine (BrdU, 10 μM, Roche Diagnostics, Mannheim, Germany) was added to the culture 4 hr before harvesting cells. Thymocytes were fixed in 70% cold ethanol for 30 min, denatured with 4 M HCl at room temperature for 10 min, and incubated with fluorescein-conjugated anti-BrdU antibody (FLUOS In Situ Cell Proliferation Kit, Roche Diagnostics) at 37°C for 45 min. Cells were analyzed on FACS-Calibur flow cytometer.

Chemotaxis Assay

Chemotaxis assay was performed as described (Kim et al., 1998; Campbell et al., 1999). In brief, 0.1 ml of a cell suspension containing 5×10^6 thymocytes was placed in a Transwell chamber with a polycarbonate membrane (6.5 mm diameter, pore size 5 μm, Costar, Cambridge, MA) inserted in 0.6 ml culture medium containing chemokines. Cells cultured for 90 min were recovered from the upper and lower chambers, measured for cell numbers, and examined for TCR-β expression by flow cytometer. Listed are representative data of adult thymocytes, though fetal thymocytes isolated from FTOC lobes gave essentially similar results.

Reverse-Transcriptase PCR Analysis of mRNA Transcripts

Total cellular RNA from thymocytes was reverse-transcribed using Superscript II reverse transcriptase (Life Technologies, Rockville, MD) and oligo-dT oligonucleotide. cDNA was PCR-amplified (30 cycles for chemokine receptors and HPRT; 33 cycles for chemokines) with Taq polymerase (Takara, Shiga, Japan) for CCR7 (5′-GAAACCCAGGAAAAACGTGC-3′ and 5′-TGCTGATGCATAGGAGCAGC-3′), CCR10 (5′-GCTCTGTTACAAGGCTGATG-3′ and 5′-TGATACAGGCTAGGAAGAGG-3′), CXCR4 (5′-CGATCAGTGTGAGTATATACAC-3′ and 5′-TCACAGATGTACCTGTCATCC-3′), CCL19 (5′-GCTAATGATGCGGAAGACTG-3′ and 5′-ACTCACATCGACTCTCTAGG-3′), CCL21 (5′-GCTGCCTTAAGTACAGCCAG-3′ and 5′-GTGTCTGTTCAGTTCTCTTGC-3′), and hypoxanthine phosphoribosyltransferase (HPRT) (5′-CACAGGACTAGAACACCTGC-3′ and 5′-GCTGGTGAAAAGGACCTCT-3′). PCR products were electrophoresed on a 1.5% agarose gel and were visualized with ethidium bromide staining.

Binding Assay of Radioactive Proteins

Carrier-free preparations of recombinant chemokines were ^{125}I-labeled by Chloramine T method. An equal amount of radioactive proteins (1×10^6 cpm) was incubated for 1 hr at 37°C with either heparin-agarose gel (Pierce, Rockford, IL; 100 μl) or Ni-nitrilotriacetate control agarose gel (Qiagen GmbH, Germany; 100 μl). Gels were washed and measured for bound radioactivity. Heparin binding (%) = [heparin-gel-bound radioactivity (cpm)/input radioactivity to heparin-gel (cpm)–Ni-gel-bound radioactivity (cpm)/input radioactivity to Ni-gel (cpm)] × 100. Background binding of the proteins to Ni-gel was in the range of 4%–24%. For the cell binding assay, an equal amount of ^{125}I-labeled radioactive proteins (5×10^7 cpm) was incubated for 1 hr at 37°C in 75% O_2 and 5% CO_2 with either an intact FTOC lobe or isolated thymocytes from an FTOC lobe. Thymocytes were washed and measured for bound radioactivity.

Immunohistochemical Analysis of the Spleen Sections

Frozen sections (5 μm) were fixed with acetone, blocked with 1% H_2O_2 in methanol and with 2.4G2 anti-FcγR antibody, and reacted with biotin-anti-Thy1.2 antibody, biotin-B220 antibody, or biotin-normal rat IgG (Pharmingen). Sections were stained with peroxidase-labeled streptavidin (Nichirei, Tokyo, Japan) and 3,3′-diaminobenzidine (Wako Pure Chemicals, Osaka, Japan). Red pulp areas and white pulp areas in the spleen were identified with the B220 and Thy1.2 staining profiles.

Confocal Microscopy Analysis of CCL19 Expression in the Thymus Sections

Mice were anaethetized and infused with 4% paraformaldehyde. Removed thymi were fixed with 4% paraformaldehyde containing 0.2 M sucrose. Frozen sections (6-8 μm) were stained with monoclonal rat antibodies (CDR1 anti-mouse cortical thymic epithelial cells [Rouse et al., 1988], MTS10 anti-mouse medullary thymic epithelial cells [Godfrey et al., 1990], G8.8 anti-mouse Ep-CAM [Nelson et al., 1996]; anti-mouse CD11c [Wu et al., 1995], MTS12 anti-mouse CD31 [Tucek et al., 1992], or MTS-15 anti-mouse fibroblasts [Gray et al., 2002]) followed by Alexa-488 conjugated anti-rat Ig (Molecular Probes, Eugene, OR). CCL21 was stained with rabbit anti-CCL21 antibody (N. Onai and K.M., unpublished data) and FITC-anti-rabbit Ig (Caltag Laboratories, Burlingame, CA). Sections were also stained with biotinylated goat anti-ELC antibody (10 μg/ml; R&D Systems) and Alexa-568 conjugated streptavidin (Molecular Probes). The confocal microscope used was a Bio-Rad MRC 1024 with a three-line Kr/Ag laser, excitation lines: 488, 568, and 647 nm. Images were obtained using LaserSharp software version 3.2 (Bio-Rad).

In Situ Hybridization for CCL19 Expression in the Thymus Sections

Fresh 10 μm tissue sections were air-dried for approximately 2 hr then fixed in 4% paraformaldehyde for 10 min. The sections were placed in 1.2% triethanolamine and acetic anhydride was added drop wise until a concentration of 0.25% was reached. The slides were washed and pre-hybridized for overnight at 4°C. Digoxygenin-labeled riboprobe was added, and the slides were incubated at 70°C for overnight. The slides were washed and incubated in 1% blocking reagent (Roche) for 1 hr. Digoxygenin signals were visualized using anti-digoxygenin-AP Fab fragment (Boehringer Mannheim) and NBT/BCIP (Boehringer Mannheim). The slides were mounted using Kaisers glycerol gelatin (Merck).

Flow Cytometric Isolation of Thymic Stromal Cells

Thymic stromal cells were isolated as described previously (Gray et al., 2002). In brief, neonatal thymic fragments from B6 mice were subjected to a series of digestions in 0.125% (w/v) collagenase/dispase (Boehringer Mannheim, Germany) with 0.1% (w/v) DNase I in RPMI1640 medium at 37°C. The final digests enriched for thymic stromal cells were stained with appropriate surface reactive stromal-specific antibodies and fluorescent conjugates. PE-conjugated anti-CD45 (clone 104, Pharmingen) was used to detect $CD45^-$ thymic endothelial and epithelial cells, with endothelium defined on the basis of CD31 expression (clone MTS-12). Cortical and medullary epithelial cells were discriminated on the basis of biotin-conjugated UEA-1 lectin binding (Vector Laboratories, Burlingame, CA). Thymic dendritic cells were defined by high expression of CD11c (biotinylated anti-CD11c, clone HL3, Pharmingen) in $CD45^+$ population. FITC-conjugated anti-rat Ig (Caltag Laboratories) was used to detect MTS-12 and APC-conjugated streptavidin (Molecular Probes) to detect biotinylated reagents. A 10% normal rat serum was employed to prevent crossreactive binding of antibodies subsequent to FITC-conjugated anti-rat Ig labeling. FcR blocking by the 2.4G2 anti-FcR antibody was performed in labeling where FITC-conjugated anti-rat Ig was not used. Cells were sorted to greater than 95% purity on a FACS-Vantage (Becton Dickson), with exclusion of dead cells using propidium iodide.

Acknowledgments

We thank Drs. K. Hieshima, M. Matsumoto, and M. Miyasaka for helpful discussion and critical comments; Dr. N. Onai for anti-CCL21 antibody; N. Masumoto and M. Kubo for technical assistance; K. Suzuki and M. Ogata for the assistance on digital movie files; and Drs. M. Matsumoto, Y. Akamatsu, and M.A. Sheard for reading the manuscript.

Received June 11, 2001; revised December 7, 2001.

References

Annunziato, F., Romagnani, P., Cosmi, L., Beltrame, C., Steiner, B.H., Lazzeri, E., Raport, C.J., Galli, G., Manetti, R., Mavilia, C., et al. (2000). Macrophage-derived chemokine and EBI1-ligand chemokine attract human thymocytes in different stage of development and are produced by distinct subsets of medullary epithelial cells: possible implications for negative selection. J. Immunol. *165*, 238–246.

Baekkevold, E.S., Yamanaka, T., Palframan, R.T., Carlsen, H.S., Reinholt, F.P., von Andrian, U.H., Brandtzaeg, P., and Haraldsen, G. (2001). The CCR7 ligand ELC (CCL19) is transcytosed in high endothelial venules and mediates T cell recruitment. J. Exp. Med. *193*, 1105–1111.

Berzins, S.P., Boyd, R.L., and Miller, J.F.A.P. (1998). The role of the thymus and recent thymic emigrants in the maintenance of the adult peripheral lymphocyte pool. J. Exp. Med. *187*, 1839–1848.

Berzins, S.P., Godfrey, D.I., Miller, J.F.A.P., and Boyd, R.L. (1999). A central role for thymic emigrants in peripheral T cell homeostasis. Proc. Natl. Acad. Sci. USA *96*, 9787–9791.

Birkenbach, M., Josefsen, K., Yalamanchili, R., Lenoir, G., and Kieff, E. (1993). Epstein-Barr virus-induced genes: first lymphocyte-specific G protein-coupled peptide receptors. J. Virol. *67*, 2209–2220.

Bleul, C.C., and Boehm, T. (2000). Chemokines define distinct microenvironments in the developing thymus. Eur. J. Immunol. *30*, 3371–3379.

Campbell, J.J., Pan, J., and Butcher, E.C. (1999). Developmental switches in chemokine responses during T cell maturation. J. Immunol. *163*, 2353–2357.

Chaffin, K.E., and Perlmutter, R.M. (1991). A pertussis toxin-sensitive process controls thymocyte emigration. Eur. J. Immunol. *21*, 2565–2573.

Cyster, J.G., and Goodnow, C.C. (1995). Pertussis toxin inhibits migration of B and T lymphocytes into splenic white pulp cords. J. Exp. Med. *182*, 581–586.

Cyster, J.G. (1999). Chemokines and cell migration in secondary lymphoid organs. Science *286*, 2098–2102.

Douek, D.C., McFarland, R.D., Keiser, P.H., Gage, E.A., Massey, J.M., Haynes, B.F., Polis, M.A., Haase, A.T., Feiberg, M.B., Sullivan, J.L., et al. (1998). Changes in thymic function with age and during the treatment of HIV infection. Nature *396*, 690–695.

Dunon, D., and Imhof, B.A. (1993). Mechanisms of thymus homing. Blood *81*, 1–8.

Fontaine-Perus, J.C., Calman, F.M., Kaplan, C., and Le Douarin, N.M. (1981). Seeding of the 10-day mouse embryo thymic rudiment by lymphocyte precursors in vitro. J. Immunol. *126*, 2310–2316.

Förster, R., Schubel, A., Breitfeld, D., Kremmer, E., Renner-Muller, I., Wolf, E., and Lipp, M. (1999). CCR7 coordinates the primary immune response by establishing functional microenvironments in secondary lymphoid organs. Cell *99*, 23–33.

Godfrey, D.I., Izon, D.J., Tucek, C.L., Wilson, T.J., and Boyd, R.L. (1990). The phenotypic heterogeneity of mouse thymic stromal cells. Immunology *70*, 66–74.

Gray, D.H.D., Chidgey, A.P., and Boyd, R.L. (2002). Analysis of thymic stromal cell populations using flow cytometry. J. Immunol. Methods *260*, 15–28.

Gunn, M.D., Tangemann, K., Tam, C., Cyster, J.G., Rosen, S.D., and Williams, L.T. (1998). A chemokine expressed in lymphoid high endothelial venules promotes the adhesion and chemotaxis of naive T lymphocytes. Proc. Natl. Acad. Sci. USA *95*, 258–263.

Hedrick, J.A., and Zlotnik, A. (1997). Identification and characterization of a novel beta chemokine containing six conserved cysteines. J. Immunol. *159*, 1589–1593.

Jotereau, F., Heuze, F., Salomon-Vie, V., and Gascan, H. (1987). Cell kinetics in the fetal mouse thymus: precursor cell input, proliferation, and emigration. J. Immunol. *138*, 1026–1030.

Kim, C.H., Pelus, L.M., White, J.R., and Broxmeyer, H.E. (1998). Differential chemotactic behavior of developing T cells in response to thymic chemokines. Blood *91*, 4434–4443.

Kotani, M., Seiki, K., Yamashita, A., and Horii, I. (1966). Lymphatic drainage of thymocytes to the circulation in the guinea pig. Blood *27*, 511–520.

Lu, B., Humbles, A., Bota, D., Gerard, C., Moser, B., Soler, D., Luster, A.D., and Gerard, N.P. (1999). Structure and function of the murine chemokine receptor CXCR3. Eur. J. Immunol. *29*, 3804–3812.

Luther, S.A., Tang, H.L., Hyman, P.L., Farr, A.G., and Cyster, J.G. (2000). Coexpression of the chemokines ELC and SLC by T zone stromal cells and deletion of the ELC gene in the *plt/plt* mouse. Proc. Acad. Natl. Sci. USA *97*, 12694–12699.

Miyasaka, M., Pabst, R., Dudler, L., Cooper, M., and Yamaguchi, K. (1990). Characterization of lymphatic and venous emigrants from the thymus. Thymus *16*, 29–43.

Murphy, P.M. (1994). The molecular biology of leukocyte chemoattractant receptors. Annu. Rev. Immunol. *12*, 593–633.

Nagira, M., Imai, T., Hieshima, K., Kusuda, J., Ridanpaa, M., Takagi, S., Nishimura, M., Kakizaki, M., Nomiyama, H., and Yoshie, O. (1997). Molecular cloning of a novel human CC chemokine secondary lymphoid-tissue chemokine that is a potent chemoattractant for lymphocytes and mapped to chromosome 9p13. J. Biol. Chem. *272*, 19518–19524.

Nelson, A.J., Dunn, R.J., Peach, R., Aruffo, A., and Farr, A.G. (1996). The murine homolog of human Ep-CAM, a homotypic adhesion molecule, is expressed by thymocytes and thymic epithelial cells. Eur. J. Immunol. *26*, 401–408.

Ngo, V.N., Tang, H.L., and Cyster, J.G. (1998). Epstein-Barr virus-induced molecule 1 ligand chemokine is expressed by dendritic cells in lymphoid tissues and strongly attracts naive T cells and activated B cells. J. Exp. Med. *188*, 181–191.

Norment, A.M., Bogatzki, L.Y., Gantner, B.N., and Bevan, M.J. (2000). Murine CCR9, a chemokine receptor for thymus-expressed chemokine that is up-regulated following pre-TCR signaling. J. Immunol. *164*, 639–648.

Picker, L.J., and Siegelman, M.H. (1999). Lymphoid tissues and organs. In Fundamental Immunology, W.E. Paul, ed. (PA: Lippincott-Raven), pp 479–531.

Poulin, J.F., Viswanathan, M.N., Harris, J.M., Komanduri, K.V., Wieder, E., Ringuette, N., Jenkins, M., McCune, J.M., and Sekaly, R.P. (1999). Direct evidence for thymic function in adult humans. J. Exp. Med. *190*, 479–486.

Premack, B.A., and Schall, T.J. (1996). Chemokine receptors: gateways to inflammation and infection. Nat. Med. *2*, 1174–1178.

Rossi, D., and Zlotnik, A. (2000). The biology of chemokines and their receptors. Annu. Rev. Immunol. *18*, 217–242.

Rossi, D.L., Vicari, A.P., Franz-Bacon, K., McClanahan, T.K., and Zlotnik, A. (1997). Identification through bioinformatics of two new macrophage proinflammatory human chemokines: MIP-3alpha and MIP-3beta. J. Immunol. *158*, 1033–1036.

Rouse, R.V., Bolin, L.M., Bender, J.R., and Kyewski, B.A. (1988). Monoclonal antibodies reactive with subsets of mouse and human thymic epithelial cells. J. Histochem. Cytochem. *36*, 1511–1517.

Scollay, R., and Godfroy, D.I. (1995). Thymic emigration: conveyor belts or lucky dips? Immunol. Today *16*, 268–273.

Scollay, R.G., Butcher, E.C., and Weissman, I.L. (1980). Thymus cell migration. Quantitative aspects of cellular traffic from the thymus to the periphery in mice. Eur. J. Immunol. *10*, 210–218.

Scollay, R., Smith, J., and Stauffer, V. (1986). Dynamics of early T cells: prothymocyte migration and proliferation in the adult mouse thymus. Immunol. Rev. *91*, 129–157.

Soto, H., Wang, W., Strieter, R.M., Copeland, N.G., Gilbert, D.J., Jenkins, N.A., Hedrick, J., and Zlotnik, A. (1998). The CC chemokine 6Ckine binds the CXC chemokine receptor CXCR3. Proc. Natl. Acad. Sci. USA *95*, 8205–8210.

Stein, J.V., Rot, A., Luo, Y., Narasimhaswamy, M., Nakano, H., Gunn, M.D., Matsuzawa, A., Quackenbush, E.J., Dorf, M.E., and von Andrian, U.H. (2000). The CC chemokine thymus-derived chemotactic agent 4 (TCA-4, secondary lymphoid tissue chemokine, 6Ckine, exodus-2) triggers lymphocyte function-associated antigen 1-mediated arrest of rolling T lymphocytes in peripheral lymph node high endothelial venules. J. Exp. Med. *191*, 61–75.

Suzuki, G., Nakata, Y., Dan, Y., Uzawa, A., Nakagawa, K., Saito, T., Mita, K., and Shirasawa, T. (1998). Loss of SDF-1 receptor expression during positive selection in the thymus. Int. Immunol. *10*, 1049–1056.

Takahama, Y. (2000). Differentiation of mouse thymocytes in fetal thymus organ culture. In T Cell Protocols. Development and Activation. K.P. Kearse, ed. (NJ: Humana Press), pp 37–46.

Tanabe, S., Lu, Z., Luo, Y., Quackenbush, E.J., Berman, M.A., Collins-Racie, L.A., Mi, S., Reilly, C., Lo, D., Jacobs, K.A., et al. (1997). Identification of a new mouse beta-chemokine, thymus-derived chemotactic agent *4*, with activity on T lymphocytes and mesangial cells. J. Immunol. *159*, 5671–5679.

Tough, D.F., and Sprent, J. (1994). Turnover of naive- and memory-phenotype T cells. J. Exp. Med. *179*, 1127–1135.

Tucek, C.L., Godfrey, D.I., and Boyd, R.L. (1992). Five novel antigens illustrate shared phenotype between mouse thymic stromal cells, thymocytes, and peripheral lymphocytes. Int. Immunol. *4*, 1021–1030.

Unkeless, J.C. (1979). Characterization of a monoclonal antibody directed against mouse macrophage and lymphocyte Fc receptors. J. Exp. Med. *150*, 580–596.

van Ewijk, W. (1991). T-cell differentiation is influenced by thymic microenvironments. Annu. Rev. Immunol. *9*, 591–615.

Wilkinson, B., Owen, J.J.T., and Jenkinson, E.J. (1999). Factors regulating stem cell recruitment to the fetal thymus. J. Immunol. *162*, 3873–3881.

Wu, L., Vremec, D., Ardavin, C., Winkel, K., Suss, G., Georgiou, H., Maraskovsky, E., Cook, W., and Shortman, K. (1995). Mouse thymus dendritic cells: kinetics of development and changes in surface markers during maturation. Eur. J. Immunol. *25*, 418–425.

Wurbel, M.A., Philippe, J.M., Nguyen, C., Victorero, G., Freeman, T., Wooding, P., Miazek, A., Mattei, M.G., Malissen, M., Jordan, B.R., et al. (2000). The chemokine TECK is expressed by thymic and intestinal epithelial cells and attracts double- and single-positive thymocytes expressing the TECK receptor CCR9. Eur. J. Immunol. *30*, 262–271.

Yoshida, R., Imai, T., Hieshima, K., Kusuda, J., Baba, M., Kitaura, M., Nishimura, M., Kakizaki, M., Nomiyama, H., and Yoshie, O. (1997). Molecular cloning of a novel human CC chemokine EBI1-ligand chemokine that is a specific functional ligand for EBI1, CCR7. J. Biol. Chem. *272*, 13803–13809.

Yoshida, R., Nagira, M., Kitaura, M., Imagawa, N., Imai, T., and Yoshie, O. (1998). Secondary lymphoid-tissue chemokine is a functional ligand for the CC chemokine receptor CCR7. J. Biol. Chem. *273*, 7118–7122.

Stromal Cells Provide the Matrix for Migration of Early Lymphoid Progenitors Through the Thymic Cortex[1]

Susan E. Prockop,* Sharina Palencia,* Christina M. Ryan,[2]* Kristie Gordon,* Daniel Gray,[‡] and Howard T. Petrie[3]*[†]

During steady state lymphopoiesis in the postnatal thymus, migration of precursors outward from the deep cortex toward the capsule is required for normal differentiation. Such migration requires, at a minimum, expression of adhesive receptors on the migrating lymphoid cells, as well as a stable matrix of their ligands persisting throughout the region of migration. In this study, we address the nature of this adhesive matrix. Although some precursor stages bound efficiently to extracellular matrix ligands, a specific requirement for the cell surface ligand VCAM-1 was also found. In situ analysis revealed that early precursors are found in intimate contact with a matrix formed by stromal cells in the cortex, a proportion of which expresses VCAM-1. In vivo administration of an anti-VCAM-1 Ab resulted in decreased thymic size and altered distribution of early precursors within the cortex. These results indicate that precursors migrating outward through the cortex may use a cellular, rather than extracellular, matrix for adhesion, and suggest that the VCAM-1$^+$ subset of cortical stroma may play a crucial role in supporting the migration of early precursors in the steady state thymus. *The Journal of Immunology,* **2002, 169: 4354–4361.**

Like other cells of hemopoietic origin, T lymphocytes must be produced throughout life to replace cells lost to senescence, trauma, and other causes. This process occurs in the thymus and involves several distinct phases. The initial phase involves recruitment into the thymus of marrow-derived progenitors that circulate in the bloodstream (reviewed in Ref. 1). It is possible that some of these thymic seeding progenitors are already committed to the lymphoid lineages, because there is a population of cells in bone marrow that has increased propensity to generate lymphoid cells (2). However, it is clear from a number of studies that the earliest precursors found within the thymus can give rise to numerous lymphoid and nonlymphoid lineages (for examples, see Refs. 3–10), suggesting that not all cells that home to the thymus are lymphoid committed (reviewed in Ref. 11). During a period of intrathymic residence that spans ~14 days (reviewed in Ref. 12), these multilineage progenitors are induced to undergo a series of differentiative events that lead to T lineage commitment (13). In addition, a great deal of proliferative expansion occurs, such that each progenitor entering the thymus gives rise to approximately one million immature progeny (12), thus generating the cells that are subsequently subjected to TCR-mediated screening.

In general, lineage commitment and proliferation are not cell autonomous processes, but rather occur in response to combinations of signals (morphogens, growth factors, hormones, etc.) that progenitor cells receive from the external microenvironment. The nature of signals that drive lineage commitment and proliferation in early intrathymic progenitors remains largely unknown. A few such signals have been identified in the form of Notch-1 (10, 14, 15), c-*kit* (16, 17), and the IL-7R (18), although the exact functions (i.e., differentiation, proliferation, survival) in some cases remain controversial. Regardless, it seems unlikely that this relatively small number of signals is adequate to explain the complex sequence of events that lead to production of a large number of T lineage progeny from a relatively few undifferentiated progenitors. To evaluate what other signals might be involved, we began from the assumption that early precursors receive specific signals from their external microenvironment that lead to T lineage commitment and/or proliferative expansion. This led us to define a stratified pattern of precursor distribution in the thymic cortex (19), wherein the earliest progenitors (CD4/8 double-negative stage 1, DN1)[4] are in the deep cortex, the next stage (DN2) in the midcortex, and the last stage (DN3) predominates in the outer third of the cortex. Transition to the early CD4/8 double-positive (pre-DP) stage, together with the most obvious wave of proliferation (20, 21), correlates with localization to the subcapsular zone (22). This is followed by a reversal in the polarity of migration, with movement of expanded DP progeny progressively deeper into the cortex toward the medulla (23).

There are two distinct categories of functions that are implicated by the behaviors described above. The first is the stratified distribution of signals that induce sequential stages of lineage commitment and proliferation in the thymic cortex. The second, and the topic of the present study, is a mechanism for moving cells between them. Directional migration of cells within tissues indicates the presence of a number of biochemical requirements. Among these are adhesion receptors on the migrating cells, as well as a stable matrix of their ligands or counterreceptors to provide the traction for cell movement. In this study, we characterize the presence of adhesion receptors on lymphoid cells traveling outward through the cortex, as well as their ability to adhere to matrix

*Memorial Sloan-Kettering Cancer Center, New York, NY 10021; [†]Weill Graduate School of Medical Sciences of Cornell University, New York, NY 10021; and [‡]Monash University Medical School, Department of Pathology, Melbourne, Australia

Received for publication July 3, 2002. Accepted for publication August 13, 2002.

The costs of publication of this article were defrayed in part by the payment of page charges. This article must therefore be hereby marked *advertisement* in accordance with 18 U.S.C. Section 1734 solely to indicate this fact.

[1] This work was supported by Public Health Service Grants A133940 and CA08748, as well as by funds from the Dewitt Wallace Foundation.

[2] Current address: Department of Microbiology and Immunology, Pennsylvania State University College of Medicine, Hershey, PA 17033.

[3] Address correspondence and reprint requests to Dr. Howard T. Petrie, Memorial Sloan-Kettering Cancer Center, Box 343, 1275 York Avenue, New York, NY 10021. E-mail address: petrieh@mskcc.org

[4] Abbreviations used in this paper: DN, double negative; DAPI, 4′,6′-diamidino-2-phenylindole; DP, double positive; ECM, extracellular matrix; FN, fibronectin; LN, laminin.

0022-1767/02/$02.00

ligands predicted by these receptors. Our data suggest that migrating lymphoid progenitors use a cellular, rather than extracellular, matrix for adhesion and migration. Combined functional and in situ analysis suggests that this cellular matrix consists of a subset of cytokeratin$^+$ cortical stromal cells that express the α_4 integrin ligand VCAM-1. Together, our findings demonstrate a close association of early lymphoid progenitors in the thymus with the stromal elements on which their differentiation depends. Furthermore, in addition to revealing unreported heterogeneity among cytokeratin$^+$ stromal cells of the thymic cortex, these studies suggest that early lymphoid progenitors and other, more mature lymphoid cells that occupy the same cortical space may nonetheless interact with very distinct stromal cell types.

Materials and Methods

Cells and Abs

Precursor thymocytes were prepared by sorting of lineage-negative thymocytes isolated from 4- to 8-wk-old C57BL/6 mice, as previously described (21). Thymic stromal cells were isolated as previously described (24). The cloned thymic stromal cell line 100-4 (25) was grown in DMEM supplemented with 10% FBS, 2 mM glutamine, and 5×10^{-5} M 2-ME. Purified anti-integrin Abs were clone 9C10 (anti-α_4), clone 5H10-27 (anti-α_5), clone GoH3 (anti-α_6), clone 9EG7 (anti-β_1), clone 346-11A (anti-β_4), and clone M293 (anti-β_7), all from BD PharMingen (San Diego, CA). Secondary Ab used for integrin detection was biotinylated goat F(ab')$_2$ anti-rat IgG (Jackson ImmunoResearch Laboratories, West Grove, PA), followed by PE-streptavidin (Molecular Probes, Eugene, OR). Anti-cytokeratin Ab was clone C-11 conjugated to FITC (Sigma-Aldrich, St. Louis, MO), recognizing cytokeratins 4, 5, 6, 8, 10, 13, and 18. Abs used to define cortical stromal cells by flow cytometry were M 5/114.15.2 and 6C3, as previously described (26). Anti-VCAM-1 Ab used for in situ analysis was clone 429 conjugated to biotin (BD PharMingen). Anti-VCAM-1 Ab used for in vitro blocking was clone M/K2.7. Abs used to identify precursor thymocytes in situ were clones PC-61 (anti-CD25) or ACK-2 (CD117) coupled to biotin. Detection of VCAM-1 or CD117 by immunohistochemistry or immunofluorescent microscopy was performed using tyramide signal amplification (NEN, Boston, MA).

Assay for adhesion to purified extracellular matrix (ECM) ligands

Murine fibronectin (FN) and laminin 1 (LN1) were purchased from Life Technologies (Carlsbad, CA). Ninety-six-well trays (Nunc 473768; Nalge Nunc International, Rochester, NY) were coated with ECM proteins by overnight incubation at 4°C with 1 (FN) or 5 μg (LN1) purified protein in 100 μl PBS. These concentrations were determined by measurement of optimal binding efficiency using unsorted DN thymocytes (i.e., lineage-depleted thymocytes). Blocking of excess protein binding was performed by incubating wells in a solution of heat-inactivated BSA (1% in PBS) for 1 h at room temperature. Purified DN precursors were added in PBS/BSA and allowed to settle for 30 min at 4°C. In any given experiment, the wells contained identical numbers of cells for each developmental stage, although the absolute number of cells varied between experiments, ranging from $4–5 \times 10^5$ cells/well. Plates were then incubated at 37°C for 30 min, followed by repeated washes in PBS/BSA. After a final wash in PBS, cells were fixed using 4% formaldehyde for 30 min at room temperature, followed by washing in PBS, treatment with 20% methanol in water (10 min at room temperature), and staining with 2% crystal violet. A single field at the center of each well was photographed, and the digital image was analyzed using the colony count function of Quantity One software (Bio-Rad, Hercules, CA). For an estimation of total cells in the well before washing, a phase-contrast image of the center of the well was used.

VCAM-1 adhesion assay

The 100-4 cells were grown in eight-well glass slide chambers (Lab-Tek; Nalge Nunc International), as described above. Purified T cell precursors ($4–5 \times 10^5$/well) were added in DMEM supplemented as described above, followed by incubation at 37°C for 1 h. The glass slide was removed from the chambers and washed by stirring in a beaker containing PBS. Fixation was then performed as described above, followed by staining in Harris' Modified Hematoxylin (Fisher Scientific, Pittsburgh, PA) and mounting. For blocking experiments, anti-VCAM-1 Ab (5 μg/ml) was added to the adherent monolayers 30 min before addition of lymphoid cells, and left in the medium during subsequent incubation.

Flow cytometry and microscopy

Thymic sections (4 μM) were prepared by cryosectioning after embedding in OCT. Immunohistochemical detection was performed using the VectaStain ABC kit (Vector Laboratories, Burlingame, CA). Staining for immunofluorescent microscopy was performed as previously described (19). Tissue counterstains were hematoxylin (immunohistochemistry) or 4′,6′-diamidino-2-phenylindole (DAPI; immunofluorescent microscopy). Digital microscopy was performed using an Olympus (Melville, NY) BX-50 microscope equipped with a mercury light source. Flow cytometric analysis was performed using a three-laser LSR cytometer (BD Biosciences, San Jose, CA).

Anti-VCAM-1 administration in vivo

Animals were injected daily for 5 days with 100 μg/day mAb recognizing VCAM-1 (clone MK-2.7) or control (nonspecific) Ab. Following this, animals were euthanized and the thymus was removed carefully. One lobe was frozen immediately for immunohistochemical and/or immunofluorescent analysis, while a single cell suspension was prepared from the other lobe. The latter was used for determination of total cellularity (by hemacytometer counting) as well as for phenotypic analysis of developmental stage by flow cytometry.

Results

Use of integrin expression profiles on intrathymic progenitors to predict adhesive substrates for cell migration

Our previous work has shown that early intrathymic precursors migrate outward through the cortex before differentiating into CD4$^+$8$^+$ cells (19). In an effort to understand the mechanisms of transcortical migration, we sought to analyze the expression of integrins by defined stages of intrathymic differentiation. Expression of integrins is implicit in cell migration through tissues, and although the mere presence of an integrin does not necessarily imply functional activity, it does indicate potential for adhesion to the corresponding ligand. It should be noted that while a number of studies have evaluated integrin expression on thymocytes, especially fetal progenitors or total DN cells, integrin expression relative to defined stages of differentiation in the postnatal progenitors has not been characterized, nor has binding to the corresponding ligands. Given the recent description of stratified regions through which progenitors migrate during differentiation (19), these were the goals of the experiments described in this work.

A number of integrins were not found at any appreciable level on DN cells, including α_1, α_2, α_3, and α_v. The latter is particularly informative, because it eliminates potential involvement of β_3-, β_5-, β_6-, and β_8-containing heterodimers in the precursor migration process. Likewise, the involvement of β_2 integrins has been largely ruled out by gene-targeting experiments (27), thus leaving β_1-, β_4-, and β_7-containing heterodimers as the major areas of interest. Analysis of these integrins and their α partners reveals substantial heterogeneity among the various stages of differentiation, as illustrated in Fig. 1. For instance, all DN stages express α_4 integrin, although DN1 express it in a bimodal pattern, and at levels that are lower than either DN2 or DN3. Likewise, α_5 integrin is expressed by all DN stages, although a bimodal distribution is again noted, this time in DN2, but not DN1 or DN3 cells. Thus, although these two integrins are consistently expressed on DN cells, they are not uniformly expressed; the relevance of this finding is addressed by other experiments in this manuscript, and in *Discussion*. Expression of integrin α_6 is fairly uniform on all DN cells, as is that of β_1. However, heterogeneity is again revealed by analysis of both β_4 integrin, which is up-regulated upon transition from DN1 to DN2, and β_7 integrin, which appears to be largely specific for DN2 cells. Thus, the functional heterodimers that can be expressed by different stages of intrathymic precursor differentiation are identifiable, and can be used to predict the potential ligands for adhesion at each stage of transcortical migration. The

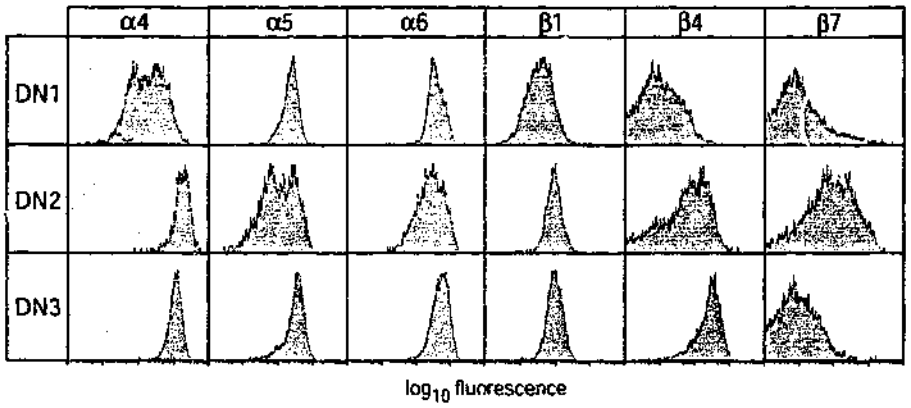

FIGURE 1. Analysis of integrin expression profiles to predict ligands for adhesion during DN precursor migration. Lineage-depleted thymocyte suspensions were stained with CD24, CD25, and CD44 Abs to reveal the various $CD4^-8^-$ stages of differentiation, as well as a panel of Abs recognizing various integrins. α_1, α_2, α_3, and α_v integrins were not found with appreciable frequency on any precursor population (not shown). However, α_4, α_5, α_6, β_1, β_4, and β_7 were expressed, as shown. In some cases (e.g., β_4 and β_7), expression fluctuated dramatically at certain developmental stages, indicating the potential for specific adhesion requirements at these stages. Possible integrin heterodimer combinations and relevant ligands for each stage are summarized in Table I. Hatched lines show the relative staining intensity of an isotype-matched nonspecific control Ab.

major predicted ligands, as summarized in Table I, were the ECM proteins FN, LN1, and LN5, as well as VCAM-1, which is generally implicated in cell-cell rather than cell-matrix interactions. The ability of integrin heterodimers on DN precursors to bind these ligands was subsequently tested, as described in the next section.

Analysis of precursor binding to ECM components

To confirm the integrin expression data shown in Fig. 1, and to further characterize the nature of the matrix for transcortical migration of lymphoid precursors, static adhesion to purified ECM proteins was performed (Fig. 2). Although static adhesion does not allow measurement of absolute affinity for a given ligand, it can be used to determine relative affinity of cells expressing a given set of receptors. Adhesion to LN5 was not tested, because it is found only in the basal layers of the thymic capsule and thymic blood vessels (28, 29), neither of which are primary sites for DN localization in the cortex (19). For the remaining ECM ligands, namely FN and LN1, 96-well tissue culture trays were coated with optimal levels of purified ECM proteins (see *Materials and Methods*), and equal numbers of cells at each stage were added. Following incubation and washing, relative levels of binding were determined. Absolute quantitation of such assays is complicated by an accumulation of cells at the edge of the well, in which the hydrodynamic forces of washing are greatly reduced. Consequently, counting was restricted to a single microscopic field at the center of the well. The number of cells in this field was quantitated using the colony-counting function of Quantity One software (Bio-Rad) and compared with the total cells present before washing (see *Materials and Methods*). Several observations were made using this assay. First, the most efficient binding was of DN3 cells to FN, with 70–80% of cells bound on average (numerous experiments were performed, but not all DN populations were examined in all experiments). DN1 also bound efficiently to FN, with a similar proportion of cells bound (60–70%). However, despite expressing multiple FN receptors (Table I), DN2 cells did not bind with appreciable frequency to FN (10–15% of cells bound). For all populations, the frequency of binding to LN1 was less than that of FN, although appreciable numbers of cells still bound at both the DN1 and DN3 stages (30–35%). However, binding of DN2 cells to LN1, although significant by the Student's *t* test for paired samples, was only trivially higher than binding to BSA alone. Together, these findings suggest that DN1 and DN3 cells express

Table I. *Integrins expressed on early intrathymic precursors, and potential ligands*

Stage	α Integrins	β Integrins	Potential Dimers	Major Ligands
DN1	$\alpha_4{}^a$, α_5, α_6	$\beta_1{}^b$	$\alpha_4\beta_1$	FN, VCAM-1
			$\alpha_5\beta_1$	FN, LN1
			$\alpha_6\beta_1$	LN1
DN2	α_4, $\alpha_5{}^a$, α_6	β_1, $\beta_4{}^a$, β_7	$\alpha_4\beta_1$	FN, VCAM-1
			$\alpha_4\beta_7$	FN, VCAM-1
			$\alpha_5\beta_1$	FN, LN1
			$\alpha_6\beta_1$	LN1
			$\alpha_6\beta_4$	LN5
DN3	α_4, α_5, α_6	β_1, β_4	$\alpha_4\beta_1$	FN, VCAM-1
			$\alpha_5\beta_1$	FN, LN1
			$\alpha_6\beta_1$	LN1
			$\alpha_6\beta_4$	LN5

[a] Bimodal expression.
[b] Low level expression.

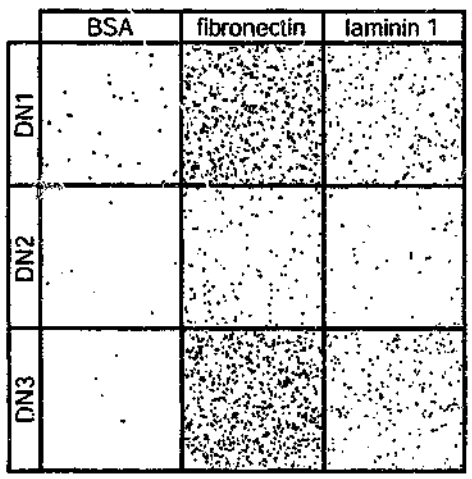

FIGURE 2. Adhesion of precursor thymocytes to ECM ligands predicted by integrin expression profiles. Equal numbers of cells were added to wells coated with FN or LN1, as indicated. After incubation and washing, bound cells were stained with crystal violet and the wells were photographed. Nonspecific binding to plates coated with BSA only was insignificant. Cells at the DN1 and DN3 stages bound with high frequency to FN (60–80% of cells bound), and somewhat less efficiently to LN1 (~30% of cells bound). However, DN2 thymocytes did not bind efficiently to either of these ECM components, despite expressing multiple relevant receptors (see Table I), indicating that DN2 cells have adhesion requirements that differ substantially from their precursors and progeny, and that may not include ECM ligands.

active FN receptors and, to a lesser extent, LN1 receptors, while DN2 cells do not bind with high affinity or frequency to either of these, despite expressing the appropriate receptors.

Analysis of precursor binding to cellular matrix components in the thymic cortex

Our previous studies suggest that DN2 cells must be highly migratory, because they span the midcortical regions between DN1 and DN3 cells (19). Directional cell migration requires a matrix for cell adhesion, yet the results shown in Fig. 2 suggest that DN2 do not bind efficiently to ECM components for which they bear receptors. DN2 cells also bear multiple receptors for VCAM-1 (Fig. 1 and Table I), a counterreceptor that is generally found in cell surface form and mediates cell-cell interactions. VCAM-1 has been shown to be expressed in human thymus by both nonhemopoietic stroma (30) and macrophages (31). Interestingly, the stromal cells expressing VCAM-1 in the former case created a reticular lattice in the cortex. To evaluate the possibility that a cellular matrix composed of VCAM-1$^+$ cells might form a substrate for cell migration across the thymic cortex, we first analyzed expression of VCAM-1 in the mouse thymus (Fig. 3). Similar to previous findings on the human thymus, we find that VCAM-1 is expressed on reticular cells that form a radially aligned matrix in the thymic cortex, while expression in the medulla is restricted to scattered cells with macrophage-like morphology, or to vascular elements. The nature of various VCAM-1$^+$ cells is further revealed by dual staining using an Ab recognizing cytokeratins (Fig. 3). Numerous phenotypes can be observed, including VCAM-1$^+$ keratin$^-$ cells with macrophage/dendritic morphology (located mainly in the medulla), and a significant number of VCAM-1$^-$ keratin$^+$ stromal cells in the cortex. However, throughout the cortex there is also a subset of keratin$^+$ cells that is VCAM-1$^+$. This finding is confirmed by flow cytometric analysis, which shows that approximately one-third of cortical stromal cells (MHC-II$^+$, 6C3$^+$; see *Materials and Methods*) are also VCAM-1$^+$ (Fig. 3). Together, the data presented in Fig. 3 reveal that VCAM-1 is expressed in the thymus on a subset of stromal cells that form a reticular matrix in the cortex. Especially given the lack of DN2 binding to ECM components, this raised the possibility that stromal cells, and in particular VCAM-1$^+$ stromal cells, might represent the substrate for precursor migration outward through the cortex, as evaluated below.

If a stromal matrix does provide the substrate for precursor migration across the cortex, then precursors and stromal cells should be in direct contact with each other. The data in Fig. 4 show that this is, in fact, the case. An Ab recognizing CD117 (c-*kit*) was used to identify early intrathymic precursors (DN1 and DN2) found in the inner and midcortex (19), together with an Ab recognizing cytokeratins, to identify the most abundant stromal cells in the cortex. The vast majority of CD117$^+$ cells were found to be in direct contact with cytokeratin$^+$ stromal cells, in support of the above hypothesis. It should be noted that in any single plane, there were always a few (one or two) precursors that did not appear to be in contact with a stromal cell, suggesting the possibility that not all lymphoid precursors remain in contact with the stromal matrix at all times. However, it is quite possible that these few cells may have been associated with a stromal cell that was above or below the plane of the tissue section being examined. In any case, the majority of precursor cells in any given plane are found to be directly in contact with a stromal cell. The intimate nature of this interaction is further revealed by high magnification views at various depths in a single tissue section (Fig. 4, *b* and *c*). Lymphoid precursors are not only in contact with stromal cells, but are virtually surrounded by reticular processes from the stromal cells that they contact. These data not only support the hypothesis that stromal cells may provide a matrix for migration of early precursors outward through the cortex, but also show that intimate lymphostromal contacts are formed during this process, providing a basis for reciprocal signals that may influence differentiation, proliferation, and/or survival of either cell type, as predicted by the findings of others (for examples, see Refs. 32–34).

To further evaluate the role of the VCAM-1$^+$ subset of cytokeratin$^+$ stroma in the above process, we first sought to demonstrate a correlation between early precursors (i.e., c-*kit*$^+$ cells) and VCAM-1$^+$ cells in the cortex. Unfortunately, detection of c-*kit* and VCAM-1 in

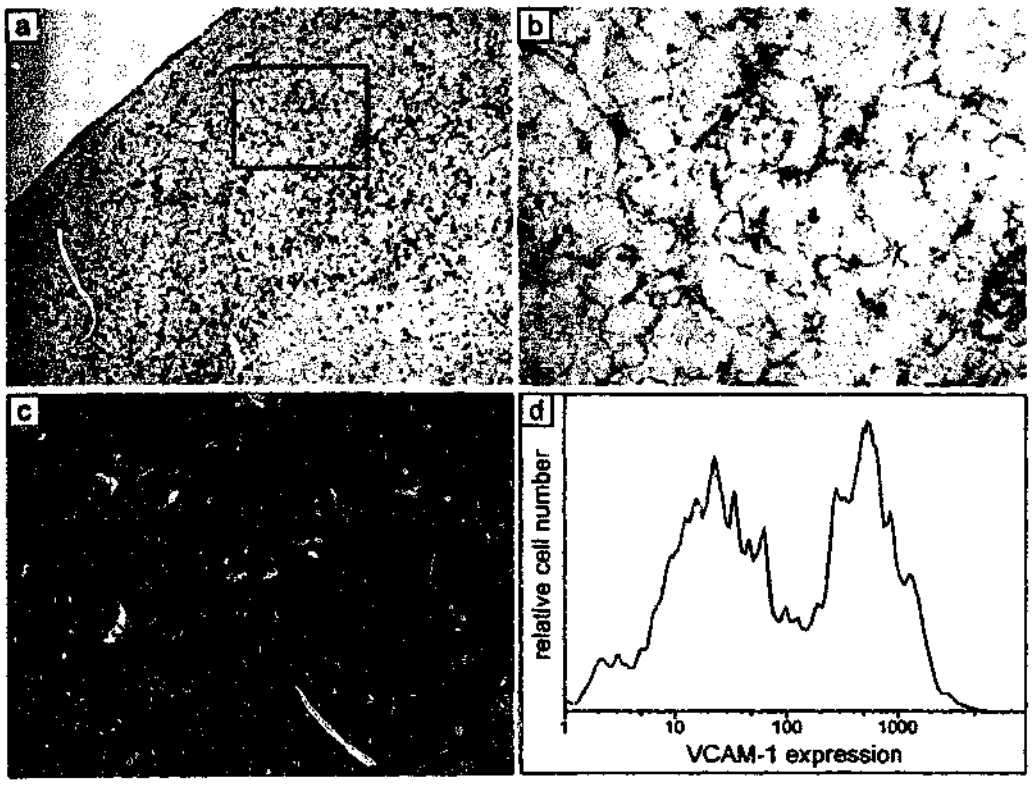

FIGURE 3. VCAM expression on a subset of the cytokeratin$^+$ stromal cell matrix of the cortex. *a*, Shows immunohistochemical detection of VCAM-1 staining (brown) on a transverse section of thymus; staining is mainly found in a reticular pattern in the cortex, as well as in vascular regions of both the medulla and cortex. *b*, Shows a higher magnification view of the area of the cortex indicated by the box in *a*. In *c*, it is shown that VCAM-1 expression (red) in the cortex corresponds to a subset of cells that also express cytokeratins (green). Flow cytometric analysis of VCAM-1 expression on cortical stromal cells (MHC-II$^+$, 6C3$^+$; see text) confirms that approximately one-third to one-half of such cells express VCAM-1 (*d*). Counterstains were hematoxylin (*a* and *b*) or DAPI (*c*). Original magnifications: *a* = ×100; *b* and *c* = ×400.

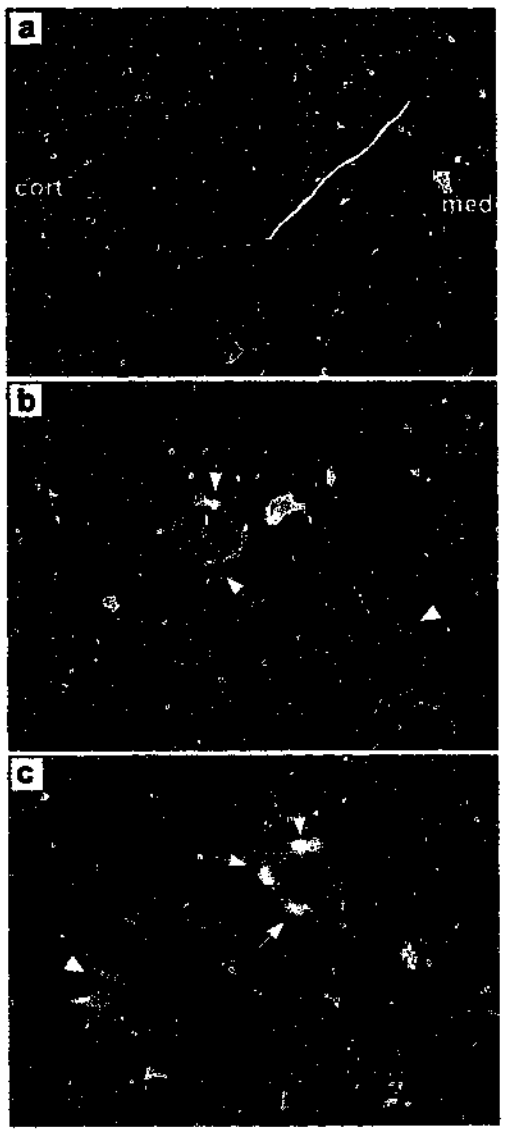

FIGURE 4. Colocalization studies reveal intimate association of early lymphopoietic precursors with the cytokeratin$^+$ stromal matrix of the cortex. *a*, Shows a lower power view (original magnification, ×100) of a transverse section of thymus, including midcortical regions and a portion of central medulla, as indicated. CD117$^+$ cells (red) are nearly always found in direct contact with cytokeratin$^+$ cells (green) that form a reticular matrix in the cortex. In *b*, a higher power view of another section is shown (original magnification, ×1000). A view from the reverse orientation is shown in *c*; the plane of focus in *b* and *c* differs by ~2 μM. The arrows around the most centrally located CD117$^+$ cell indicate a cytokeratin$^+$ cell seen from above in *b*, and through the center of the CD117$^+$ cell in *c*; note that the processes from the cytokeratin$^+$ cell virtually envelop the CD117$^+$ precursor. A similar relationship can be seen in a second precursor-stromal pair in this field (marked by an arrowhead), albeit at a different tissue depth.

the thymus is difficult, requiring some form of enzymatic amplification (either peroxidase alone or peroxidase/tyramide; see *Materials and Methods*) to be detected. It is not clear whether this results from low Ag levels on target cells, or whether the Abs and/or Ab conjugates are of low affinity, although it is worth noting that multiple clones and multiple direct conjugates have been used with similar results. Consequently, a functional assay for interaction of early precursors was used, in which binding to a cloned VCAM-1$^+$ thymic stromal line (100-4, the gift of A. Farr, Seattle, WA) was tested (Fig. 5). In this assay, DN1 cells bound in a relatively nonspecific manner to both the stromal cells and the plastic substrate; consequently, the ability of DN1 cells to bind specifically to VCAM-1 cannot be reliably determined. However, both DN2 and DN3 cells bound specifically to these VCAM-1$^+$ cells in a manner that could be blocked almost completely by preincubation with anti-VCAM-1. This finding

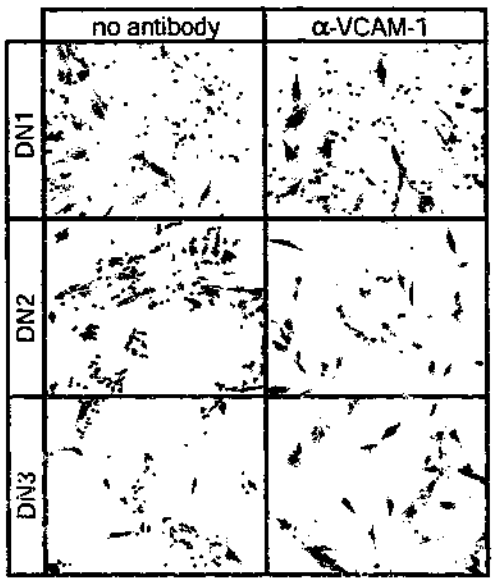

FIGURE 5. Adhesion of precursor thymocytes to stromal cells via VCAM-1. The ability of DN precursors to adhere to VCAM-1 expressed by thymic stromal cells was tested by a coincubation assay. Equal numbers of purified precursors were added to each well, followed by incubation, washing, fixation, and staining with hematoxylin. Thymocytes appear as small, darkly stained dots, while thymic stromal cells are large, reticular, and less darkly stained. DN1 thymocytes adhered in a relatively nonspecific manner to stromal cell cultures, as evidenced by binding to noncellular regions of the plastic substrate; such binding could not be blocked with an anti-VCAM-1 Ab. However, DN2 and DN3 precursors adhered specifically to the VCAM-1$^+$ stromal cells, but not to the surrounding plastic. This adhesion specifically involved VCAM-1, because it could be blocked almost completely by pretreatment of the stromal culture with an anti-VCAM-1 Ab.

is most revealing in relation to the DN2 subset, which had poor affinity for ECM ligands under similar assay conditions (Fig. 2). Because the anatomic location of DN2 cells is intermediate between that of DN1 (inner cortex) and DN3 (outer cortex), the reliance of this stage on cell surface-expressed VCAM-1 for adhesion strongly implicates requirement for a cellular, rather than extracellular, matrix for transmigration of early precursors between different cortical microenvironments.

In vivo effects of anti-VCAM-1 administration on the thymus

The data presented to this point show that early lymphoid precursors directly interact with stromal cells during migration outward through the cortex, and strongly implicate adhesion to this stromal matrix via a VCAM-1-dependent mechanism. To confirm the relevance of this data, an in vivo assay was highly desirable. Several factors complicate such analysis. First, disruption of lymphoid receptors for VCAM-1 results in an inability of bone marrow precursors to intravasate and travel to the thymus (35), making interference with α_4 integrins problematic. Second, it is possible that VCAM-1 may be involved not just in the intrathymic migration process, but in the interaction of blood-borne progenitors with vascular endothelium in thymic blood vessels, and thus in entry of early precursors into the thymus. Inhibition of entry into the thymus and inhibition of early precursor differentiation inside the thymus could have similar phenotypes, i.e., an overall reduction in thymocyte number, thus making it difficult to unconditionally distinguish between these two potential roles for VCAM-1.

With this caveat in mind, we performed such experiments, using in vivo administration of a mAb against VCAM-1 for 5 consecutive days in mice. Overall, the size of the thymus was reduced by approximately one-third, both in terms of cross sectional area (Fig. 6) and cell number (Table II), in animals receiving anti-VCAM-1

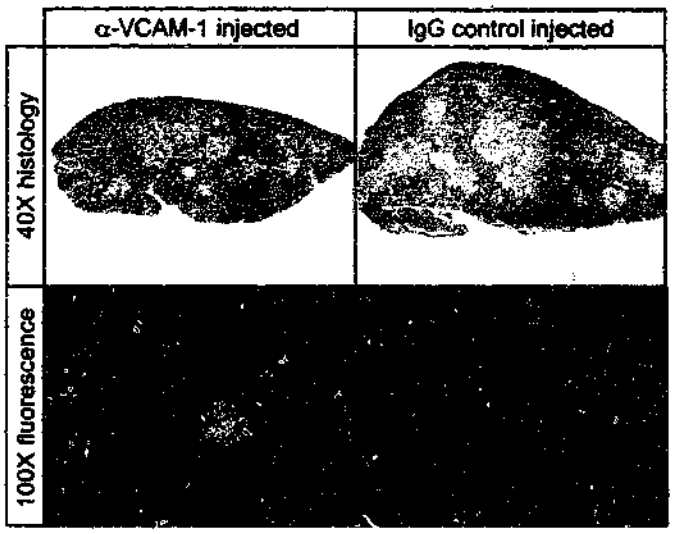

FIGURE 6. Reduced thymic size and altered precursor distribution and frequency resulting from anti-VCAM-1 administration in vivo. The *top two panels* show hematoxylin staining (original magnification, ×40) of transverse sections of thymus from a mouse treated for 5 consecutive days with an anti-VCAM-1 Ab (*left*) or a control Ab (*right*). In each case, sections were selected as those having the greatest cross sectional area. Anti-VCAM-1-treated thymuses were smaller, had fewer cells (see Table II), and have a reduced cell density per unit area. The *bottom panels* show higher power views (original magnification, ×100) of a portion of the thymus from mice treated similarly, indicating the presence of $CD117^+$ precursors (red). $CD117^+$ precursors were less frequent and more centrally located in mice treated with anti-VCAM-1 Ab, compared with controls. Dashed lines in immunofluorescent images represent the boundaries of medullary regions; counterstain is DAPI (blue).

Ab vs a nonspecific control Ab. The density of cells in the anti-VCAM-1-injected thymus was different from that of controls, with the cortex assuming a less densely packed appearance (i.e., more space between cells). The frequency and anatomic distribution of early ($CD117^+$) precursors were also influenced, with fewer cells being present overall, and markedly fewer cells in the mid- to outer cortex of anti-VCAM-1-injected mice. Overall, the proportion of total $CD4^-8^-$ cells did not differ substantially in thymuses from anti-VCAM-1 injected vs controls (Table II). Likewise, the proportion of individual DN subsets, including the $CD117^+$ stages (DN1 and DN2), was not dramatically affected (data not shown). This result is to be expected given the relatively short period of VCAM-1 administration (5 days) compared with the total life span of DN cells (~2 wk; see Ref. 12), especially because the transit time through the $CD117^+$ stages is at least 10 days. Thus, 5 days of anti-VCAM-1 administration can effectively block migration to the outer cortex without substantially changing the number of precursor cells that are present. Administration of Ab for longer periods incurs the risk of anti-Ig immune responses in either VCAM-1- or nonspecific Ab-treated mice. Nonetheless, 5 days of anti-VCAM-1 Ab had clear effects on both thymic size and precursor distribution. The fact that early progenitors were biased toward the inner cortex in anti-VCAM-1-treated animals further suggests that VCAM-1 must play a role in intrathymic migration in addition to any potential role in precursor entry; effects on precursor entry alone should result in an accumulation of precursors in the outer, rather than the inner, cortex. Thus, our findings are consistent with a requirement for VCAM-1 in the intrathymic migration of early progenitors, although an additional role in precursor entry cannot be excluded by these studies.

Table II. *Effects of in vivo administration of anti-VCAM-1 Ab*[a]

Treatment Type	Total Cells[b]	% of Cells in Phenotype		
		$CD4^-8^-$	$CD4^+8^+$	Mature
Anti-VCAM-1	110 ± 27	5 ± 3	88 ± 9	6 ± 4
IgG control	146 ± 37	6 ± 1	86 ± 2	8 ± 2

[a] Mean ± SD for three to six experiments.
[b] Total of $\times 10^{-6}$ per lobe of the thymus.

Discussion

In this study, we used integrin expression profiles (Fig. 1 and Table I) to predict the mechanical requirements for migration of immature precursors from the deep cortex to the capsule. Although deep cortical (DN1) and outer cortical (DN3) stages were capable of efficient binding to ECM ligands predicted by integrin expression profiles, DN2 cells that span the midcortex were not. This led us to evaluate binding to alternative matrix ligands, specifically the cell surface-expressed integrin counterreceptor VCAM-1. Functional and in situ studies revealed that lymphoid progenitors migrating outward through the cortex were found in intimate contact with a radially aligned stromal cell matrix (Fig. 4), a subset of which was $VCAM\text{-}1^+$ (Fig. 3). Although technical limitations prevented us from performing direct colocalization studies of VCAM-1 and early precursors in situ, the capacity for these cells to interact in a VCAM-1-specific manner was demonstrated by in vitro binding (Fig. 5). Furthermore, administration of an anti-VCAM-1 Ab in vivo resulted in reduced thymic size and cortical density, as well as a reduction in the presence of early progenitors in the outer cortex (Fig. 6). This phenotype is consistent with a role for $VCAM\text{-}1^+$ stromal cells in providing the adhesive matrix for intrathymic precursor migration, although, as mentioned earlier (see *Results*), VCAM-1 could also play a role in the entry of precursors into the thymus. Our data conclusively show that early lymphoid progenitors form intimate contacts with a matrix composed of cortical stromal cells (Fig. 4); that they express receptors for VCAM-1 (Fig. 1 and Table I), which is found on components of this cellular matrix (Fig. 3); and that they bind specifically to VCAM-1 on cloned cortical stromal cells in vitro (Fig. 5). Together with supportive results from in vivo studies (Fig. 6 and Table II), these findings provide direct evidence for intimate interactions between stromal cells and early lymphoid progenitors during their migration across the cortex, and further suggest that VCAM-1 and α_4 integrins (respectively) are probably responsible for this interaction. Although inducible deletion of VCAM-1 has been reported to have no obvious effect on the distribution of thymic subsets (36), deletion was performed in the immediate postnatal period, when the embryonic wave of thymic precursor differentiation predominates (reviewed in Ref. 1). Thus, a requirement for VCAM-1 in either the extravasation or transcortical migration of progenitors in the steady state thymus may not be obvious from such experiments. Furthermore, the overall size of the thymus in gene-targeted animals was not reported, and consequently the results of those studies may be completely consistent with those obtained by us using in vivo Ab administration (Fig. 6 and Table II).

It should be noted that stromal cells in the thymic cortex are scattered (Fig. 4), such that not every cortical lymphocyte (which are mostly DP cells) can be in contact with a stromal cell at any one time. Consequently, the finding that early progenitors do remain in contact with stromal cells during their migration across the cortex may reveal important principles about the differentiation process, as follows. Stromal cells are generally believed to be responsible for establishing the thymic microenvironment (reviewed in Refs. 37 and 38), and consequently, for inducing the steady state production of mature T lymphocytes from uncommitted progenitors. Our previous

work has shown that although stromal cells from various cortical regions may be morphologically indistinct, they can be functionally differentiated, and establish a series of stratified microenvironments in which distinct stages of early precursor differentiation occur (19). Many of the signals that induce cellular differentiation, including those known to be important for intrathymic differentiation, such as Notch and c-*kit* ligands (see above), exist as cell surface proteins. Thus, successful differentiation of early lymphoid progenitors may require direct, sequential interactions with stromal cell-expressed ligands in each cortical region (for an example, see Ref. 22). Interstitial migration, i.e., migration along an ECM, could leave many such interactions to chance, while migration along a matrix of the very cells that generate these signals would ensure the efficiency of required interactions. This does not mean that the cortical stromal matrix exists merely to support DN migration and differentiation, because DP cells undoubtedly have a requirement for stromal cells as well. In fact, given that VCAM-1 expression reveals clear heterogeneity among cytokeratin$^+$ cortical stroma (Fig. 3), it is conceivable that DN and DP cells may use quite different stromal cell types, despite being present in the same cortical regions. Likewise, the ECM plays a required role in the differentiation, proliferation, and/or survival of lymphoid progenitors (39), either by direct signaling to the progenitors themselves, or through the organization of other stromal cells in their corresponding microenvironments.

A requirement for cell migration in progenitor differentiation is not unique to the steady state thymus. Of course, migration into and/or away from different microenvironments is a well-known paradigm of differentiation in the embryo. In addition, progenitor migration between different extracellular microenvironments is an integral component of steady state differentiation in a variety of postnatal tissues, including the epidermis (40), intestinal crypts (41), germ cells (42, 43), and even bone marrow (44, 45). Frequently, the divergence of independent cell fates, i.e., commitment to one lineage vs another, or self-renewal vs differentiation, is intricately linked to the position of a given stem/progenitor cell relative to other cells in its microenvironment. It is likely that progenitors in the thymus undergo a similar process, because they not only migrate, but make numerous cell fate choices as well, including (for instance) divergence of α/β vs γ/δ lineages, or the decision to differentiate or remain (albeit temporarily) in an undifferentiated state (46). The signals that regulate this asymmetry in the thymus are largely unknown. However, it is worth noting that integrin expression analysis reveals heterogeneity among otherwise homogeneous DN1 and DN2 subsets, in which many such cell fate decisions occur (see Fig. 1). It is interesting to speculate that such changes in integrin expression may, in fact, be linked to asymmetry of cell fates, as it is in differentiating epidermis (see Ref. 40). However, not only are integrins nonhomogenously expressed on DN cells, but their ligands are nonhomogenously distributed in the thymus (this study, and Refs. 28, 29, and 47). Further structural and biochemical mapping of specific regions in which asymmetric cell fate decisions take place thus represents an important next step in deciphering the signals for steady state T cell production in the postnatal thymus.

Acknowledgments

We thank Dr. Andrew Farr for the 100-4 cell line, Dr. Svetlana Mazel for initial characterization of integrin expression, and Drs. Filippo Giancotti (Memorial Sloan-Kettering Cancer Center) and Yoji Shimizu (University of Minnesota, Minneapolis, MN) for helpful discussions.

References

1. Dunon, D., and B. A. Imhof. 1996. T cell migration during ontogeny and T cell repertoire generation. *Curr. Top. Microbiol. Immunol. 212:79.*
2. Kondo, M., I. L. Weissman, and K. Akashi. 1997. Identification of clonogenic common lymphoid progenitors in mouse bone marrow. *Cell 91:661.*
3. Matsuzaki, Y., J. Gyotoku, M. Ogawa, S. Nishikawa, Y. Katsura, G. Gachelin, and H. Nakauchi. 1993. Characterization of c-*kit* positive intrathymic stem cells that are restricted to lymphoid differentiation. *J. Exp. Med. 178:1283.*
4. Michie, A. M., J. R. Carlyle, T. M. Schmitt, B. Ljutic, S. K. Cho, Q. Fong, and J. C. Zuniga-Pflucker. 2000. Clonal characterization of a bipotent T cell and NK cell progenitor in the mouse fetal thymus. *J. Immunol. 164:1730.*
5. Zuniga-Pflucker, J. C., J. Di, and M. J. Lenardo. 1995. Requirement for TNF-α and IL-1α in fetal thymocyte commitment and differentiation. *Science 268:1906.*
6. Rodewald, H. R., P. Moingeon, J. L. Lucich, C. Dosiou, P. Lopez, and E. L. Reinherz. 1992. A population of early fetal thymocytes expressing FcγRII/III contains precursors of T lymphocytes and natural killer cells. *Cell 69:139.*
7. Wu, L., C. L. Li, and K. Shortman. 1996. Thymic dendritic cell precursors: relationship to the T lymphocyte lineage and phenotype of the dendritic cell progeny. *J. Exp. Med. 184:903.*
8. Ardavin, C., L. Wu, C. L. Li, and K. Shortman. 1993. Thymic dendritic cells and T cells develop simultaneously in the thymus from a common precursor population. *Nature 362:761.*
9. Petrie, H. T., R. Scollay, and K. Shortman. 1992. Commitment to the T cell receptor-$\alpha\beta$ or -$\gamma\delta$ lineages can occur just prior to the onset of CD4 and CD8 expression among immature thymocytes. *Eur. J. Immunol. 22:2185.*
10. Radtke, F., A. Wilson, G. Stark, M. Bauer, J. van Meerwijk, H. R. MacDonald, and M. Aguet. 1999. Deficient T cell fate specification in mice with an induced inactivation of Notch1. *Immunity 10:547.*
11. Katsura, Y., and H. Kawamoto. 2001. Stepwise lineage restriction of progenitors in lympho-myelopoiesis. *Int. Rev. Immunol. 20:1.*
12. Shortman, K., M. Egerton, G. J. Spangrude, and R. Scollay. 1990. The generation and fate of thymocytes. *Semin. Immunol. 2:3.*
13. Wu, L., F. Livak, and H. T. Petrie. 1998. TCR-independent development of pluripotent T-cell precursors. In *Molecular Biology of B-cell and T-cell Development.* J. G. Monrow and E. V. Rothenberg, eds. Humana Press, Totowa, p. 285.
14. Washburn, T., E. Schweighoffer, T. Gridley, D. Chang, B. J. Fowlkes, D. Cado, and E. Robey. 1997. Notch activity influences the $\alpha\beta$ versus $\gamma\delta$ T cell lineage decision. *Cell 88:833.*
15. Robey, E., D. Chang, A. Itano, D. Cado, H. Alexander, D. Lans, G. Weinmaster, and P. Salmon. 1996. An activated form of Notch influences the choice between CD4 and CD8 T cell lineages. *Cell 87:483.*
16. Rodewald, H. R., K. Kretzschmar, W. Swat, and S. Takeda. 1995. Intrathymically expressed c-*kit* ligand (stem cell factor) is a major factor driving expansion of very immature thymocytes in vivo. *Immunity 3:313.*
17. Akashi, K., and I. L. Weissman. 1996. The c-*kit*$^+$ maturation pathway in mouse thymic T cell development: lineages and selection. *Immunity 5:147.*
18. Peschon, J. J., P. J. Morrissey, K. H. Grabstein, F. J. Ramsdell, E. Maraskovsky, B. C. Gliniak, L. S. Park, S. F. Ziegler, D. E. Williams, C. B. Ware, et al. 1994. Early lymphocyte expansion is severely impaired in interleukin 7 receptor-deficient mice. *J. Exp. Med. 180:1955.*
19. Lind, E. F., S. E. Prockop, H. E. Porritt, and H. T. Petrie. 2001. Mapping precursor movement through the postnatal thymus reveals specific microenvironments supporting defined stages of early lymphoid development. *J. Exp. Med. 194:127.*
20. Penit, C., B. Lucas, and F. Vasseur. 1995. Cell expansion and growth arrest phases during the transition from precursor (CD4$^-$8$^-$) to immature (CD4$^+$8$^+$) thymocytes in normal and genetically modified mice. *J. Immunol. 154:5103.*
21. Tourigny, M. R., S. Mazel, D. B. Burtrum, and H. T. Petrie. 1997. T cell receptor (TCR)-β gene recombination: dissociation from cell cycle regulation and developmental progression during T cell ontogeny. *J. Exp. Med. 185:1549.*
22. Takahama, Y., J. J. Letterio, H. Suzuki, A. G. Farr, and A. Singer. 1994. Early progression of thymocytes along the CD4/CD8 developmental pathway is regulated by a subset of thymic epithelial cells expressing transforming growth factor β. *J. Exp. Med. 179:1495.*
23. Penit, C. 1988. Localization and phenotype of cycling and post-cycling murine thymocytes studied by simultaneous detection of bromodeoxyuridine and surface antigens. *J. Histochem. Cytochem. 36:473.*
24. Gray, D. H., A. P. Chidgey, and R. L. Boyd. 2002. Analysis of thymic stromal cell populations using flow cytometry. *J. Immunol. Methods 260:15.*
25. Nelson, A. J., C. H. Clegg, and A. G. Farr. 1998. In vitro positive selection and anergy induction of class II-restricted TCR transgenic thymocytes by a cortical thymic epithelial cell line. *Int. Immunol. 10:1335.*
26. Surh, C. D., E. K. Gao, H. Kosaka, D. Lo, C. Ahn, D. B. Murphy, L. Karlsson, P. Peterson, and J. Sprent. 1992. Two subsets of epithelial cells in the thymic medulla. *J. Exp. Med. 176:495.*
27. Shier, P., G. Otulakowski, K. Ngo, J. Panakos, E. Chourmouzis, L. Christjansen, C. Y. Lau, and W. P. Fung-Leung. 1996. Impaired immune responses toward alloantigens and tumor cells but normal thymic selection in mice deficient in the β_2 integrin leukocyte function-associated antigen-1. *J. Immunol. 157:5375.*
28. Kim, M. G., G. Lee, S. K. Lee, M. Lolkema, J. Yim, S. H. Hong, and R. H. Schwartz. 2000. Epithelial cell-specific laminin 5 is required for survival of early thymocytes. *J. Immunol. 165:192.*
29. Lannes-Vieira, J., M. Dardenne, and W. Savino. 1991. Extracellular matrix components of the mouse thymus microenvironment: ontogenetic studies and modulation by glucocorticoid hormones. *J. Histochem. Cytochem. 39:1539.*
30. Salomon, D. R., L. Crisa, C. F. Mojcik, I. K. Ishii, G. Klier, and E. M. Shevach. 1997. Vascular cell adhesion molecule-1 is expressed by cortical thymic epithelial cells and mediates thymocyte adhesion: implications for the function of $\alpha_4\beta_1$ (VLA4) integrin in T-cell development. *Blood 89:2461.*

31. Reza, J. N., and M. A. Ritter. 1994. Differential expression of adhesion molecules within the human thymus. *Dev. Immunol. 4:55.*
32. Klug, D. B., C. Carter, E. Crouch, D. Roop, C. J. Conti, and E. R. Richie. 1998. Interdependence of cortical thymic epithelial cell differentiation and T-lineage commitment. *Proc. Natl. Acad. Sci. USA 95:11822.*
33. Van Ewijk, W., G. Hollander, C. Terhorst, and B. Wang. 2000. Stepwise development of thymic microenvironments in vivo is regulated by thymocyte subsets. *Development 127:1583.*
34. Hollander, G. A., B. Wang, A. Nichogiannopoulou, P. P. Platenburg, W. Van Ewijk, S. J. Burakoff, J. C. Gutierrez-Ramos, and C. Terhorst. 1995. Developmental control point in induction of thymic cortex regulated by a subpopulation of prothymocytes. *Nature 373:350.*
35. Arroyo, A. G., J. T. Yang, H. Rayburn, and R. O. Hynes. 1996. Differential requirements for α_4 integrins during fetal and adult hematopoiesis. *Cell 85:997.*
36. Leuker, C. E., M. Labow, W. Muller, and N. Wagner. 2001. Neonatally induced inactivation of the vascular cell adhesion molecule 1 gene impairs B cell localization and T cell-dependent humoral immune response. *J. Exp. Med. 193:755.*
37. Anderson, G., and E. J. Jenkinson. 2001. Lymphostromal interactions in thymic development and function. *Nat. Rev. Immunol. 1:31.*
38. Van Ewijk, W., E. W. Shores, and A. Singer. 1994. Cross talk in the mouse thymus. *Immunol. Today 15:214.*
39. Anderson, G., K. L. Anderson, E. Z. Tchilian, J. J. Owen, and E. J. Jenkinson. 1997. Fibroblast dependency during early thymocyte development maps to the $CD25^+$ $CD44^+$ stage and involves interactions with fibroblast matrix molecules. *Eur. J. Immunol. 27:1200.*
40. Fuchs, E. 1998. Beauty is skin deep: the fascinating biology of the epidermis and its appendages. *Harvey Lect. 94:47.*
41. Marshman, E., C. Booth, and C. S. Potten. 2002. The intestinal epithelial stem cell. *BioEssays 24:91.*
42. Orth, J. M., W. F. Jester, L. H. Li, and A. L. Laslett. 2000. Gonocyte-Sertoli cell interactions during development of the neonatal rodent testis. *Curr. Top. Dev. Biol. 50:103.*
43. Matzuk, M. M., K. H. Burns, M. M. Viveiros, and J. J. Eppig. 2002. Intercellular communication in the mammalian ovary: oocytes carry the conversation. *Science 296:2178.*
44. Kondo, Y., K. Irie, M. Ikegame, S. Ejiri, K. Hanada, and H. Ozawa. 2001. Role of stromal cells in osteoclast differentiation in bone marrow. *J. Bone Miner. Metab. 19:352.*
45. Shackney, S. E., S. S. Ford, and A. B. Wittig. 1975. Kinetic-microarchitectural correlations in the bone marrow of the mouse. *Cell Tissue Kinet. 8:505.*
46. Foss, D. L., E. Donskoy, and I. Goldschneider. 2001. The importation of hematogenous precursors by the thymus is a gated phenomenon in normal adult mice. *J. Exp. Med. 193:365.*
47. Kutlesa, S., U. Siler, A. Speiser, J. T. Wessels, I. Virtanen, P. Rousselle, L. M. Sorokin, C. A. Muller, and G. Klein. 2002. Developmentally regulated interactions of human thymocytes with different laminin isoforms. *Immunology 105:407.*